AD

USAAVLABS TECHNICAL REPORT 65-38

COMPONENT TESTING
XV-9A HOT CYCLE RESEARCH AIRCRAFT
SUMMARY REPORT

By

G. D. Deveaux

November 1965

U. S. ARMY AVIATION MATERIEL LABORATORIES

FORT EUSTIS, VIRGINIA

CONTRACT DA 44-177-AMC-877(T)

HUGHES TOOL COMPANY

DDC Availability Notice

Qualified requesters may obtain copies of this report from DDC.

This report has been furnished to the Department of Commerce for sale to the public.

Disclaimer

The findings in this report are not to be construed as an official Department of the Army position, unless so designated by other authorized documents.

When Government drawings, specifications, or other data are used for any purpose other than in connection with a definitely related Government procurement operation, the United States Government thereby incurs no responsibility nor any obligation whatsoever; and the fact that the Government may have formulated, furnished, or in any way supplied the said drawings, specifications, or other data is not to be regarded by implication or otherwise as in any manner licensing the holder or any other person or corporation, or conveying any rights or permission, to manufacture, use, or sell any patented invention that may in any way be related thereto.

Trade names cited in this report do not constitute an official indorsement or approval of the use of such commercial hardware or software.

Disposition Instructions

Destroy this report when it is no longer needed. Do not return it to the originator.

DEPARTMENT OF THE ARMY
U. S. ARMY AVIATION MATERIEL LABORATORIES
FORT EUSTIS, VIRGINIA 23604

This report was prepared by the Hughes Tool Company, Aircraft Division, under the provisions of Contract DA 44-177-AMC-877(T) to document service life substantiation of various critical components of the XV-9A aircraft. The test objectives were completed with generally satisfactory results.

This report is furnished for information and to report on the status of the project.

Task IM121401D14403
Contract DA 44-177-AMC-877(T)
USAAVLABS Technical Report 65-38
November 1965

COMPONENT TESTING
XV-9A HOT CYCLE RESEARCH AIRCRAFT
SUMMARY REPORT

Report HTC-AD 64-26 (385-T 16)

by

G. D. Deveaux

Prepared by

Hughes Tool Company, Aircraft Division
Culver City, California

for

U. S. ARMY AVIATION MATERIEL LABORATORIES
FORT EUSTIS, VIRGINIA

SUMMARY

The tests of the various structural components of the XV-9A Hot Cycle Research Aircraft have been accomplished in accordance with U. S. Army Aviation Materiel Laboratories Contract DA 44-177-AMC-877(T).

These component tests included fatigue tests of the blade root-end and constant section areas, hub gimbal system, spar-to-segment and root-fitting-to-spar attachments, and material evaluation tests of the blade spars. Sealing tests were conducted on the joint between the Y-duct and triduct in the hub area, the joint area between the gas generator and diverter valve, and the fixed-duct joint on the rotor blade. Blade natural frequency tests were conducted to ensure that the natural frequencies of the rotor blade would not be in a critical frequency range. The instrumented flight blade was calibrated in a test fixture before the flight test program.

FOREWORD

This report was prepared in accordance with clause 1, paragraph i (3c) of U. S. Army Contract DA 44-177-AMC-877(T), and summarizes the component testing conducted under clause 1, paragraph d, of subject contract and under clause 1, paragraph c, of Modification No. 6 to subject contract.

This work was performed at the Hughes Tool Company, Aircraft Division, Culver City, California, under the direction of Mr. H. O. Nay, Program Manager, Hot Cycle Programs, and Mr. C. R. Smith, Engineering Project Manager, Hot Cycle Research Aircraft; and under the direct supervision of Mr. H. G. Smith, Chief, Structures Analysis and Test, and Mr. G. D. Deveaux, Head, Structures Test.

The contract became effective on 29 September 1962. The component test program was completed 15 March 1965.

CONTENTS

ILLUSTRATIONS

TABLES

Figure 1. XV-9A Hot Cycle Research Aircraft.

INTRODUCTION

This report covers the component testing conducted on various structural components of the XV-9A Hot Cycle Research Aircraft. The testing has provided information necessary for design development of the aircraft and has supplied data necessary for rotor system fatigue-life calculations.

The blade root-end fatigue test was conducted to provide information for rotor fatigue-life calculations. The blade constant-section fatigue test and an additional blade root-end fatigue test provided additional information for rotor fatigue-life calculations. Reduced scale spar-to-segment and root-fitting-to-spar attachments fatigue tests provided data for optimizing the attachment of the spars to the segments.

Three component tests were conducted involving sealing problems: (1) sealing of the Y-duct to the triduct that forms a manifold for ducting the gas generator exhaust to the rotor blades, (2) sealing of the area between the gas generator exhaust section and the diverter valve, and (3) sealing of the fixed-duct joint on the rotor blade.

A proof loading was performed on a pair of bonded spars to a 2.5-g loading condition to ensure the structural integrity of the laminated rotor blade spars. In addition, preliminary developmental testing was conducted on laminated spars to investigate potential local buckling problems. Material evaluation tests were conducted to aid in selection of proper static and fatigue strength materials for the rotor blade spars. A structural integrity test was conducted on the laminated spars simulating a possible hot-gas duct rupturing with its gases impinging upon the spar. A functional proof test was conducted on the blade-tip closure valve to verify its reliability. A fatigue test was conducted on the reinforced hub gimbal system assembly.

Blade natural frequency tests (nonrotating) were performed to obtain information for comparison with the original titanium spar frequencies, and to supply information to ensure that the natural frequencies of the rotor blade would not be in a critical frequency range. The instrumented flight rotor blade was calibrated in a test fixture to permit reducing data during the whirl test and flight test programs.

HUB GIMBAL SYSTEM FATIGUE TEST

SUBJECT

This test constituted an endurance evaluation of the hub gimbal bearing and adjacent rotor hub support structure under radial and axial thrust loads with oscillating motion. It was conducted in the HTC-AD structures test laboratory from December 1963 through February 1964.

PURPOSE

The purpose of this test was to substantiate the hub gimbal bearing and surrounding hub support structure for a 100-hour life in support of the XV-9A whirl and flight test programs.

SUMMARY OF RESULTS

The hub gimbal bearing successfully completed a 106.3-hour endurance test at the following load conditions:

Radial	11,470 pounds steady
Axial thrust	0 to 4170 pounds at 8 cps
Oscillation	$\pm 10^{o}$ at 4 cps

Although inspection of the bearing revealed some fretting in the heavily loaded radial zone, the bearing was serviceable at the completion of the test.

TEST SPECIMEN

The test specimen consisted of the hub gimbal bearing and the necessary hub support structure to duplicate a typical bearing installation (HTC-AD drawing 385-0511, Hub Assembly, modified for axial thrust provisions by drawing 385-1203).

TEST SETUP

The bearing and hub gimbal support structure was tested in a fixture that simulated the bearing installation and provided the necessary steady radial load, cyclic axial thrust load, and oscillatory motion (HTC-AD drawing 385-9613).

A vari-drive unit was used to provide the oscillating motion to the test fixture. Figure 2 shows the test setup and actuating mechanism.

INSTRUMENTATION

The instrumentation used consisted of an integrally designed link to measure the radial bearing loads. The axial thrust loads were measured by a bending bridge circuit installed on the arms of the thrust spring system. Both the radial and axial thrust transducers were calibrated prior to testing for their respective use.

TEST PROCEDURE

The 11,475 pounds of radial load applied to the bearing was provided by a jack screw system reacting against the outer bearing housing. The axial load, 0 to 4170 pounds at 8 cps, was applied by a cantilever spring system engaged on a cam surface and induced by the ± 10 degrees of oscillatory motion. The oscillation of the specimen was provided by a drive crank mechanism operating at 4 cps.

A greasing schedule of every four hours was performed throughout the test, using a MIL-G-25537 oscillating bearing grease to conform to the planned XV-9A maintenance.

See Figure 3 for a general schematic of setup and load application.

TEST RESULTS

The hub gimbal bearing and hub support structure successfully completed a 106.3-hour endurance test without failure. This included 1.531×10^6 cycles of oscillation and 3.062×10^6 cycles of axial thrust loading.

The hub gimbal bearing was submitted to the materials engineering laboratory for inspection and analysis, with the following results:

1. Fifteen rollers showed evidence of fretting (heavily loaded zone).
2. Seven rollers revealed slight evidence of fretting (slightly loaded zone).
3. Eight rollers showed no evidence of fretting.
4. Mating surfaces on the bearing races also indicated areas of fretting.

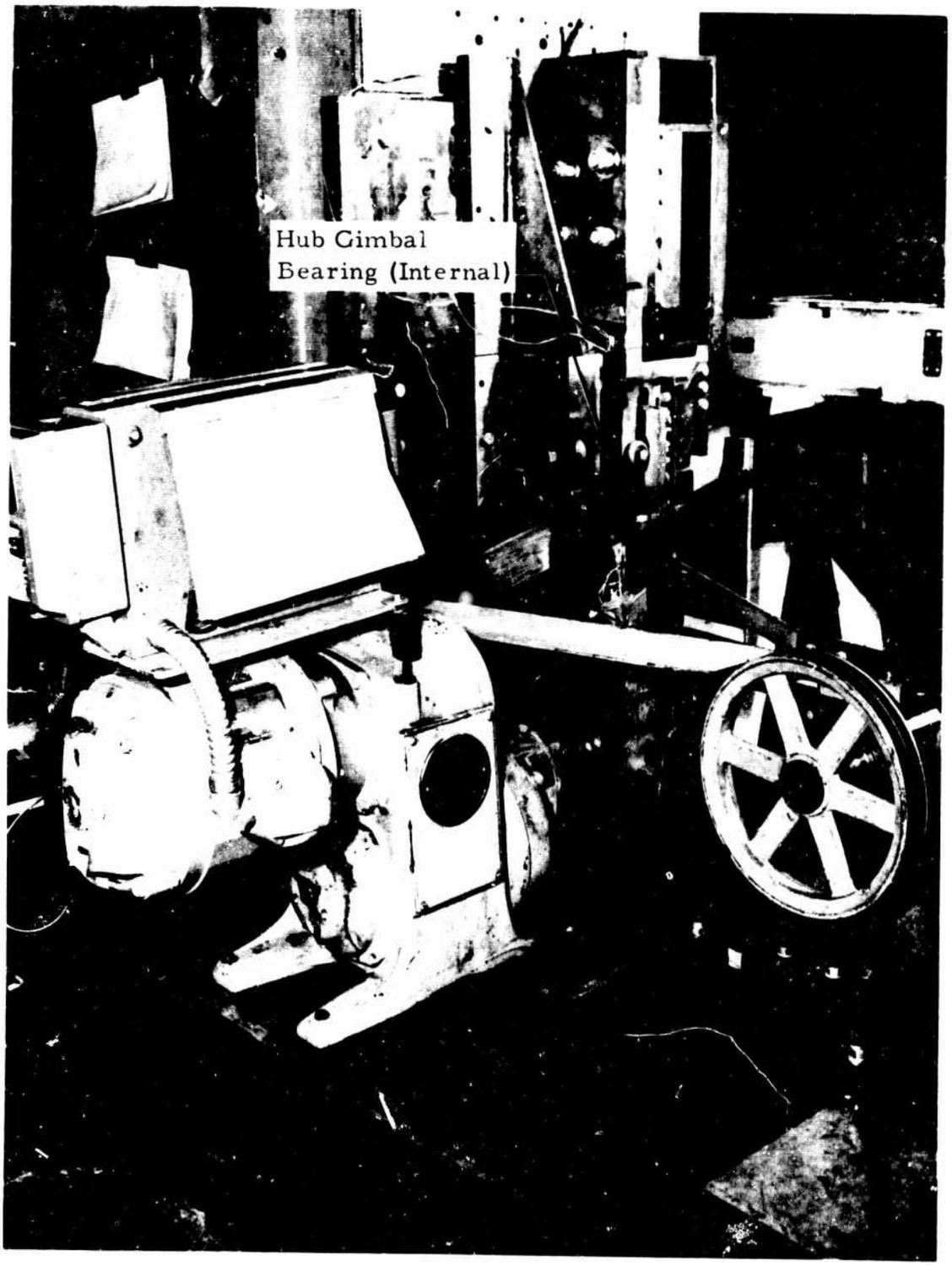

Figure 2. Hub Gimbal System Fatigue Test Setup.

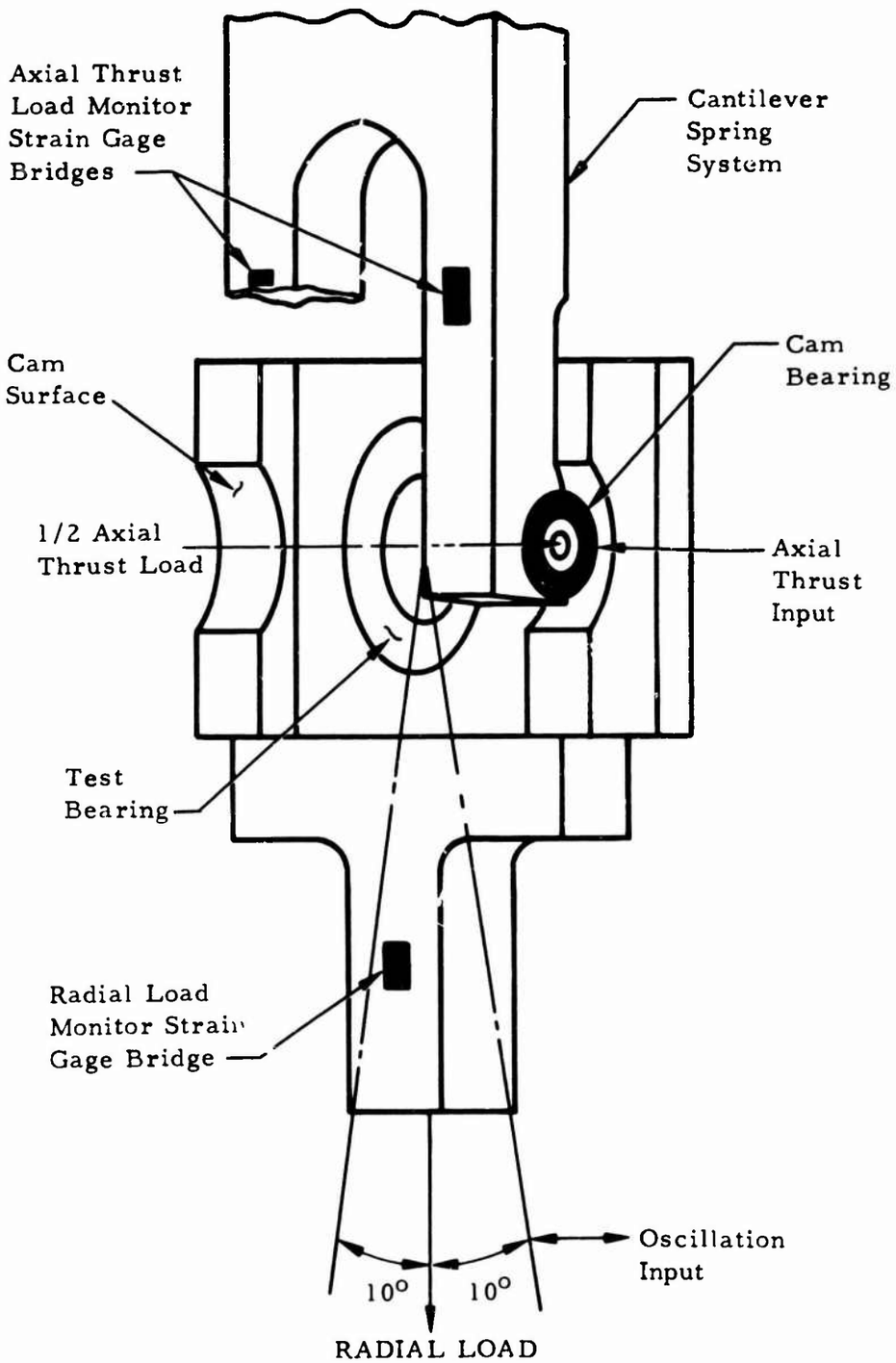

Figure 3. Hub Gimbal System Fatigue Test Loading Schematic.

5. The roller bearing cages showed slight signs of wear due to axial thrust loadings.

Figures 4 and 5 show the bearing and hub support structure conditions after the endurance test. The bearing was serviceable at the completion of the test.

Figure 4. Hub Gimbal System Bearing After Completion of Test.

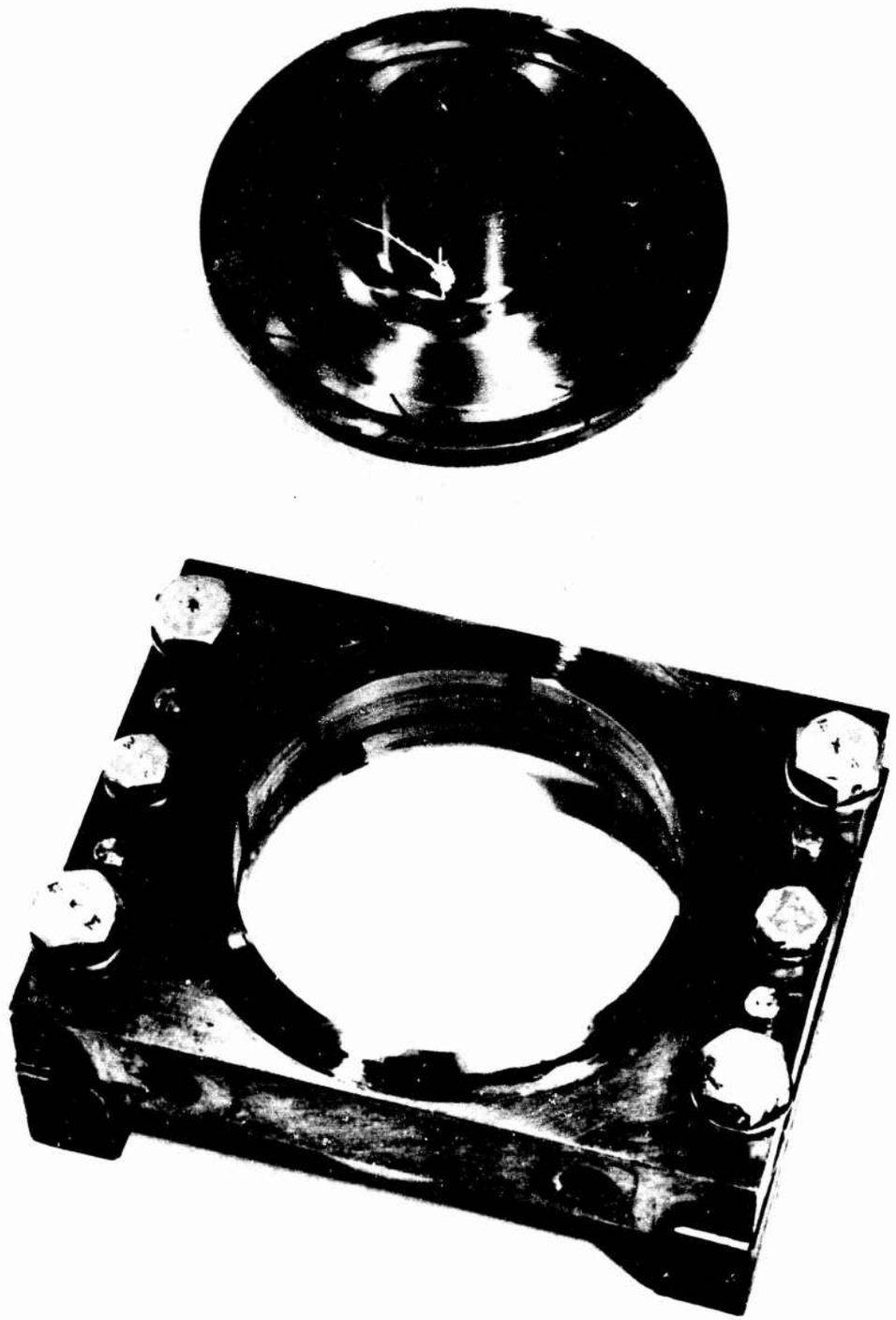

Figure 5. Hub Gimbal System Thrust Bearing After Completion of Test.

Y-DUCT AND TRIDUCT PRESSURE AND TEMPERATURE TESTS

SUBJECT

These were a leakage test and a proof test of the reduced-weight Y-duct and triduct under pressure and temperature conditions. They were conducted in the manufacturing facility and on the whirl test tower between January and May 1964.

PURPOSE

The purpose of these tests was to demonstrate that the reduced-weight Y-duct and triduct are structurally adequate to withstand the pressures and temperatures anticipated during the XV-9A flight test program.

SUMMARY OF RESULTS

AMBIENT AIR PRESSURE TESTS

The Y-duct and triduct assemblies were pressurized separately to 36 psig and indicated zero leakage. When pressure of the two ducts was checked, a leakage rate of less than 16 cfm at 26 psig was indicated.

HOT GAS PRESSURE AND TEMPERATURE TESTS

These tests, performed during the whirl test program, subjected the duct assembly to maximum pressures and temperatures of the YT-64 gas generators. No appreciable leakage or damage was detected in the duct assembly.

TEST SPECIMEN

The test specimen consisted of the Y-duct assembly (HTC-AD drawing 385-1603) and the triduct assembly (HTC-AD drawing 385-1605) with the carbon seals (HTC-AD drawing 285-0509) installed. The Y-duct is the stationary portion of the ducting system and the triduct is the rotating portion of the ducting system.

TEST SETUP AND PROCEDURE

AMBIENT AIR PRESSURE TESTS

The ducts were set up in the rotor hub and shaft assembly fixture for these tests. All ports were blocked by bulkhead plates to form a completely sealed chamber. One of the lower Y-duct plates had a bulkhead fitting to allow pressurization of the chamber. The opposite bulkhead had a fitting for a pressure gage to read chamber pressure. Figure 6 shows the general test setup. Figure 7 shows a general schematic of the pressurization system. The instrumentation consisted of a 0- to 60-cfm flowmeter, and a pressure gage for monitoring the chamber pressure.

HOT GAS PRESSURE AND TEMPERATURE TESTS

The Y-duct/triduct assembly, installed on the rotor hub, was subjected to the maximum pressures and temperatures of the YT-64 gas generators at intermediate and full power settings during the whirl test program.

TEST RESULTS

AMBIENT AIR PRESSURE TESTS

The complete Y-duct/triduct assembly attained a leakage rate of less than 16 cfm at 26 psig. For the individual Y-duct and triduct assemblies, no leakage was encountered up to 36 psig.

HOT GAS PRESSURE AND TEMPERATURE TESTS

Inspection of the Y-duct and triduct assemblies during and following the whirl test program revealed no appreciable system leakage and no damage to the duct assemblies.

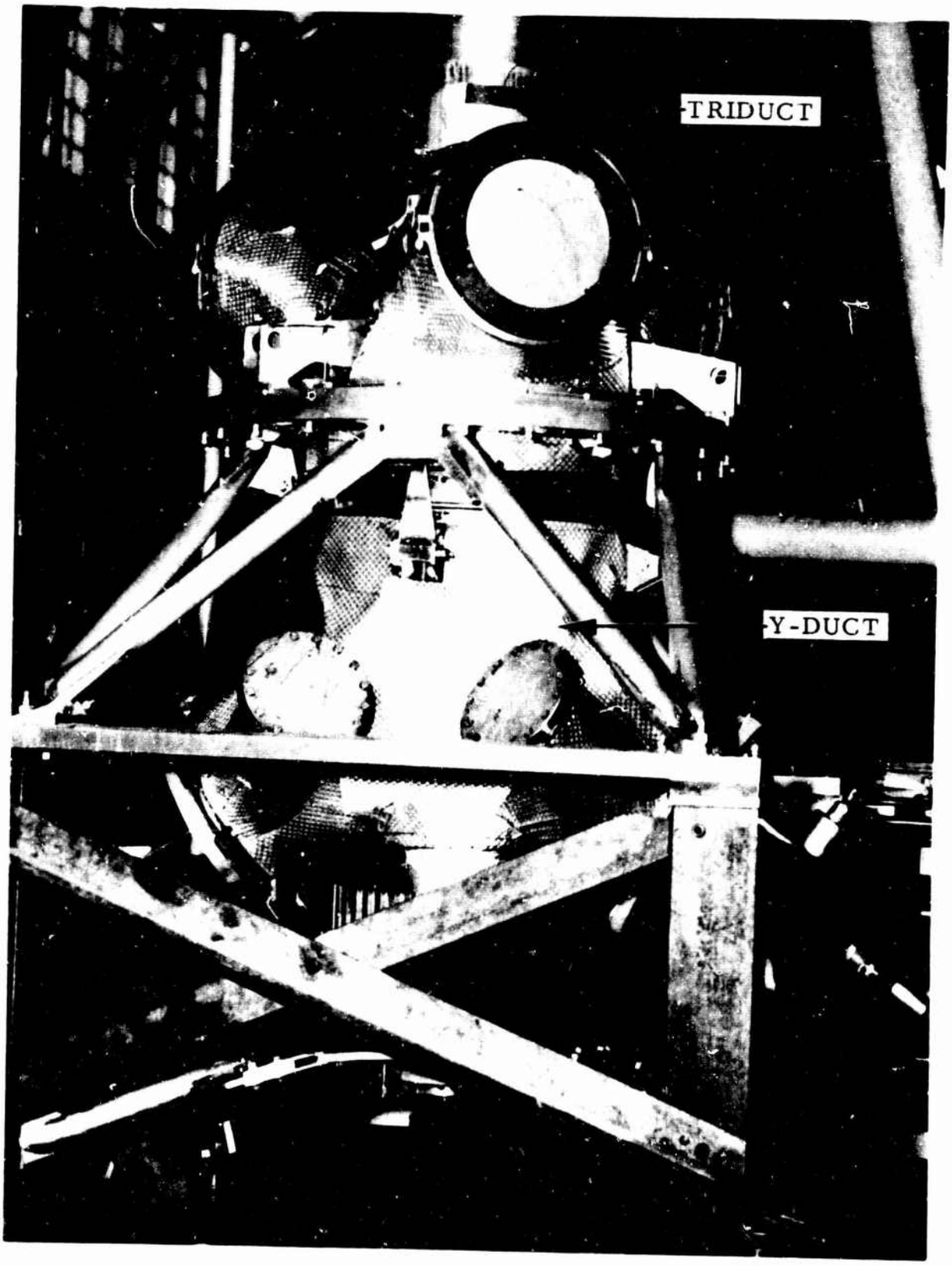

Figure 6. Y-Duct and Triduct Test Setup.

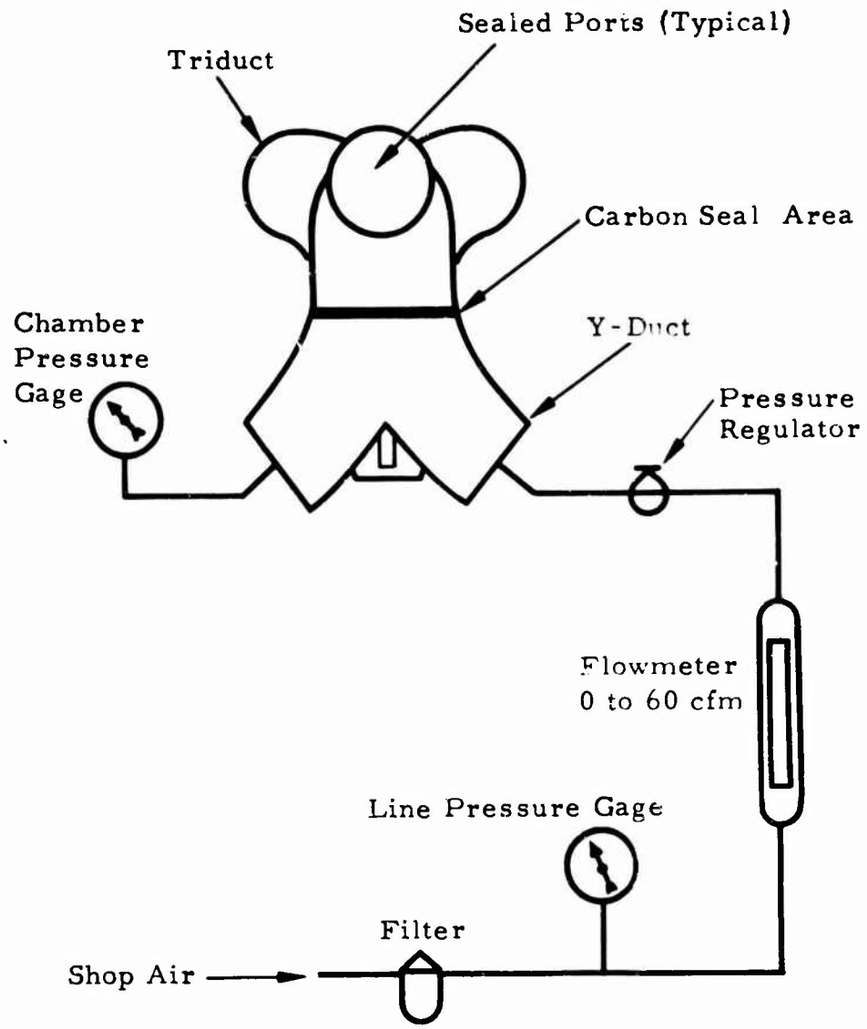

Figure 7. Y-Duct and Triduct Schematic - Pressure Test.

FIXED-DUCT JOINT SEAL TEST

SUBJECT

This test was conducted to provide an adequate seal in the fixed-duct joints of the root-end of the XV-9A rotor blade. It was conducted at the HTC-AD structures test laboratory during October 1963.

PURPOSE

The purpose of this test was to provide a seal with minimum leakage under high temperature and pressure conditions across load-carrying fixed ducting in the XV-9A rotor blade.

SUMMARY OF RESULTS

The fixed-duct joint test specimen successfully completed a 100-hour test under simulated pressure, temperature, and loading with no leakage of the seal throughout the test.

TEST SPECIMEN

The test specimen consisted of two duct segments joined together by a clamp, duplicating the duct joint assembly found in the XV-9A rotor blade hot gas ducting system.

The seal used (HTC-AD drawing number 285-0507-33) was made from 0.063-inch-thick A-286 corrosion-resistant steel AMS 5525. A high-temperature joint sealing compound was used between the metal seal and the two fixed-duct facings.

TEST SETUP AND INSTRUMENTATION

The test specimen was installed in a test fixture to duplicate flapping bending moment, torsion, centrifugal force, hot gas temperatures, and pressure. Shown in Figure 8 is a general schematic indicating the loads applied and instrumentation locations.

Instrumentation required to monitor the test consisted of a pressure transducer, two strain-gaged tension rods, a strain-gaged input load cell, and four chromel-alumel thermocouples placed internally on the duct wall. These electronic devices were recorded on a direct-writing

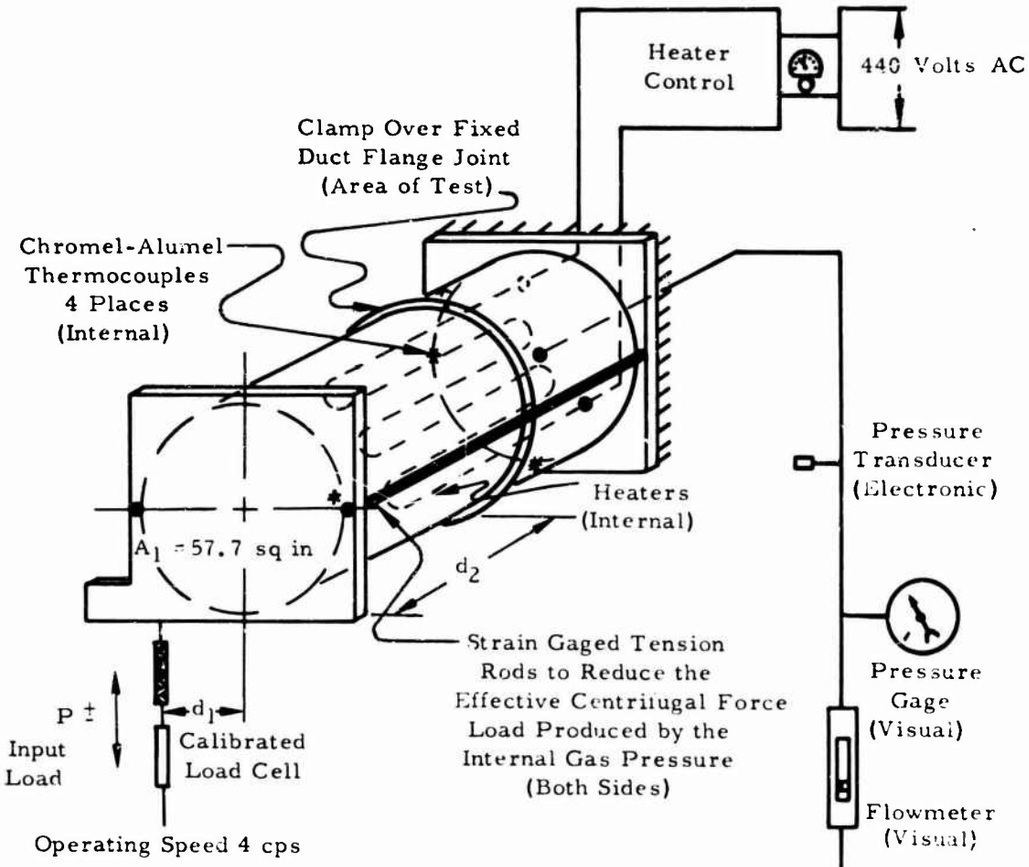

Pertinent Data

A_1 = Area (acted upon by internal pressure)
Simulated gas pressure = 27.5 psig
Centrifugal force = 580 lb
Torque = ±600 in -lb ($\pm P \times d_1$)
Flapping moment = 228 ±1591 in -lb ($\pm P \times d_2$)
(steady moment is produced by the weight of the end plate + additional weight necessary to obtain desired moment)
Temperature = 1200°F
P = ±130 lb d_1 = 4.62 in d_2 = 12.25 in
Tension in rods (each) = 503 lb
Centrifugal force produced by gas pressure = 1585 lb

Figure 8. Fixed-Duct Joint Seal Test Loading Schematic.

oscillograph at periodic intervals during the test. Additional visual aid equipment included a calibrated flowmeter and a pressure gage.

A standard air regulator was used to control the line air input pressure. A transformer was used to adjust the heaters to the desired temperature level.

TEST PROCEDURE

Temperature and pressure were simultaneously increased in the fixed-duct joint test chamber. The preload in the tension rods was then checked to ensure that the clamp area was correctly loaded. Upon reaching the test temperature and pressure, the cyclic input load was applied by an eccentric vari-drive operating at 4 cps. Oscillograph records were taken of the electronic monitoring devices and were recorded at periodic intervals throughout the test.

Presented in Figure 9 is a photograph of the fixed-duct seal test setup.

TEST RESULTS

The fixed-duct joint seal test successfully completed 100 hours of running under the following conditions:

Temperature	1200°F
Pressure	27.5 psig
Centrifugal load	580 lb
Torsion	±600 in -lb
Flapping bending	±228 ±1591 in -lb
Operating cyclic load speed	4 cps
Leakage rate	nil

CONCLUSIONS

The fixed-duct joint with the reinforced duct clamps, the metal spacer, and joint sealant compound produced a seal superior to that provided by the previously used plain asbestos gasket. The asbestos gasket had previously broken under loading and gas pressures, and had contributed to the overall leakage of the system. This condition was caused by the inability of the soft gasket material to take the flexural motions required in this area.

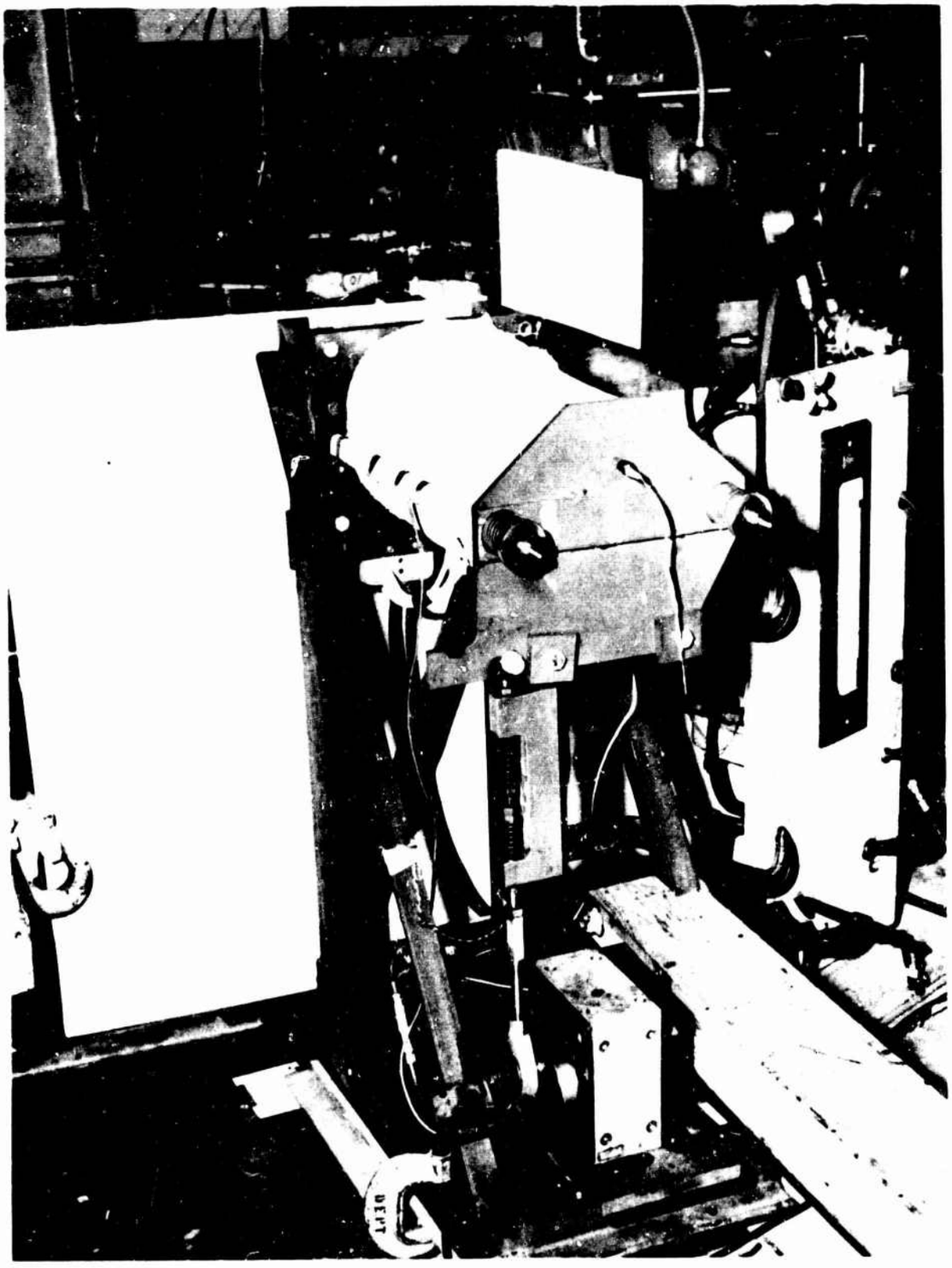

Figure 9. Fixed-Duct Joint Test Setup.

GAS GENERATOR-DIVERTER VALVE SEAL TEST

SUBJECT

This test concerned functional adequacy of the seal between the gas generator and the diverter valve. It was conducted in the HTC-AD structures test laboratory during January and February 1964.

PURPOSE

The purpose of this test was to determine leakage rates under various conditions and to prove the structural adequacy of the seal under simulated operational conditions.

SUMMARY OF TEST RESULTS

The leakage flow of air past the gas generator-diverter seal was found to be 13 pounds per minute at 800°F and 30 psig. The YT-64 gas generator develops a flow of approximately 1,500 pounds per minute at 26 psig. This leakage by the seal represented a conservative loss of less than 1 percent.

TEST SPECIMEN

The test specimen consisted of a gas generator-diverter valve seal assembly (HTC-AD drawing 385-7106).

TEST SETUP AND INSTRUMENTATION

The gas generator-diverter valve seal was set up in a test fixture that supported the seal similarly to the method used in the aircraft. A dummy gas generator exhaust section was used to provide a heater base and end cap for the heat chamber system. The general setup is shown in the schematic diagram, Figure 10. Figure 11 shows the setup and instrumentation.

The instrumentation consisted of iron-constantan thermocouples placed in the area of the gas generator-diverter valve seal in the free air stream. These thermocouples were used to measure the representative gas temperatures. A standard pressure gage was used to measure the chamber air pressure. A 0- to 60-cfm flowmeter attached to the plant air supply was used. It was controlled by a standard air pressure regulator.

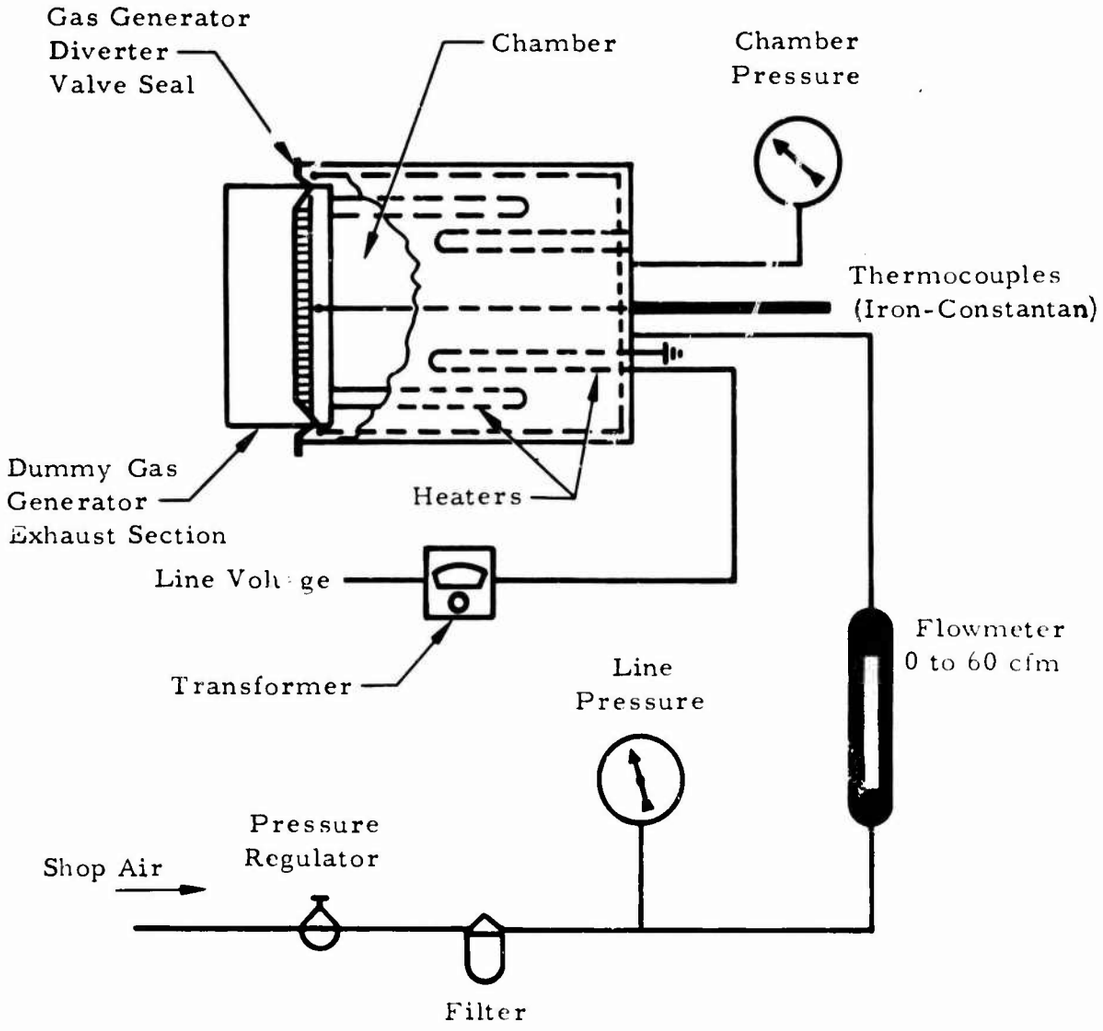

Figure 10. Gas Generator-Diverter Valve Seal Test Loading Schematic.

Figure 11. Gas Generator-Diverter Valve Seal Test Setup.

TEST RESULTS

Presented in Figure 12 is a plot of the leakage versus airflow test data at various temperatures. The leakage flow of air past the gas generator-diverter seal was found to be 13 pounds per minute at 800°F and 30 psig. Due to support requirements in the test setup, the center pipe or duct was not allowed to float. This condition resulted in some eccentricity, which was cause for leakage in excess of that anticipated for the aircraft.

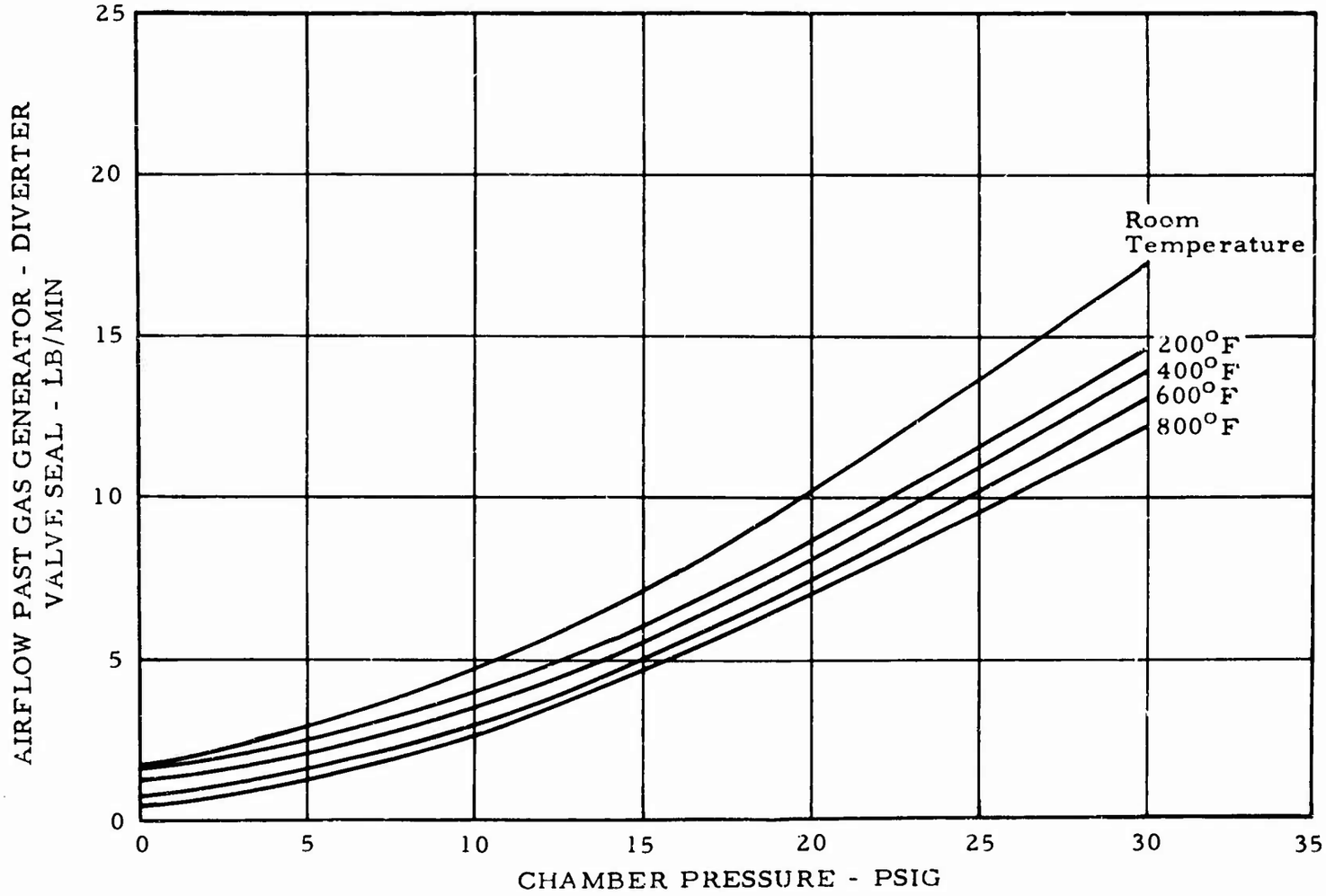

Figure 12. Air Mass Flow Past Seal Versus Chamber Pressure and Temperature.

MATERIALS EVALUATION TESTS

TENSILE AND FATIGUE PROPERTIES

SUBJECT

These tests evaluated static tensile and tension-tension fatigue strength properties of the rotor blade spar material, AM 355 CRT sheet. They were performed in the HTC-AD structures test laboratory from January 1963 through July 1963.

PURPOSE

The purpose of these tests was to provide static tensile and axial tension-tension fatigue test data at room and elevated temperatures, with subsequent fatigue data on performance of various manufacturing finishes on the spar material.

SUMMARY OF RESULTS

The material selected for the spar material was AM 355 CRT sheet strip with basic static tensile properties of 200, 000 psi yield stress and 220, 000 psi ultimate stress.

The fatigue endurance limit for the unnotched specimen was 130, 000 psi maximum stress.

The fatigue endurance limit for the notched specimen with a central unloaded 0. 25-inch-diameter hole was 90, 000 psi maximum stress.

TEST SPECIMENS

Tensile Test Coupons

The tensile test coupons were machined from AM 355 CRT sheet to a typical configuration according to Federal Test Method Standard 151a and incorporated a reduced center section width of 0. 50 inch. The longitudinal and transverse specimens were geometrically similar except for the grain direction of the material. The specimens were polished by hand and inspected prior to testing.

Fatigue Test Coupons, Unnotched Specimens

These fatigue test coupons were machined from AM 355 CRT sheet to a test section width of 0. 25 inch with a typical blend radius of 2. 25 inches. All surfaces were polished and inspected prior to testing.

Fatigue Test Coupons, Notched Specimens

The notched fatigue test specimens were machined to a constant width of 0. 69 inch with a 0. 25-inch-diameter hole in the center. The holes underwent various treatments and finishes, which are described in detail in the Test Results section. The edges of the specimens were polished to prevent the occurrence of failures at the outer edges of the specimens.

Shown in Figure 13 are typical AM 355 CRT test specimens used throughout the static and fatigue test evaluations.

TEST PROCEDURE AND INSTRUMENTATION

Static Tests

The static tensile tests were performed in a 5, 000-pound capacity test machine. This test machine utilized a recorder to automatically plot load versus deflection. The heat source for the elevated temperature portion of the test was supplied by a radiant heat quartz lamp oven. The temperature of the specimen was measured by a potentiometer connected to the specimen by two iron-constantan thermocouples.

Fatigue Tests

The fatigue coupon tests were performed on an axial tension fatigue test machine. This test machine is a below-resonance type, operating at 30 cycles per second, with the cycles recorded on a mechanical counter. Steady and vibratory loads were monitored from a strain gage load cell set up in series with the test specimen. This setup is shown in Figure 14.

The heat source for the elevated temperature portion of the fatigue test was supplied by a radiant heat quartz lamp oven. The temperature was measured by a potentiometer connected to the specimen by an iron-constantan thermocouple. This setup is shown in Figure 15.

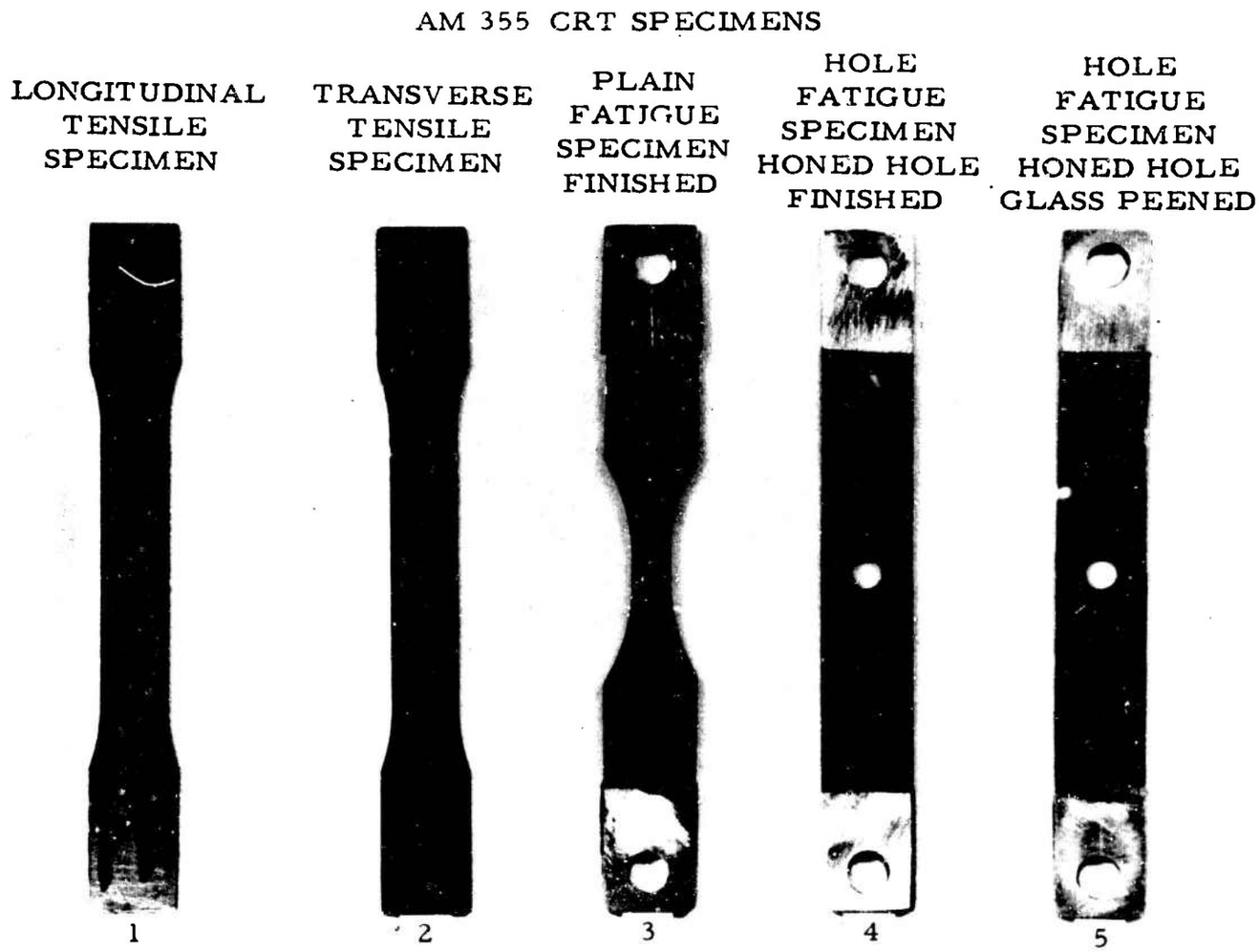

Figure 13. Materials Evaluation - Static and Fatigue Test Coupons.

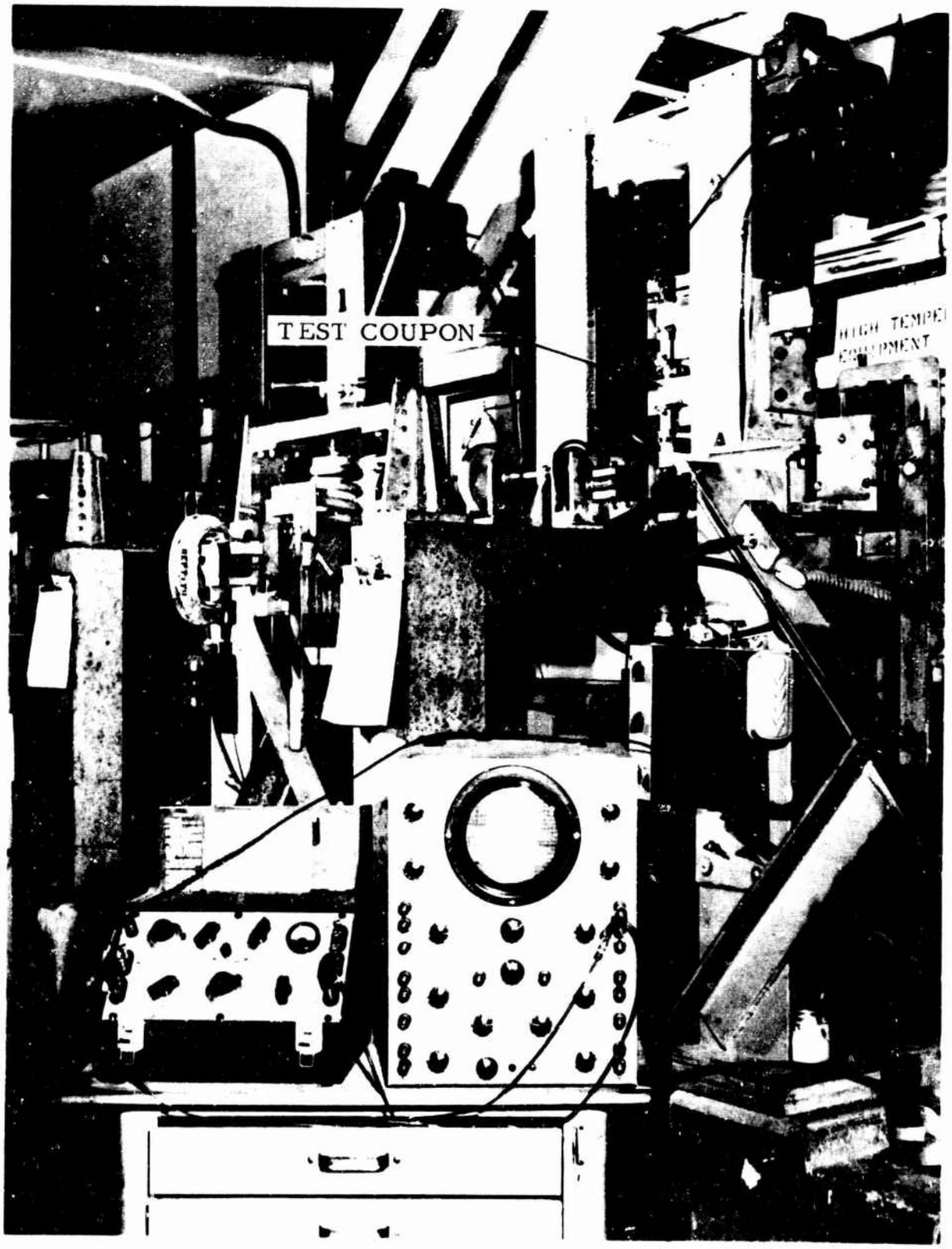

Figure 14. Materials Evaluation - Fatigue Test Setup.

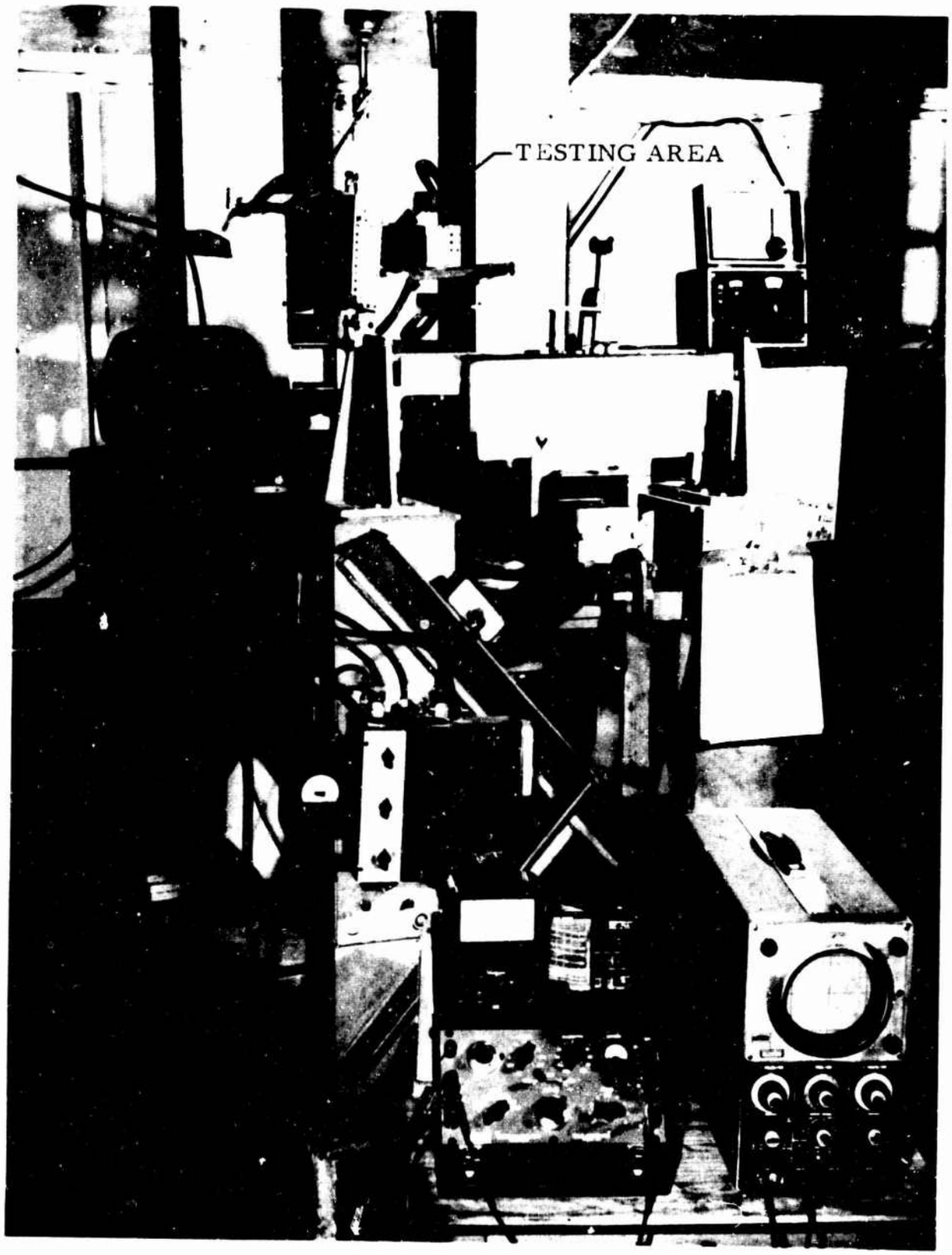

Figure 15. Materials Evaluation - High Temperature Fatigue Test Setup.

TEST RESULTS

Presented in Table 1 are the static tensile properties of AM 355 CRT longitudinal and transverse specimens.

TABLE 1
STATIC TENSILE PROPERTIES - AM 355 MATERIAL

Specimen Number	Thickness (in)	F_{ty} (0.2% Offset) (ksi)	F_{tu} (ksi)	% Elongation	500-Gram Knoop Hardness Test: Knoop Hardness Number	500-Gram Knoop Hardness Test: Rockwell R_c
		A. Longitudinal Coupons				
83-5-33	0.0493	201.6	226.4	20.0	513.2	48.2
X-7-9	0.0507	201.0	226.5	20.0	511.6	48.1
82-5-33	0.0504	206.0	228.0	19.5	511.6	48.1
83-3-7-9	0.0499	203.3	227.3	19.5	514.8	48.3
82-3-7-9	0.0499	202.4	228.3	19.5	498.0	47.2
X-51-5355-57	0.0500	200.0	225.3	20.5	486.0	46.4
X-59-61-63-65	0.0499	198.3	225.0	20.5	498.0	47.2
X-37	0.0498	202.0	226.7	21.0	505.5	47.7
81-3-7-9	0.0507	195.0	225.0	20.5	505.5	47.7
80-5-33	0.0506	187.4	217.0	20.0	496.5	47.1
83-5-35-37	0.0258	185.0	224.4	19.5	501.0	47.4
83-5-39-41	0.0259	186.4	221.6	19.5	507.0	47.8
83-5-43-45	0.0260	186.7	225.0	20.5	518.0	48.5
83-5-47-49	0.0260	185.6	223.7	19.5	505.5	47.7
83-5-49-53	0.0260	197.0	229.0	20.0	502.5	47.5
83-5-51-53	0.0258	191.7	223.0	18.0	495.0	47.0
83-5-53-51	0.0259	187.4	219.0	18.5	473.0	45.5
83-5-55	0.0259	193.4	221.0	17.0	507.0	47.8
83-5-55-57	0.0258	184.3	222.5	20.0	480.0	46.0
X-11-13	0.0260	197.7	237.3	20.0	484.5	46.3
X-15-17	0.0258	187.4	224.4	20.0	496.5	47.1
X-19-21	0.0252	193.0	226.8	19.0	490.5	46.7
X-23	0.0255	196.0	226.0	21.5	487.5	46.5
X-25-27-29	0.0256	193.3	224.0	20.0	490.5	46.7
X-31-33-35	0.0257	191.3	223.6	20.0	490.5	46.7
82-5-57	0.0253	195.5	222.5	16.5	484.5	46.3
82-5-51-53	0.0257	190.0	221.4	19.5	490.5	46.7
82-5-47-49	0.0257	190.0	221.4	18.0	487.5	46.5

TABLE 1 (Continued)

Specimen Number	Thickness (in)	F_{ty} (0.2% Offset) (ksi)	F_{tu} (ksi)	% Elongation	500-Gram Knoop Hardness Test: Knoop Hardness Number	500-Gram Knoop Hardness Test: Rockwell R_c
82-5-47	0.0260	195.0	223.6	18.0	507.0	47.8
82-5-45-55	0.0254	190.4	222.4	19.5	478.6	45.9
82-5-43	0.0260	195.0	215.5	17.5	492.0	46.8
82-5-39-41	0.0260	191.9	220.2	21	487.5	46.5
82-5-35-37	0.0256	190.5	220.2	19.5	486.0	46.4
81-3-17	0.0257	185.0	220.8	20.5	474.4	45.6
83-3-11-13	0.0260	195.0	219.7	17.5	499.5	47.3
83-3-15-17	0.0257	190.4	222.4	20.0	486.0	46.4
83-3-19-21	0.0250	193.0	220.5	20.0	483.0	46.2
83-3-23-25	0.0257	195.0	222.0	19.5	493.5	46.9
83-3-27-29	0.0258	192.8	225.6	20.0	484.5	46.3
83-3-31	0.0252	191.1	218.7	19.0	490.5	46.7
82-3-11-13	0.0258	190.4	221.5	19.0	484.5	46.3
82-3-15	0.0260	190.8	217.9	19.0	481.5	46.1
82-3-17	0.0250	189.0	221.8	19.5	487.5	46.5
82-3-19-21	0.0250	189.7	217.5	17.0	458.0	44.4
82-3-23-25	0.0255	190.7	222.5	19.5	492.0	46.8
82-3-27	0.0259	189.2	221.5	18.0	486.0	46.4
82-3-27-29	0.0260	188.0	221.4	19.5	477.2	45.8
82-3-31	0.0251	187.2	218.4	18.0	467.4	45.1
X-39-41-43	0.0254	192.0	225.0	21.0	504.0	47.6
X-45-47-49	0.0255	192.5	225 6	19.0	469.0	45.2
80-285-0121-3-1A	0.0255	186.0	214.3	19.0	461.0	44.6
80-285-0121-3-2A	0.0255	183.0	214.3	23.5	462.5	44.7
80-285-0121-3-3A	0.0255	185.0	219.0	21.0	467.5	45.1
80-285-0121-5-1A	0.0253	191.4	219.3	17.5	469.0	45.2
80-285-0121-5-2A	0.0254	185.3	221.3	19.0	480.0	46.0
80-285-0121-5-3A	0.0254	187.0	221.2	18.0	481.5	46.1
81-285-0121-3-1A	0.0256	189.0	217.7	17.5	463.2	44.8
81-285-0121-3-2A	0.0256	188.0	219.6	20.0	466.0	45.0
81-285-0121-3-3A	0.0252	187.5	218.0	20.0	457.0	44.4
81-285-0121-5-1A	0.0253	197.0	223.8	19.0	478.6	45.9
81-285-0121-5-2A	0.0253	193.0	223.0	19.0	478.6	45.9
81-285-0121-5-3A	0.0254	197.0	224.4	20.0	468.8	45.2
82-285-0121-5-1A	0.0254	193.0	221.0	18.5	489.0	46.6
82-285-0121-5-2A	0.0255	191.0	223.3	20.5	498.0	47.2
82-285-0121-5-3A	0.0255	200.0	225.0	21.0	492.0	46.8
82-285-0121-3-1A	0.0254	191.0	218.0	18.0	475.8	45.7
82-285-0121-3-2A	0.0252	189.8	221.9	19.5	461.8	44.7

TABLE 1 (Continued)

Specimen Number	Thickness (in)	F_{ty} (0.2% Offset) (ksi)	F_{tu} (ksi)	% Elongation	500-Gram Knoop Hardness Test: Knoop Hardness Number	500-Gram Knoop Hardness Test: Rockwell R_c
82-285-0121-3-3A	0.0256	195.0	223.8	20.0	492.0	46.8
83-285-0121-3-1A	0.0285	195.0	225.3	20.0	490.5	46.7
83-285-0121-3-2A	0.0258	195.0	225.0	22.0	480.0	46.0
83-285-0121-3-3A	0.0256	193.0	221.5	20.0	464.6	44.9
83-285-0121-5-1A	0.0254	192.0	225.0	20.0	471.6	45.4
83-285-0121-5-2A	0.0255	200.0	224.0	20.0	475.8	45.7
83-285-0121-5-3A	0.0253	198.0	225.0	20.0	477.2	45.8
81-3-11-13	0.0255	192.0	221.0	20.5	477.2	45.8
81-3-15-17	0.0255	187.2	218	20.5	477.2	45.8
81-3-19-21	0.0254	179.0	217.5	23.0	454.8	44.2
81-3-23-25	0.0253	189.0	222.2	20.5	474.4	45.6
81-3-27-29	0.0255	189.0	222.2	20.0	489.0	46.6
81-3-31	0.0255	188.0	218.5	20.0	475.8	45.7
80-5-35-37	0.0257	199.0	227.0	19.0	486.0	46.4
80-5-39-41	0.0254	197.6	225.5	19.0	492.0	46.8
80-5-43-45	0.0256	193.0	221.7	18.0	487.5	46.5
80-5-47-49	0.0256	192.0	222.5	19.0	492.0	46.8
80-5-51-53	0.0257	196.0	226.4	20.0	475.8	45.7
80-5-55-57	0.0256	200.4	231.0	18.0	507.0	47.8
37-39	0.0255	197.3	230.6	17.5	478.6	45.9
33-59-61	0.0495	200.4	231.0	20.0	496.5	47.1
41-43	0.0254	195.6	226.6	17.0	480.0	46.0
45-47	0.0255	197.3	229.0	20.0	513.2	48.2
37-39	0.0254	199.2	226.8	17.5	529.2	49.2
33-59-61	0.0500	201.2	228.0	17.5	516.4	48.4
41-43	0.0254	199.0	227.0	16.5	475.8	45.7
45-47	0.0255	198.0	228.0	17.0	480.0	46.0
37-39	0.0254	195.7	227.0	17.0	501.0	47.4
33-59-61	0.0499	197.8	231.0	21.0	492.0	46.8
41-43	0.0254	199.0	226.0	17.0	495.0	47.0
45-47	0.0256	198.0	224.0	17.0	502.5	47.5
7-9	0.0505	203.3	227.0	19.5	498.0	47.2
11-13	0.0255	198.4	230.0	20.5	493.5	46.9
15-17	0.0255	191.3	223.2	21.5	471.6	45.4
19-21	0.0256	190.6	226.0	22	489.0	46.6
23-25	0.0252	194.0	227.4	19.0	486.0	46.4
27-29	0.0254	193.7	226.4	20.0	492.0	46.8
31	0.0252	189.6	226.0	19.5	486.0	46.4
63-65	0.0255	191.2	226.4	17.0	484.5	46.3

TABLE 1 (Continued)

Specimen Number	Thickness (in)	F_{ty} (0.2% Offset) (ksi)	F_{tu} (ksi)	% Elongation	500-Gram Knoop Hardness Test: Knoop Hardness Number	500-Gram Knoop Hardness Test: Rockwell R_C
81-5-35-36-37	-	-	-	-	477.2	45.8
81-5-39-41	-	-	-	-	484.5	46.3
81-5-43-45	-	-	-	-	478.6	45.9
81-5-47-49	-	-	-	-	478.6	45.9
81-5-51-53	-	-	-	-	493.5	46.9
81-5-55-57	-	-	-	-	464.6	44.9
80-5-39-41	-	-	-	-	499.5	47.3
1-49-51	0.0255	197.3	225.8	15.0	483.0	46.2
2-49-51	0.0256	198.8	227.0	15.0	513.2	48.2
3-49-51	0.0256	197.0	225.4	22.0	489.0	46.6
1-53-55	0.0258	192.5	222.7	18.0	490.5	46.7
2-53-57	0.0257	197.2	226.8	18.0	496.5	47.1
3-53-55	0.0257	196.0	223.6	19.5	480.0	46.0
1-57	0.0256	190.5	222.6	18.0	486.0	46.4
2-57	0.0256	198.8	226.6	18.0	507.0	47.8
3-57	0.0256	197.3	223.4	17.5	470.2	45.3
80-5-33	-	-	-	-	502.5	47.5
80-5-35-37	-	-	-	-	477.2	45.8
80-5-39-41	-	-	-	-	508.5	47.9
80-5-43-45	-	-	-	-	496.5	47.1
80-5-47-49	-	-	-	-	483.0	46.2
80-5-51-53	-	-	-	-	504.0	47.6
80-5-55-57	-	-	-	-	498.0	47.2
80-3-7-9	0.0497	199.0	228.7	18.5	513.2	48.2
80-3-11-13	0.0253	187.5	226.2	21.5	466.0	45.0
80-3-15-17	0.0255	190.6	219.0	18.0	481.5	46.1
80-3-19-21	0.0254	182.0	219.5	22.5	460.4	44.6
80-3-23-25	0.0250	193.6	224.2	18.0	477.2	45.8
80-3-27-29	0.0253	187.5	216.4	20.0	477.2	45.8
80-3-31	0.0253	190.6	224.7	20.0	449.2	43.8
12-16-X	-	-	-	-	484.5	46.3
		B. Transverse Coupons				
T-1	0.041	209.0	240.5	14.0	-	-
T-2	0.041	213.7	253.7	14.0	-	-
T-3	0.041	224.6	232.2	16.0	-	-
T-4	0.041	209.0	240.5	14.0	-	-
T-6	0.026	199.0	232.0	12.5	-	-

TABLE 1 (Continued)

Specimen Number	Thickness (in)	F_{ty} (0.2% Offset) (ksi)	F_{tu} (ksi)	% Elongation	500-Gram Knoop Hardness Test: Knoop Hardness Number	500-Gram Knoop Hardness Test: Rockwell R_c
T-7	0.026	205.0	233.6	10.0	-	-
T-8	0.026	209.6	233.7	12.0	-	-
T-9	0.026	206.1	266.6	13.5	-	-
	C. Elevated Temperature, 400°F, Coupons					
L-4	0.041	197.5	209.0	3.0 (longitudinal)		-
T-5	0.041	187.5	215.5	3.5 (transverse)		-

Fatigue test data are presented in Figures 16 and 17 and in Tables 2 through 9 for the unnotched and notched specimens. A brief description of each specimen group and manufacturing process covered in the tables is as follows:

Table 2, unnotched specimen completely polished prior to testing, 0.041-inch-thick material.

Table 3, unnotched specimen polished prior to testing, 0.026-inch-thick material.

Table 4, notched specimen, 0.25-inch-diameter hole, glass bead peening to the following specifications: Almen N intensity of 0.004 to 0.006.

Table 5, notched specimen, 0.25-inch-diameter reamed hole, 0.026-inch-thick material.

Table 6, notched specimen 0.25-inch-diameter hole, various reamed holes, 0.026-inch-thick material.

Table 7, notched specimen, bonded together as a laminated pack, 0.25-inch-diameter hole, bored and honed, separated into specimens and tested without additional surface treatments; 0.026-inch-thick material. Figure 17 contains a comparison of fatigue life in relation to lamination location in the bonded pack.

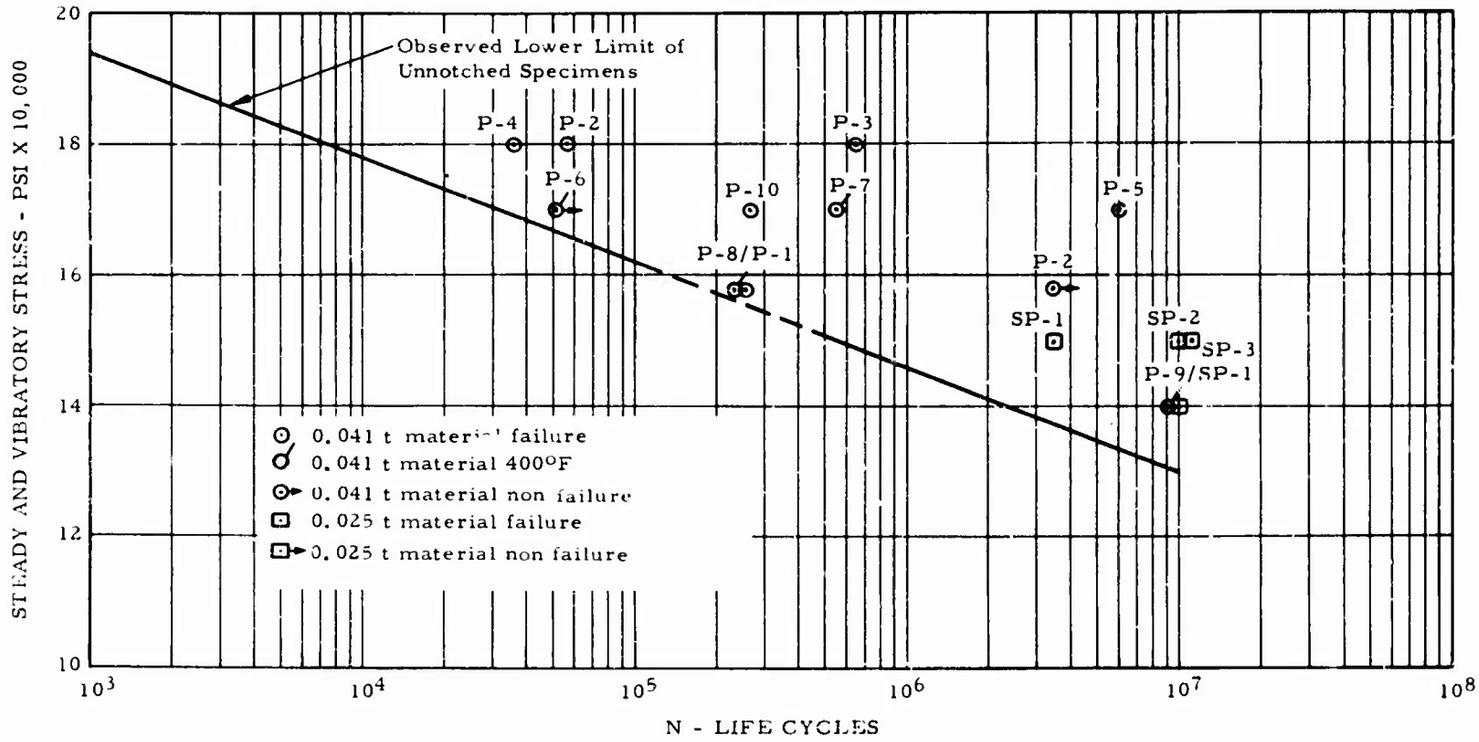

Figure 16. Materials Evaluation - Unnotched Fatigue Test S/N Data

Material AM 355 CRT
Hole Coupon Specimen

Mean Stress 80,000 psi
Vibratory Stress ±25,000 psi
Bond Pack Sample

Specimen bonded with adhesive
Hole drilled, reamed, and honed.
Sample then split apart. No additional treatment performed on holes.

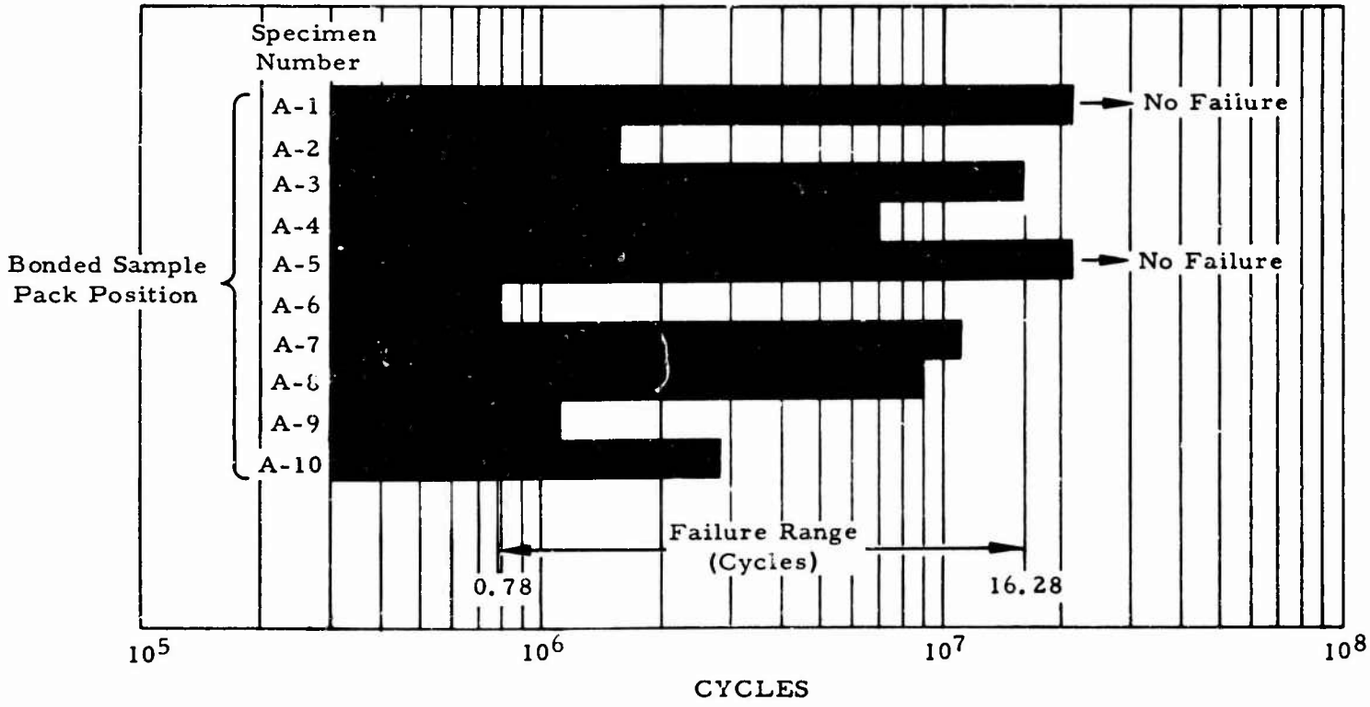

Figure 17. Materials Evaluation - Bonded Sample Failure Bar Graph

Table 8, notched specimen, 0.25-inch-diameter honed hole.

Table 9, notched specimen manufactured from material that had been stretched to 1-percent elongation to alleviate waviness and camber present in the AM 355 CRT strip stock. The specimen had a 0.25-inch-diameter hole, bored and honed.

TABLE 2
FATIGUE TEST - PLAIN AM 355 MATERIAL (0.041 INCH THICK)

Specimen Number	Treatment or Configuration	Material Thickness (in)	Stress Steady ± Cyclic (psi)	Total Cycles x 10^6	Temp
P-1	Unnotched specimen polished completely	0.041	80,000 ±78,000	0.254	Room
P-2	↓	↓	80,000 ±78,000	3.455	↓
P-2			94,500 ±85,500	0.055	
P-3			94,500 ±85,500	0.651	
P-4			94,500 ±85,500	0.036	
P-5			87,500 ±82,500	6.194	Room
P-6			87,500 ±82,500	0.051*	400°F
P-7			87,500 ±82,500	0.556	400°F
P-8			80,000 ±78,000	0.231	400°F
P-9	↓	↓	80,000 ±60,000	9.353	400°F
P-10	Unnotched specimen polished completely	0.041	87,500 ±82,500	0.263	Room

*Indicates invalid failure through thermocouple spotweld

TABLE 3
FATIGUE TEST - UNNOTCHED AM 355 MATERIAL (1/4-INCH-DIA HOLE)

Specimen Number	Treatment or Configuration	Material Thickness (in)	Stress Steady ± Cyclic (psi)	Total Cycles x 10^6	Temp
SP-1	Unnotched specimen polished completely	0.026	80,000 ±60,000	10.106	Room
SP-1	↓	↓	80,000 ±70,000	3.384	↓
SP-2			80,000 ±70,000	9.936	
SP-3	Unnotched specimen polished completely	0.026	80,000 ±70,000	11.242	Room

TABLE 4
FATIGUE TEST - NOTCHED AM 355 MATERIAL SHOT PEENED

Specimen Number	Treatment or Configuration	Material Thickness (in)	Stress PSI Steady ± Cyclic	Total Cycles x 10^6	Temp
GP-1	Notched 0. 25 in.-dia hole, glass bead peen	0. 041	80, 000 ±20, 000	4. 692	Room
GP-1	↓	↓	80, 000 ±30, 000	2. 441	↓
GP-2			60, 000 ±40, 000	10. 000	
GP-2			80, 000 ±40, 000	5. 364	
GP-3			80, 000 ±40, 000	0. 250	
GP-4			80, 000 ±40, 000	7. 727	Room
GP-5			80, 000 ±40, 000	0. 019	400°F
GP-6			80, 000 ±30, 000	10. 324	400°F
GP-6			80, 000 ±40, 000	4. 277	400°F
GP-7			80, 000 ±40, 000	0. 235*	400°F
GP-8			80, 000 ±40, 000	0. 202	400°F
GP-9	↓	↓	80, 000 ±40, 000	2. 362	400°F
GP-10	Notched 0. 25-in -dia hole, glass bead peen	0. 041	80, 000 ±40, 000	1. 515	400°F

*Indicates invalid failure through alignment hole.

TABLE 5
FATIGUE TEST - NOTCHED AM 355 MATERIAL (0. 025 INCH THICK)

Specimen Number	Treatment or Configuration	Material Thickness (in)	Stress Steady ± Cyclic (psi)	Total Cycles x 10^6	Temp
R-1	Notched 0. 25-in -dia hole, reamed	0. 026	80, 000 ±25, 000	0. 082	Room
R-2	↓	↓	↓	0. 050	↓
R-3				0. 050	
R-4				0. 131	
R-5	↓	↓	↓	0. 096	↓
R-6	Notched 0. 25-in -dia hole, reamed	0. 026	80, 000 ±25, 000	0. 136	Room

TABLE 6
FATIGUE TEST - NOTCHED AM 355 MATERIAL
(1/4-INCH-DIA, 0.025 THICKNESS)

Specimen Number	Treatment or Configuration	Material Thickness (in)	Stress Steady ± Cyclic (psi)	Total Cycles x 10^6	Temp
M-1	Notched 0.25 in -dia hole, mfg defects	0.026	80,000 ±30,000	0.355	Room
M-2			80,000 ±40,000	0.056	
M-3			80,000 ±40,000	0.073	
M-4			80,000 ±25,000	11.090	
M-5				10.839	
M-6				10.696	
M-7				1.209	
M-8				6.918	
M-9				12.116	
M-10	Notched 0.25-in -dia hole, mfg defects	0.026	80,000 ±25,000	10.297	Room

TABLE 7
FATIGUE TEST - NOTCHED AM 355 MATERIAL
(1/4-INCH-DIA, REAMED)

Specimen Number	Treatment or Configuration	Material Thickness (in)	Stress Steady ± Cyclic (psi)	Total Cycles x 10^6	Temp
B-1	Notched specimen, bonded; 0.25-in -dia hole; bored, separated into specimens	0.026	80,000 ±25,000	14.499	Room
B-2				1.582	
B-3				16.278	
B-4				6.874	
B-5				13.054	
B-6				0.776	
B-7				11.164	
B-8				8.874	
B-9				1.123	
B-10	Notched specimen bonded; 0.25 in -dia hole; bored, separated into specimens	0.026	80,000 ±25,000	2.838	Room

TABLE 8
FATIGUE TEST - NOTCHED AM 355 MATERIAL
(BONDED, SEPARATED)

Specimen Number	Treatment or Configuration	Material Thickness (in)	Stress Steady ± Cyclic (psi)	Total Cycles x 10^6	Temp
HH-1	Notched, 0.25-in dia hole, honed	0.041	39,700 ±38,800	0.060*	Room
HH-2	↓	↓	39,700 ±38,800	10.951	↓
HH-2			43,500 ±41,000	15.351	
HH-2			47,000 ±42,500	5.776	
HH-3			80,000 ±78,000	0.060	Room
HH-4			80,000 ±78,000	0.009	400°F
HH-5			80,000 ±40,000	0.037	Room
HH-6			80,000 ±40,000	0.028	400°F
HH-7			10,000 ±40,000	10.267	Room
HH-7	Notched, 0.25-in dia hole, honed	0.041	80,000 ±40,000	0.030	400°F

*Indicates invalid failure through retention pad.

TABLE 9
FATIGUE TEST - NOTCHED AM 355 MATERIAL
(1/4-INCH-DIA STRETCHED)

Specimen Number	Treatment or Configuration	Material Thickness (in)	Stress Steady ± Cyclic (psi)	Total Cycles x 10^6	Temp
SM-1	Notched 0.25-in -dia hole, stretched mat'l and honed	0.026	80,000 ±25,000	0.075	Room
SM-2	↓	0.026	80,000 ±25,000	0.070	Room
SM-3	Notched 0.25-in -dia hole, stretched mat'l and honed	0.026	80,000 ±25,000	0.234	Room

THERMAL CONDUCTIVITY

SUBJECT

This testing concerned limited medium to high temperature evaluation of various structural materials used in the XV-9A rotor blade spars. Tests were conducted in the HTC-AD structures test laboratory in June 1963.

PURPOSE

The purpose of this test was to establish heat transfer coefficients for various materials used in the XV-9A rotor system.

TEST SPECIMENS

Laminated Sample

This sample consisted of fifteen laminations of AM 355 CRT 0. 025-inch sheet strip bonded together with a high temperature adhesive. Dimensions of the sample were as follows: width = 1. 56 in , length = 4. 56 in , final thickness after bonding = 0. 448 in (glue line average thickness = 0. 004 in), area = 7. 02 sq in , volume = 3. 145 cu in.

Composite Sample

This sample was manufactured from a high temperature adhesive that is an epoxy-phenolic, aluminum filled, and fiber glass backed composite material. This sample consisted of laminations of fiber glass and filler laid up to an approximate 0. 30-inch thickness. Dimensions of the sample were as follows: width = 1. 59 in , length = 4. 55 in , thickness = 0. 293 in , area = 7. 23 sq in. , volume = 2. 118 cu in.

Titanium Sample (AMS 4928-6 Al-4V Ti)

This sample was cut from a previous fatigue test specimen blade spar. Dimensions of the sample were as follows: width = 1. 60 in , length = 4. 36 in , thickness = 0. 448 in , area = 6. 97 sq in , volume = 3. 123 cu in.

Solid AM 355 Sample (AMS 5743)

This sample was cut from an equalized and oven tempered AM 355 round bar stock. It was heat treated to the proper mechanical and physical properties (R_C hardness 38 - 43). Dimensions of the sample were as follows: diameter = 2.25 in , thickness = 0.441 in , area = 3.974 sq in , volume = 1.753 cu in.

TEST SETUP AND INSTRUMENTATION

A 0.375-inch-thick, 9-x 10-inch aluminum plate was set up to act as a heat transfer media. One side was coated with lamp black to readily absorb the radiated heat. Approximately 6 inches below the surface of this aluminum plate, a 9-inch quartz lamp assembly was set up as the primary heat source. The temperature of the plate was monitored by two iron-constantan thermocouples spotwelded to the top surface of the plate. The heat generated by the quartz lamps was controlled by a transformer and monitored by the upper surface aluminum plate thermocouples.

Each specimen was set up in an asbestos block to prevent heat conduction through the edges.

Time was monitored by a second-counting electric clock that has an independent start/stop system.

Temperatures were monitored through a galvanometer, with readings recorded in millivolts.

Each sample had an iron-constantan thermocouple spotwelded at the geometric center on both upper and lower surfaces, except the bonding material sample, which had to depend on surface contact.

The aluminum plate was notched to allow the samples to maintain full contact with the aluminum plate and provide access for the thermocouple lead wire on the bottom.

TEST PROCEDURE

The temperature of the plate was stabilized at the desired test level and each specimen in turn was placed on the aluminum plate. The timer was started at the instant of full contact of the specimen with

the hot plate. Temperature readings were taken at 30-second intervals until each specimen's temperature stabilized. The aluminum plate was monitored at frequent intervals to ensure that the proper test temperature was maintained.

Each sample, in turn, was tested by the preceding method, with plate temperatures stabilized at 100°, 200°, 300°, 400°, 500°, and 600° F intervals.

TEST RESULTS

Heat transfer data were recorded, and are presented in time-versus-temperature plots for each of the four materials tested. Figures 18 through 21 show these data.

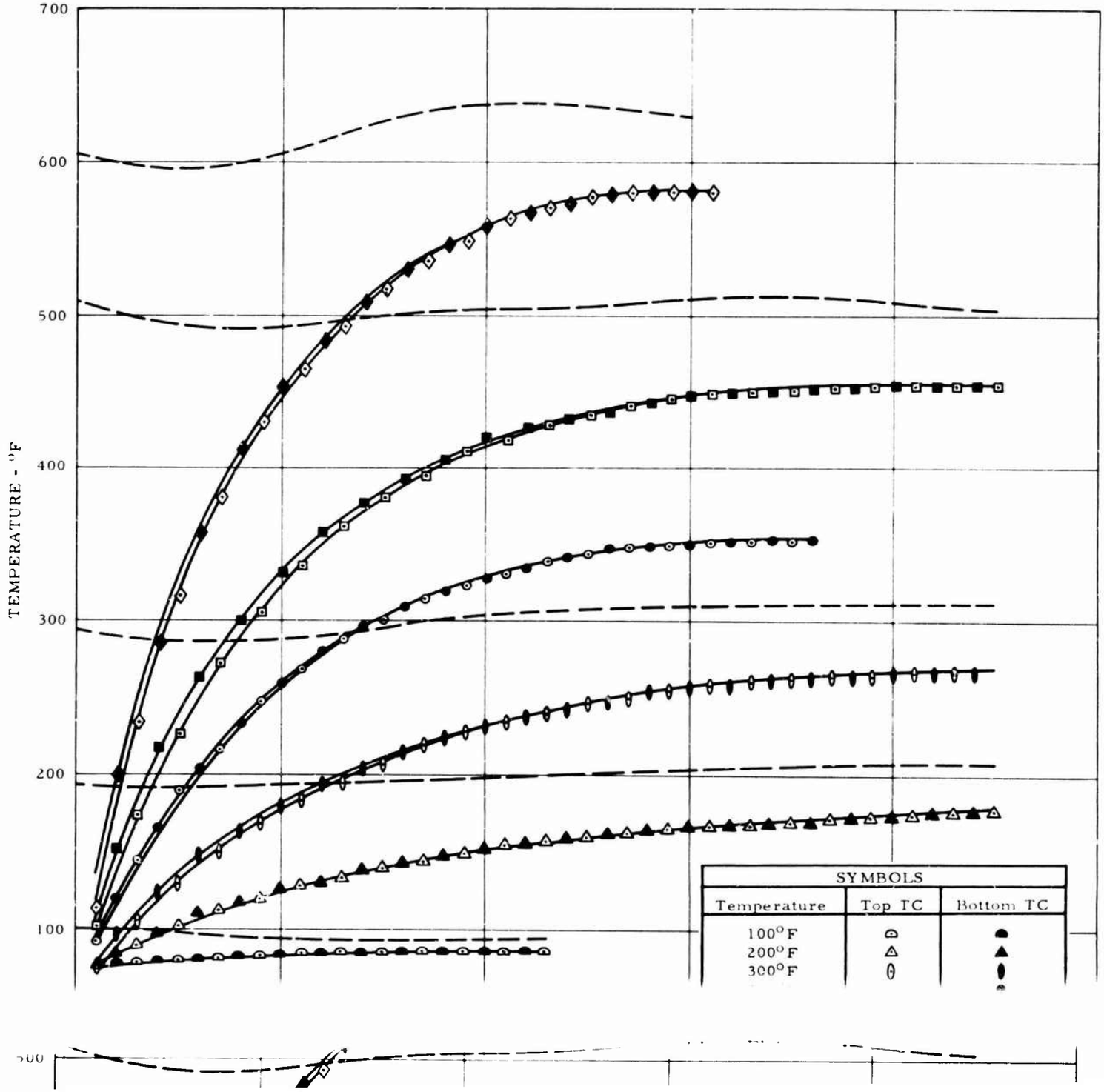
700
600
500
400
300
200
100
TEMPERATURE - °F
SYMBOLS
Temperature
Top TC
Bottom TC
100°F
200°F
300°F

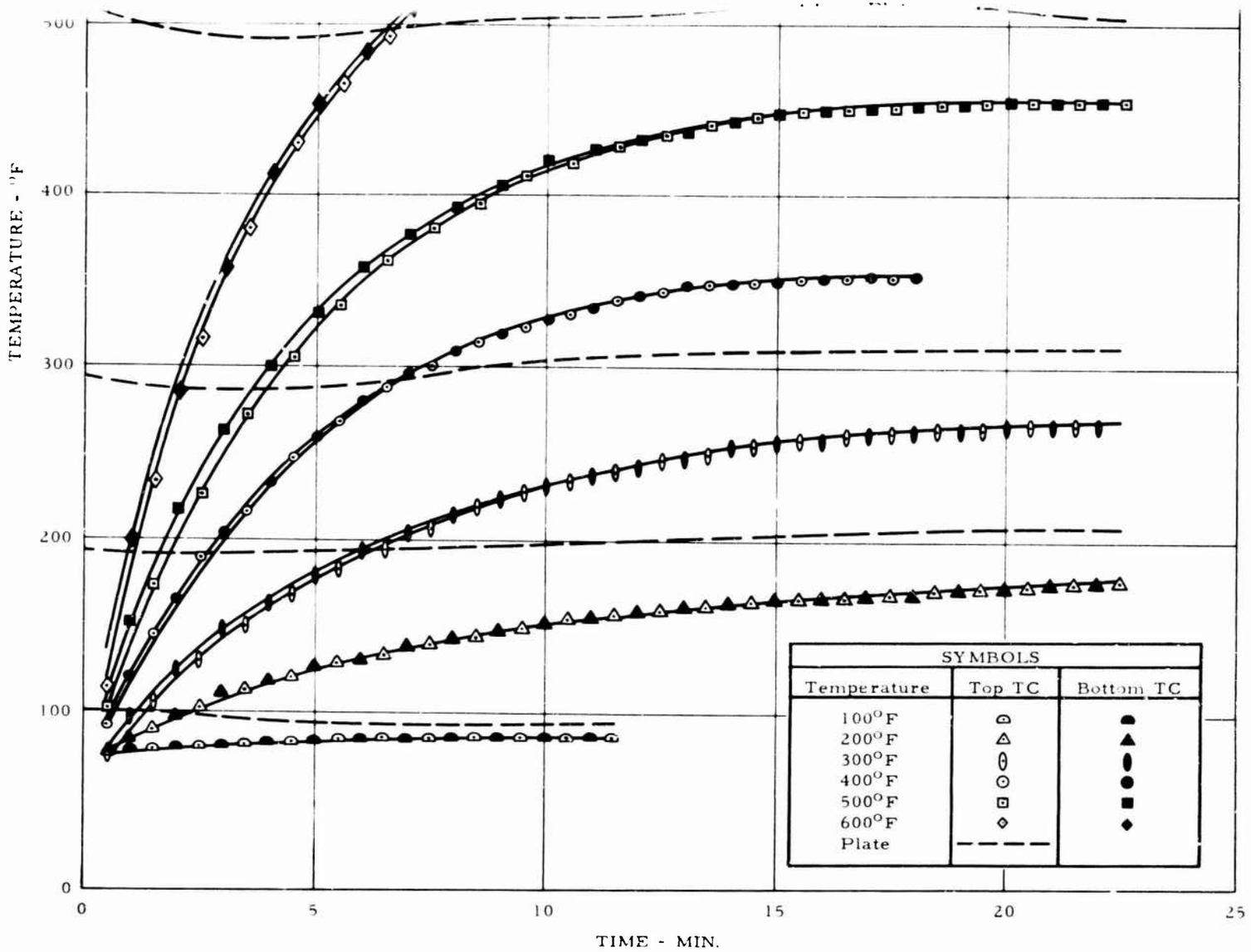

Figure 18. Material Evaluation - Heat Transfer Data - AM 355.

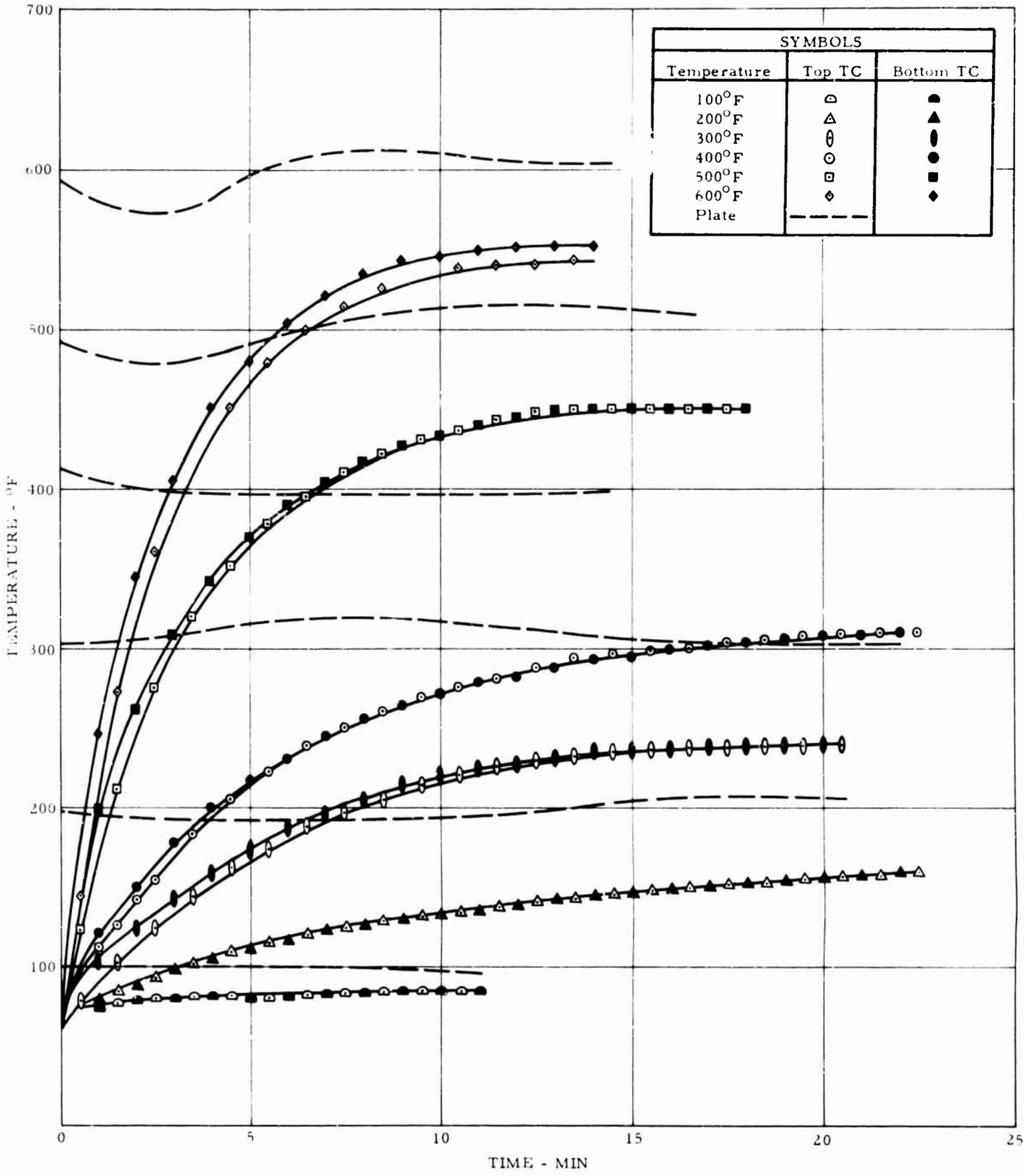

Figure 19. Material Evaluation - Heat Transfer Data - Titanium.

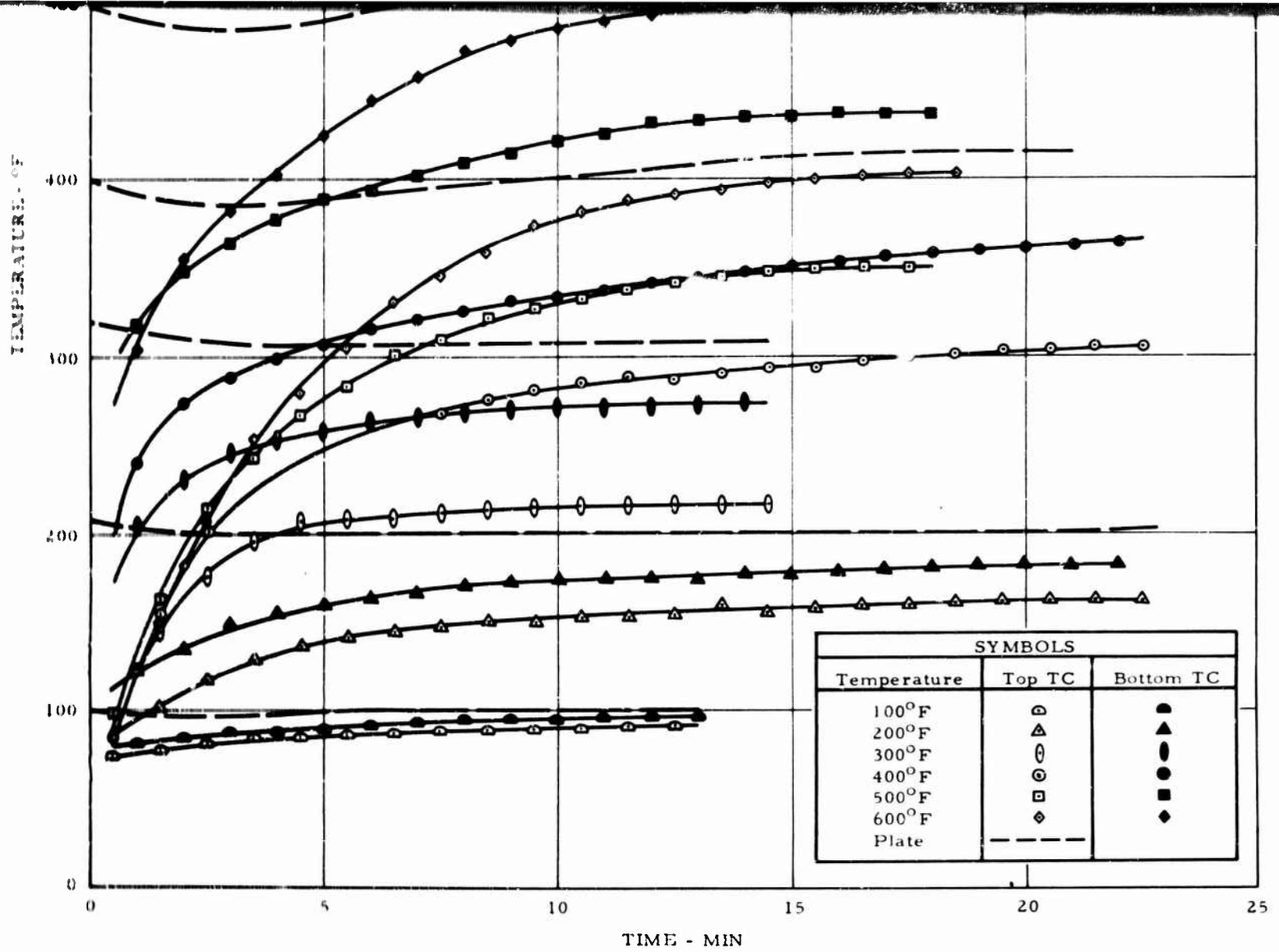

Figure 20. Material Evaluation - Heat Transfer Data - Bonded Specimen.

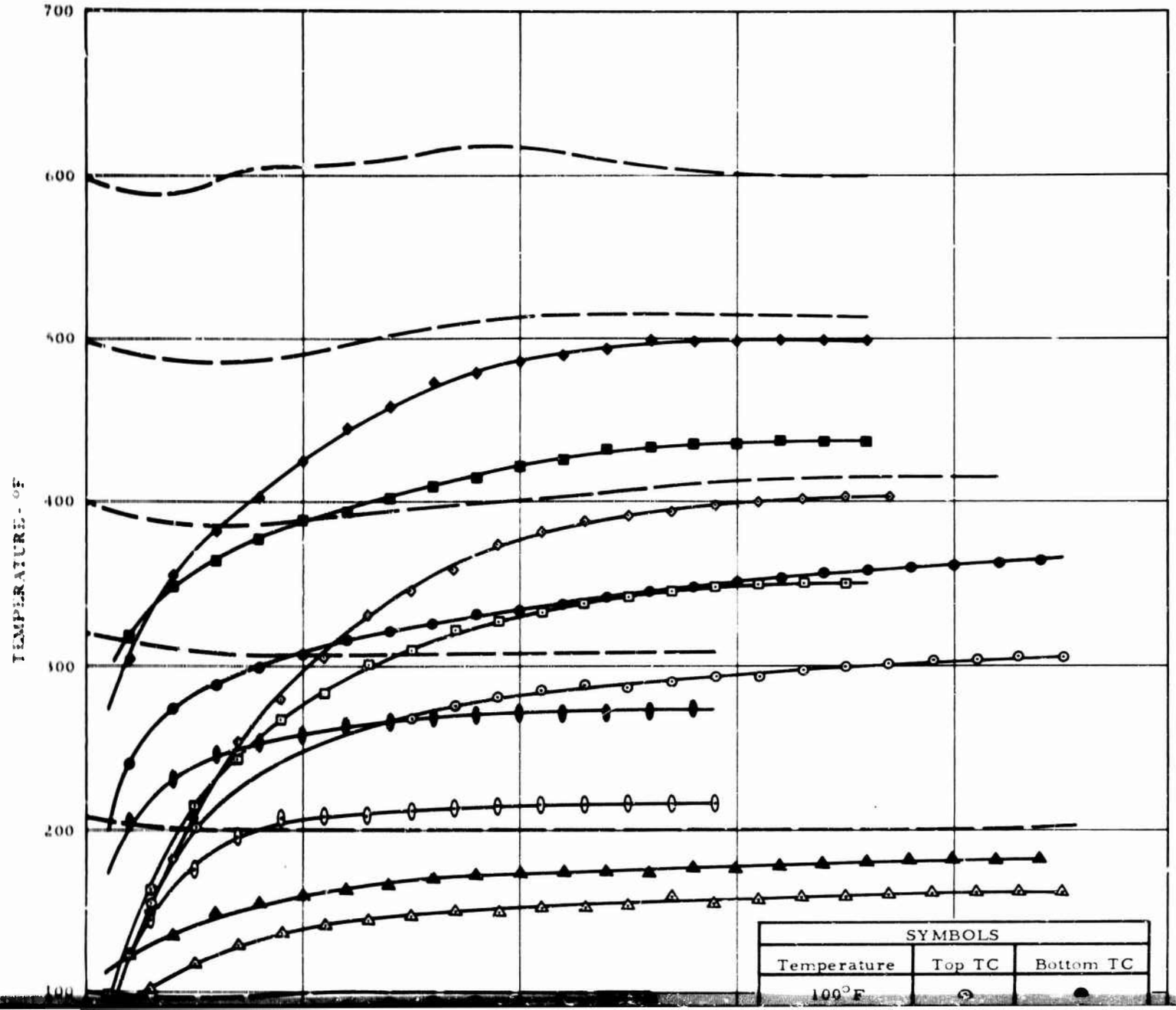
700
600
500
400
300
200
100
TEMPERATURE - °F
SYMBOLS
Temperature
Top TC
Bottom TC
100°F

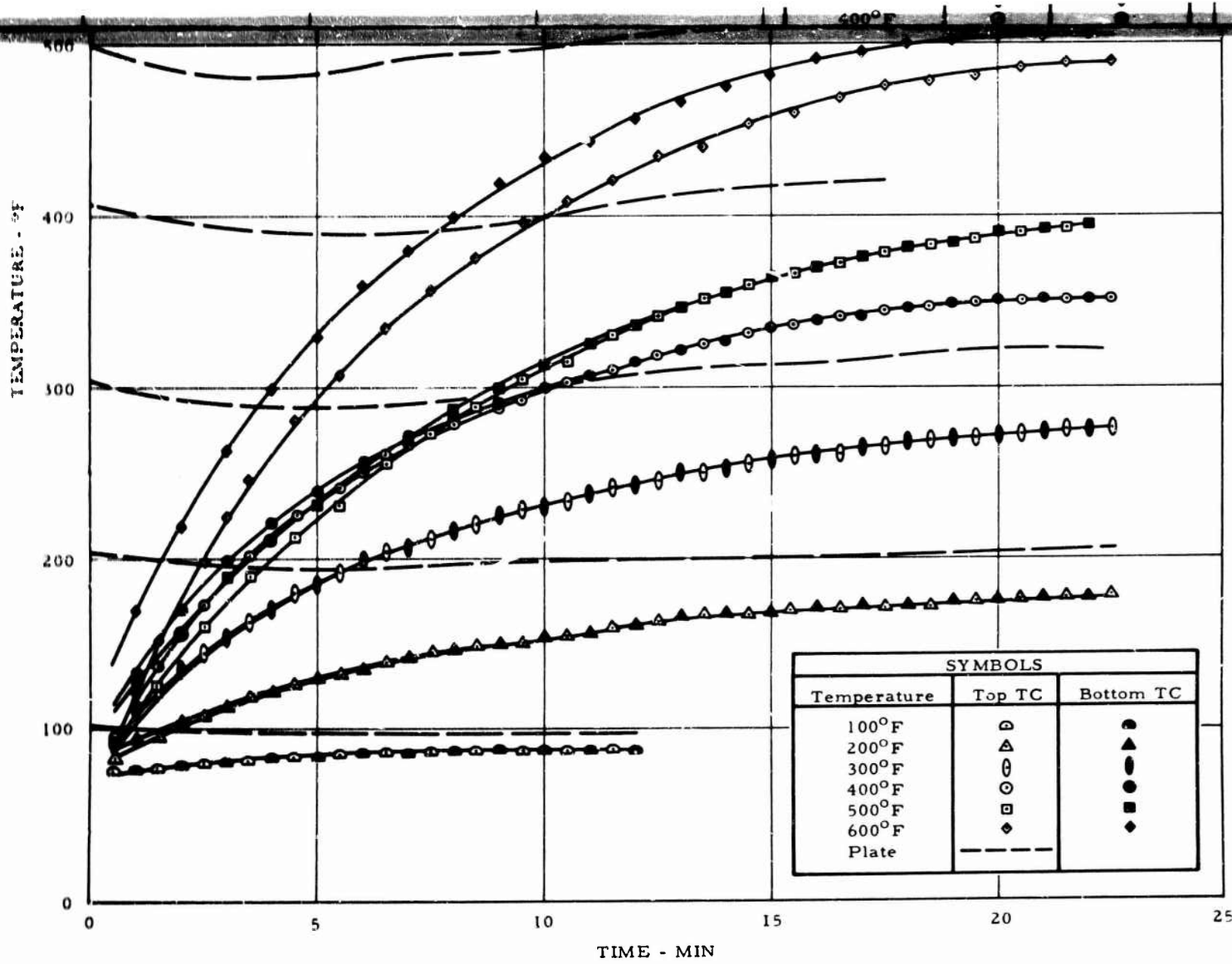

Figure 21. Material Evaluation - Heat Transfer Data - Laminated Specimen.

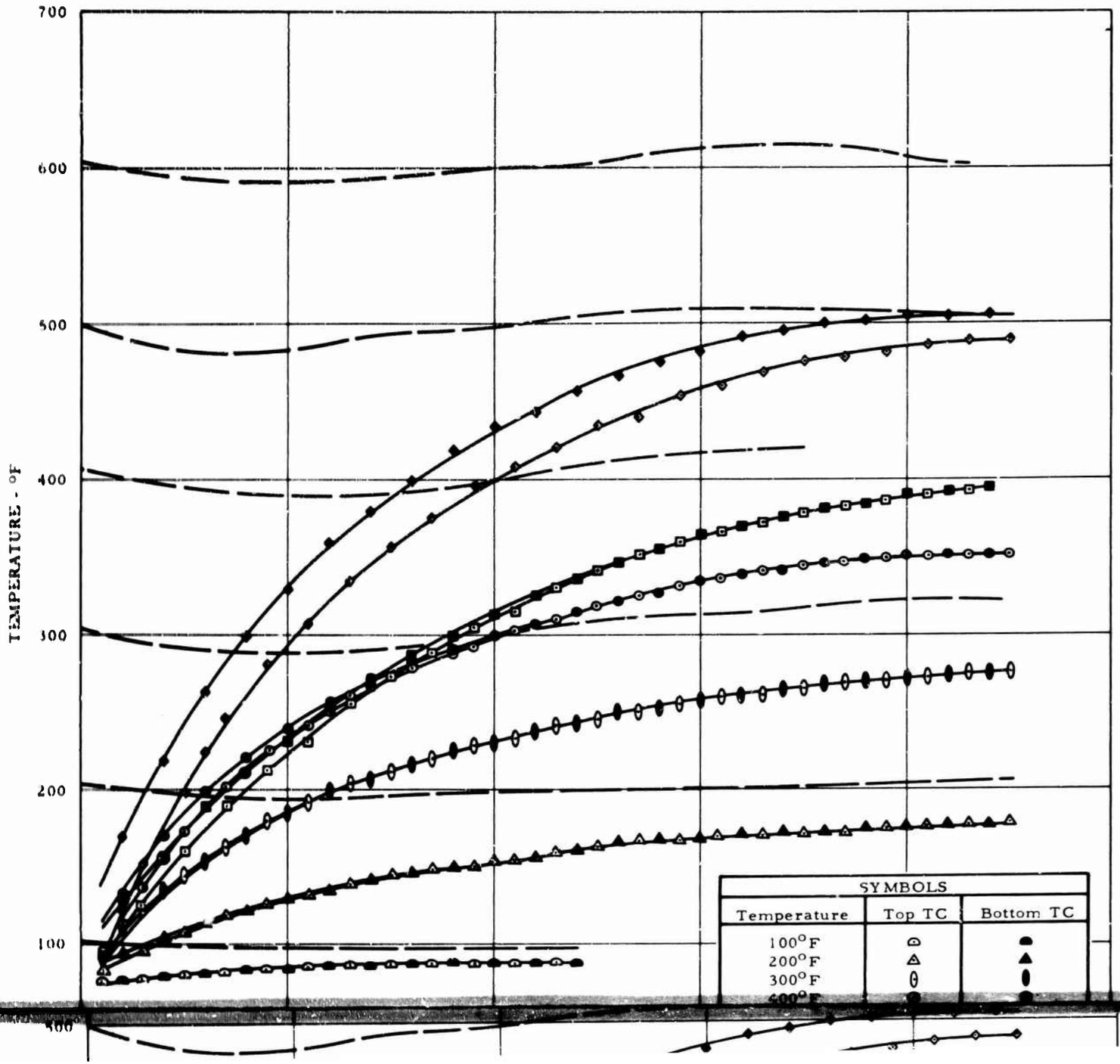
700
600
500
400
300
200
100
TEMPERATURE - °F
SYMBOLS
Temperature
Top TC
Bottom TC
100°F
200°F
300°F
400°F

FATIGUE TEST OF SPAR MATERIAL WITH HOT GAS IMPINGEMENT

SUBJECT

This test concerned high temperature fatigue strength of the rotor blade spar material subjected to hot gas impingement. It was conducted in the AD structures test laboratory in April 1964.

PURPOSE

The purpose of this test was to substantiate that the rotor blade spar design will withstand hot gas impingement from a ruptured duct for a sufficient period of time to ensure a safe landing of the aircraft.

SUMMARY OF RESULTS

The test specimen successfully completed a 2.3-hour test at 1050°F for a total of 33,130 load cycles, operating at 4 cps (design rotor rpm).

TEST SPECIMEN

The test specimen simulated a section of the rear laminated rotor blade spar, duplicating the thickness at blade station 169.0. The material was AM 355 CRT sheet, bonded together with a high-temperature adhesive.

A sketch of the laminated spar section is shown in Figure 22. Shielding consisted of 0.005-in aliron; 0.012-in type 301 stainless steel, duplicating the sheet metal blade segment construction; and 0.010-in teflon-impregnated fiber glass sheet used as an antifretting material.

TEST SETUP

The specimen and shield were set up in a simple hydraulic axial loading system designed to apply steady and vibratory loads to the specimen. The loads were derived from the centrifugal force, cyclic chordwise moment, and steady and cyclic flapwise moments encountered on the spar at blade station 169. Based on the nominal thickness of the spar lamina and the measured width of the machined specimen, the steady and cyclic stresses applied to the test specimen were 72,980 ±17,870 psi. Figures 23 and 24 show the specimen assembly and the general test setup.

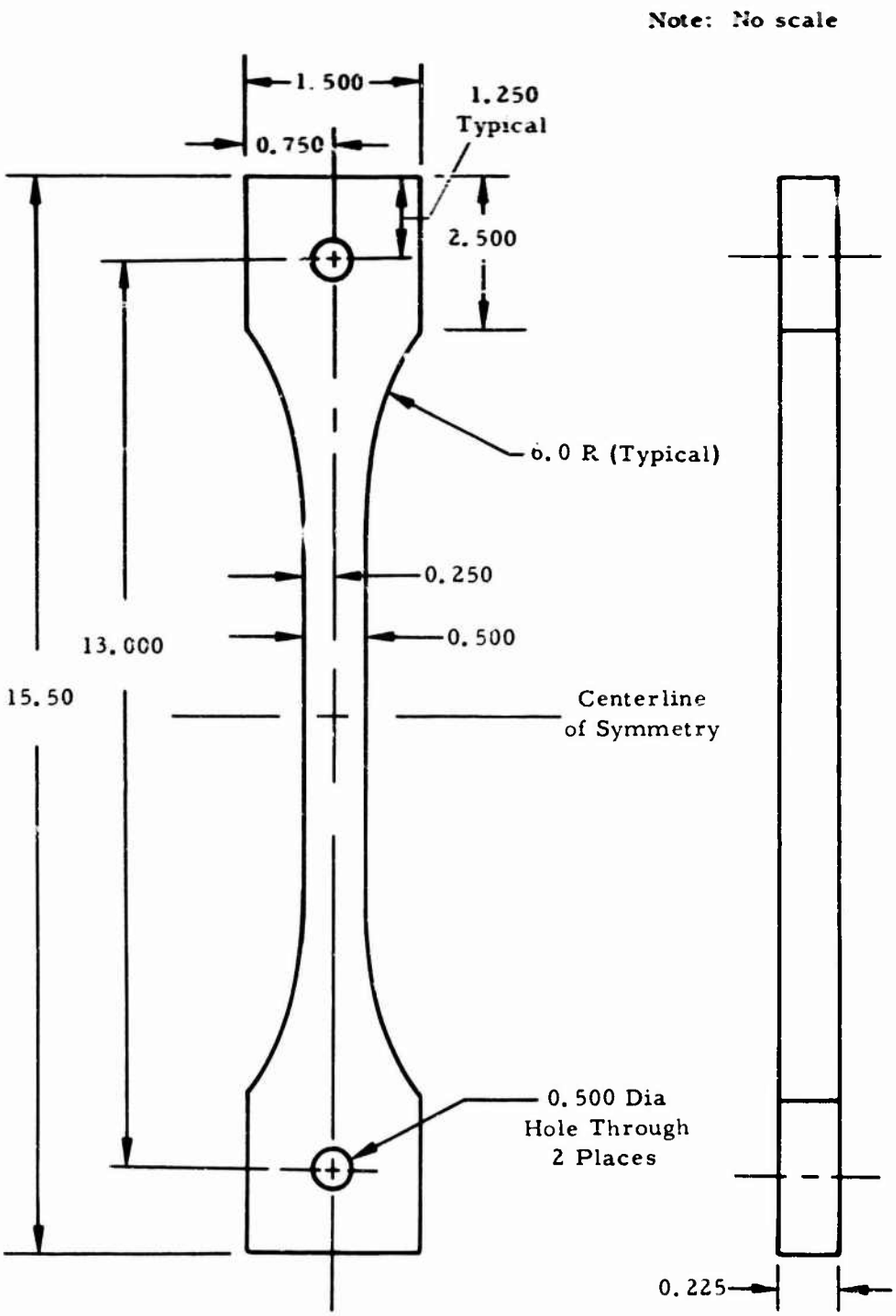

Material: AM 355 CRT Strip
Bonded With Adhesive

Figure 22. Fatigue Test of Spar Material With Hot Gas Impingement - Test Specimen.

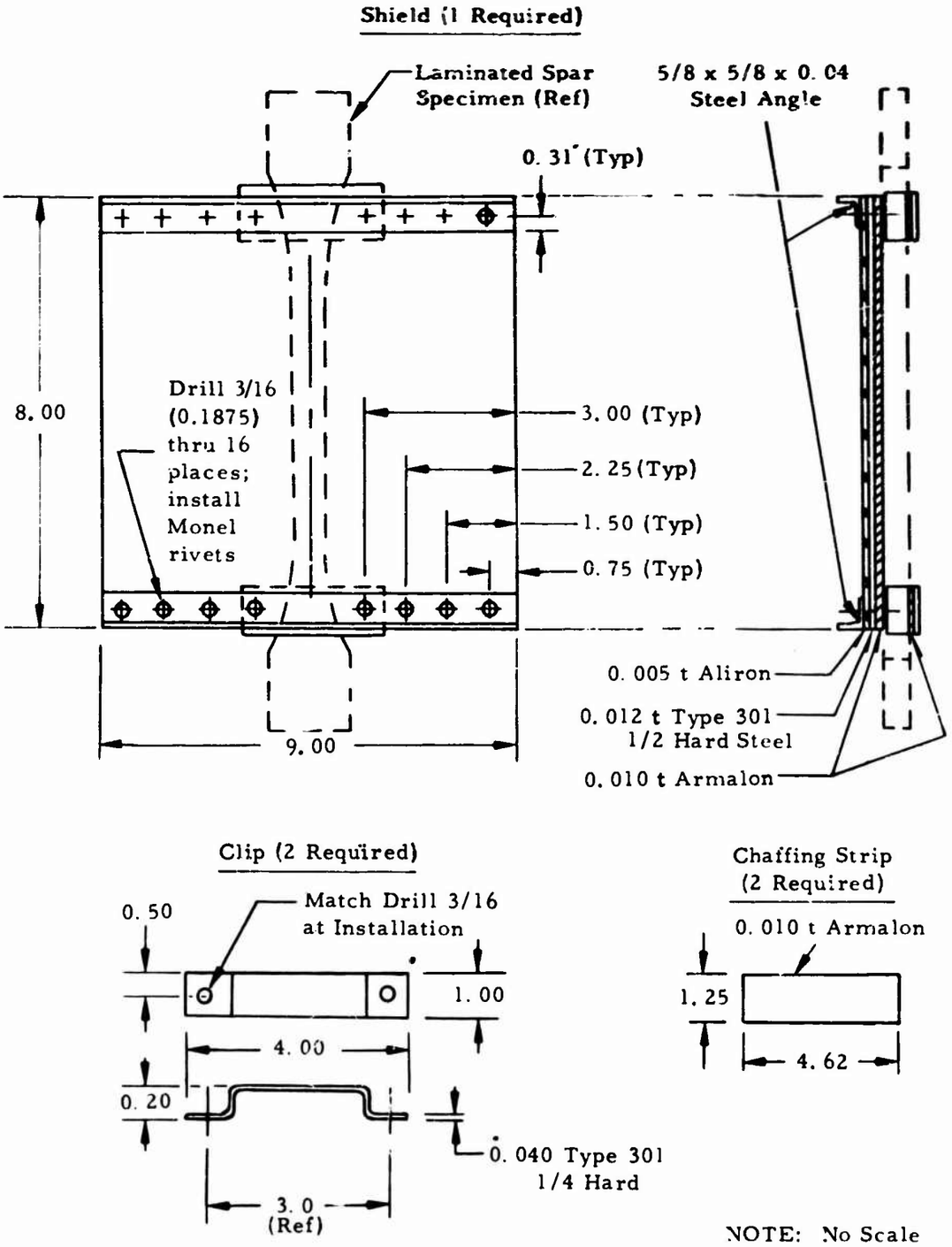

Figure 23. Fatigue Test of Spar Material With Hot Gas Impingement - Test Specimen Assembly.

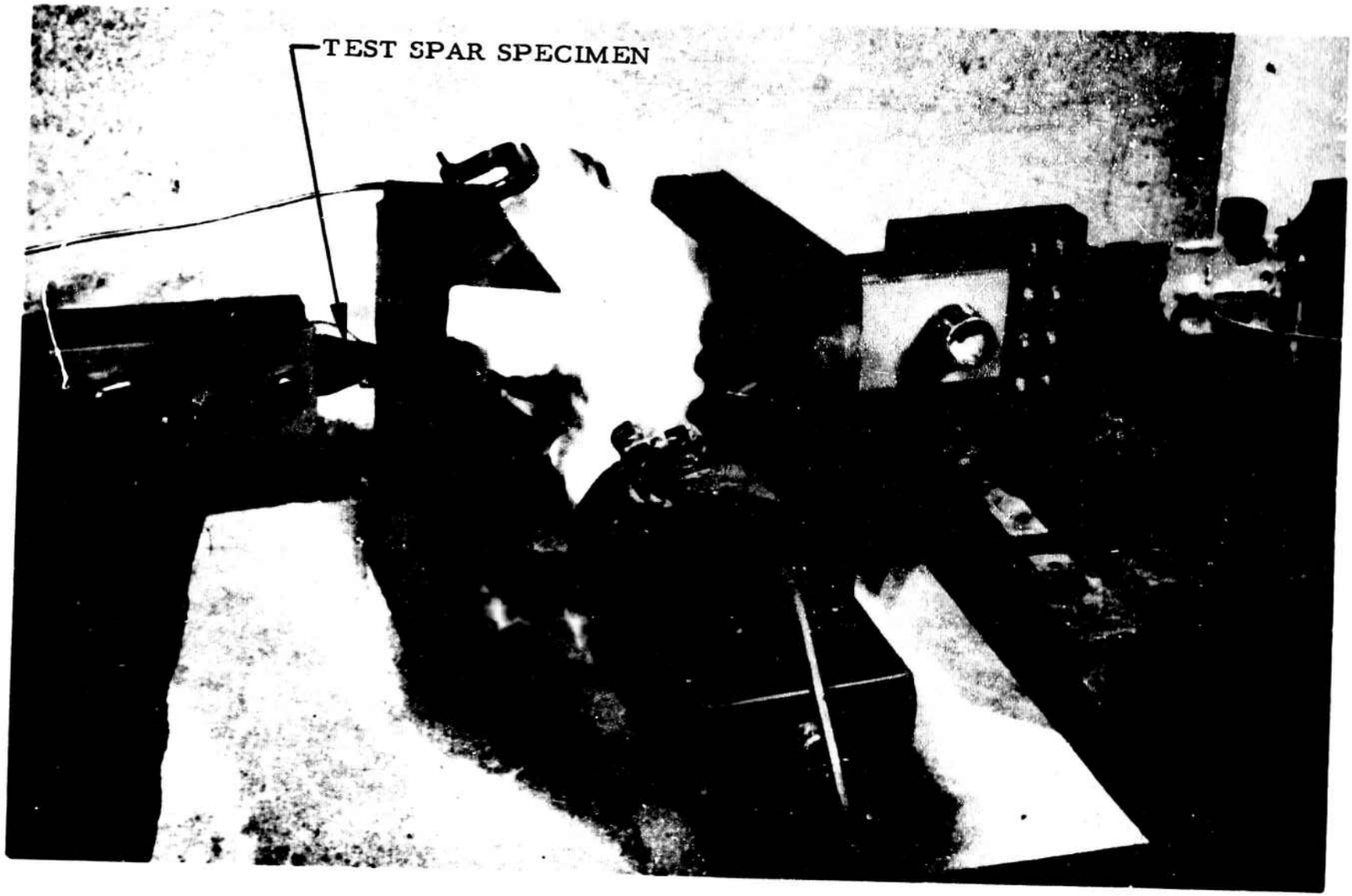

Figure 24. Fatigue Test of Spar Material With Hot Gas Impingement - Test Operation.

The heat source was provided by a 4.0-inch-diameter blowtorch impinging on the aliron shield.

INSTRUMENTATION

LOAD MEASUREMENTS

The steady load was monitored by an SR-4 strain indicator from an axial bridge circuit installed on a load cell link that had been calibrated for known loads. The vibratory load was monitored through the same link, but was connected to a dynagraph (oscillograph) to record the dynamic loads. A cycle counter was placed in series with the hydraulic cylinder to record the load cycles.

TEMPERATURE MEASUREMENTS

The temperatures were recorded and monitored by two iron-constantan thermocouples. One thermocouple was placed in the geometric center of the aliron shield, 0.25 inch from the shield in the stream of hot gas and flame. This thermocouple was connected to a continuous recording potentiometer. The second thermocouple was installed on the outermost lamina of the pack, the side opposite the flame. This thermocouple was connected to the dynagraph, and recorded continuously throughout the test.

TEST PROCEDURE

The steady load on the specimen was hydraulically applied and recorded with an SR-4 strain indicator. The cyclic load was monitored on the dynagraph. The blowtorch was adjusted to bring the aliron shield thermocouple to the operating temperature of 1050°F. A record was maintained of both time and cycles from the counter, and the test was monitored for 2 hours.

TEST RESULTS

The specimen successfully completed a 2.3-hour fatigue test at 1050°F gas temperature. Load cycles on the specimen totaled 33,130. The average temperature recorded on the outermost lamina of the bonded pack was 385°F. The steady and cyclic loading maintained during the test was +8210 ±2010 pounds.

The condition of the test specimen after completion of the test was as follows:

Aliron shield:	Discoloration and warpage of the thin sheet.
Armalon sheet:	In the top area, teflon material dissipated, leaving fiber glass support material flaking and brittle.
Laminated spar section:	No visible damage; the lamination still remained as a unit. No visible damage to the adhesive. The specimen was disassembled after test.

STATIC TESTS OF MISCELLANEOUS FITTINGS

ROTOR BLADE SPAR BUCKLING TEST

SUBJECT

These tests concerned static uniform bending strength of a two-segment portion of the XV-9A blade constant section. They were conducted at the HTC-AD structures test laboratory between February and April 1963.

PURPOSE

The purpose of these tests was to determine the structural adequacy of various unbonded and bonded laminated front and rear spar configurations.

SUMMARY OF RESULTS

The bonded front and rear spar configuration utilizing adhesive successfully withstood 117,000 inch-pounds of flapwise bending moment (2.78 g) without any visible signs of buckling.

TEST SPECIMEN

Description

The specimen simulated a two-segment portion of the XV-9A blade constant section at station 90 (HTC-AD drawing 385-9601). The front and rear spars consisted of AM 355 CRT stainless steel laminations. The adhesive used in the bonded spar configurations was a high temperature, aluminum filled, fiber glass reinforced, epoxy-phenolic resin.

Configuration

Specimen 1

This specimen consisted of unbonded spar laminations. The rear spar was reinforced by a hat section that was riveted to the trailing edge segment and bore against the lower edge of the rear spar. The front spar was reinforced by a 0.25-inch steel plate and was secured to the face of the spar by the spar-to-segment attachment bolts.

Specimen 2

This specimen was similar to specimen 1, except that the rear spar was reinforced by a channel and bracket clips that were secured to the face of the spar by the spar-to-segment attachment bolts. The front spar was reinforced with 0.44-inch steel plate with overlapping channel brackets.

Specimen 3

The specimen was fabricated using bonded laminated spars and included the reinforcing devices of specimen 2.

Specimen 4

This specimen was similar to specimen 3 with all reinforcing devices removed.

TEST SETUP AND PROCEDURE

Each specimen configuration was installed in a test fixture designed to apply a uniform flapwise bending moment to the specimen. A 400,000-pound test machine was used to apply the loads. A schematic of the test setup is shown in Figure 25.

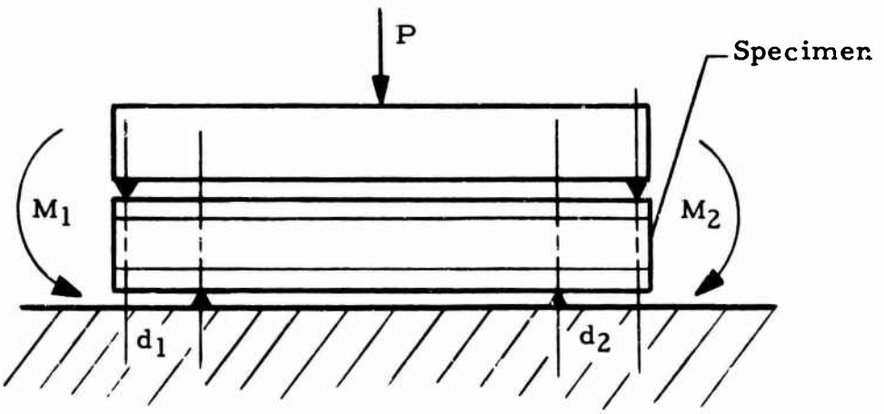

P = vertical load produced by test machine; $d_1 = d_2$; therefore, $M_1 = M_2$; $M = 1/2\ Pd$

Figure 25. Spar Buckling Test Loading Schematic.

Dial gages were mounted on the front and rear spars and measured the deflections of the spars during each test. Loads were applied in increments in order to observe the deflections of the front and rear spars. Figure 26 shows the bending moment versus blade span for a 1-g load condition. Figure 27 shows the test setup.

TEST RESULTS

Specimen 1

The front and rear spar buckled at 37, 800-inch-pound bending moment, 0. 90 g. Figure 28 shows the deflections of the front and rear spar.

Specimen 2

The front and rear spar buckled at 48, 000-inch-pound bending moment, 1. 14 g. Figure 29 shows the deflections of the front and rear spar.

Specimen 3

This specimen was loaded to 102, 000-inch-pound bending moment, 2. 42 g, without any visible signs of buckling. Figure 30 shows the deflections of the front and rear spar.

Specimen 4

This specimen was loaded to 117, 000-inch-pound bending moment, 2. 78 g, without any visible signs of buckling. Figure 31 shows the deflections of the front and rear spar.

ROTOR BLADE REAR SPAR PROOF LOAD TEST

SUBJECT

This test concerned a proof load test of the full length XV-9A bonded laminated rotor-blade rear spars. This test was conducted in October 1963 at the manufacturing facility.

PURPOSE

The purpose of this test was to ensure the structural integrity of the bonded rear spar laminations under a simulated 2. 5-g bending moment.

SUMMARY OF RESULTS

The bonded rear spars successfully withstood the 2. 5-g loading condition with no ill effects.

TEST SPECIMEN

The test specimen consisted of two laminated blade rear spars (HTC-AD drawing 385-1108) bolted to a wood beam shear web.

TEST SETUP AND PROCEDURE

The test specimen was mounted in a fixture at the inboard end of the spars and at blade station 73. 0. The specimen was subjected to cantilever loading at three spanwise blade stations: 140, 240, and 300.

Test loads applied were for a 2. 5-g ground flapping condition, shown in Figure 32. The loads were applied at the three stations by means of weight pans and weight bars. Tip deflections were measured at each incremental loading. The setup is shown in Figure 33.

Test Results

The bonded rear spar successfully withstood the 2. 5-g loading condition. The following table gives the tip deflections recorded.

TABLE 10
ROTOR BLADE SPAR PROOF TEST - TIP DEFLECTION

Station 140 Load (lb)	Station 240 Load (lb)	Station 300 Load (lb)	Spar Moment (in -lb)	Deflection (in)	g
16	153	24	49, 000	23. 0	1. 11
59	253	57	73, 600	37. 0	1. 67
102	353	90	98, 000	50. 0	2. 22
124	402	107	110, 400	58. 0	2. 50

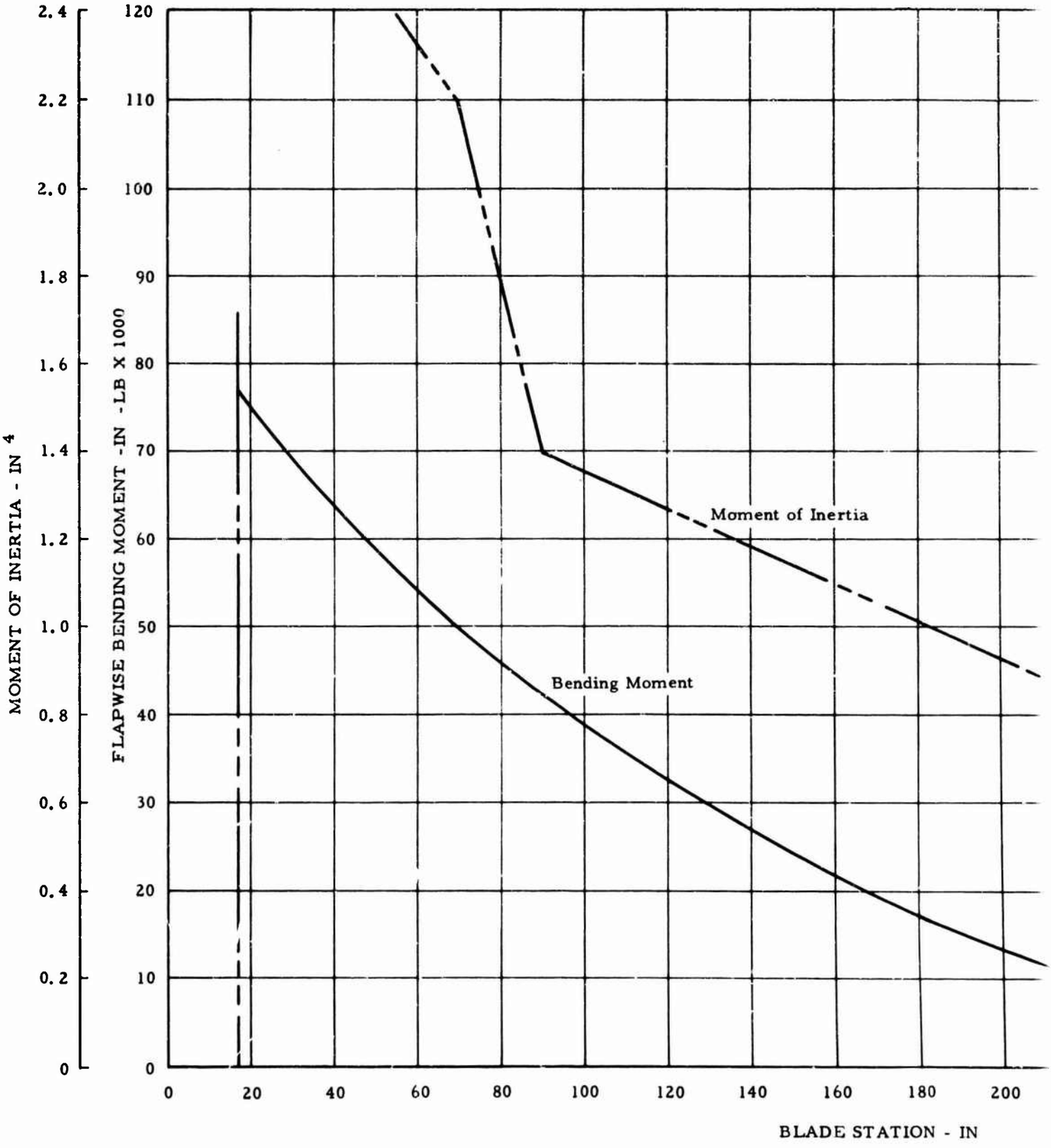

Figure 26. Spar Buckling Test - Blade Bending Mome
1-g Loading on Blade.

A

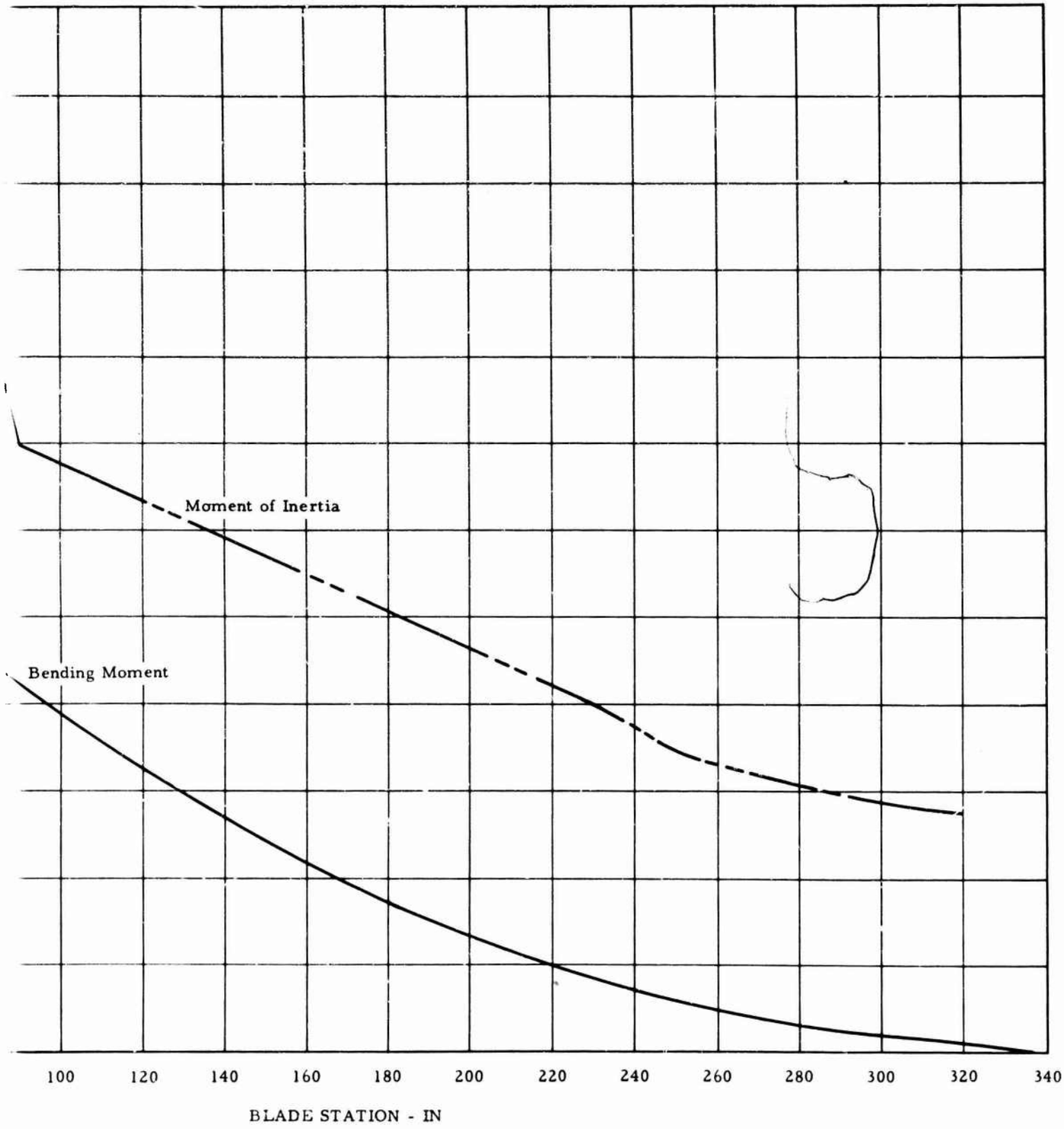

Spar Buckling Test - Blade Bending Moment Distribution - 1-g Loading on Blade.

B

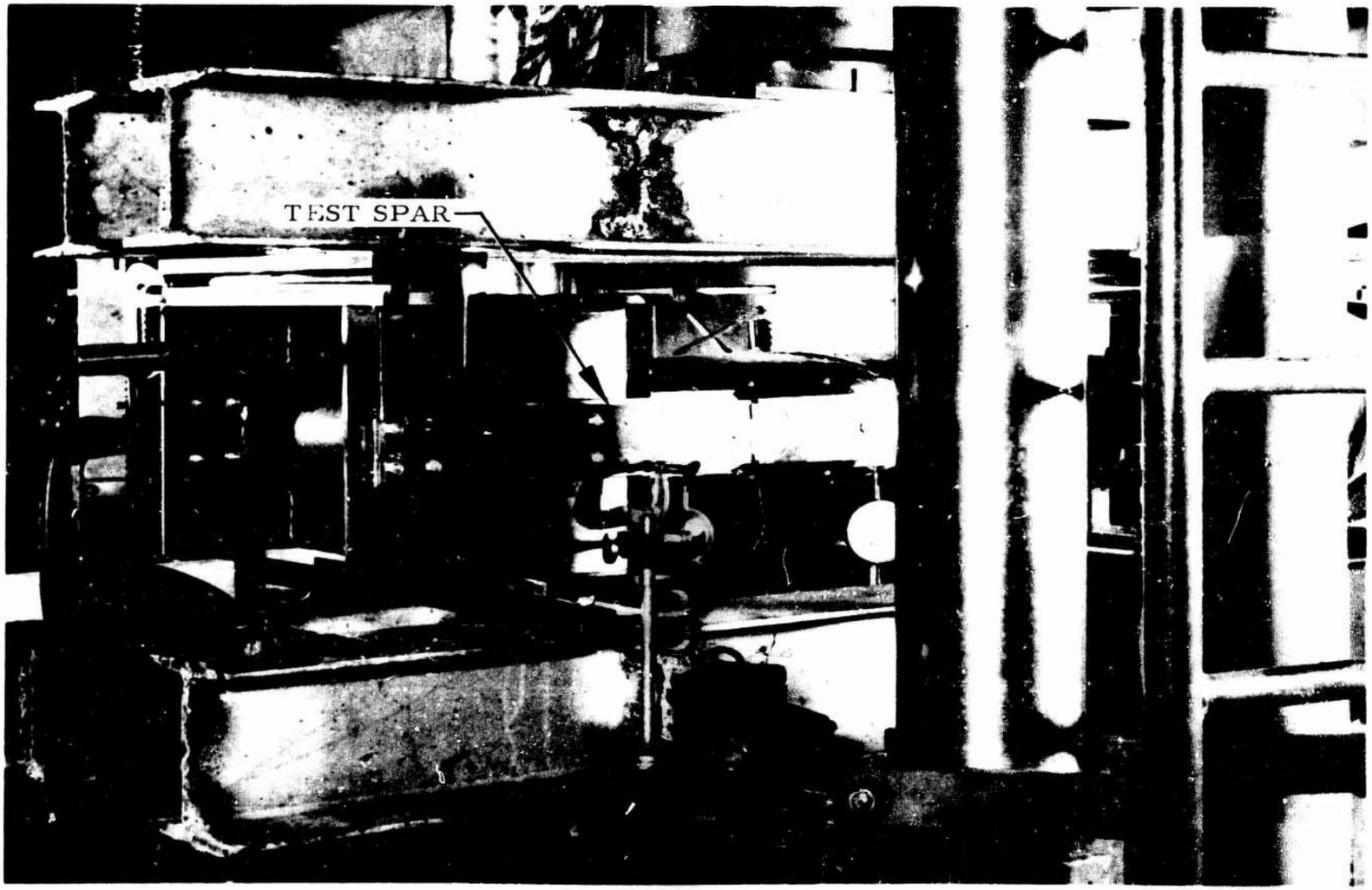

Figure 27. Spar Buckling Test - General Test Setup.

Laminated Spar Buckling Configuration;
Unbonded Spar, Clips, Hat Section, and 0.25-Inch Block
Test 1

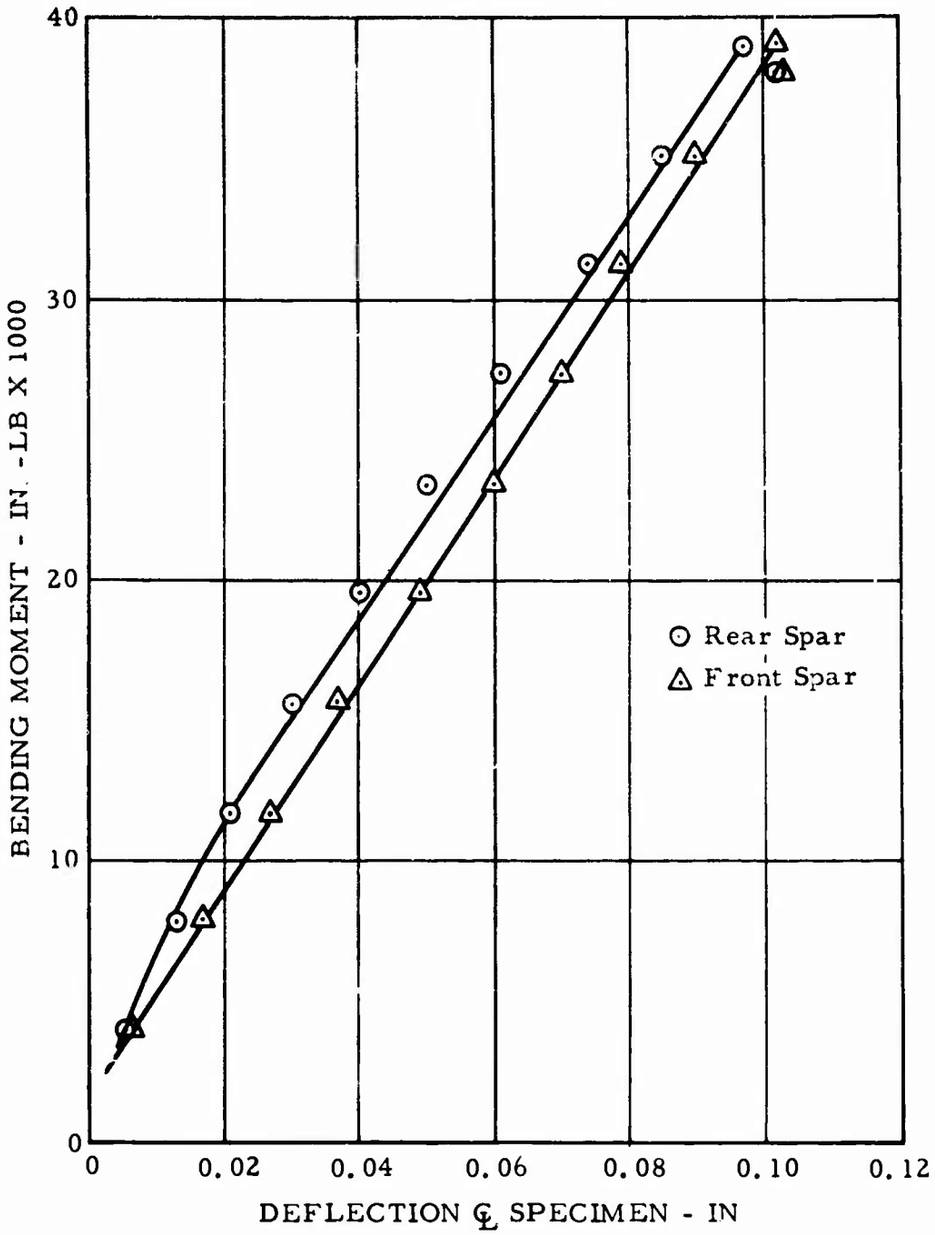

Figure 28. Spar Buckling Test - Unbonded Spar - Deflection.

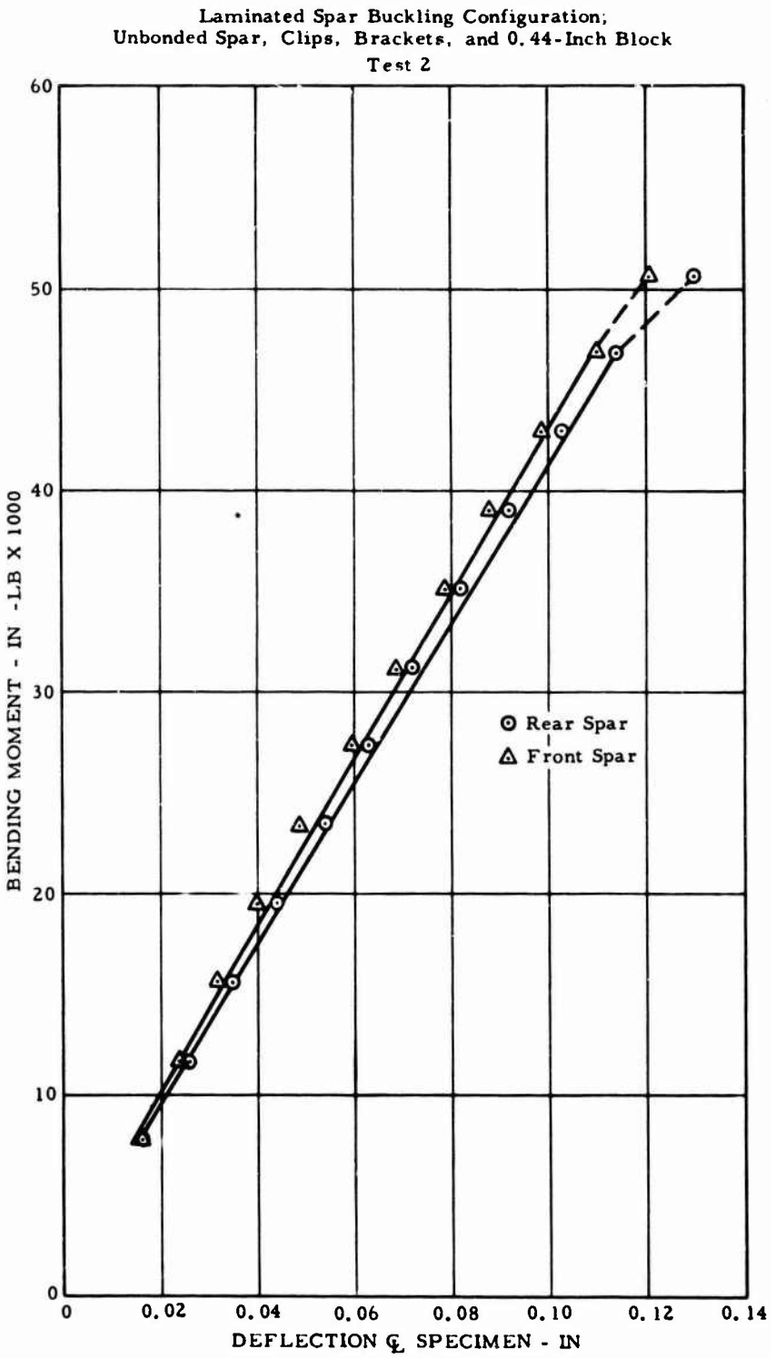

Figure 29. Spar Buckling Test - Unbonded Spar With Mechanical Restraint - Deflection.

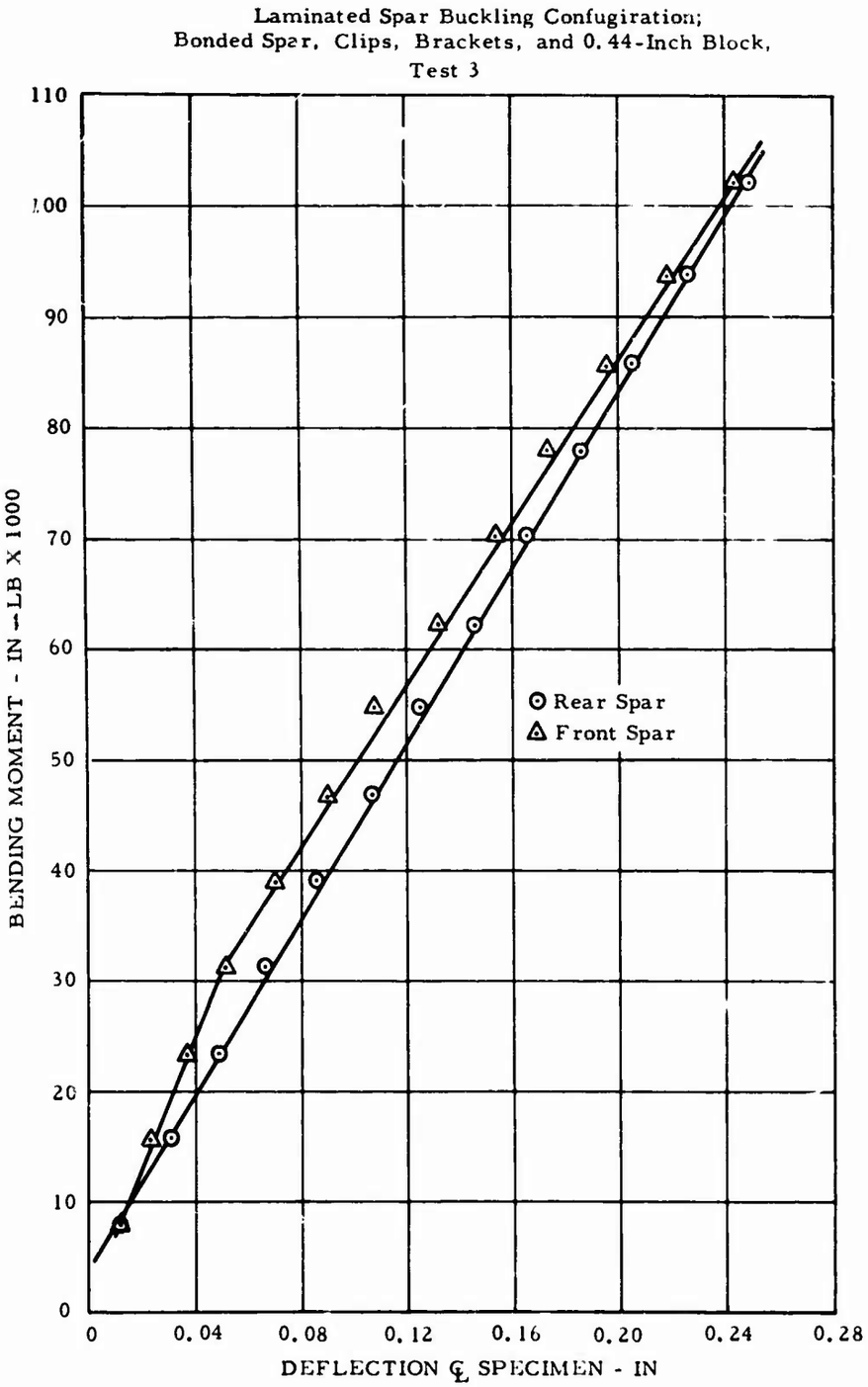

Figure 30. Spar Buckling Test - Bonded Spar With Mechanical Restraint - Deflection.

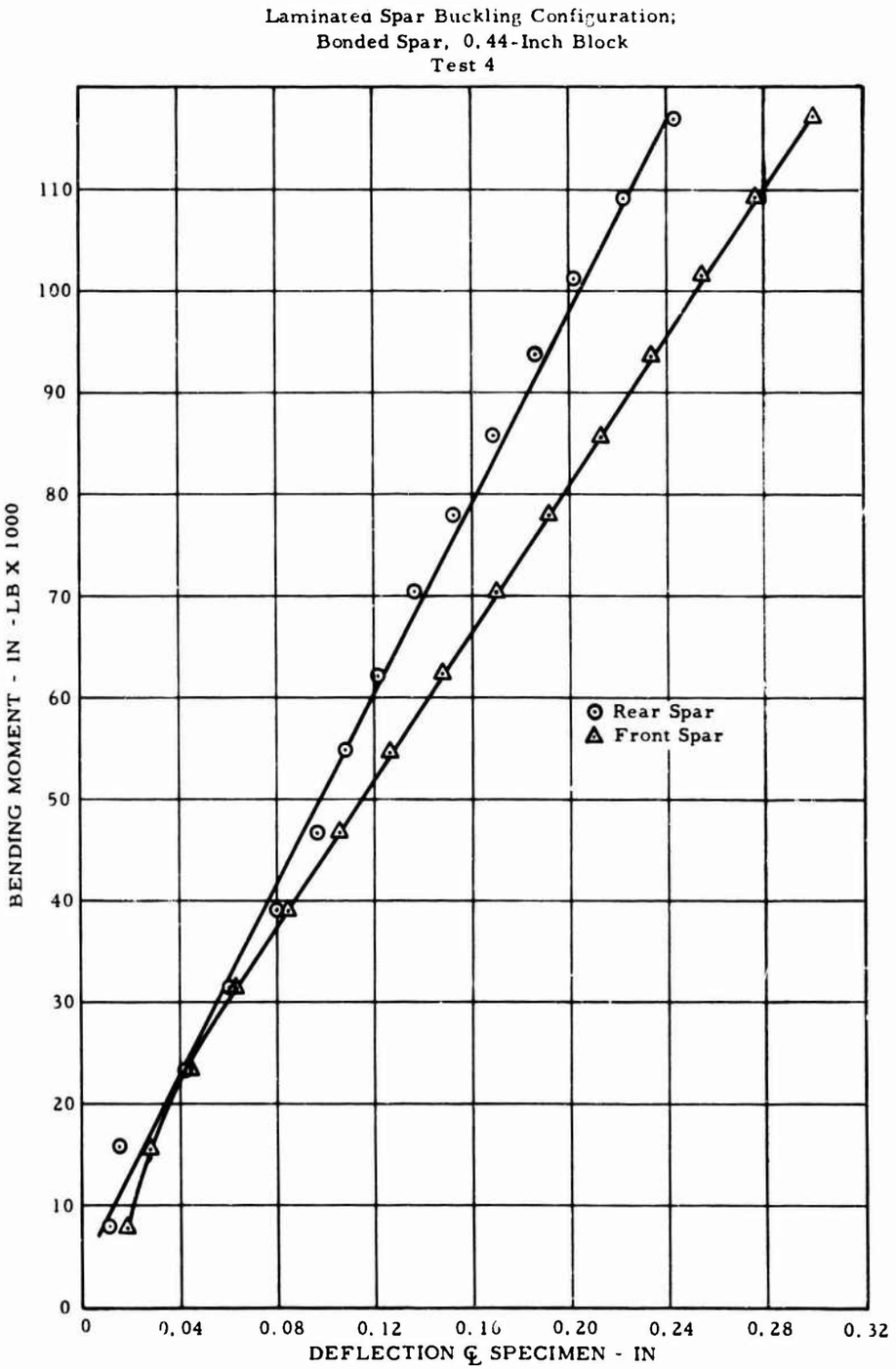

Figure 31. Spar Buckling Test - Bonded Spar Final Configuration - Deflection.

ROTOR BLADE CHORDWISE SHEAR TEST

SUBJECT

This test concerned chordwise shear stiffness of the rotor blade spar and segment combination. It was conducted in the HTC-AD structures test laboratory in January 1963.

PURPOSE

The purpose of this test was to obtain the proportion of chordwise shear carried in the titanium spars to the chordwise shear carried in the blade flexure of the constant section of the blade.

TEST SPECIMEN

The test specimen consisted of the XV-9A rotor blade (HTC-AD drawing 285-0100) with the titanium spars installed as tested in the original whirl test program, but without the leading and trailing edge aerodynamic fairings.

TEST SETUP

The test setup is shown in Figure 34. A fixture was attached to the existing bolt holes in the skin of a main rotor blade in order to apply a shear load across a representative blade flexure. This specimen was used to obtain preliminary shear distribution information to be incorporated into new spar design studies. Because of the large percentage of shear carried by the flexures, tests utilizing stainless steel spars were not considered.

The fixture was loaded using a turnbuckle arrangement. The load was read on a dial indicator load ring.

One dial indicator was mounted normal to the rear spar on the side of the blade. Another dial indicator was mounted on the top of the blade. Both dial indicators measured shear deflections in the chordwise direction.

TEST PROCEDURE

With the spars bolted to the blade segments on each side of the flexure, a load was applied to the fixture. Load and deflection were recorded.

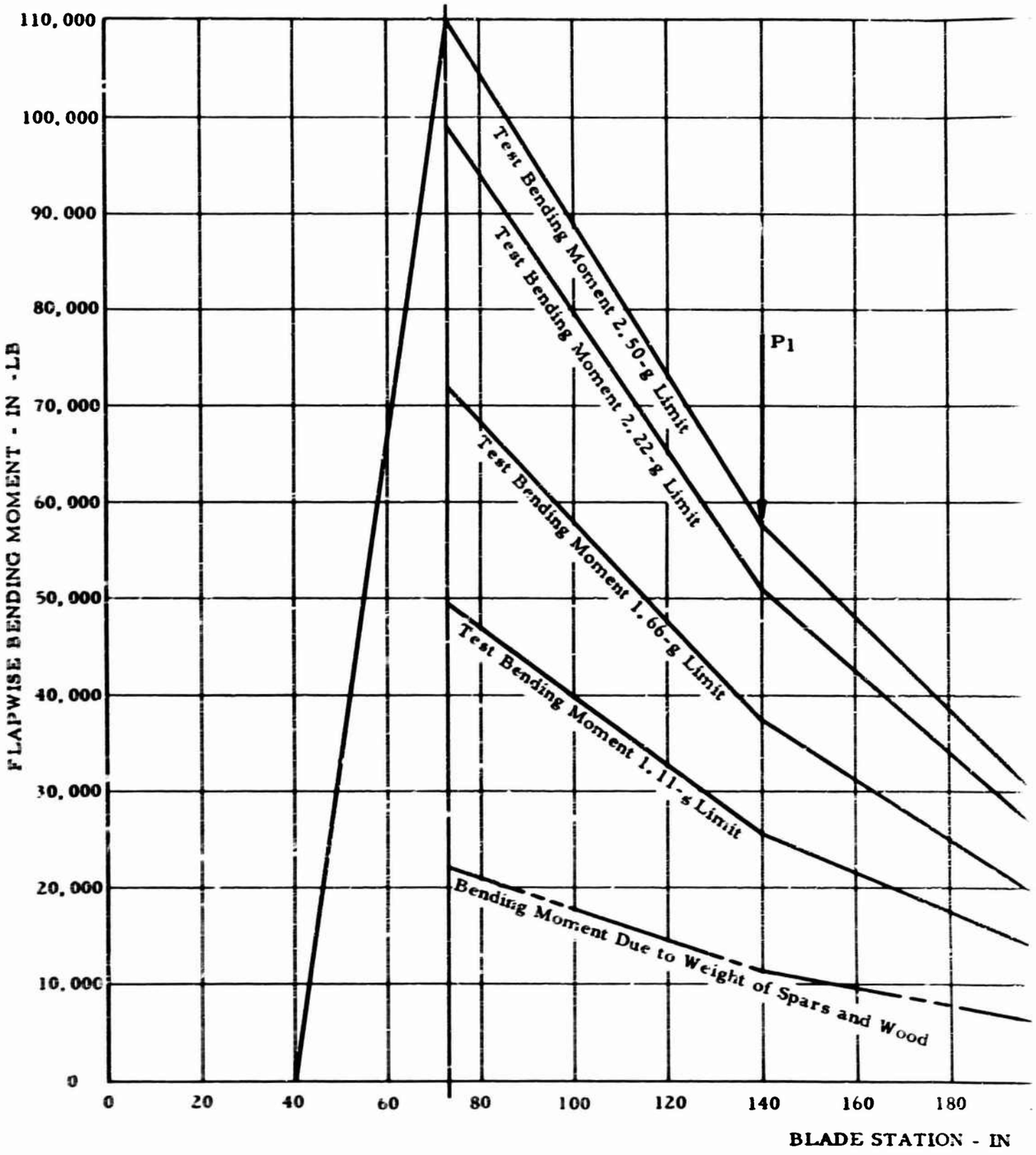

Figure 32. Rotor Blade Spar F Moment Distributio

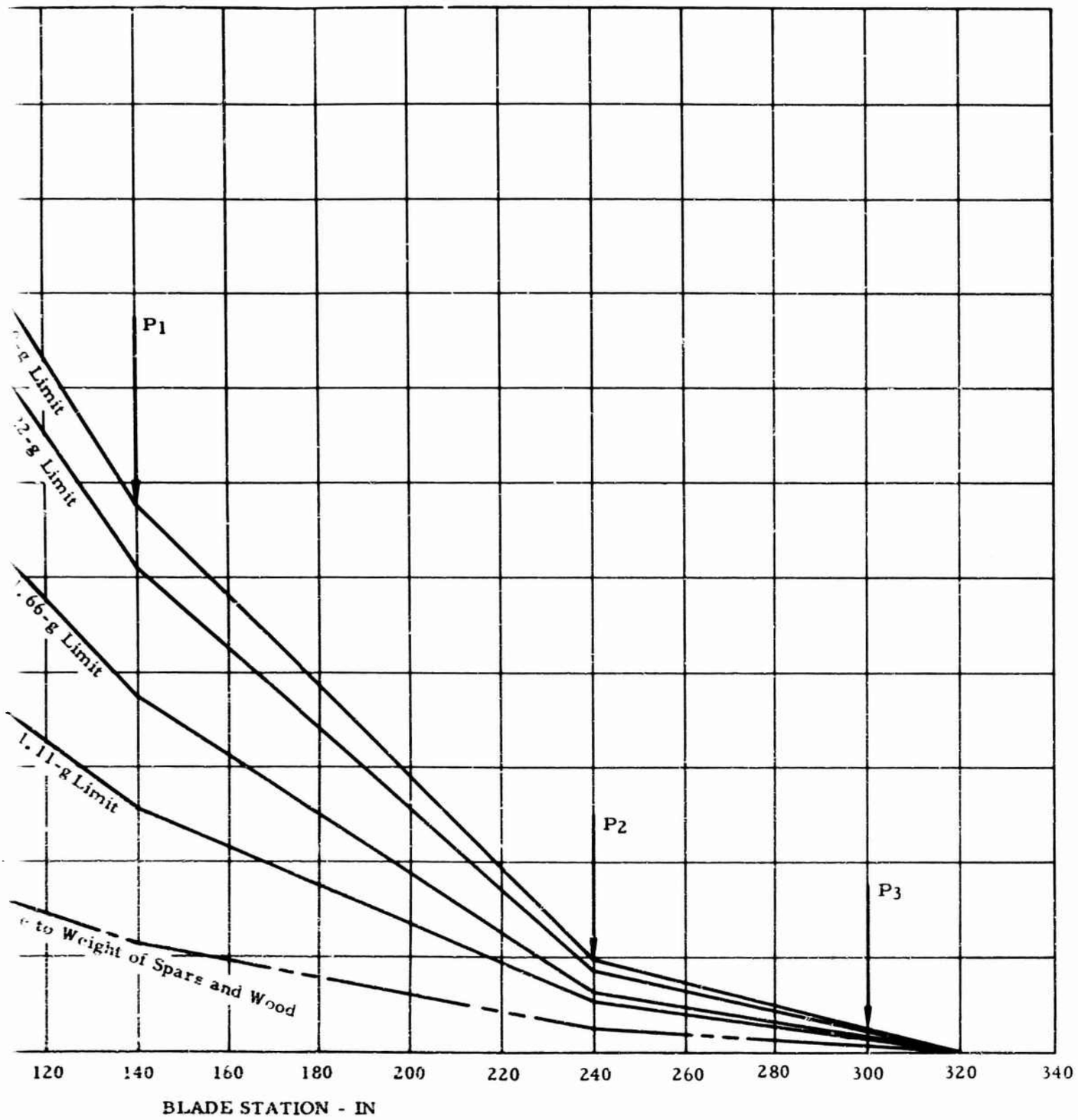

Figure 32. Rotor Blade Spar Proof Test - Bending Moment Distribution.

Figure 33. Rotor Blade Spar Proof Test at 2.5-g Condition.

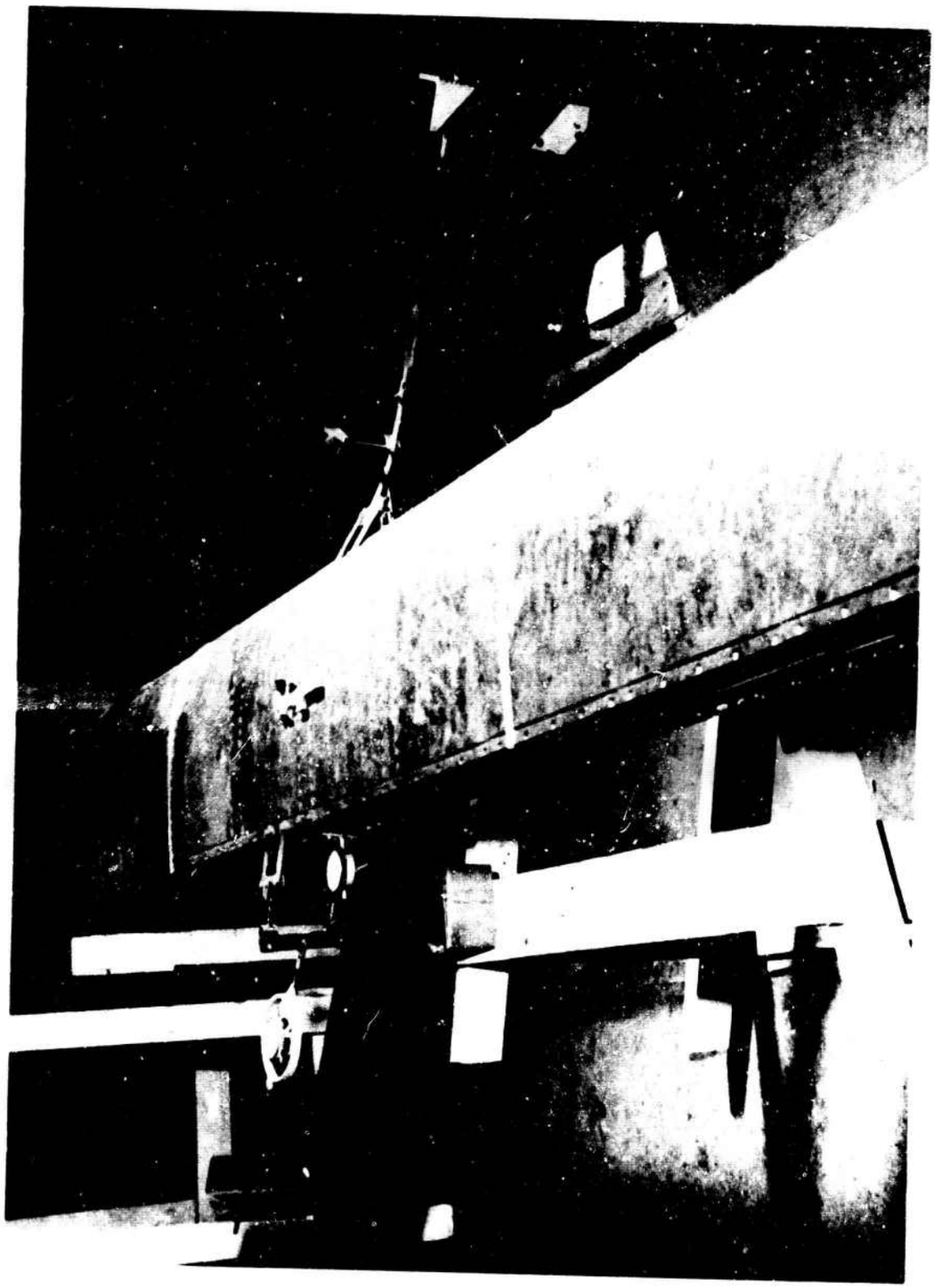

Figure 34. Rotor Blade Flexure Shear Test Setup.

With the spar attaching bolts loosened, again an equivalent load was applied to the fixture. Load and deflection were recorded.

TEST RESULTS

On Figures 35 and 36, load versus deflection curves are plotted for the spars-bolted and spars-unbolted conditions.

Because of the friction hysteresis and high chordwise stiffness in the blade specimen, only an approximate distribution of shear between the spars and the flexures can be determined. The shear carried by the flexure was between 90 and 98.5 percent.

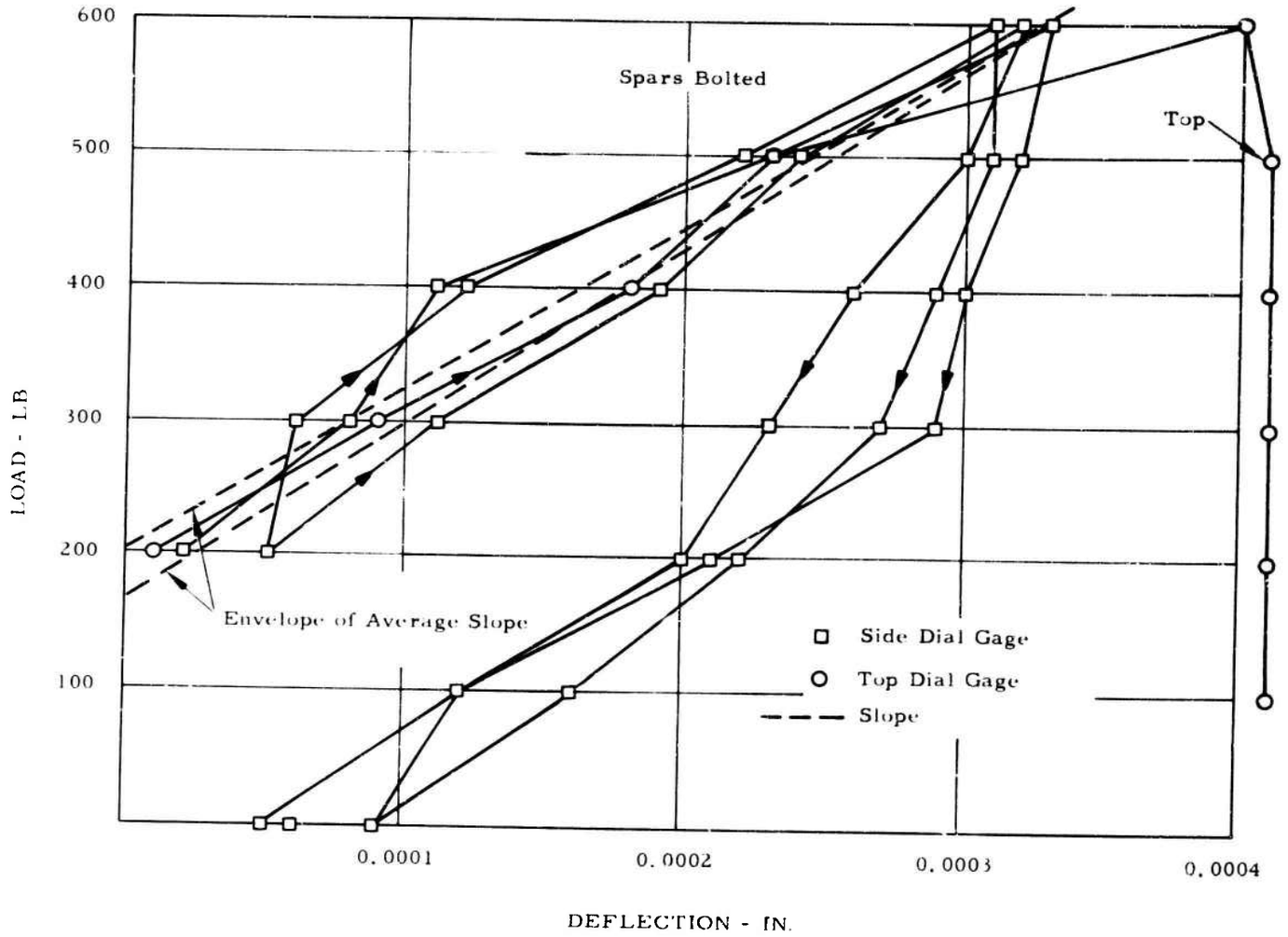

Figure 35. Rotor Blade Flexure Deflection Results - Spars Bolted.

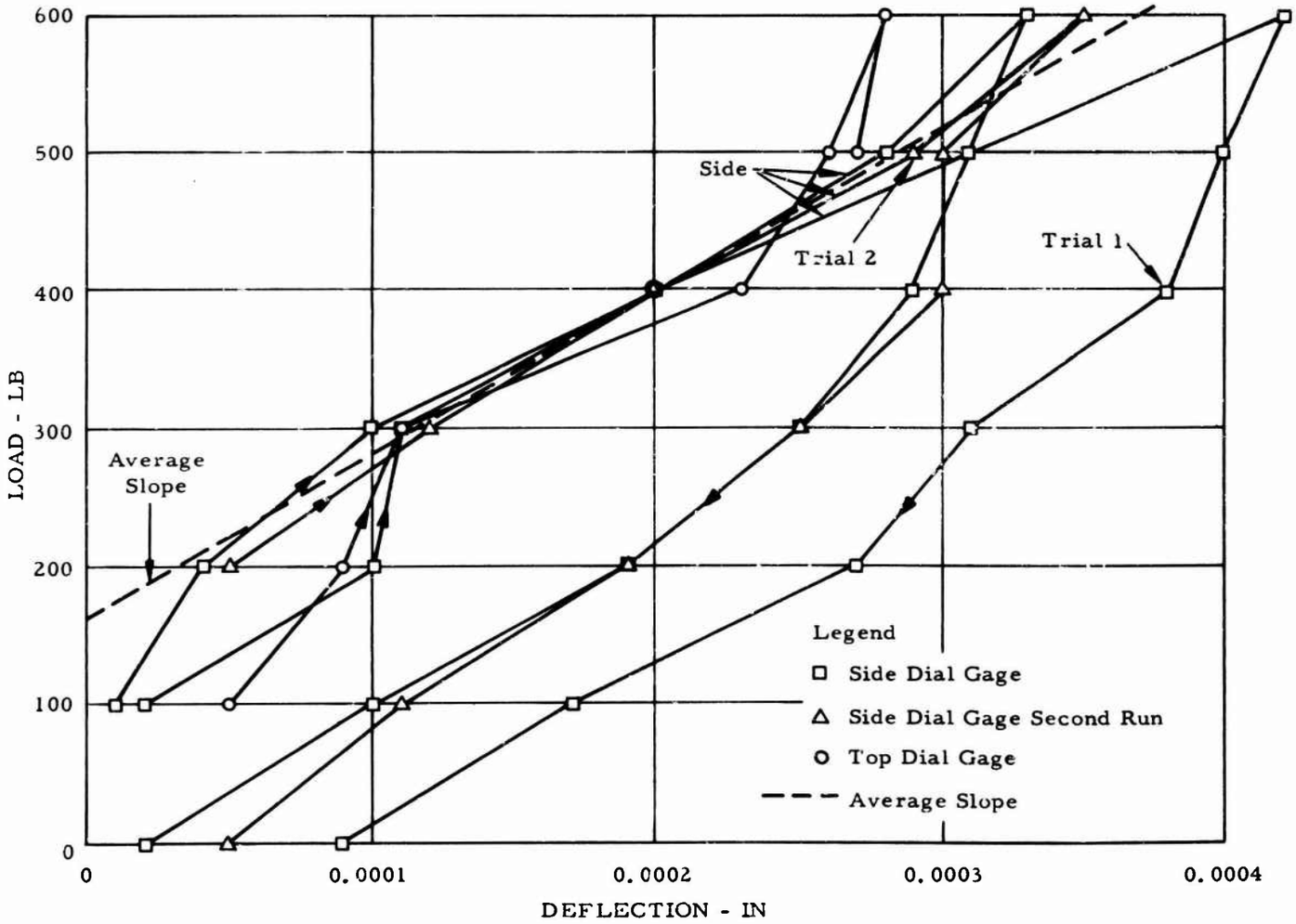

Figure 36. Rotor Blade Flexure Deflection Results - Spars Unbolted.

BLADE SHAKE TEST

SUBJECT

This test concerned a survey of the nonrotating natural frequencies of the XV-9A rotor blade supported in a horizontal leading-edge-down position. It was conducted in the HTC-AD structures test laboratory in November 1963.

PURPOSE

The purpose of this test was to determine the fundamental, second, and third nonrotating flapwise bending natural frequencies and mode shapes as set up in a horizontal position.

SUMMARY OF RESULTS

The flapwise natural frequencies and mode shapes for the first, second, and third modes were determined, and are presented below. The mode shapes for all three natural frequencies and their phase relationship with a fixed accelerometer located at station 324 are presented in Figure 37. Also included in Figure 37 are the approximate observed nodal points, which closely coincided with accelerometer indications.

Mode	Frequency (CPS)
First	2.5 - *(3.9 - 4.3)
Second	7.7 - 8.3
Third	18.0 - 18.4
Torsion	22.8 - 23.0

TEST SPECIMEN

The test specimen consisted of a complete XV-9A rotor blade (HTC-AD drawing 385-1100) less blade retention straps. This blade had both leading-and-trailing-edge sections with pressure probes installed and was complete except for the blade-tip closure valve and its functioning equipment.

*See Discussion of Test Results.

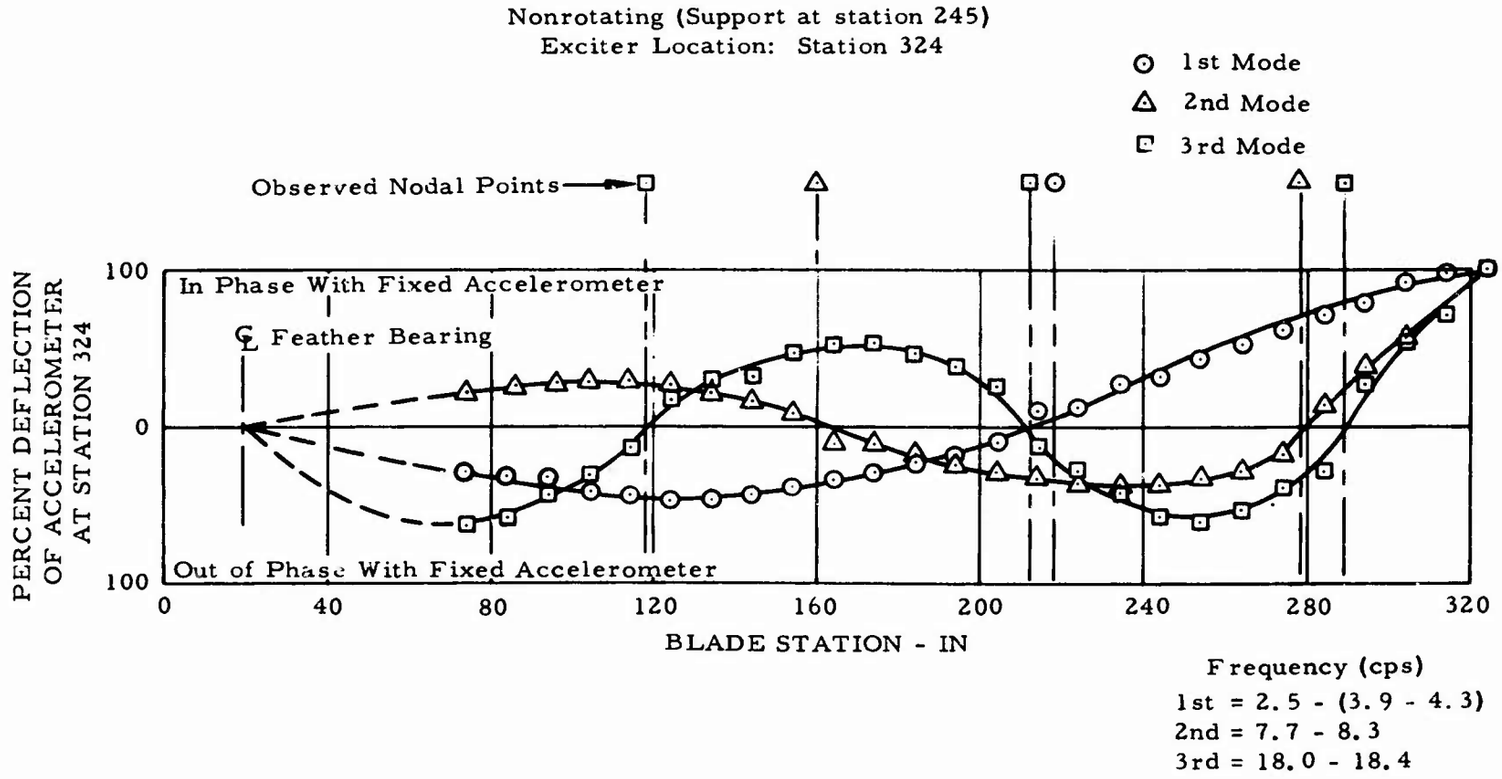

Figure 37. Rotor Blade Shake Test - Flapping Mode Shapes.

TEST SETUP AND PROCEDURE

The test blade was set up in a fixture to accept the feathering bearing portion of the blade. This fixture was then installed on the static test jig that formed the major reacting structure.

The blade was rigged in a horizontal position, leading edge down, and supported at blade station 245 by an elastic cord bungee and strap system. Figures 38 and 39 show the test setup.

The blade was excited by an electromagnetic shaker system, console model T-57, exciter unit model S-6A, and attached to the blade by a vacuum linkage system. The system allows complete movement of the exciter to any station along the blade span without mechanical attachments.

Instrumentation required for testing was two accelerometers — one at a fixed station and the other a roving pickup to investigate various phase angles and mode shapes of the blade at various stations. Signals from the accelerometers were simultaneously fed into a dynagraph (oscillograph), and from these records phase relationships and mode shapes were determined.

DISCUSSION OF TEST RESULTS

The frequency spread of the various resonances indicates that the XV-9A rotor blade is a highly damped body in which no precise sharp peaks were encountered. In the first mode, the blade, when excited as a free body at 2.5 cps (no exciter attachment), would completely damp out its excitations within 3 to 4 cycles; whereas, when the exciter was attached to the blade, resonance did occur at 2.5 cps, but remained relatively flat in response until the 3.9 to 4.3 cps region, when the accelerometer traces peak out.

The second and third modes again indicate the same trend: no sharp resonant peaks, but relatively flat across the resonant frequency range.

During part of the frequency investigations, a torsional mode was discovered at 22.8 to 23.0 cps.

The bungee support system was later changed to blade station 218 (first mode nodal point), where the natural frequencies were again rechecked and were found to coincide with reported test results.

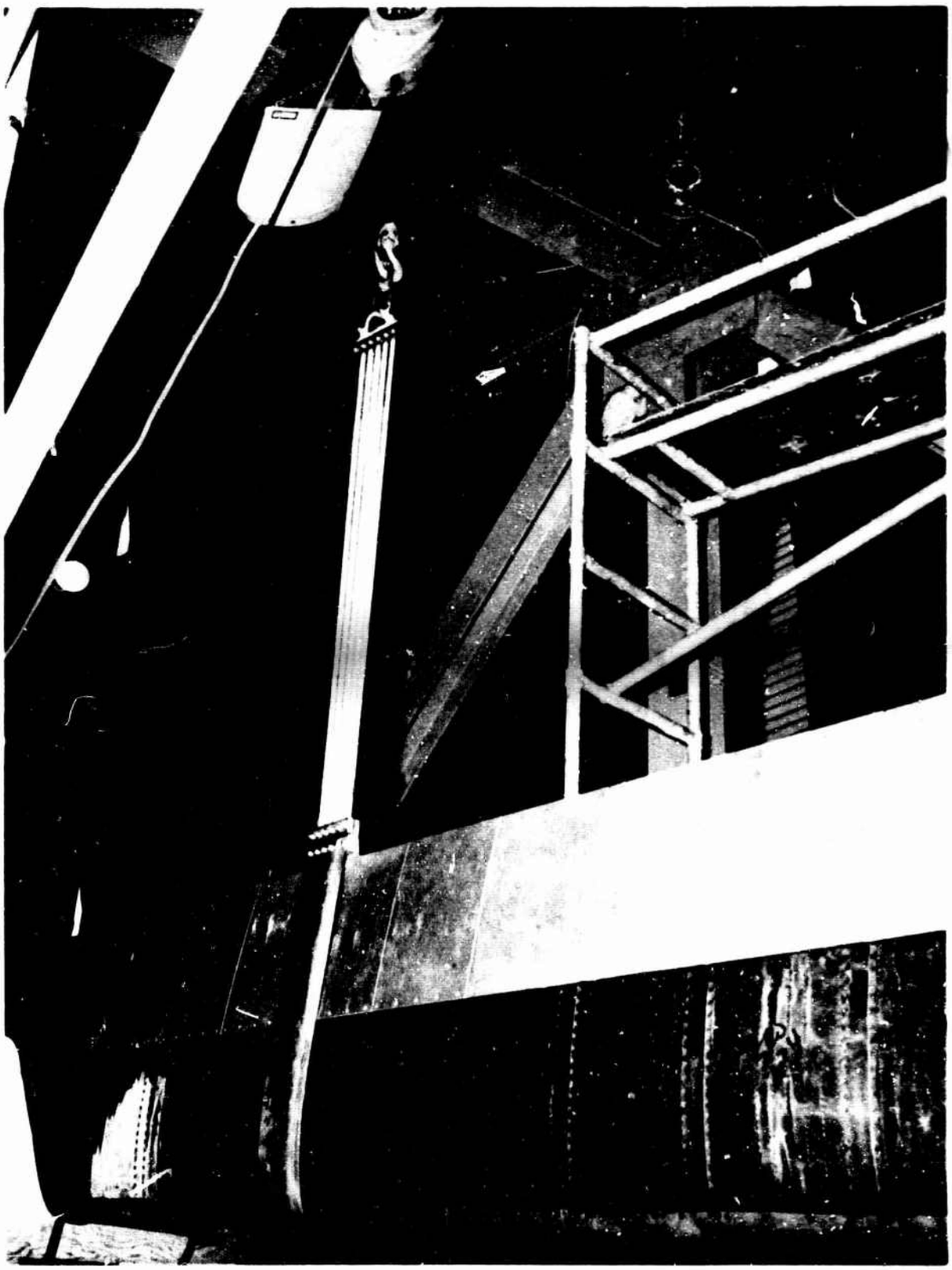

Figure 38. Rotor Blade Shake Test - Bungee Support System.

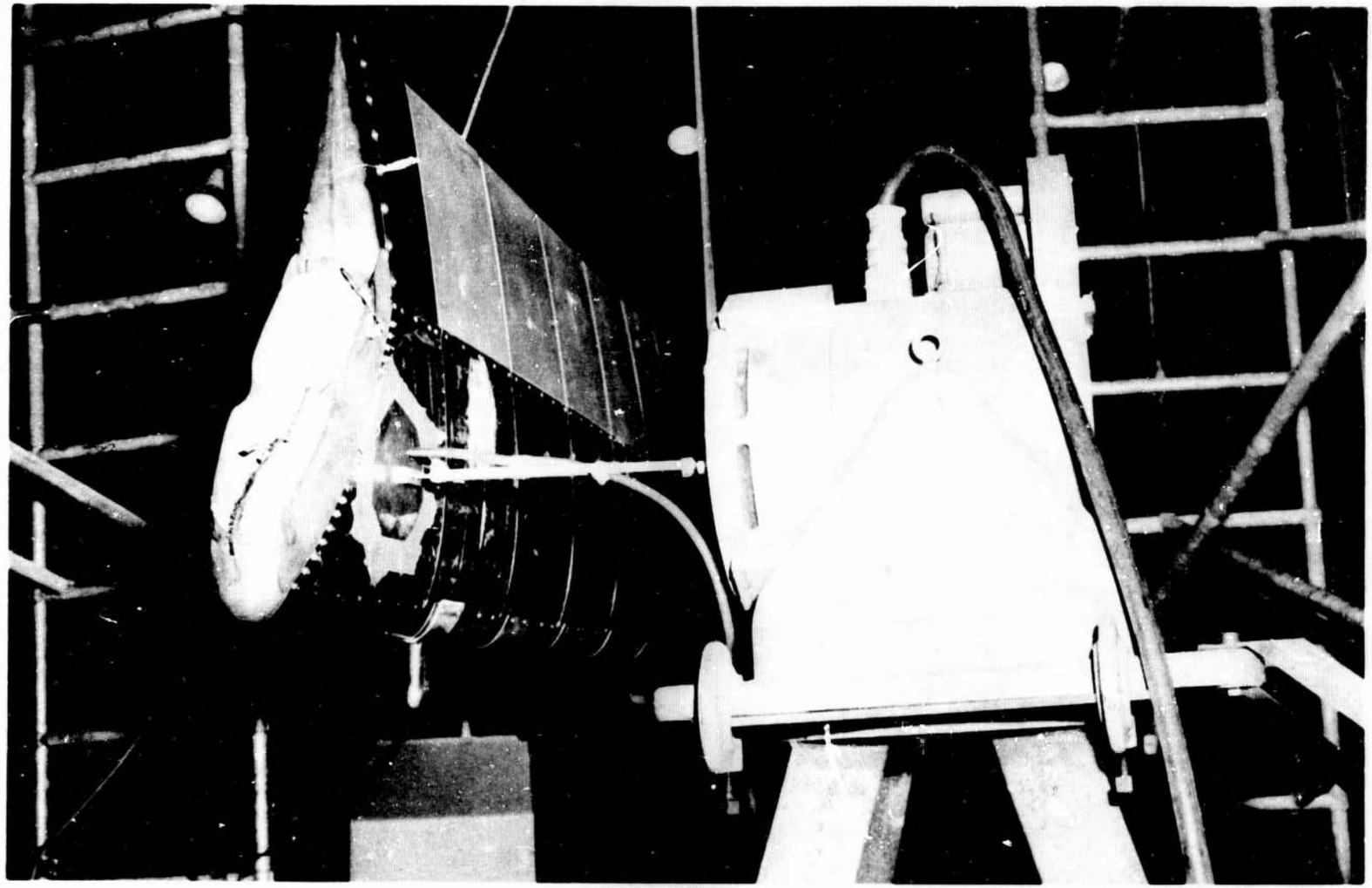

Figure 39. Rotor Blade Shake Test - Shaker Attachment.

BLADE STATIC DEFLECTION AND CALIBRATION TEST

SUBJECT

This test concerned static deflection and calibration of the instrumented XV-9A rotor blade – color code identification, blue. The test was conducted at the HTC-AD structures test laboratory during November 1963.

PURPOSE

The purpose of this test was to provide the flight test and whirl test programs with calibration and static deflection data.

SUMMARY OF RESULTS

The instrumented blade of the rotor system was calibrated in flapwise bending, chordwise bending, and torsion conditions. Tip deflections were recorded, and a blade torsional spring rate was established for the full length of the blade.

TEST SPECIMEN

The test specimen consisted of a flight rotor blade (HTC-AD drawing 385-1100) without the trailing edge sections installed.

TEST SETUP AND INSTRUMENTATION

The rotor blade was installed in a test fixture in the structures test facility. This fixture accepts the feathering bearing housing in the root-end portion of the blade. Located outboard at blade station 73.44 was a reacting ring, used to aid in calibration as a simple cantilever beam.

The instrumentation consisted of bending and axial bridge circuits to measure the various whirl and flight loads. These bridges are shown in Figure 40. All strain gage bridge systems were routed to a switching unit and data were read on an SR-4 strain indicator. Data were recorded for the appropriate calibration setups.

TEST PROCEDURE

The test was conducted in three phases: (1) flapwise bending in both directions (Figure 41), (2) chordwise bending in both directions (Figure 42),

and (3) torsion in clockwise and counterclockwise directions (Figure 43). Simultaneously, while the above tests were being conducted, tip deflections were recorded for the flapwise and chordwise conditions, and angular deflections for the torsion conditions.

The blade was loaded at the tip, station 320; for the flapwise condition, up to 160 pounds in 20-pound increments, and for the chordwise condition up to 400 pounds in 50-pound increments. The blade torsion condition was accomplished up to 10,000 inch-pounds in 20-pound increments on a 66-2/3-inch arm.

TEST RESULTS

The calibrations for the flapwise, chordwise, and torsion conditions, shown in Figures 44 through 50, are presented in a plotted form of calibration parameter versus strain output of the bridge.

Tip deflections for the above conditions are presented in Figures 51 through 53.

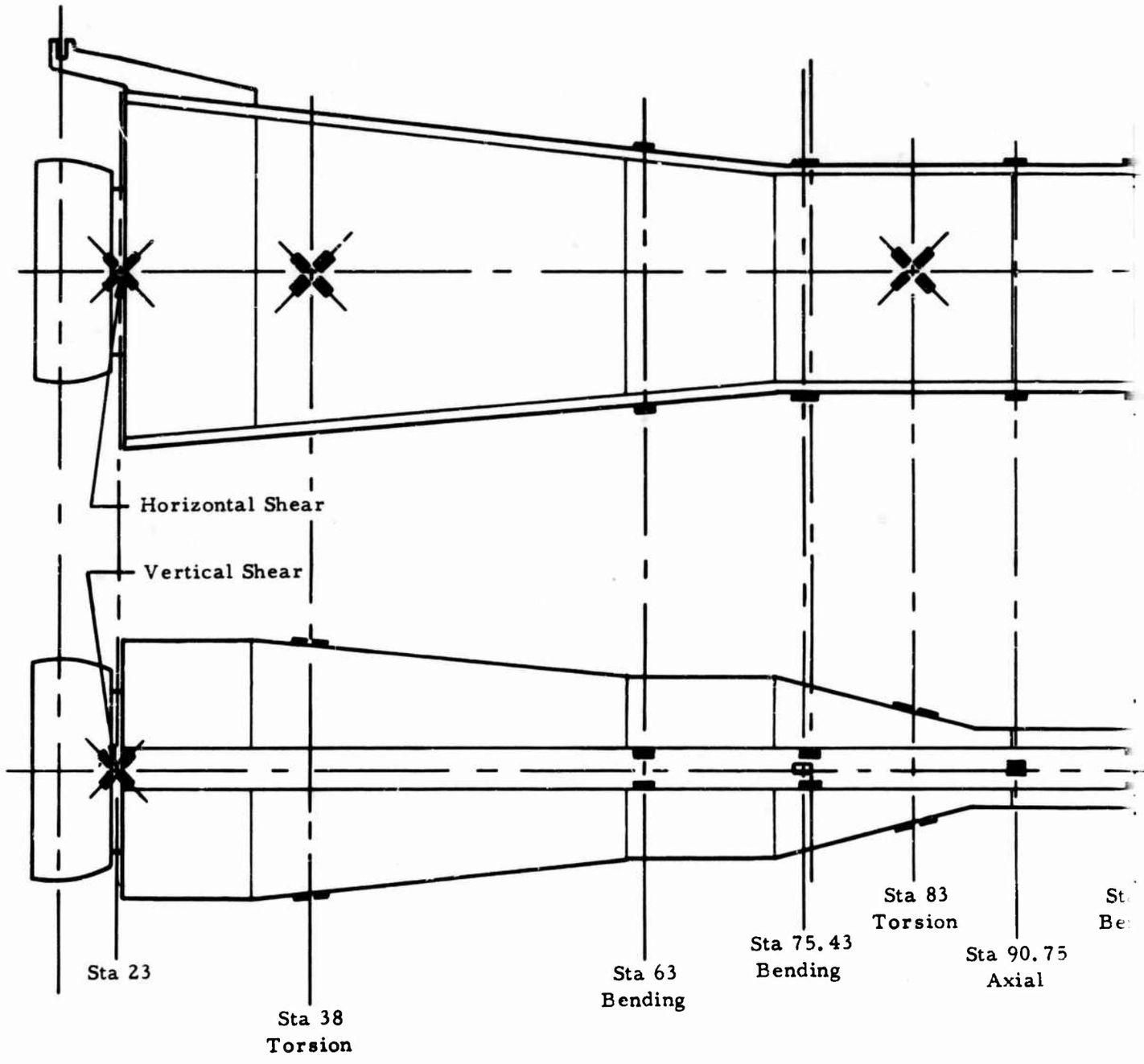

Figure 40. Blade Static Deflection Test - Instrumentation Location.

A

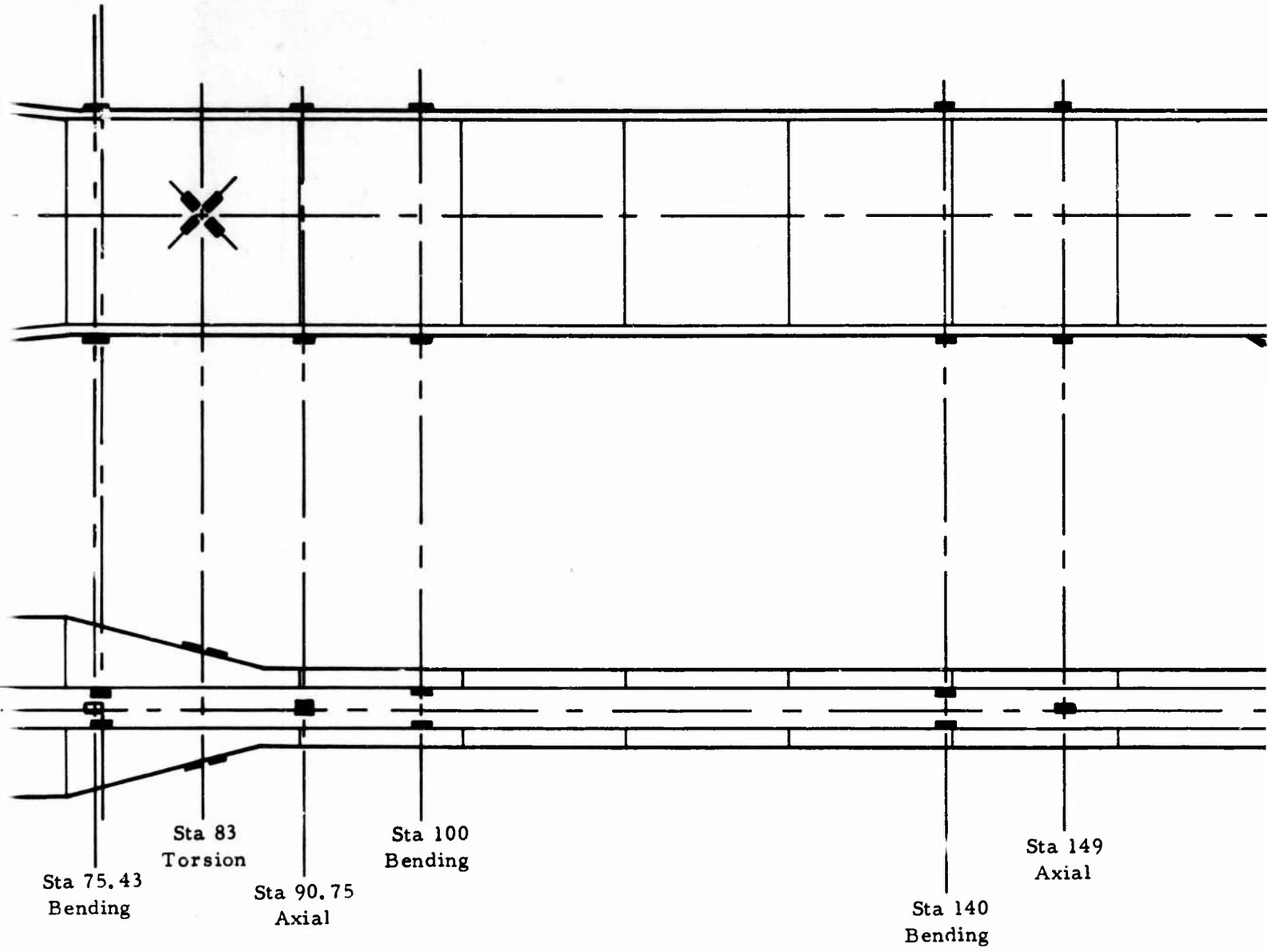

on Location.

B

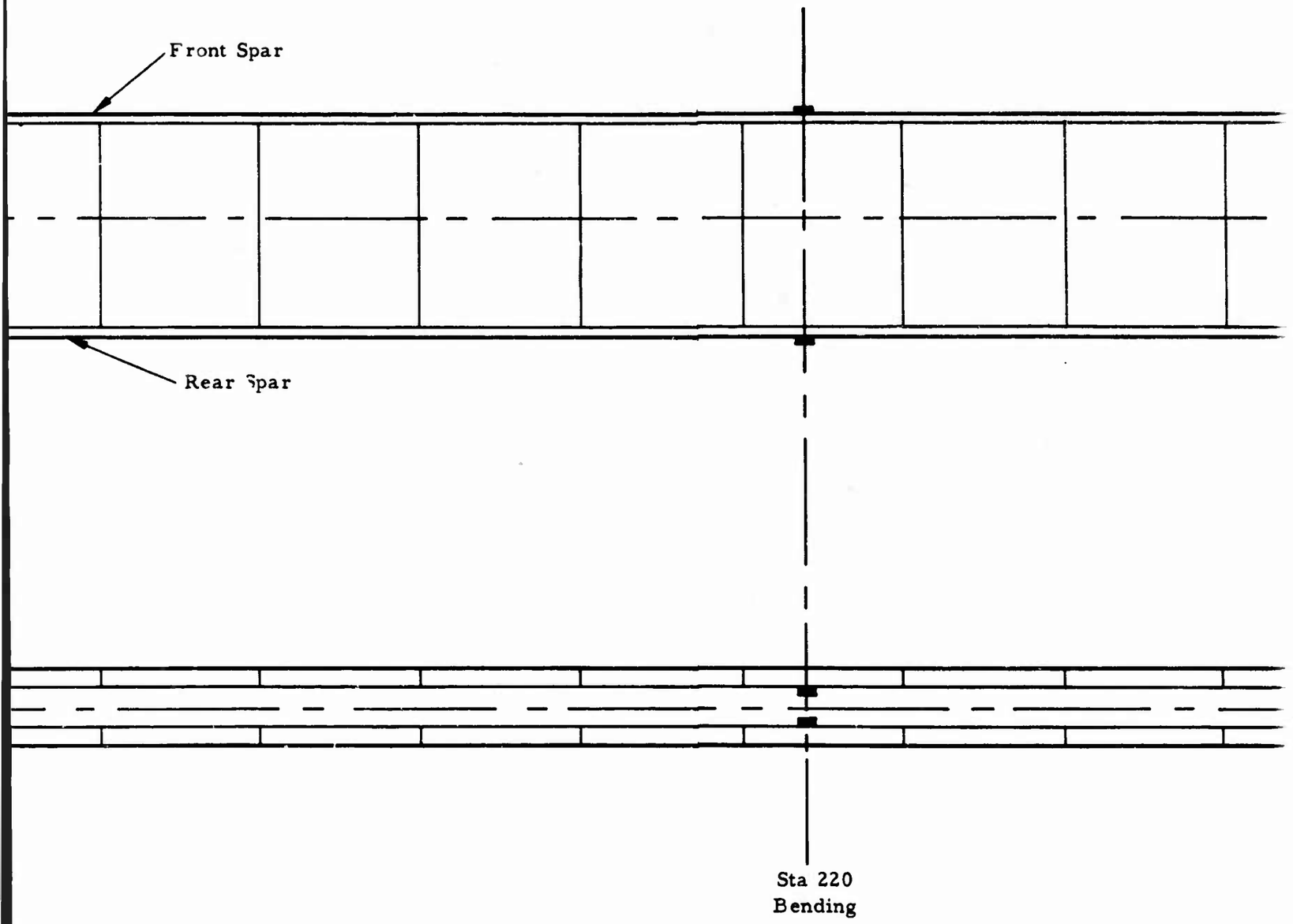

C

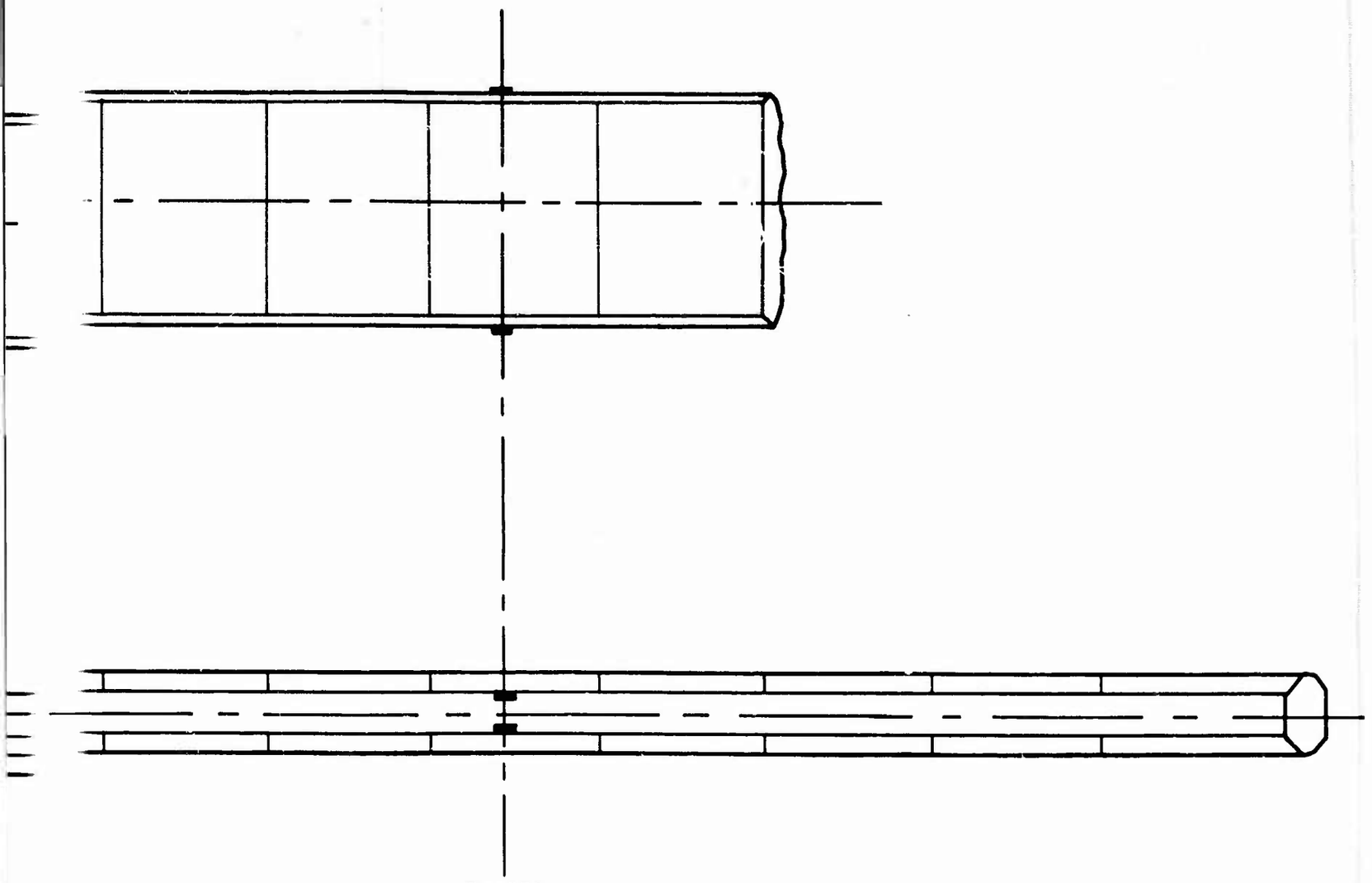

Sta 270
Bending

D

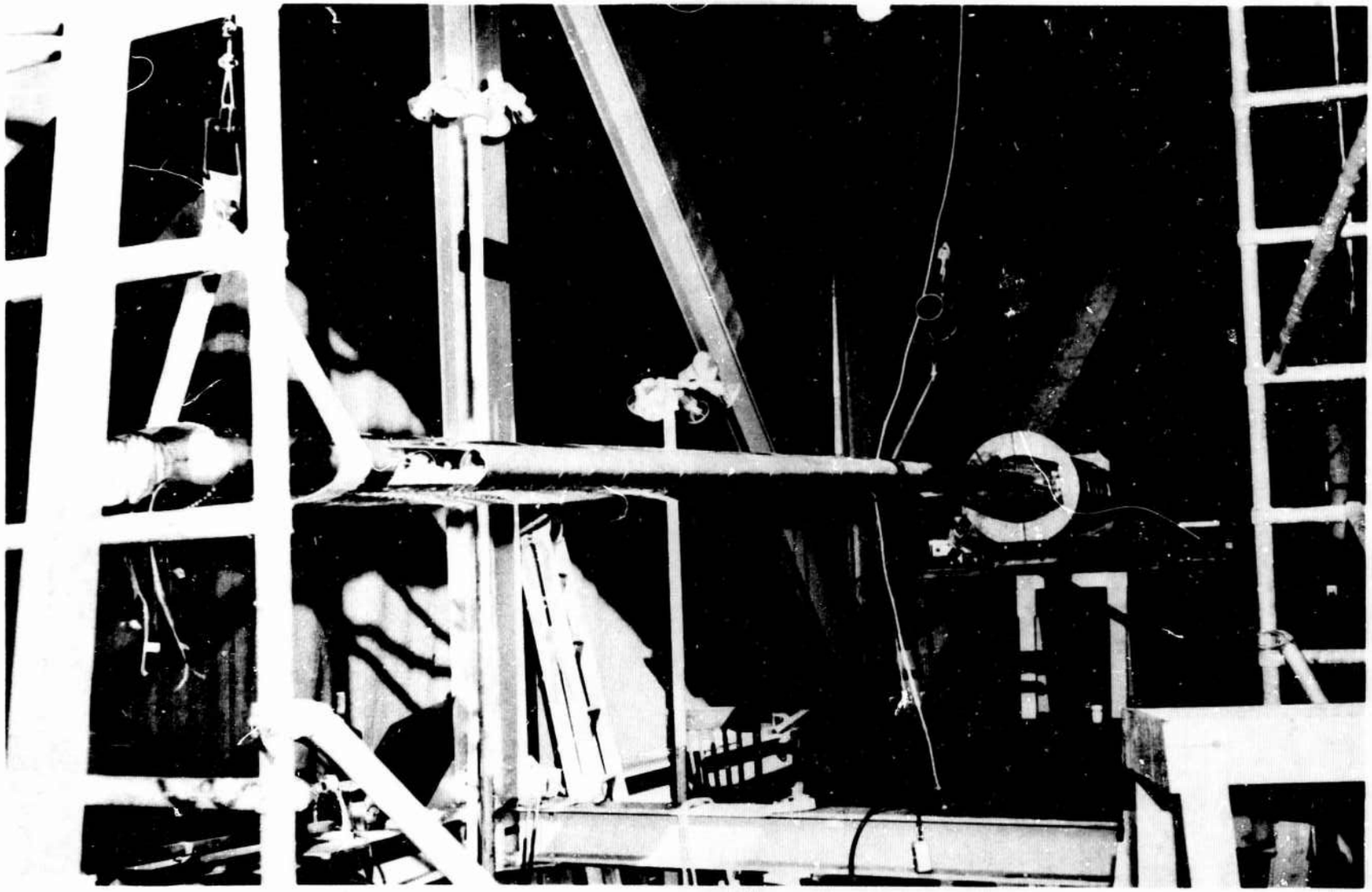

Figure 41. Blade Static Deflection Test - Flapwise Blade Setup.

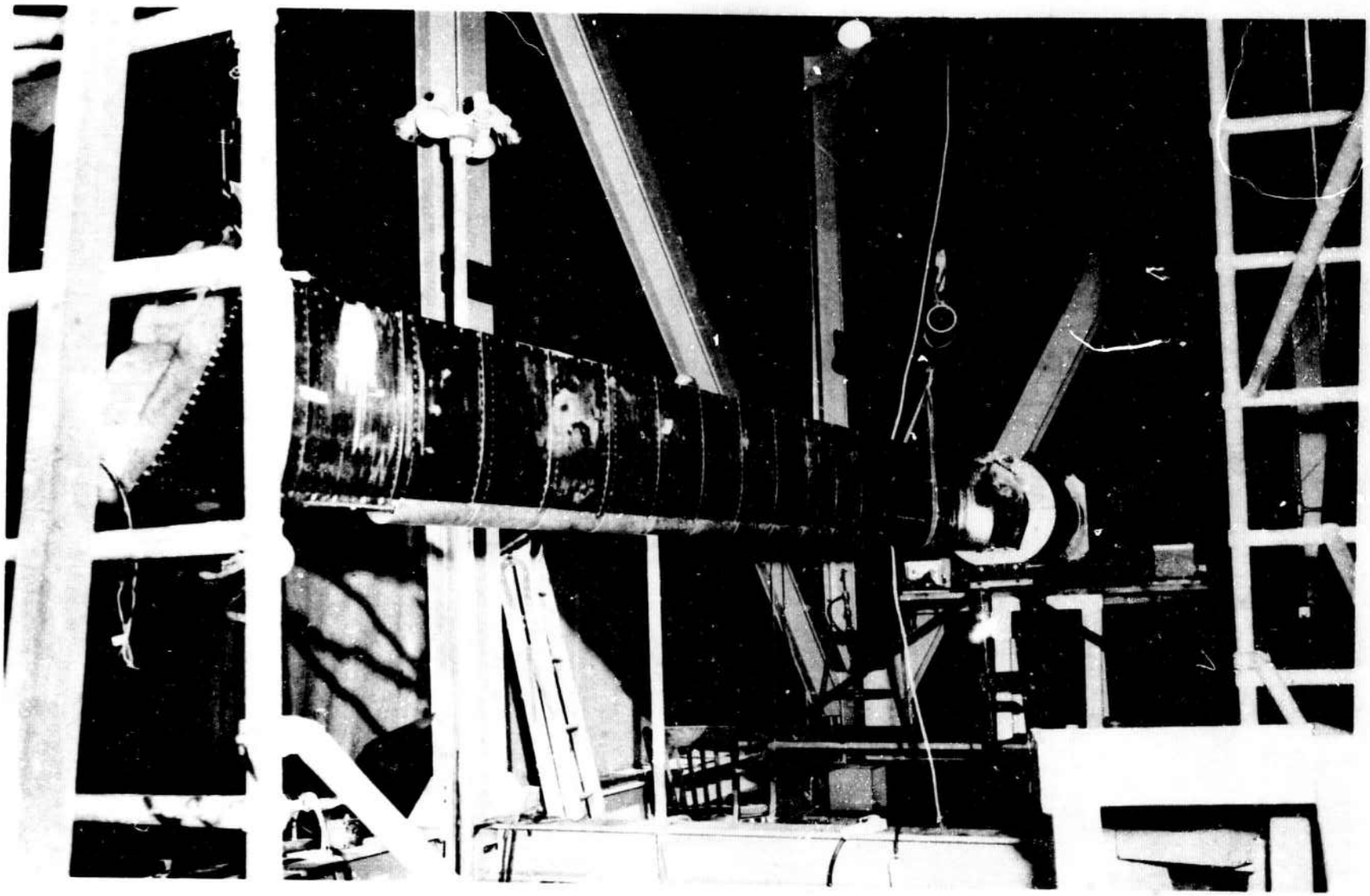

Figure 42. Blade Static Deflection Test - Chordwise Blade Setup.

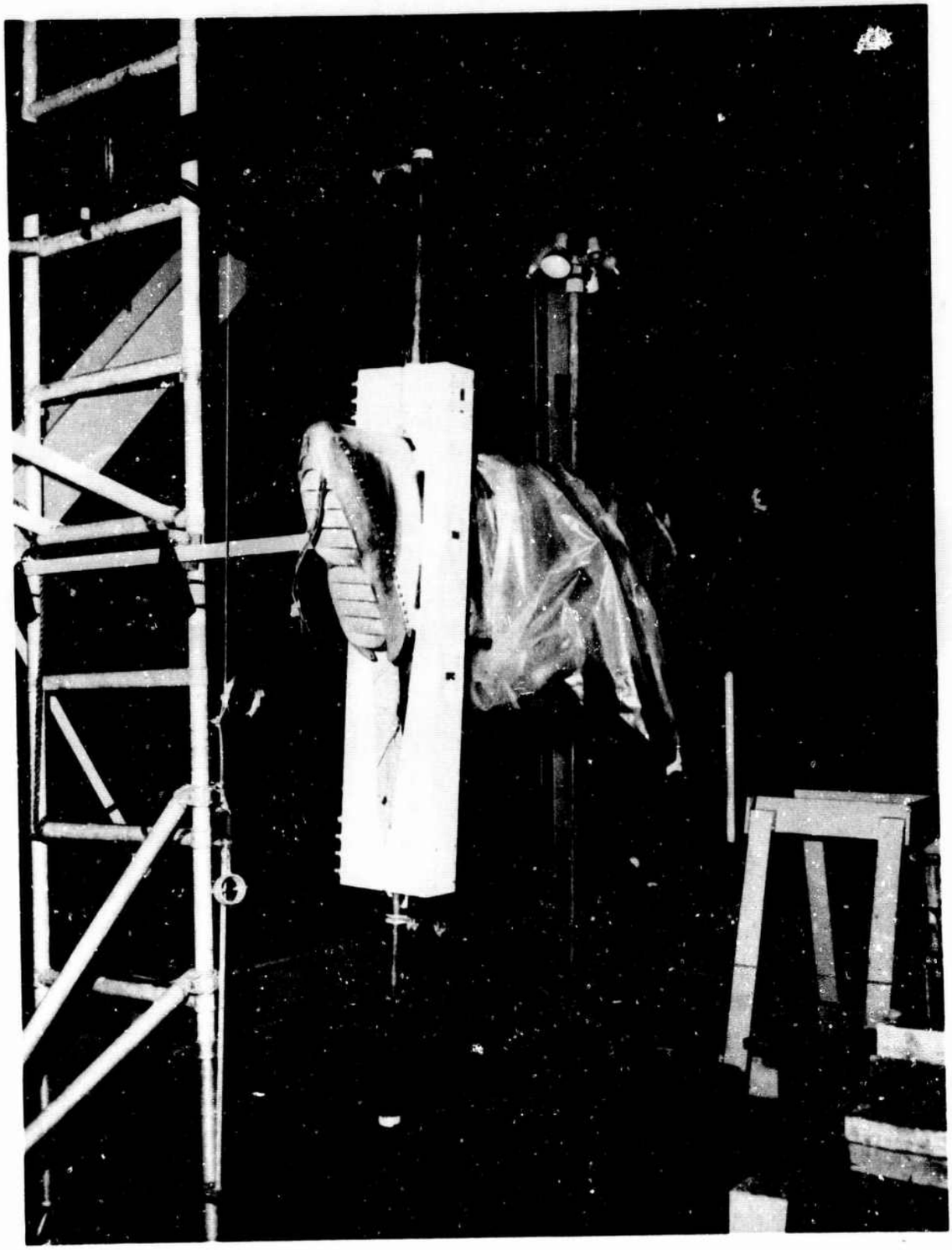

Figure 43. Blade Static Deflection Test - Torsion Blade Setup.

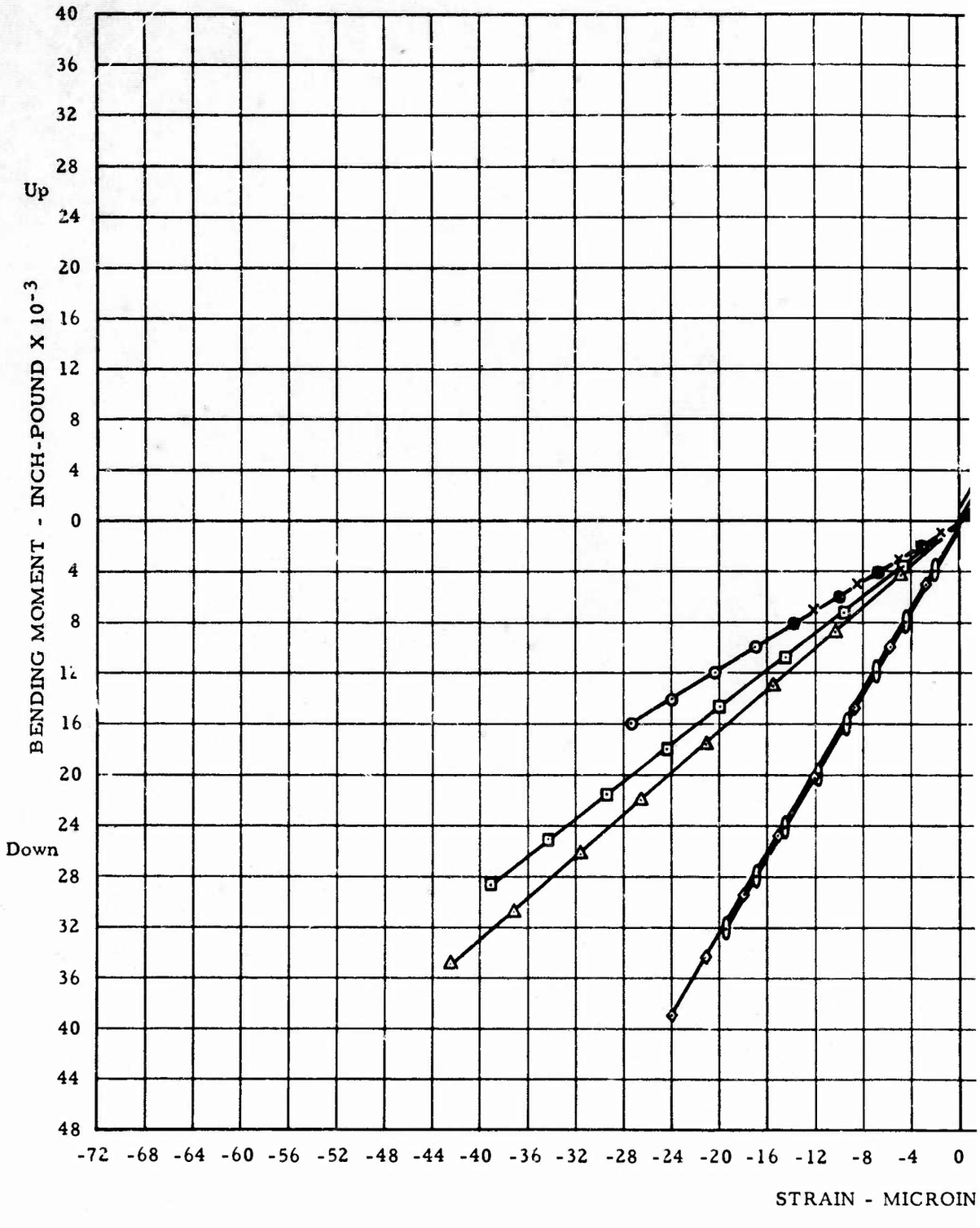

Figure 44. Blade Static Deflection Test -

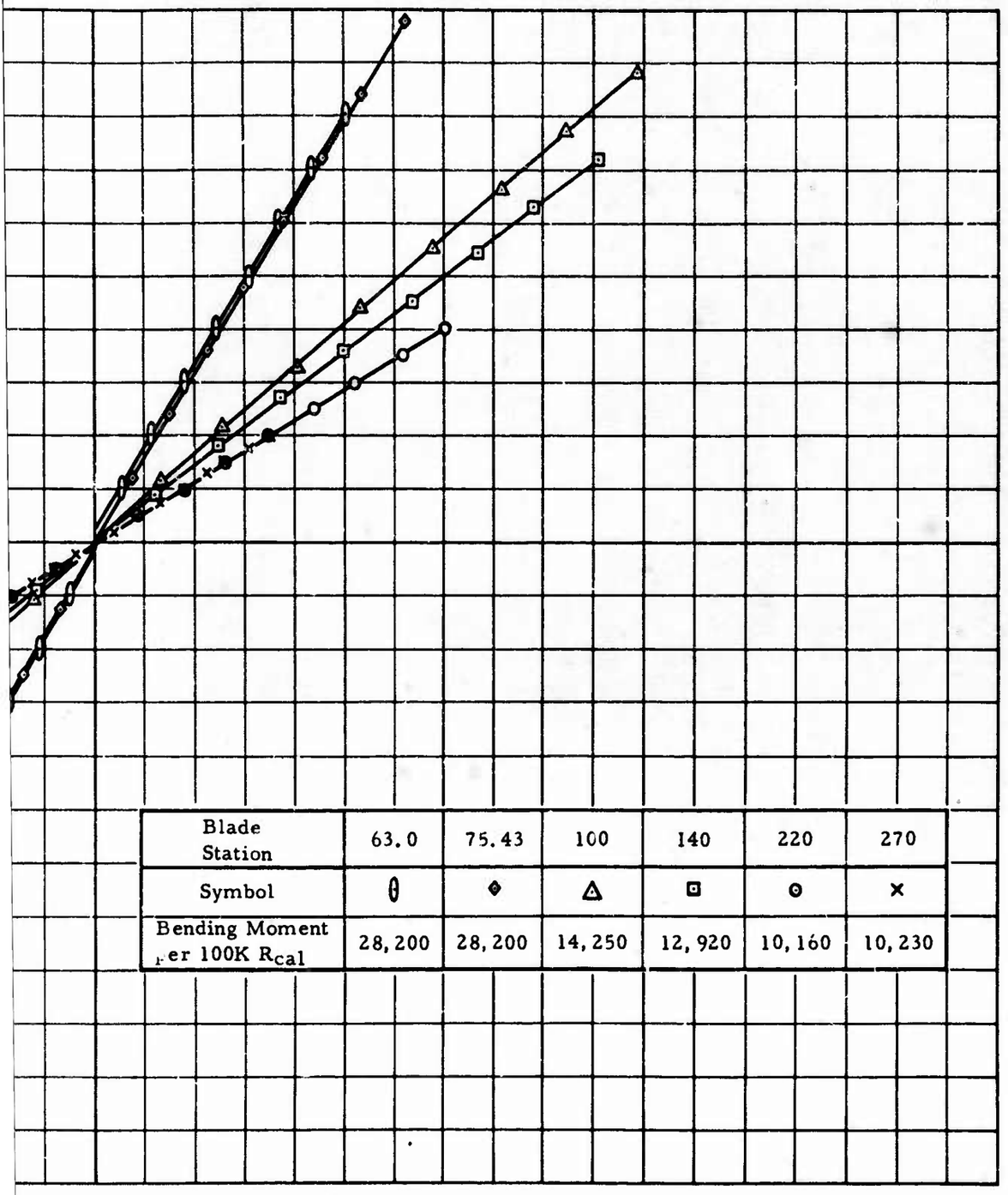

Blade Station	63.0	75.43	100	140	220	270
Symbol	θ	◈	△	▫	⊙	×
Bending Moment per 100K R_{cal}	28,200	28,200	14,250	12,920	10,160	10,230

-4 0 4 8 12 16 20 24 28 32 36 40 44 48 52 56 60 64 68 72

MICROINCH/INCH X 10^{-2}

ı Test - Flapwise Bending, Rear Spar.

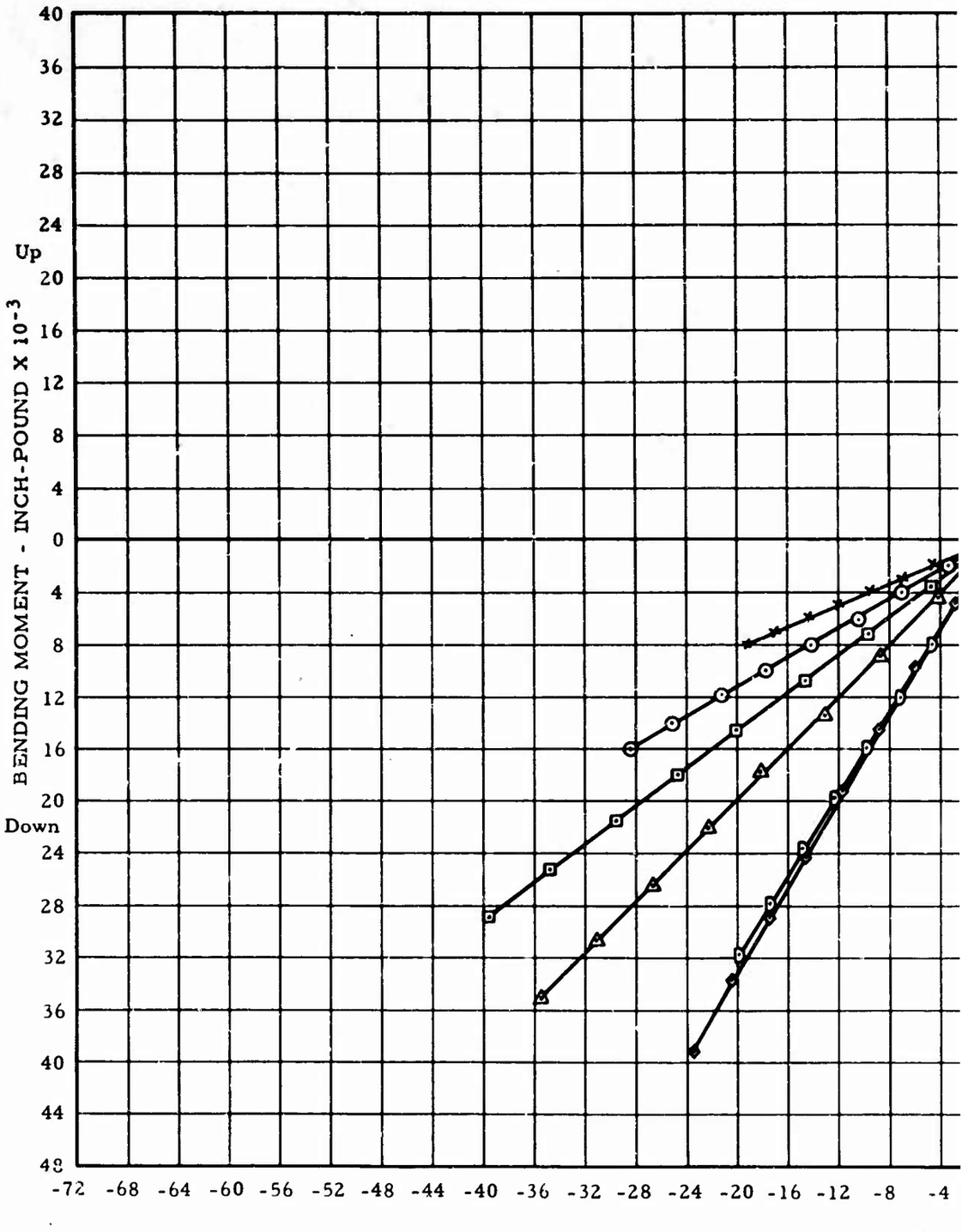

Figure 45. Blade Static Def

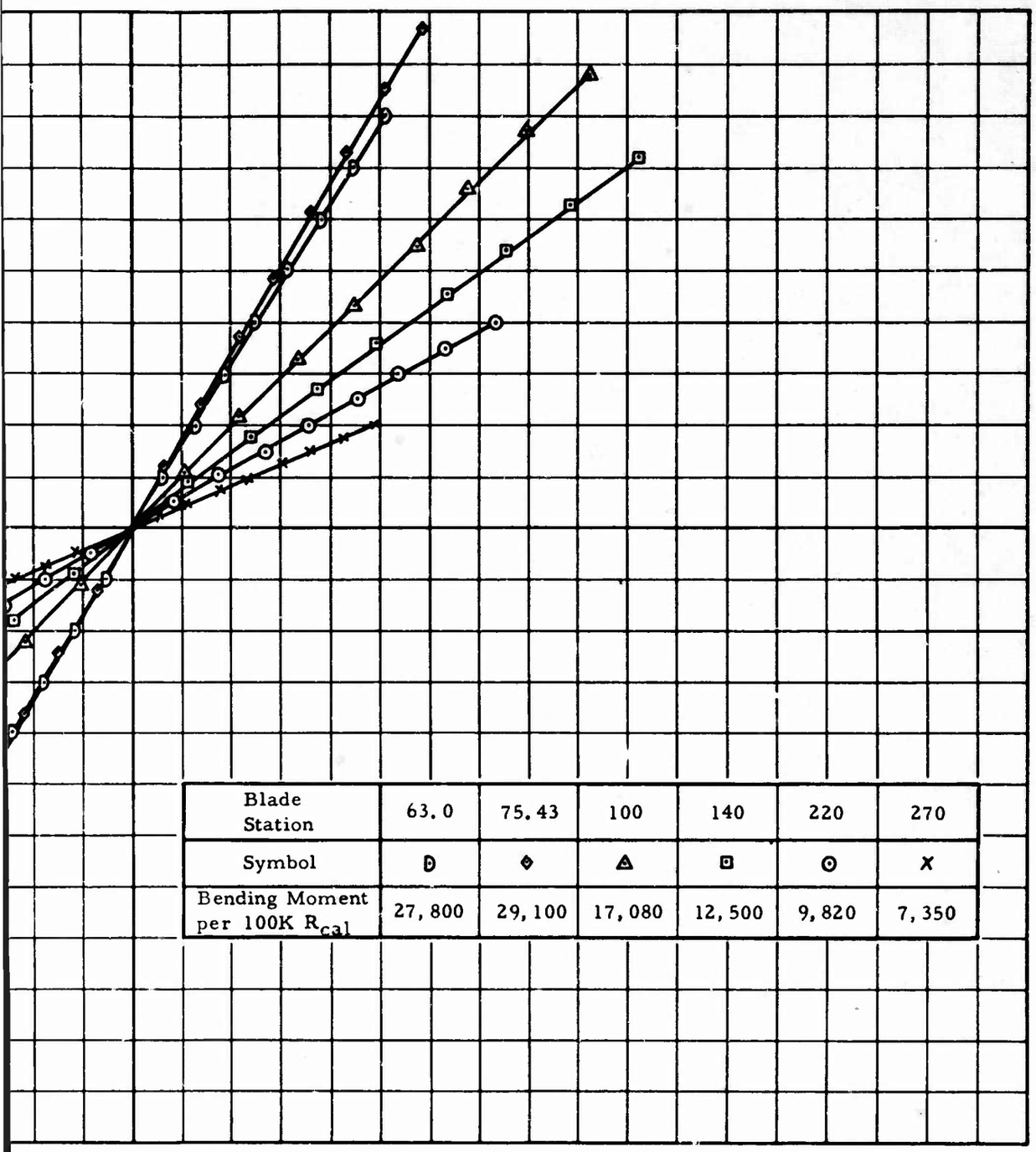

Blade Station	63.0	75.43	100	140	220	270
Symbol	D	◆	△	□	⊙	X
Bending Moment per 100K R_{cal}	27,800	29,100	17,080	12,500	9,820	7,350

-8 -4 0 4 8 12 16 20 24 28 32 36 40 44 48 52 56 60 64 68 72

N - MICROINCH/INCH X 10^{-2}

atic Deflection Test - Flapwise Bending, Front Spar.

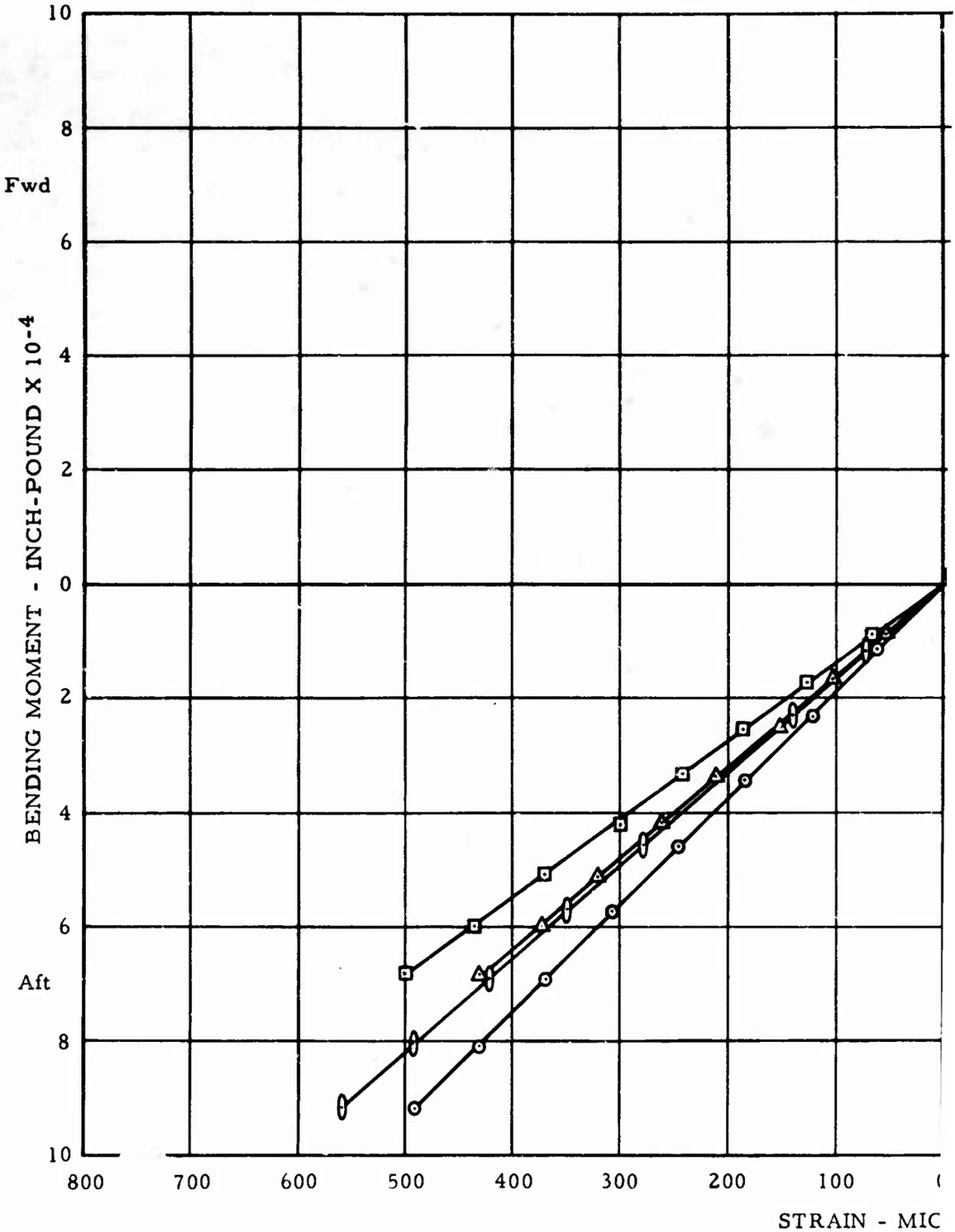

Figure 46. Blade Static

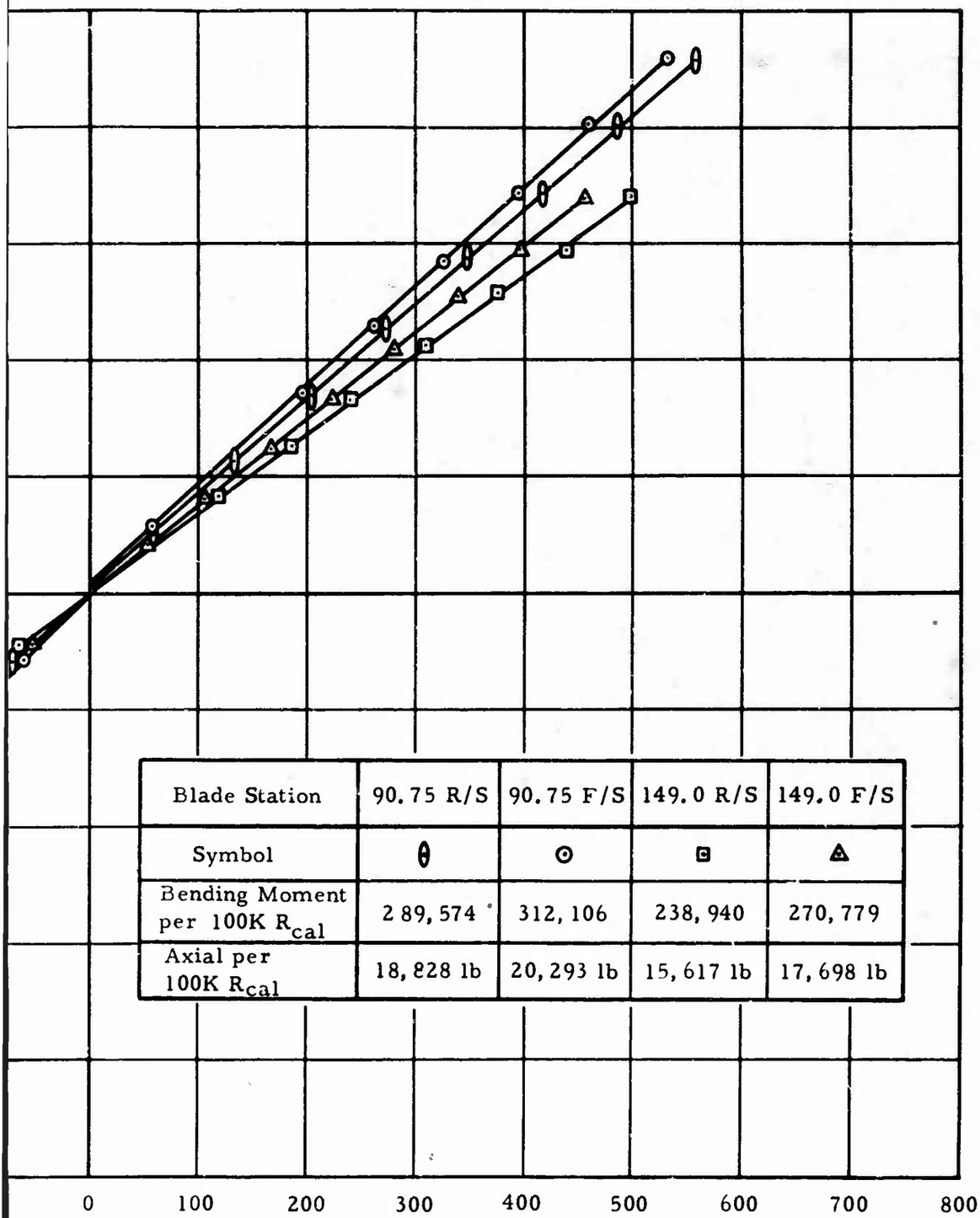

Blade Station	90.75 R/S	90.75 F/S	149.0 R/S	149.0 F/S
Symbol	θ	⊙	⊡	△
Bending Moment per 100K R_{cal}	289,574	312,106	238,940	270,779
Axial per 100K R_{cal}	18,828 lb	20,293 lb	15,617 lb	17,698 lb

0 100 200 300 400 500 600 700 800

- MICROINCH/INCH

Static Deflection Test - Chordwise Bending.

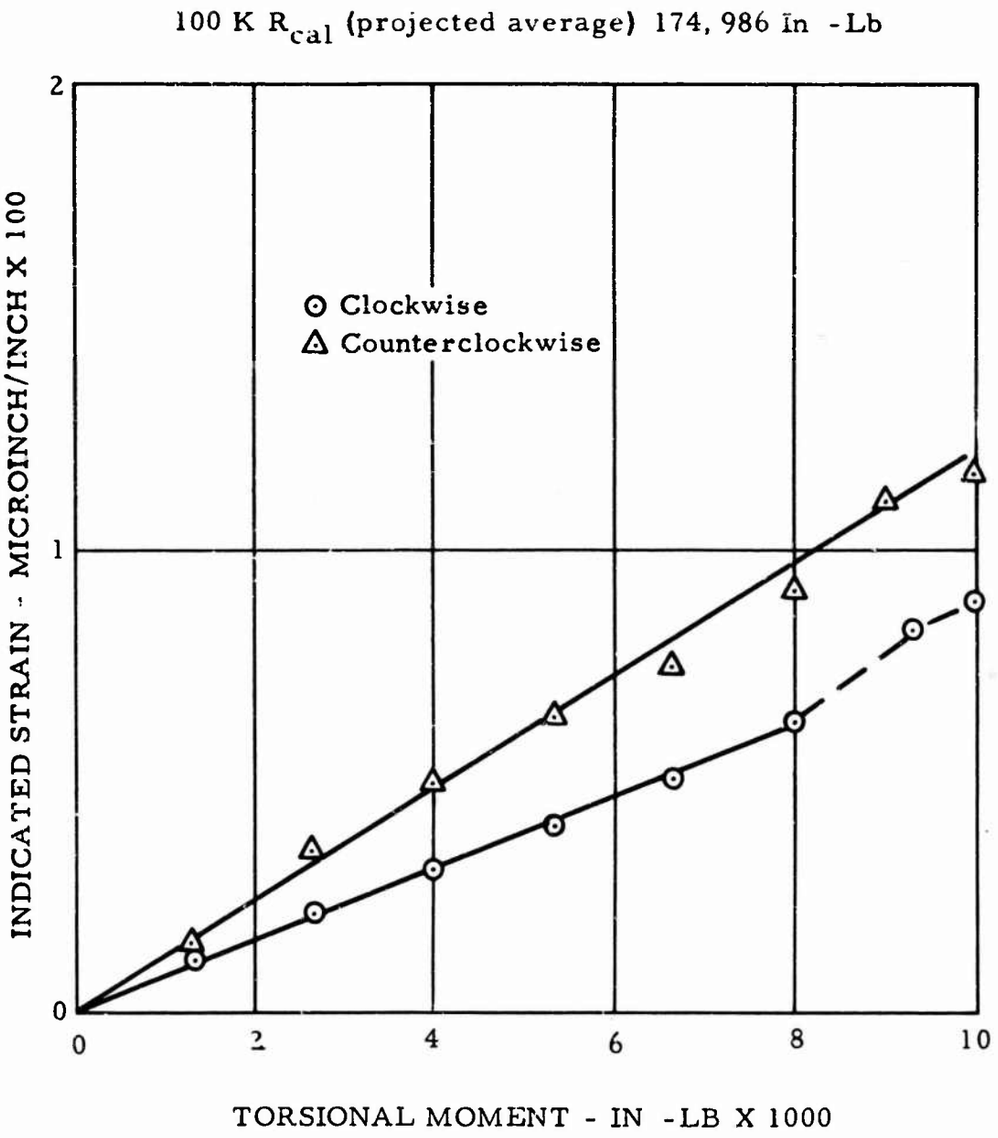

Figure 47. Blade Static Deflection Test - Torsion, Station 38.

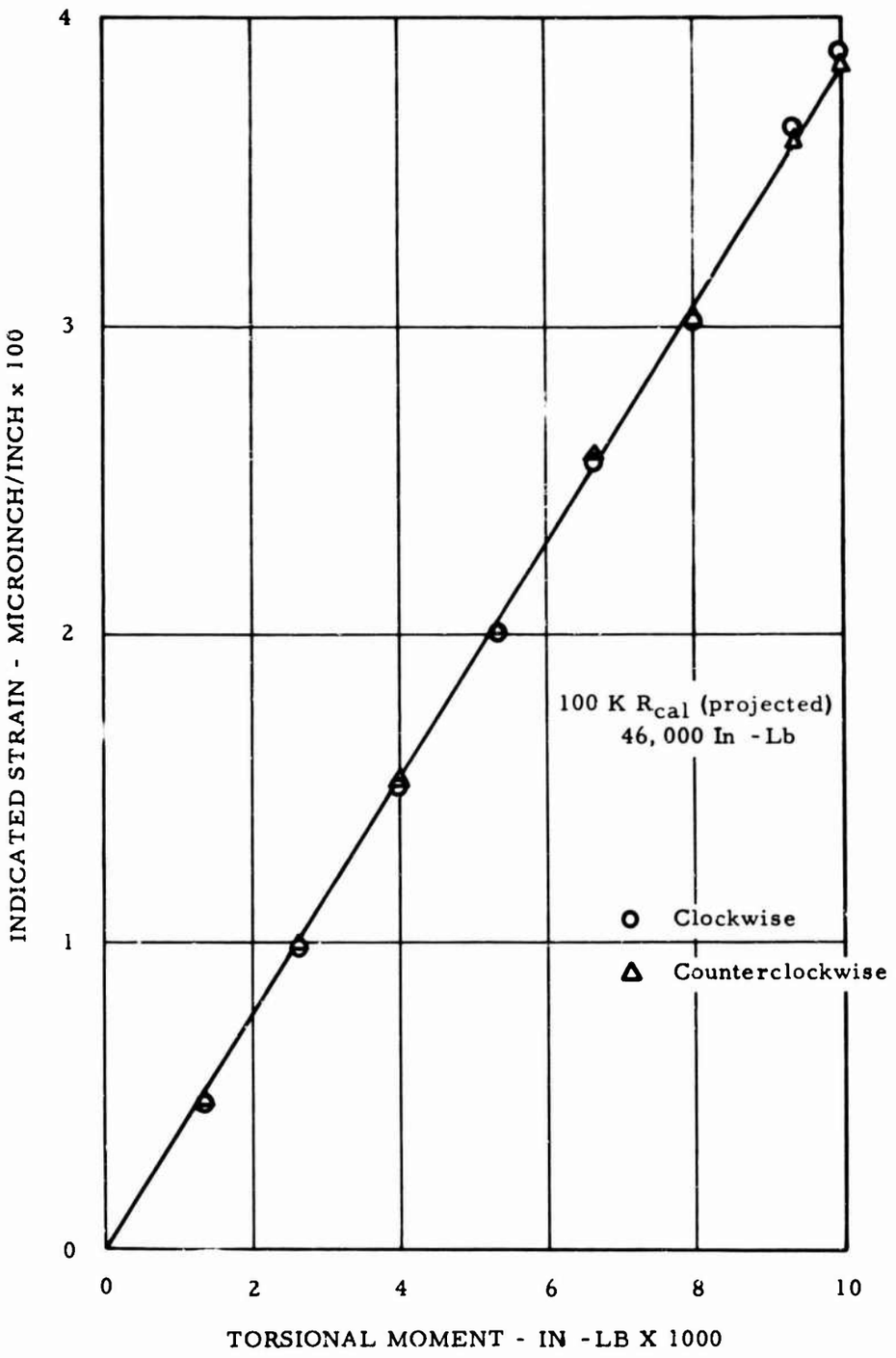

Figure 48. Blade Static Deflection Test - Torsion, Station 83.

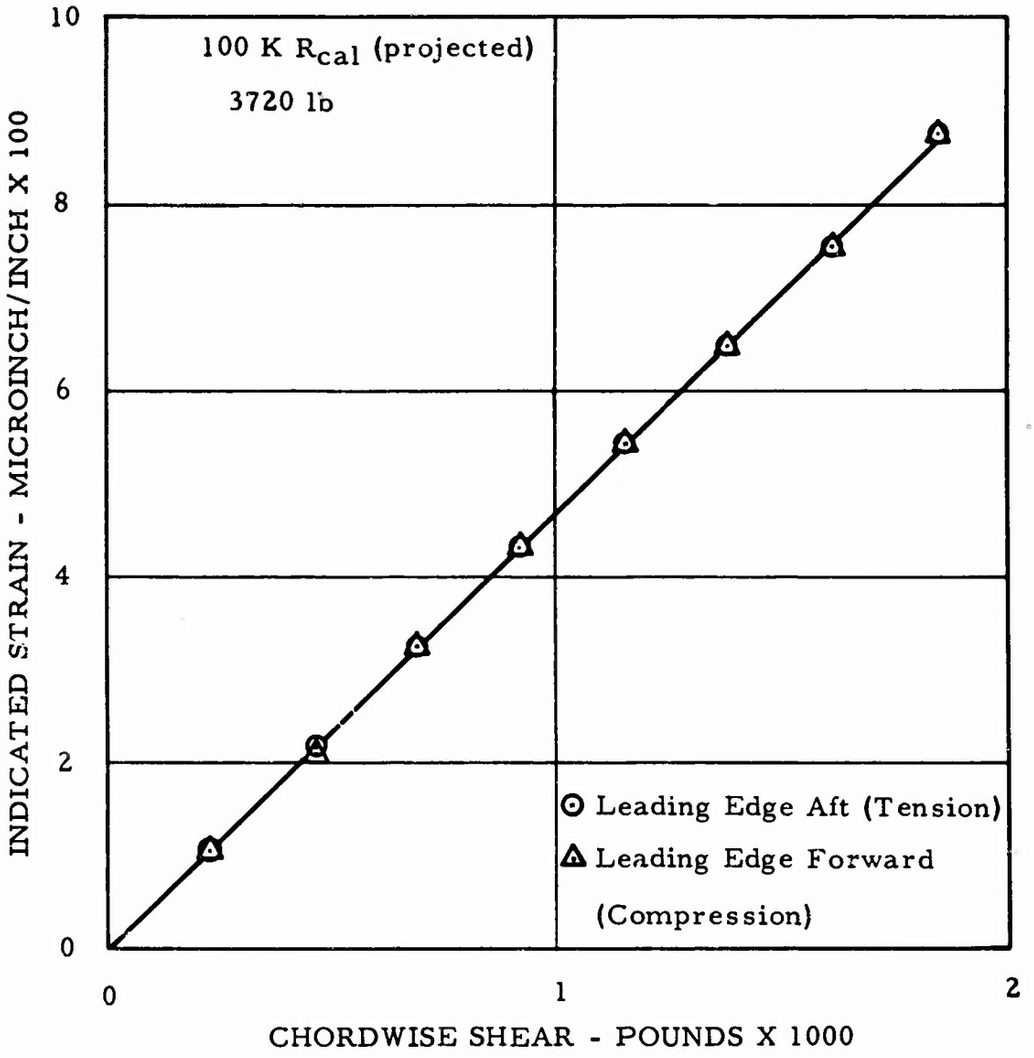

Figure 49. Blade Static Deflection Test - Chordwise Shear.

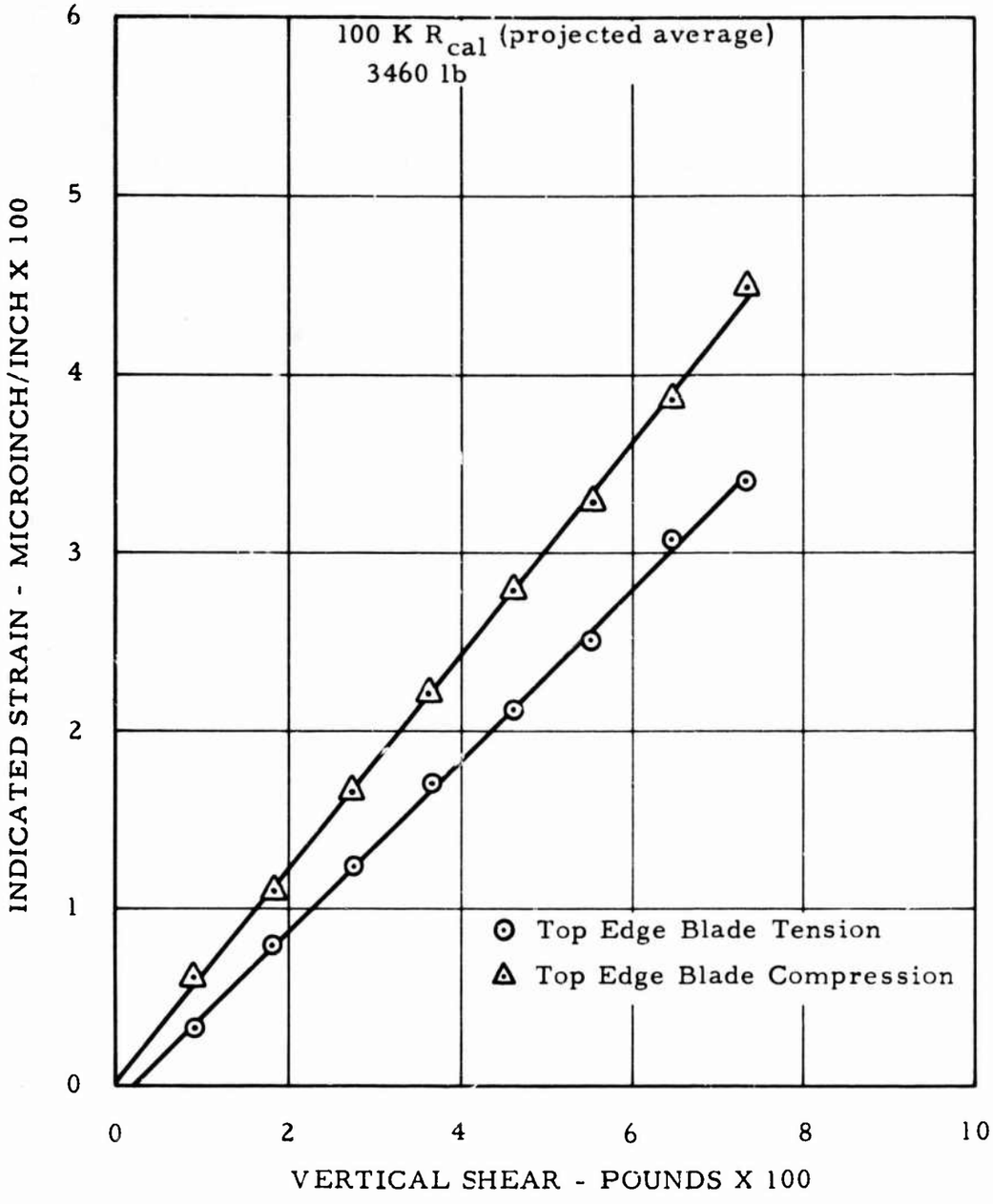

Figure 50. Blade Static Deflection Test - Vertical Shear.

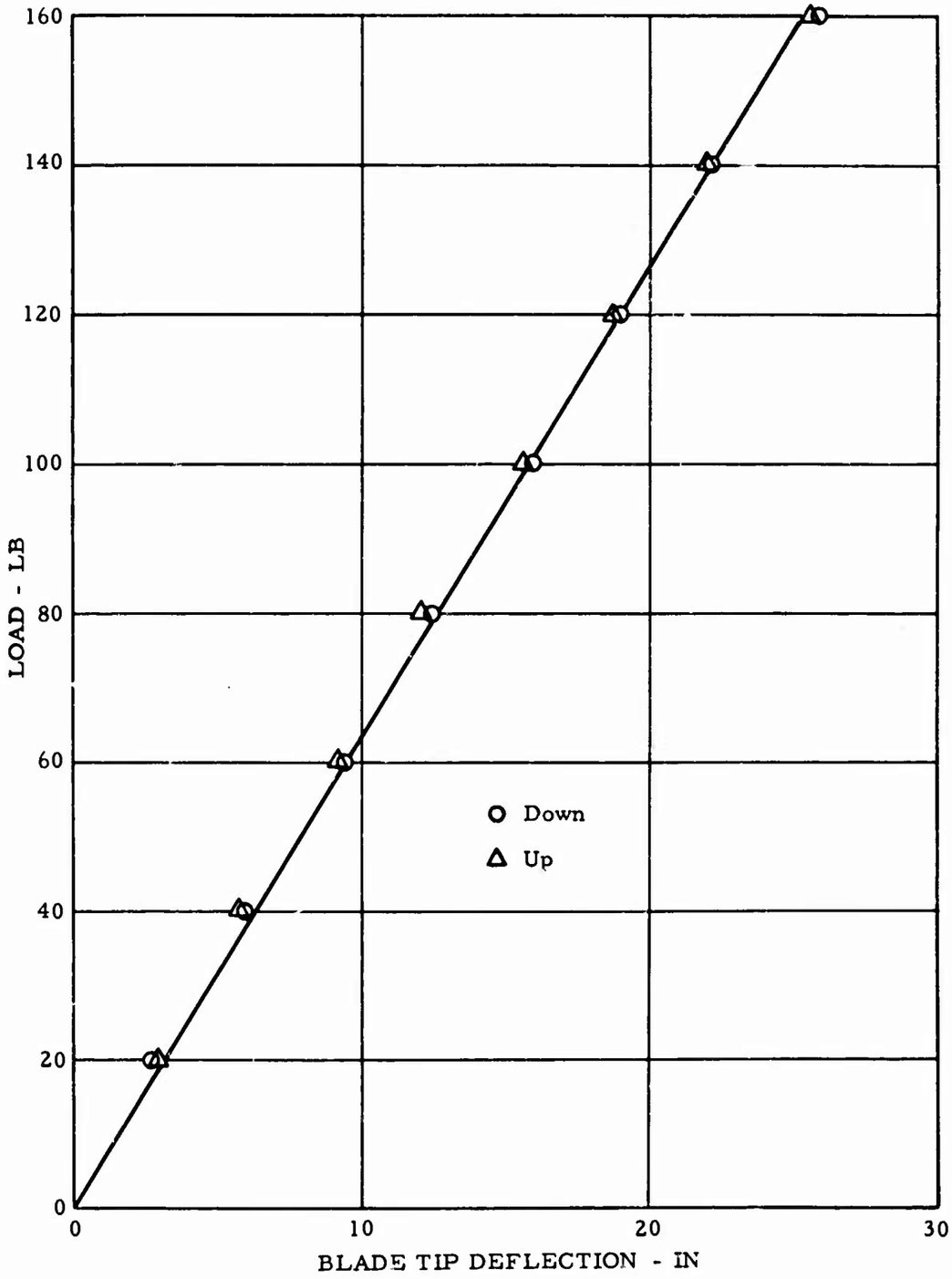

Figure 51. Blade Static Deflection Test - Tip Deflection, Flapping.

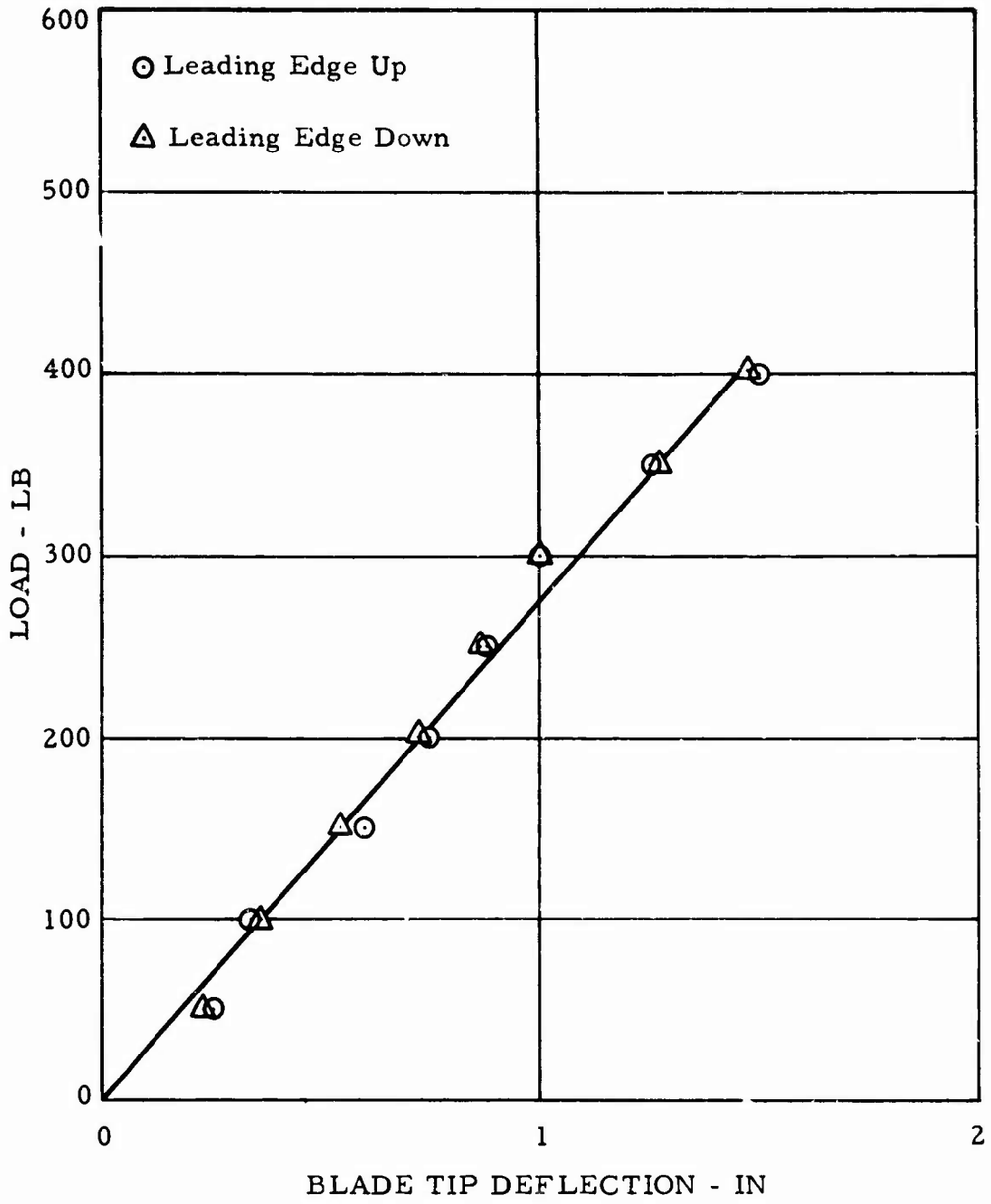

Figure 52. Blade Static Deflection Test - Tip Deflection, Chordwise.

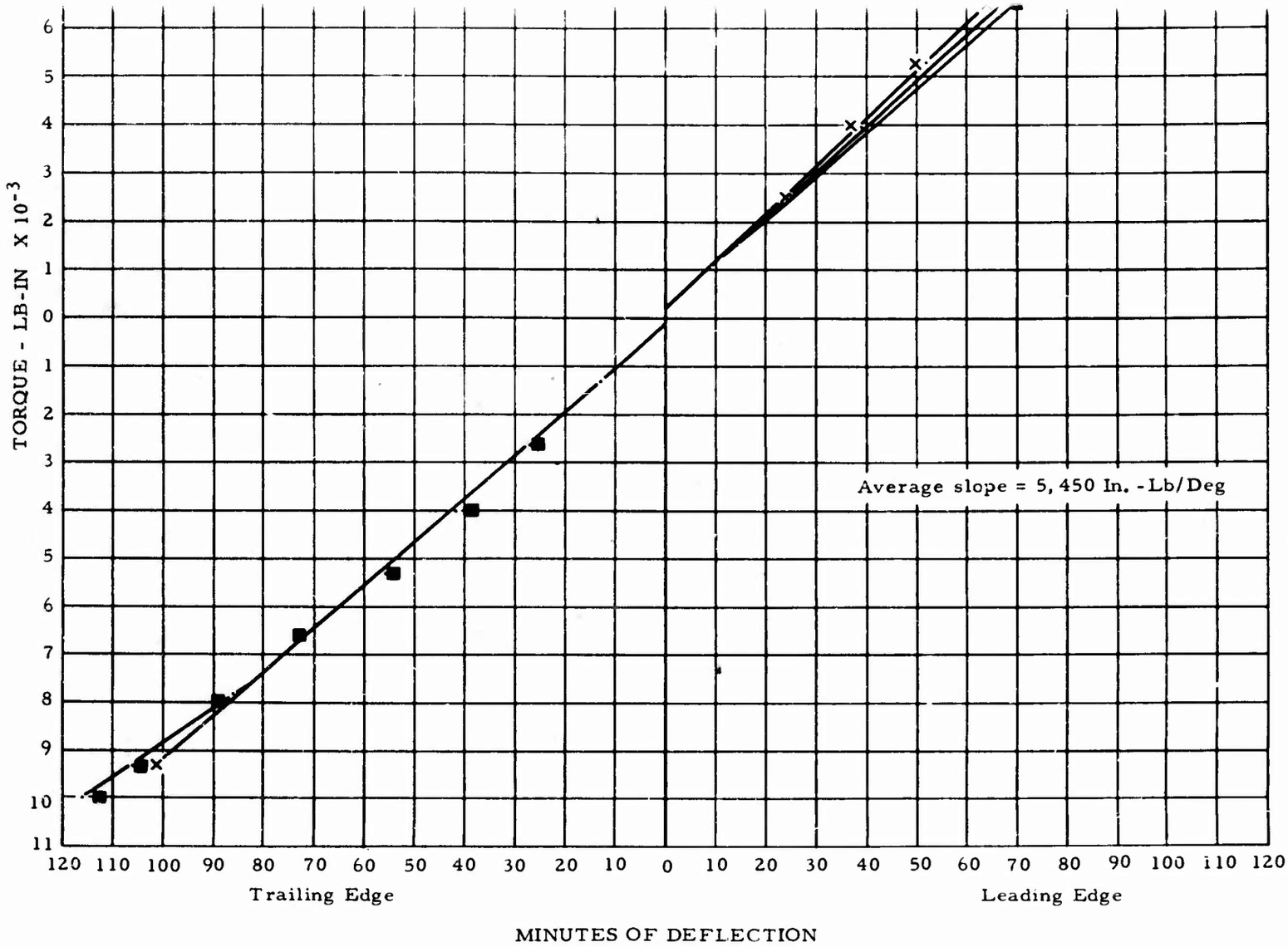

Figure 53. Blade Static Deflection Test - Torsion Deflection at Tip.

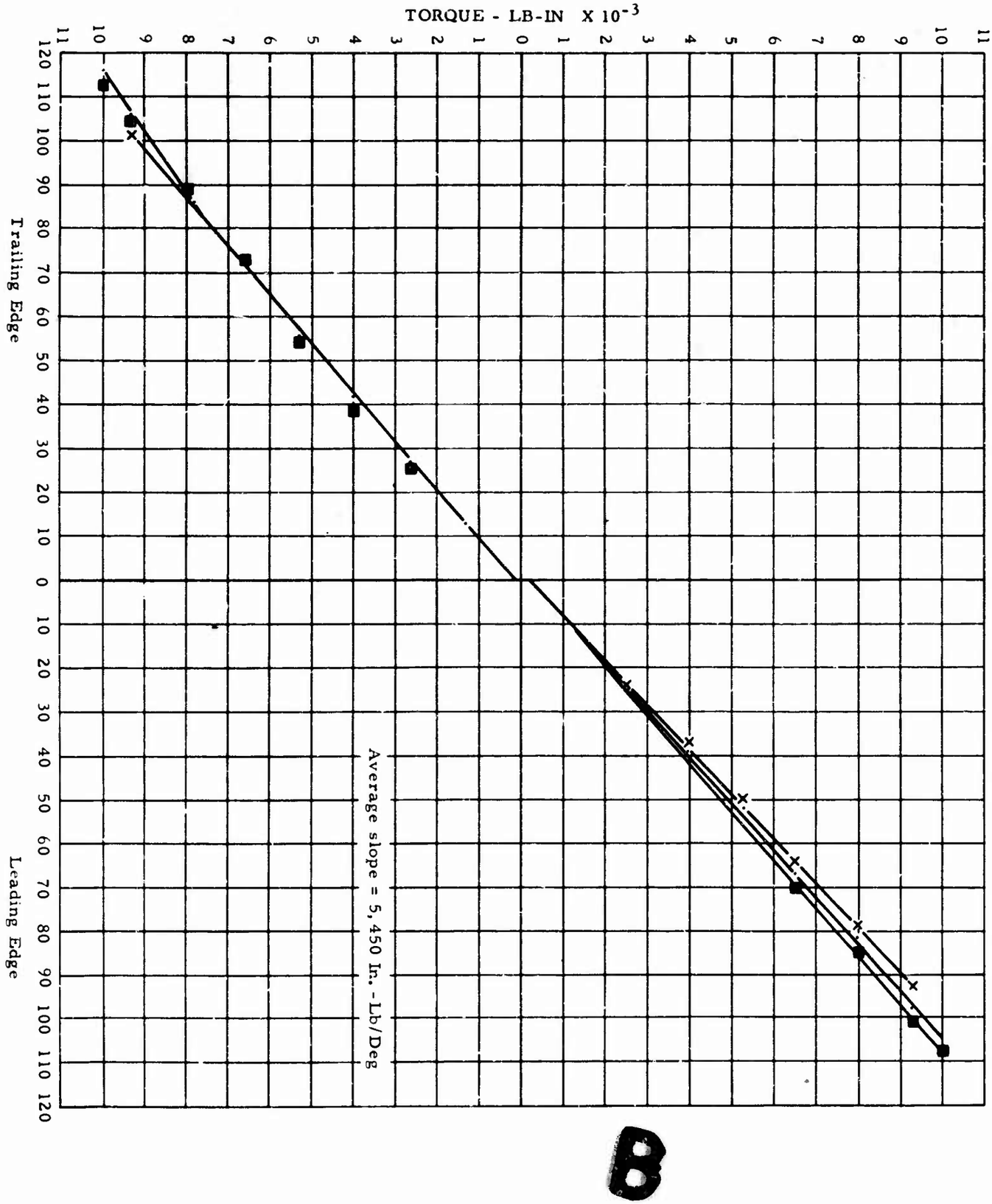
TORQUE - LB-IN X 10^{-3}
11 10 9 8 7 6 5 4 3 2 1 0 1 2 3 4 5 6 7 8 9 10 11
120 110 100 90 80 70 60 50 40 30 20 10 0 10 20 30 40 50 60 70 80 90 100 110 120
Trailing Edge
Leading Edge
Average slope = 5,450 In. -Lb/Deg

8

BLADE-TIP CLOSURE VALVE FUNCTIONAL TEST

SUBJECT

This was a functional test of the blade-tip closure valve and actuation mechanism. It was conducted at the whirl test site during whirl testing in May 1964.

PURPOSE

The purpose of this test was to substantiate the functional operation of the blade-tip closure valve and its actuation system prior to installation on the aircraft.

SPECIMEN

The test specimen consisted of a blade-tip cascade assembly (HTC-AD drawing 385-1124) with a cylinder assembly (HTC-AD drawing 385-1112) attached to a transition duct (HTC-AD drawing 385-9629).

TEST SETUP AND INSTRUMENTATION

The test specimen and transition duct assembly was attached to the yaw control supply duct (gas bled from the stationary Y-duct in the hot gas transfer system) as installed on the whirl test stand (see Figure 54). The necessary hot gas was supplied by the YT-64 gas generator engines as installed in the power module. A butterfly valve in the transition duct was used to control the hot gas supply to the blade-tip closure valve.

Two springs, applying a 35-pound force, were attached to each of the tip closure vanes to simulate the effects of centrifugal force.

A separate air system for cycling the blade-tip closure valve actuating cylinder was supplied by a pressurized accumulator with a normal operating range of 2800 psig. The instrumentation consisted of a position light indicator to monitor the valve position and a linear potentiometer rigged to the actuating mechanisms with its signal output (indicating valve position) recorded on an oscillograph.

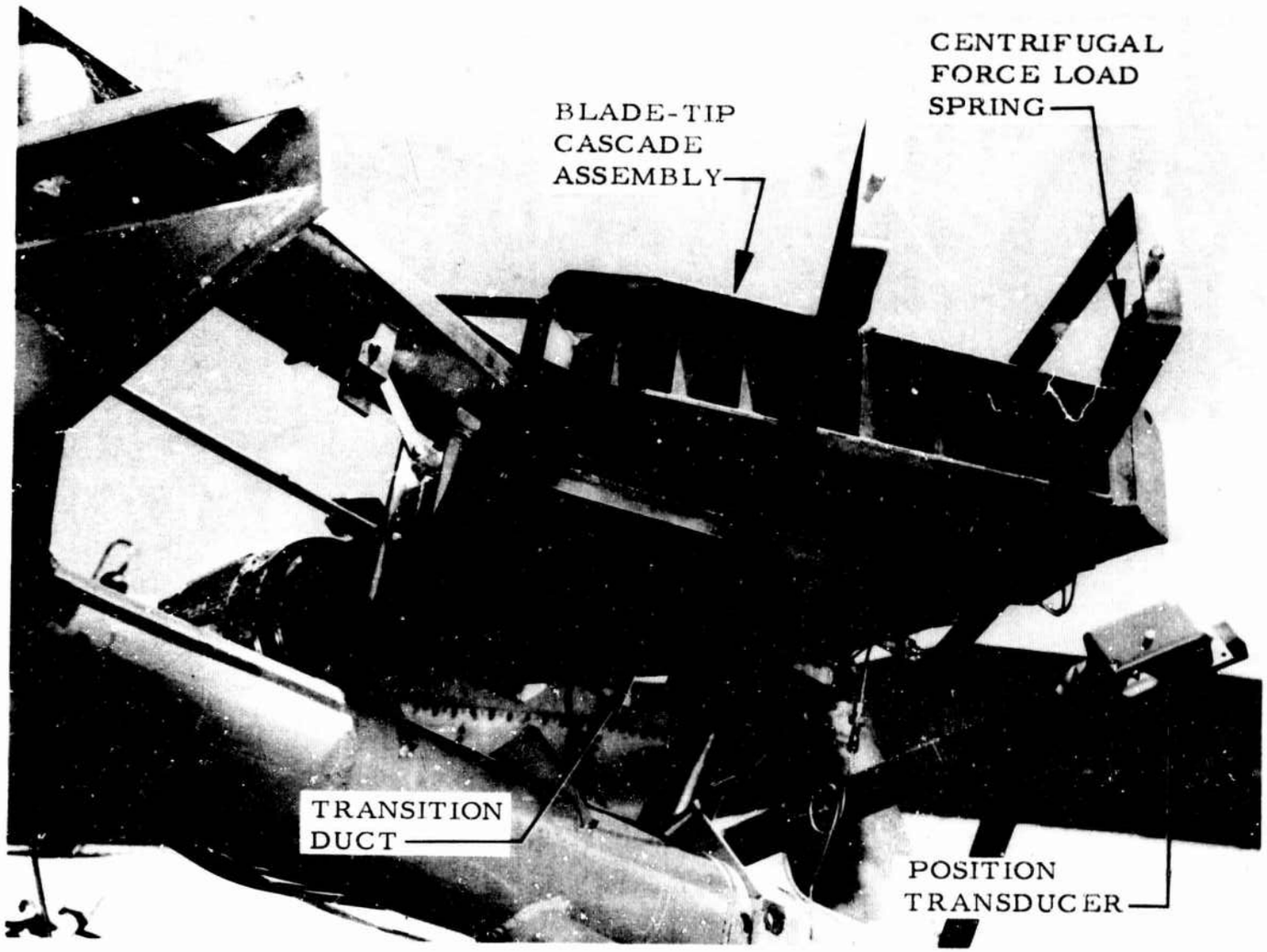

Figure 54. Blade-Tip Closure Valve Functional Test Setup.

TEST RESULTS

A total of 55 cycling functions was performed on the blade-tip closure valve at operating temperatures and pressures. A rework after the first few operating cycles was necessary as a result of insufficient clearances in the high-temperature running condition. The rework consisted of removing material from the ends of the movable vanes to provide 0.010-inch cold clearance.

No other problems were encountered during the remaining portion of the test. The tip closure valve cylinder operated satisfactorily with accumulator pressure ranging from 2800 psig to as low as 1000 psig.

During the testing of the blade-tip closure valve the rotor conditions were as follows:

Collective pitch setting	7 degrees
Rotor speed (N_R)	243 rpm
Lift	15,500 pounds

BLADE ROOT-END FATIGUE TESTS

SUBJECT

These tests concerned the fatigue strength of the XV-9A rotor blade root-end area. They were conducted from February through April 1964 and in January 1965 at the HTC-AD whirl test site.

PURPOSE

The purpose of these tests was to substantiate the structural fatigue capabilities of the blade root-end for the flight test program of the XV-9A, for 100 flight hours.

SUMMARY OF RESULTS

Based on the following results for specimens 1 and 2, an S-N curve was constructed and was used to calculate blade service life, which is reported in Reference 1.

SPECIMEN 1

A fatigue crack in the laminated spar was discovered at blade station 90 after 0.468×10^6 cycles of fatigue test loading under conditions described under Test Procedure.

SPECIMEN 2

A fatigue crack in the laminated front spar was discovered at blade station 94.12 after 0.413×10^6 cycles of the loads described under Test Procedure.

TEST SPECIMENS

The fatigue test specimens basically duplicated the XV-9A rotor blade root-end area, including the retention straps.

GENERAL DESCRIPTION

The rotor-blade spars consisted of 0.025- and 0.050-inch laminated AM 355 CRT sheet strips bonded together with a high-temperature

adhesive. The AM 355 spar material has a 200,000- to 220,000-psi ultimate tensile strength after straightening.

The laminated spars in turn were bonded to root-end fittings that were machined from AM 355 billet stock in an annealed condition. The root-end fittings were then tempered and aged to within 10 percent of the tensile properties of the AM 355 CRT sheet material.

The completed spars were bolted to the inboard blade segments per the flight blade configuration.

DETAIL DRAWINGS OF TEST SPECIMEN

285-0113	Segment assembly
285-0121-3	Strap assembly, forward
285-0121-5	Strap assembly, aft
285-0138	Structural installation
285-0139	Structure installation
285-0165	Coupling assembly - flexure
285-0166	Structure installation
385-1100	Rotor blade assembly
385-1114	Fitting - front spar
385-1115	Fitting - rear spar
385-9617-3	Laminated front spar*
385-9617-5	Laminated rear spar*
285-0326-9	Bearing (pitch control blade)**

TEST SETUP

The test specimen was set up in a test fixture (HTC-AD drawing 385-9602). This test fixture was capable of applying various types of loading to the specimen. See Figure 55 for a general schematic showing the specimen and types of loading applied. The root-end area front spar with pitch arm link is shown in Figure 56. The station 159 torque arrangement system and the flapwise drive system view from the leading

* These test spars duplicated the flight blade spars up to station 120. The remaining portion of the spars preserved structural continuity and provided load application provisions. The flight blade spar drawing number is 385-1108.

**The bearing reacted all steady and vibratory torque applied to the specimen in a manner similar to the flight ship.

edge is shown in Figure 57. The station 63-73 torque device and a view of the root-end fitting rear spar are shown in Figure 58. The centrifugal load application system is shown in Figure 59. The chordwise drive system linkage and the feed input system from the flapping motion are shown in Figures 60 and 61.

INSTRUMENTATION

The instrumentation, which consisted of two 20-channel balance and calibration units and a recording oscillograph with an integral developer, served two functions: (1) to monitor the external load inputs statically and dynamically, and (2) to monitor the moment distributions as applied to the specimen.

EXTERNAL LOADING

Centrifugal force load cell - Set up in series with the specimen; monitored centrifugal force loadings.

Torsion bars, station 159 - Measured steady and vibratory loads at station 159 in the form of steady and cyclic torsion.

Leaf spring, station 68 - Measured the vibratory torsion input at station 68. 0.

Pitch arm link - Set up as a reaction member, it measured the steady and vibratory torsion as applied to the specimen.

BLADE SPECIMEN

Presented in Figure 62 is a sketch showing the strain gage bridges installed on the test blade specimen, and duplicating the root-end area of the XV-9A instrumented flight blade. Flapwise bending bridges were located at:

Specimen 1

Station 53, front and rear root-end fitting
Station 63, front and rear root-end fitting
Station 71. 5, front and rear root-end fitting
Station 75. 4, front and rear root-end fitting
Station 85. 0, front and rear laminated spar
Station 112, front and rear laminated spar

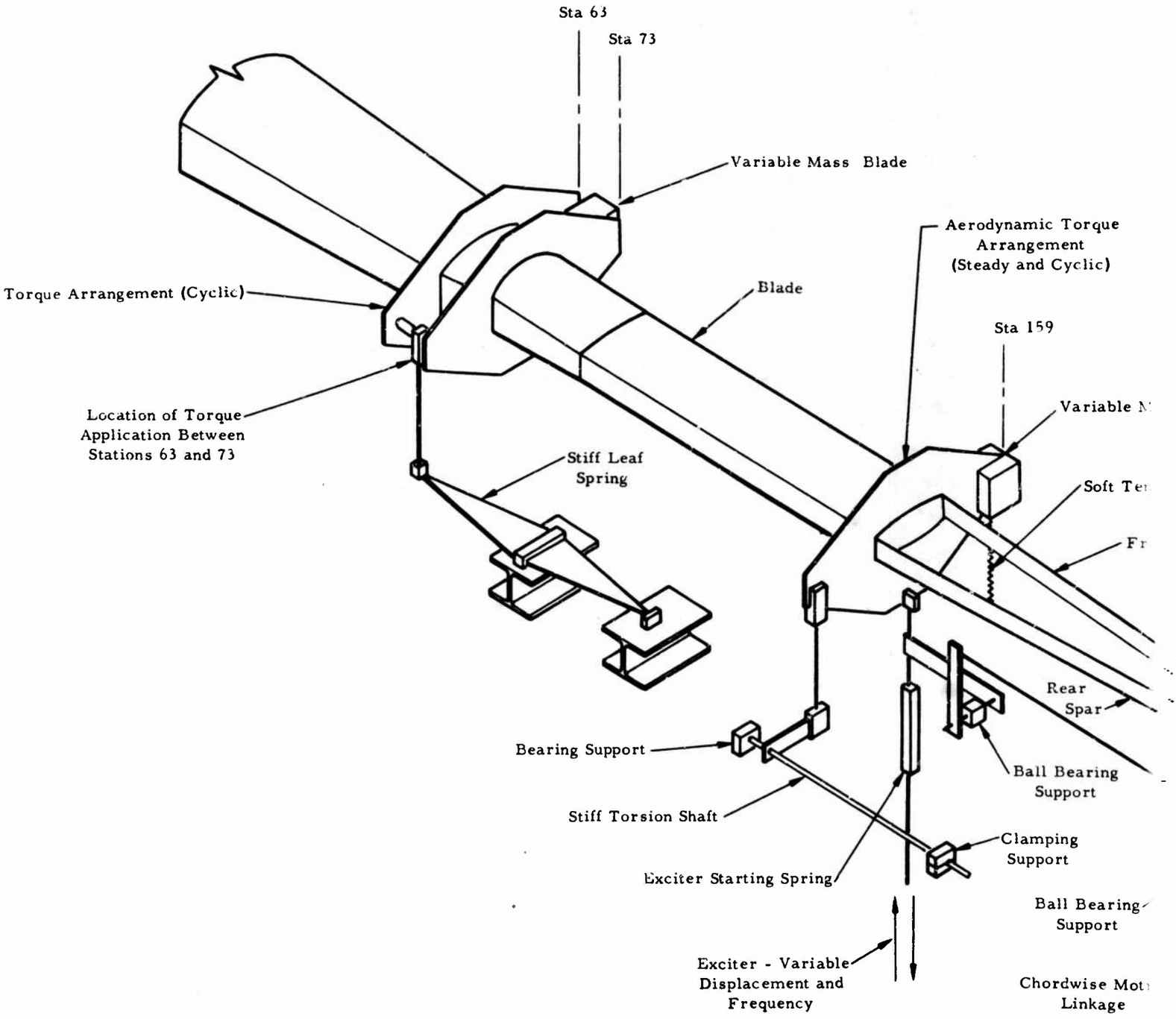

Figure 55. Blade Root-End Fatigue Test - Loading

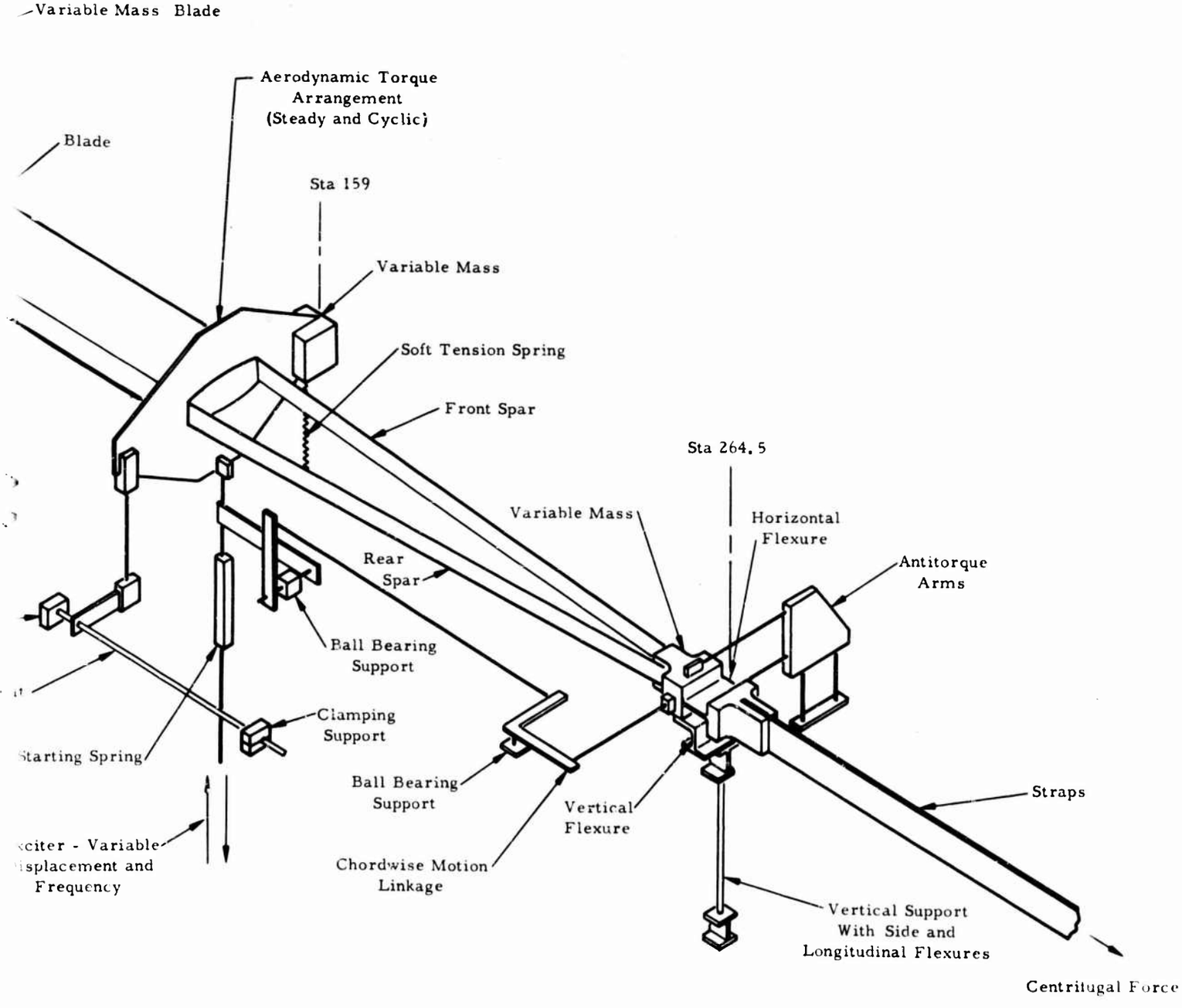

Blade Root-End Fatigue Test - Loading Schematic.

B

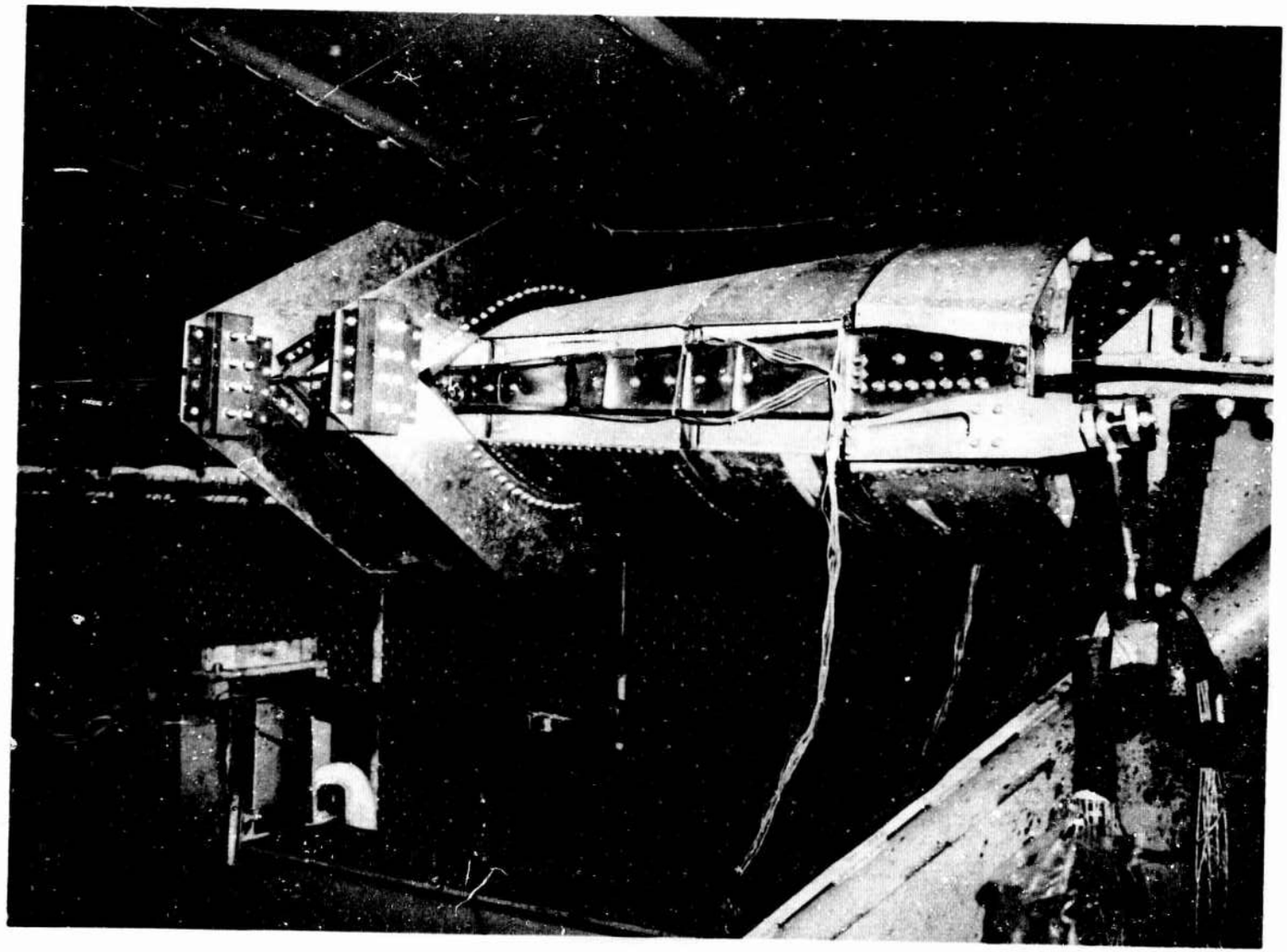

Figure 56. Blade Root-End Fatigue Test Fixture - Leading Edge of Specimen.

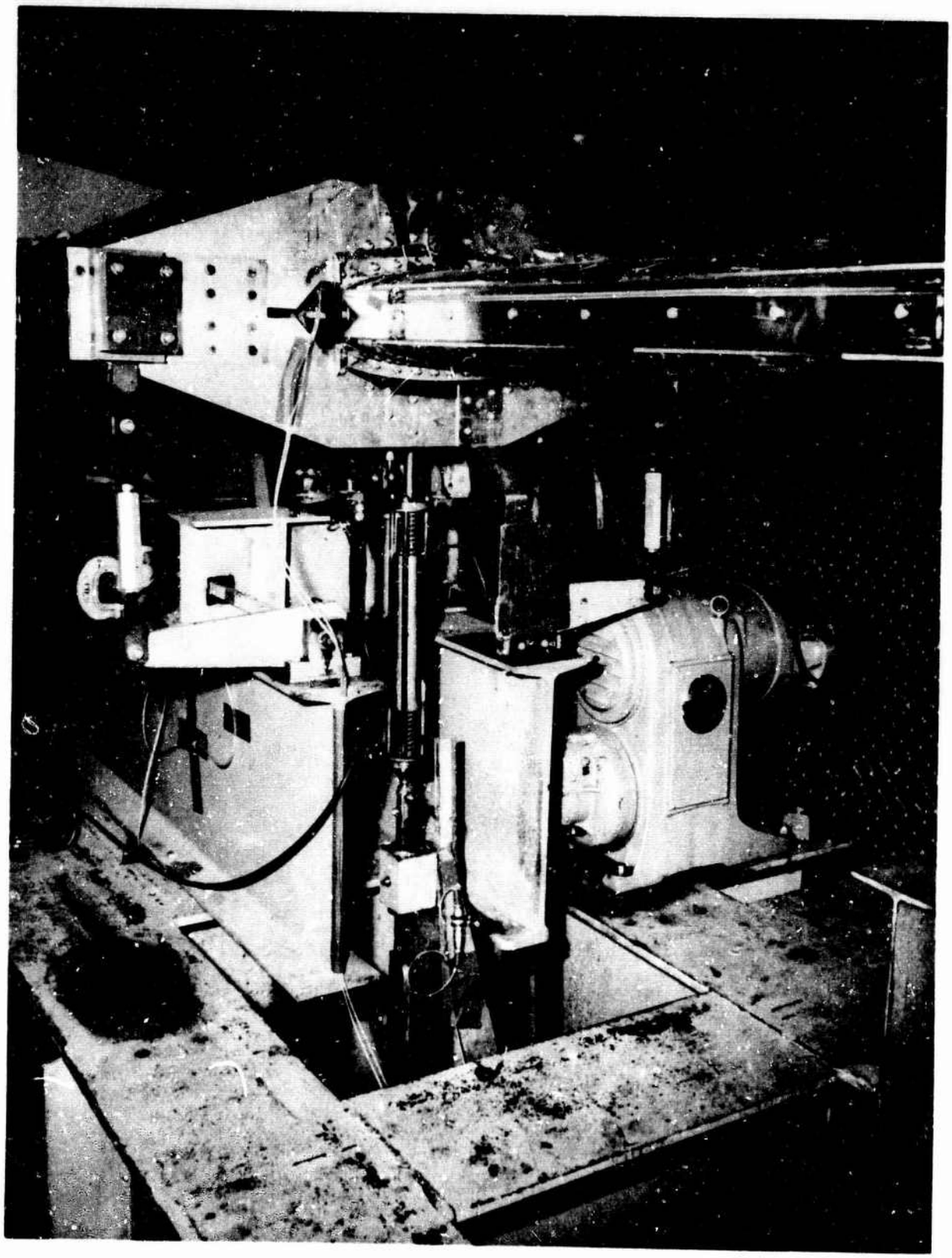

Figure 57. Blade Root-End Fatigue Test Fixture - Drive System.

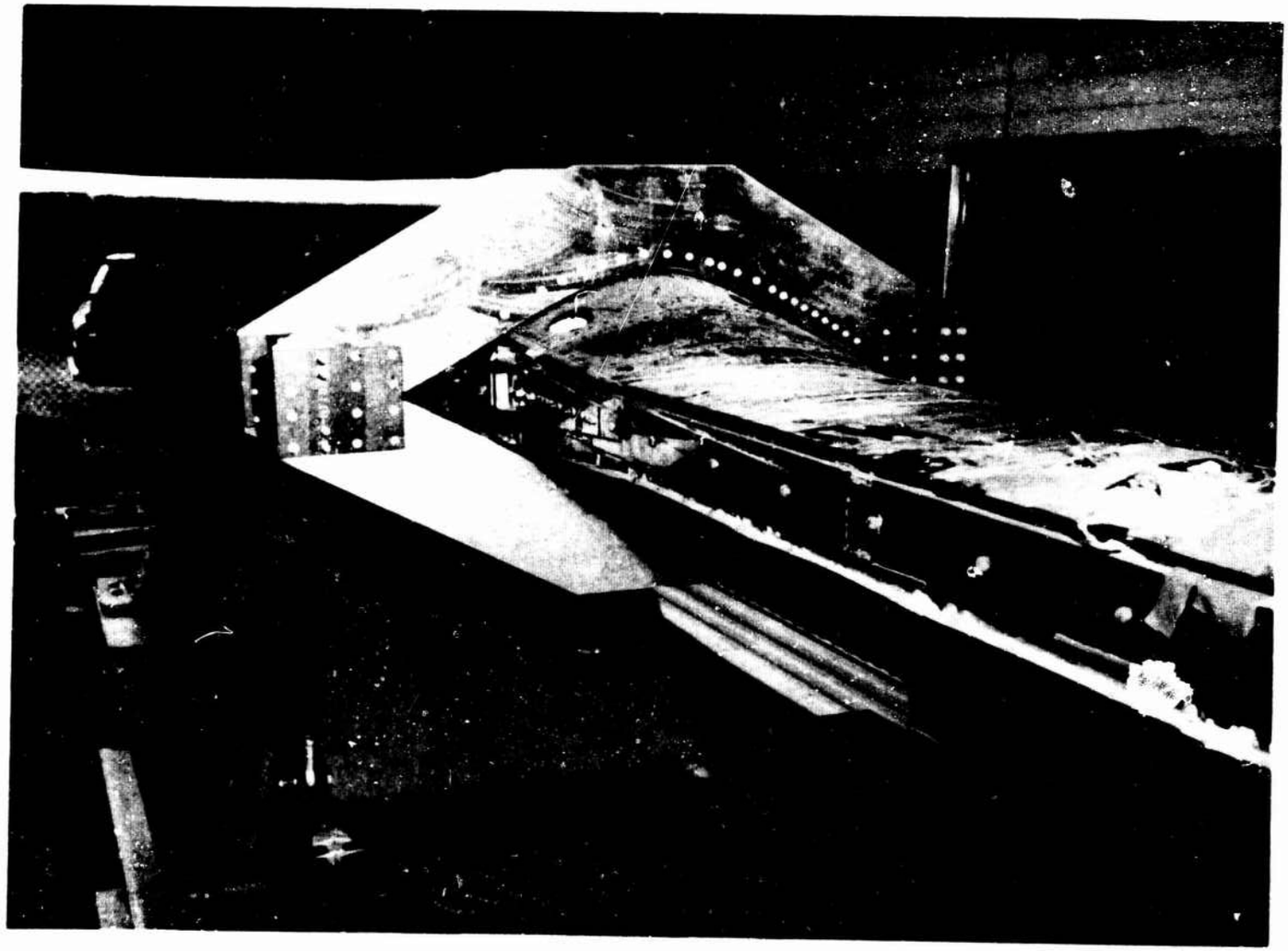

Figure 58. Blade Root-End Fatigue Test Fixture - Trailing Edge of Specimen

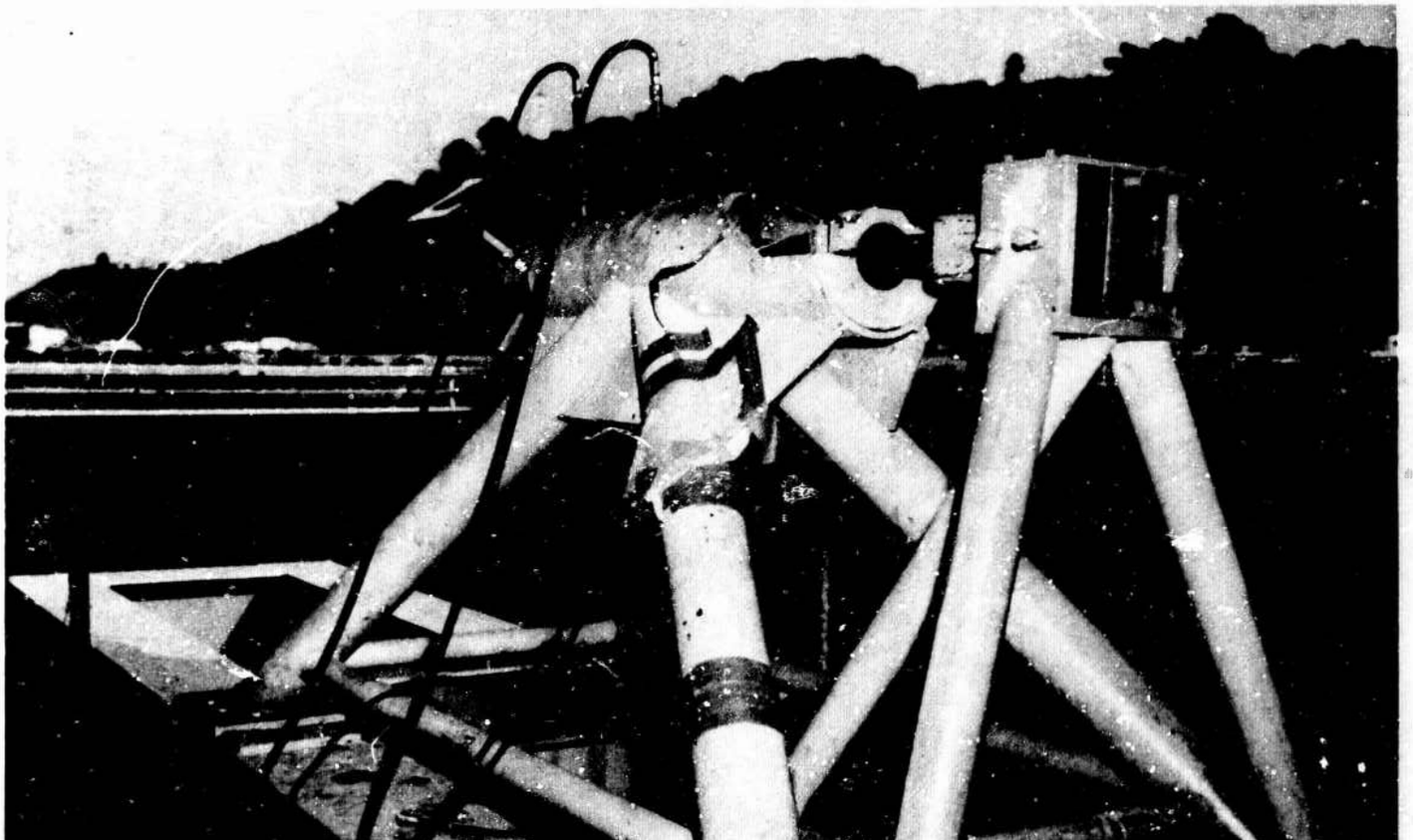

Figure 59. Blade Root-End Fatigue Test Fixture - Centrifugal Loading System.

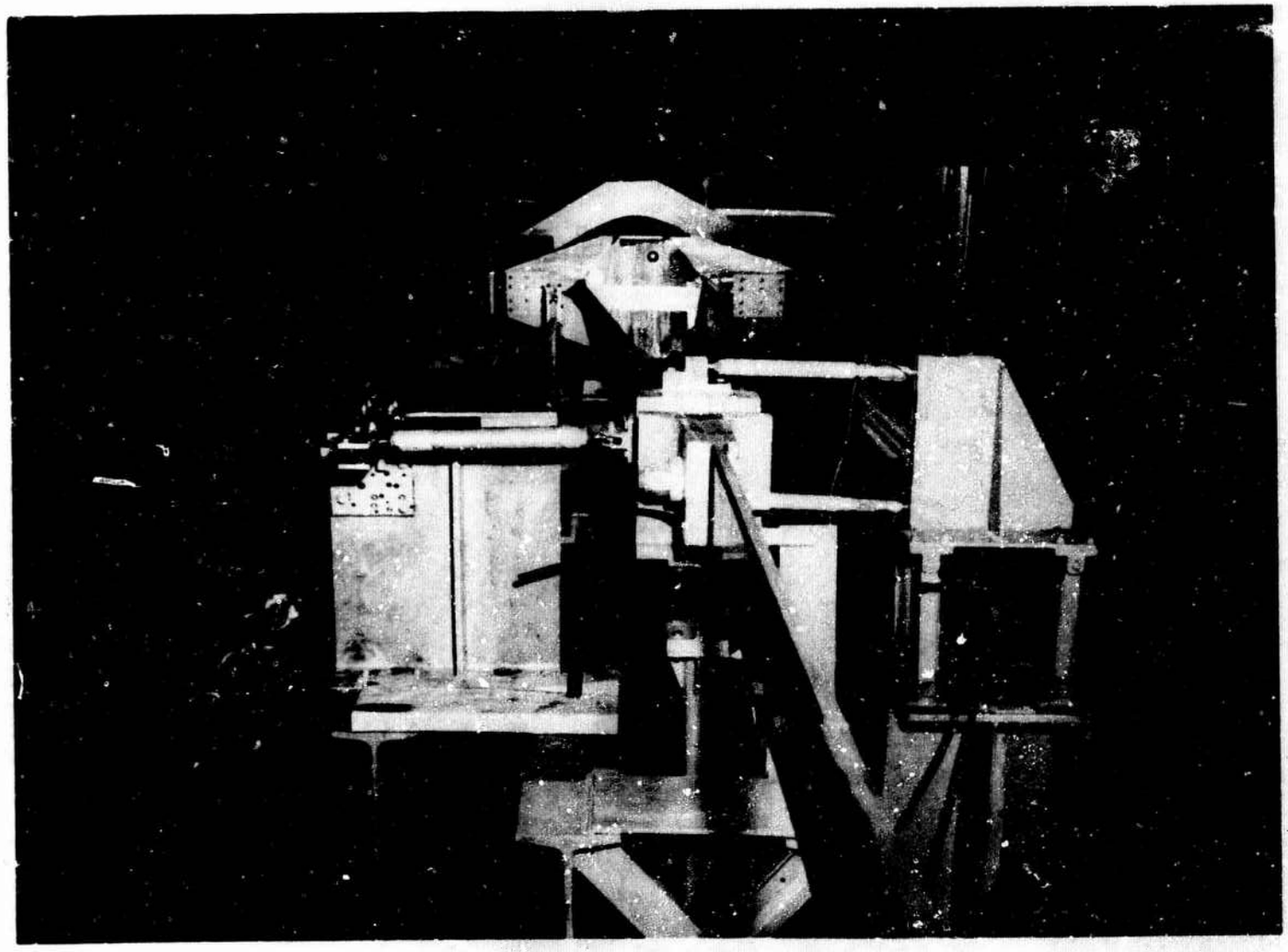

Figure 60. Blade Root-End Fatigue Test Fixture - Chordwise Input Mechanism.

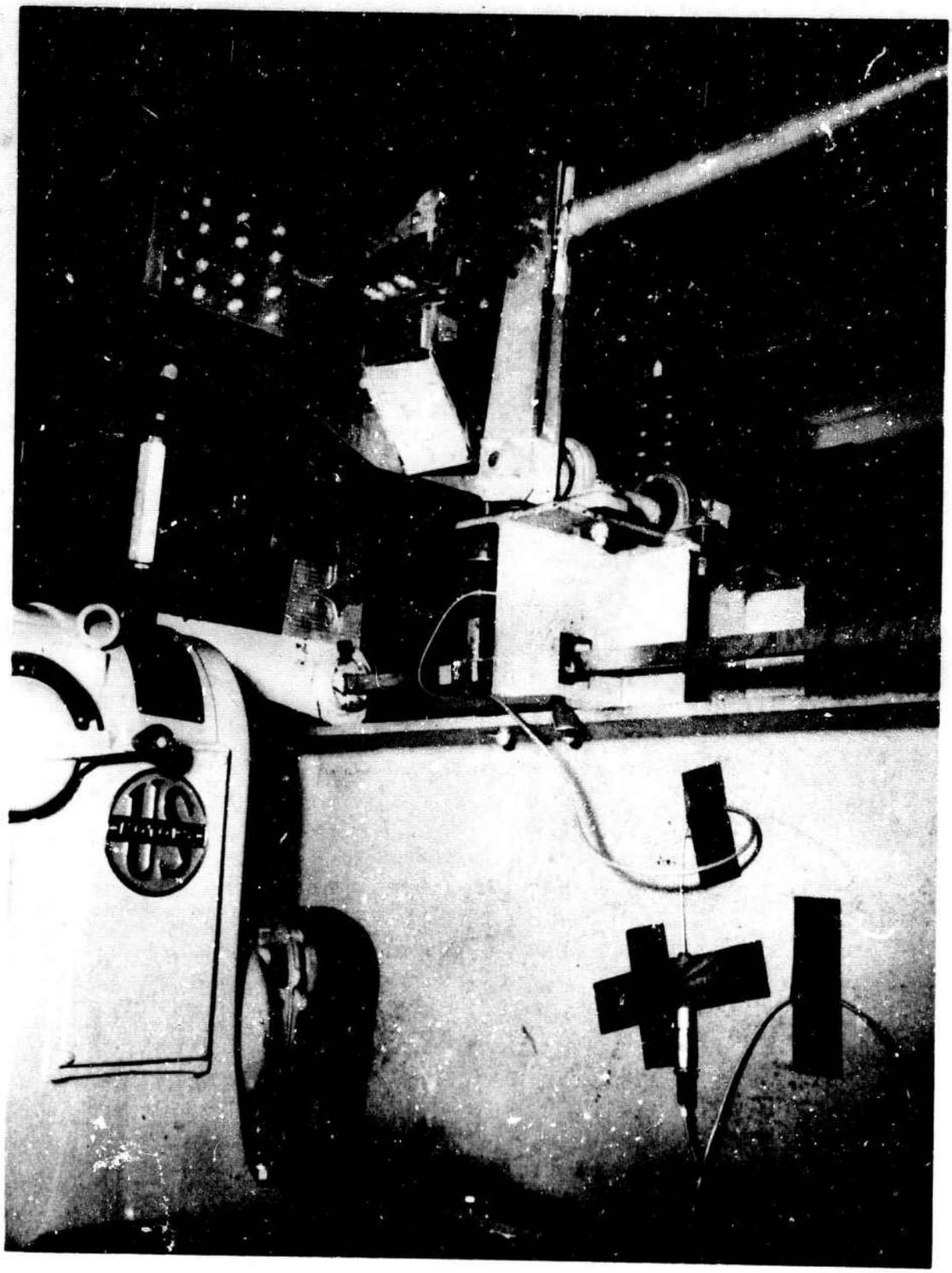

Figure 61. Blade Root-End Fatigue Test Fixture - Chordwise Actuating Mechanism.

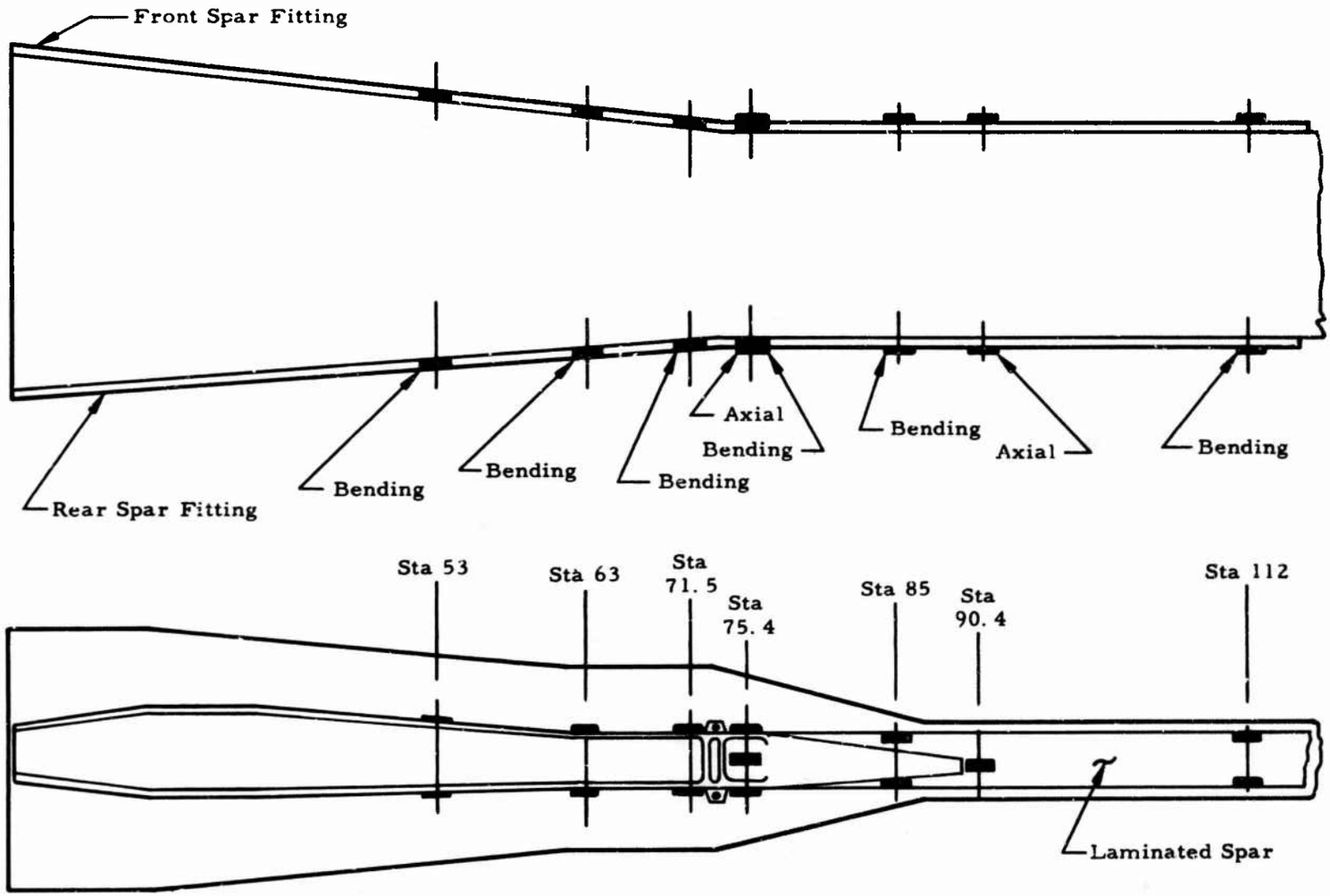

Figure 62. Blade Root-End Fatigue Test - Instrumentation Locations - Specimen 1.

Specimen 2

Station 53. 5, front and rear root-end fitting
Station 63. [illegible] front and rear root-end fitting
Station 72. 2[illegible], front and rear root-end fitting
Station 76. 12, front and rear root-end fitting
Station 88. 75, front and rear laminated spar
Station 112. 5, front and rear laminated spar

Chordwise axial bridges were located at:

Specimen 1

Station 75. 4, front and rear root-end fitting
Station 90. 4, front and rear root-end fitting

Specimen 2

Station 76. 12, front and rear root-end fitting
Station 79. 62, front and rear root-end fitting
Station 91. 00, front and rear laminated spar

All load cells and blade strain-gage bridge circuits were routed to a calibration, balance, and switching unit prior to being fed into the oscillograph.

During testing operations, the critical bending stations 63 and 73 (determined by whirl test to be the critical bending locations) and the axial load at station 90. 43, were set up for constant monitoring on a separate direct-writing oscillograph.

A pair of accelerometers, located at station 159, measured horizontal and vertical accelerations and aided in maintaining proper load levels on the direct-writing oscillograph.

TEST PROCEDURE

Prior to setting the specimen in the test fixture, all the external load cells were calibrated in a test machine.

The test specimen was installed in the test fixture and all gages on the specimen were calibrated versus known moments or loads and appropriate constants were derived from this information. Checks were made to see if data were repeatable and linear.

On setting up the test, all external load cells were recorded on a strain indicator in a null load condition. The pitch arm link was connected from the fixture to the specimen. The centrifugal force was applied through the hydraulic cylinder and monitored by the centrifugal force load cell. The torsion bars at station 159 were hooked up to apply a steady torsion in the system. This was cross-checked by the pitch arm link readings.

The leaf spring torque system at station 68 applied vibratory torsion, and its reading was monitored on the recording oscillograph.

All external bridges were monitored, and the following steady loads were applied to the specimens:

Centrifugal force	= 116,000 lb
Steady torsion, station 159	= +13,000 in -lb
Pitch arm link	= 800 lb (reaction load between the link and the vertical reaction flexure at station 19)

The dynamic loads applied to the specimen were as follows:

Specimen 1

Flapwise bending moment, station 73	±14,000 in -lb
Chordwise bending moment, station 90.43	±85,000 – 90,000 in -lb
Torsion at station 159.0	±7,300 in -lb
Torsion at station 68.0	±18,000 in -lb
Pitch arm link, torsion at station 19.0	±25,500 in -lb

Specimen 2

	Phase 1	Phase 2
Flapwise bending moment, station 76.12	±13,300 in-lb	±13,000 in -lb
Chordwise bending moment, station 91.0	±92,000 in -lb	±84,300 in -lb
Torsion at station 159.0	±6,000 in -lb	±3,000 in -lb
Torsion at station 68.0	±15,900 in -lb	±8,000 in -lb
Pitch arm link, torsion at station 19.0	±21,900 in -lb	±11,000 in -lb

For the dynamic loadings, the flapping bending moments were excited by the crank-type drive system approaching the flapwise natural frequencies. The chordwise loading was excited by a coupling system utilizing the flapping drive system displacement.

The chordwise bending system had a longer effective length, hence a lower natural resonant frequency. For this testing, the magnitude of the chordwise loads required that the chordwise natural frequency be the determining factor in selecting the speed requirements of the test. Both flapping and chordwise moments are monitored on the specimen.

The cyclic torsion moment at station 159 was determined by the deflection and frequency at that station in conjunction with a cantilevered mass. The torsion bar system gives the differential torsion moment superimposed over the steady torsion moment.

The cyclic torsion moment at station 68 was determined by the deflection and frequency of the cantilevered mass at that station, which was reacted by the leaf spring on the other side, thus setting up the vibratory couple.

The pitch arm link was relatively stationary in the root-end system, but reacted the torsion inputs as a couple with the vertical flexure system.

Presented in Figure 63 is a typical oscillographic trace of the dynamic loadings as recorded during the fatigue test of the root-end specimen.

TEST RESULTS

SPECIMEN 1

A total of 468, 152 cycles was applied before a crack was noted in the front spar through the bolt hole at approximately station 90. Testing was terminated at this point. Of these cycles, 32, 100 were accumulated during preliminary runs, some of which were at a higher load level. See Table 11 for a breakdown of this test.

Upon removal and inspection of the spars, the following failures were noted:

1. On the rear spar, at station 90, one outboard lamination was cracked. See Figure 64.

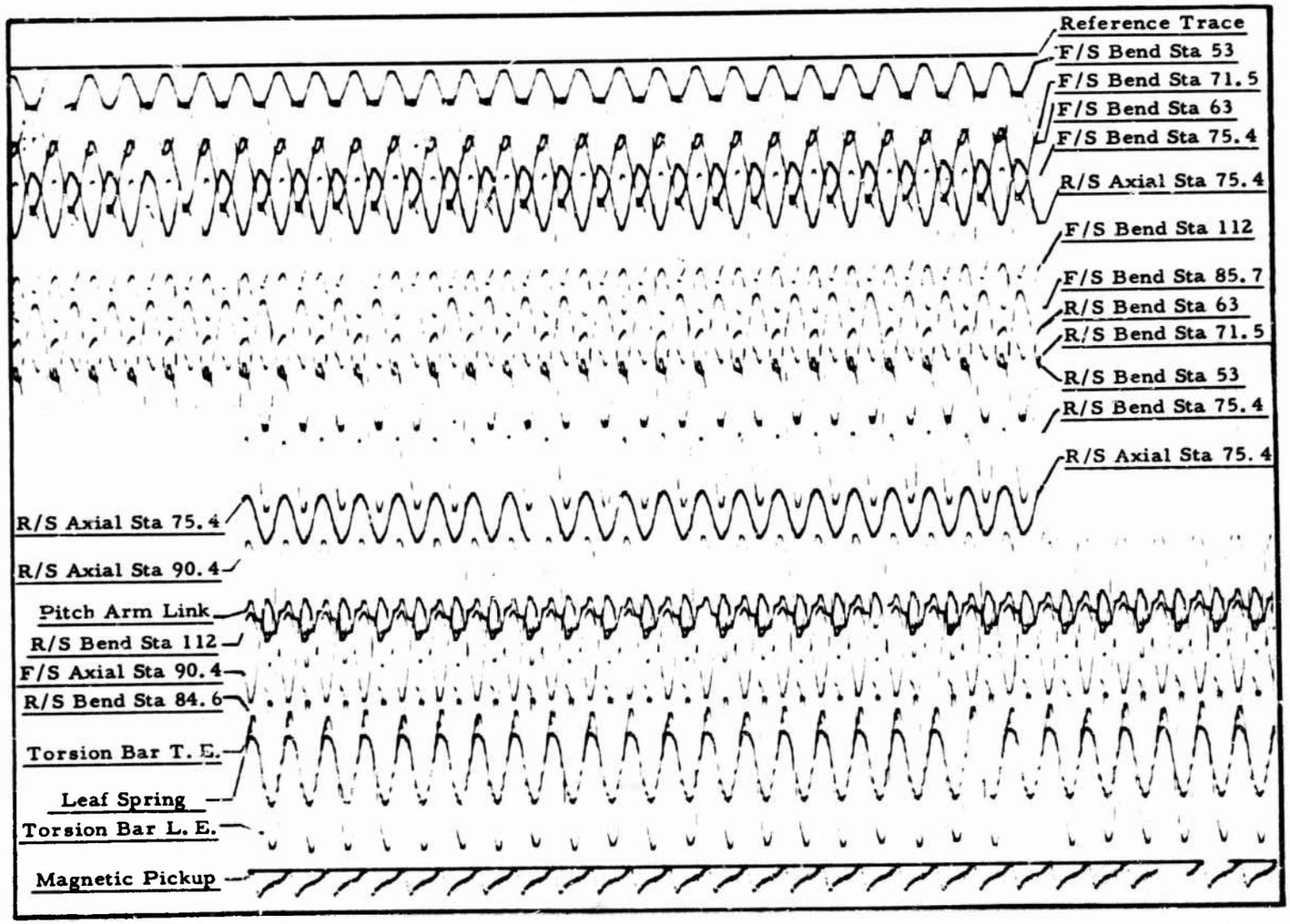

Figure 63. Blade Root-End Fatigue Test - Oscillograph Record at Test Load Level.

TABLE 11
BREAKDOWN OF CYCLES ACCUMULATED ON BLADE ROOT-END FATIGUE TEST SPECIMEN 1

Date	Ref. Roll	Load Cycles	Speed (cps)	Front Spar Bending 75.43	Front Spar Axial 75.43	Rear Spar Axial 75.43	Rear Spar Bending 75.43	Front Spar Axial 90.43	Rear Spar Axial 90.43	Remarks
1/2/64	A	1,244	11.2	9,050	15,150	13,500	9,850	-	-	-
1/3/64	1	1,356	11.3	7,250	1,430	892	8,650	-	-	-
1/4/64	2	500	↓	↓	↓	↓	↓	-	-	-
1/6/64	3	500	↓	↓	↓	↓	↓	-	-	-
1/9/64	4	500	↓	↓	↓	↓	↓	-	-	-
1/10/64	5	500	↓	↓	↓	↓	↓	-	-	-
1/10/64	6	500	↓	7,250	1,430	892	8,650	-	-	-
1/10/64	7	500	↓	3,320	7,720	6,800	3,380	-	-	-
1/10/64	8	500	↓	↓	↓	↓	↓	-	-	-
1/10/64	9	500	↓	↓	↓	↓	↓	-	-	-
1/10/64	10	500	↓	↓	↓	↓	↓	-	-	-
1/10/64	11	500	11.3	3,320	7,720	6,800	3,380	-	-	-
1/10/64	12	1,000	9.3	10,700	10,450	10,450	11,250	-	-	-
1/13/64	13	500	9.1	6,900	7,650	7,660	9,240	-	-	-
1/14/64	14	500	9.1	6,300	7,350	7,690	8,900	3,250	3,630	(a)
2/4/64	15 & 16	1,000	9.1	9,560	5,860	6,470	10,750	2,170	2,738	-
2/5/64	17 & 18	1,000	9.1	-	8,940	8,030	11,550	3,580	4,310	-
2/5/64	19 & 20	1,000	9.0	-	9,550	10,850	10,850	4,080	4,790	-
2/7/64	21 & 22	1,000	8.8	7,200	7,650	7,100	9,030	3,225	3,695	-
2/7/64	23 & 24	1,000	8.8	10,650	3,580	2,470	13,209	1,800	1,162	-
2/7/64	Investigated edgewise-flapwise coupling effect									
2/10/64	25 & 26	1,000	8.8	11,650	11,150	9,850	11,110	4,840	4,360	-
2/11/64	27 & 28	1,000	8.8	11,910	10,080	7,850	12,200	4,980	4,590	-
2/12/64	29 & 30	1,000	8.7	12,000	9,560	5,750	18,800	4,510	4,035	-
2/12/64	31 & 32	1,000	8.7	11,400	8,610	6,350	14,420	3,870	3,530	Tuning runs
2/13/64	33 & 34	1,000	8.5	11,650	8,930	6,160	15,300	4,240	3,830	-
2/13/64	35 & 36	1,000	8.5	13,700	10,850	8,150	15,300	5,100	4,510	-

2/18/64	39	1,000	8.5	9,775	(Station o3B)		11,450	5,750	5,380	(86,000)
2/18/64	40	1,000	8.5	12,500	-	-	14,400	7,940	6,850	(114,500)
2/18/64	41	1,000	8.5	9,250	-	-	10,050	6,330	6,150	(96,000)
2/19/64	42	1,500	8.5	11,000	-	-	12,460	7,340	6,775	(108,900)
2/19/64	43	1,500	8.4	13,000	-	-	15,500	8,620	8,000	(128,000)
2/19/64	44	1,000	8.5	14,400	(22,500)		16,700	9,000	8,400	(133,500)
2/19/64	44	1,000	8.6	14,800	(24,250)		16,900	9,450	8,670	(139,000)
2/20/64	45	500	8.5	15,500	(11,320)		19,700	6,330	5,555	
2/20/64	46	500	8.5	12,900	(9,460)		13,800	5,320	4,700	
2/20/64	47	500	8.5	15,250	-	-	18,750	6,330	5,680	-
2/21/64	48	500	8.5	11,250	-	-	13,800	5,750	5,100	-
2/21/64	49	500	8.5	12,800	-	-	15,400	7,270	6,250	-
2/21/64	50	500	8.5	12,600	-	-	15,400	6,575	5,950	-
2/21/64	51	500	8.5	-	-	-	14,400	-	-	-
			Start of fatigue runs (cycles to date = 32,100)							
2/21/64	52	45,300	8.5	11,400	-	-	14,600	5,690	5,055	-
	53 & 54									
2/24/64	55 & 56	15,480	8.5	11,200	-	-	14,900	5,900	5,290	-
2/24/64		88,632	8.5	11,300	-	-	14,700	5,570	5,400	-
2/25/64	60 & 61	30,600	8.5	11,320	-	-	15,000	5,880	5,560	-
			Failed coupling[c], station 154 (patched)							
3/3/64	-	8,160	Failed leading edge strap pack[d] (188,172 cycles +)							
3/18/64	-	10,200	8.5	12,650	-	-	15,400	6,120	6,180	-
			Cracked flexure[e], station 45; drilled stop holes; continued run							
3/20/64	-	38,780	8.5	12,600	-	-	14,000	5,600	6,240	-
3/23/64	-	12,750	Constant monitoring of the direct writing oscillograph					-		-
3/24/64	-	15,300	horizontal and vertical accelerometer					-	-	-
3/25/64	-	23,970	8.5	-	-	-	-	-	-	-

Stopped to repair cracked flexures at stations 45 and 85

TABLE 11 (Continued)

Date	Ref. Roll	Load Cycles	Speed (cps)	Front Spar Bending 75.43	Front Spar Axial 75.43	Rear Spar Axial 75.43	Rear Spar Bending 75.43	Front Spar Axial 90.43	Rear Spar Axial 90.43	Remarks
4/7/64	-	36,720	8.5	-	-	-	-	-	-	-
4/8/64	-	78,540	8.5	-	-	-	15,700	6,030	6,050	-
4/9/64	-	31,620	8.5	-	-	-	-	-	-	-

Cycles including 32,100 preliminary runs = 468,152.

(a) Shortened test fixture straps.
(b) Values in parentheses are chordwise bending moments (in -lb) at station 90.43.
(c) Coupling of electroformed nickel and not representative of final blade couplings.
(d) As a result of insufficient clampup of strap pack retention bolts, the strap packs were replaced and the proper clampup of the retention bolts was obtained. No further problems were encountered.
(e) This coupling had experienced more than 2 million cycles in previous fatigue test and could have sustained damage.

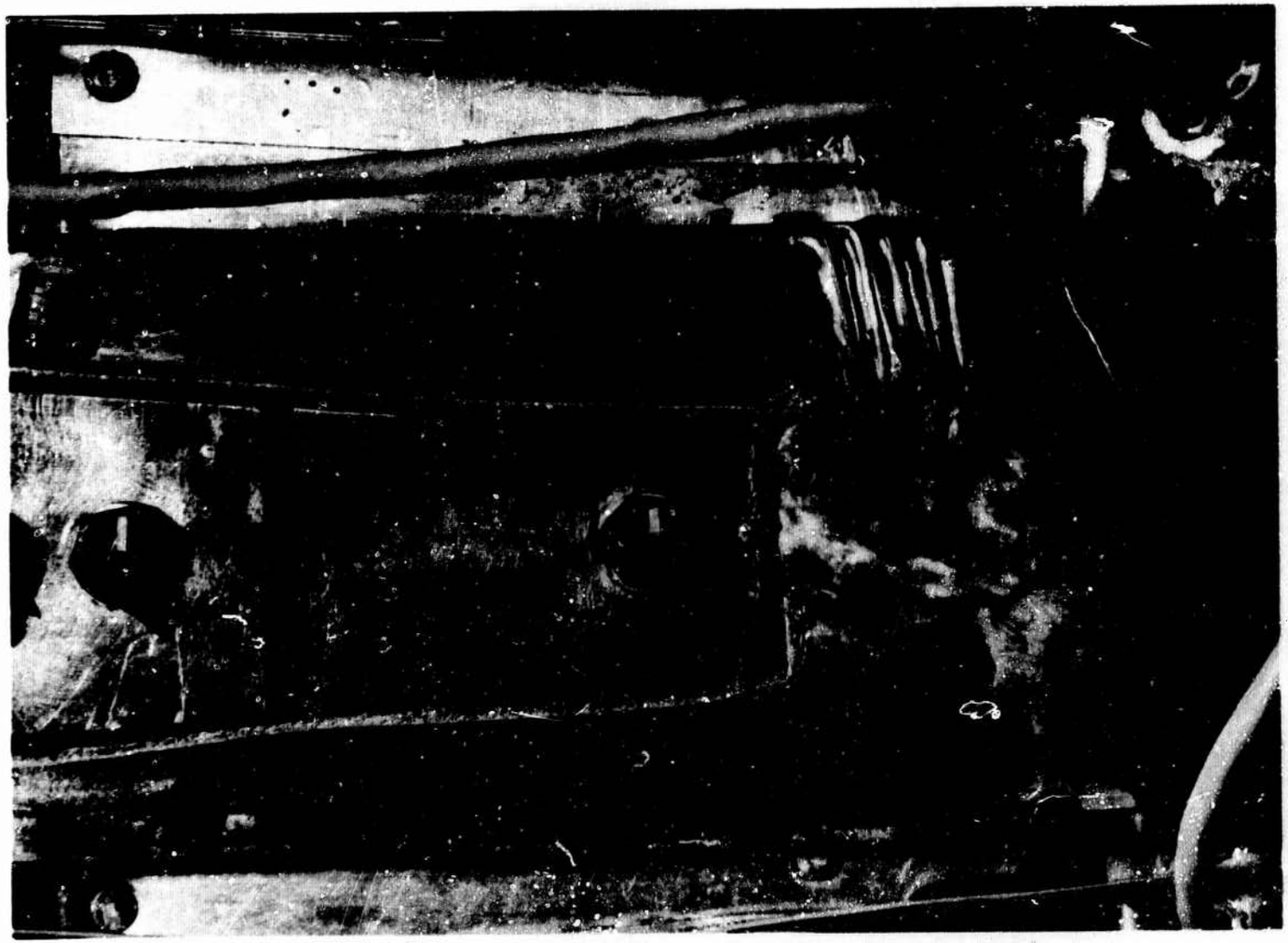

Figure 64. Blade Root-End Fatigue Test - Rear Spar Fatigue Crack.

2. On the front spar, at station 90, the five most outboard laminations were cracked. See Figure 65.

3. Cracks were found in the laminations next to the segments at several of the attaching bolt holes. See Figure 66.

4. Holes for the bolts attaching the spars to the segments were cocked as much as 4 degrees, due to the lamination slipping during the bonding operation. (This manufacturing discrepancy was corrected and does not exist on the flight blade spars.)

5. Holes in the segments were also found to be oversize on the test specimen.

6. Failure of the bond between the root-end fitting and the spar at the first bolt was noted (at approximately station 90).

The most serious failure on the root-end fatigue test was the crack in the spar at station 90. At this point, the bond failure indicated the probability that the bond strength was insufficient to allow the required local load transfer from the laminated spar to the root fitting. There is also the possibility that the bolt had picked up a disproportionate share of the load, as is the tendency for the first bolt in a bolted connection.

The other failures occurring during the fatigue test can be attributed to the following:

1. Cracked flexures, because of the fact that they had been used in the previous fatigue test and possibly damaged.

2. Segment attach bolt failures, because of the cocked holes in the spar plus the oversize holes in the segment causing the bolt to fail in bending across the minor thread diameter.

3. Cracks in the spar lamination next to the segment, attributed to the cocked and oversize holes.

SPECIMEN 2

A total of 413, 000 cycles was applied before a crack through the bolt hole at station 94. 12 was detected, at which time the test was terminated. Of this total, 256, 000 cycles were at the Phase 1 loads and the

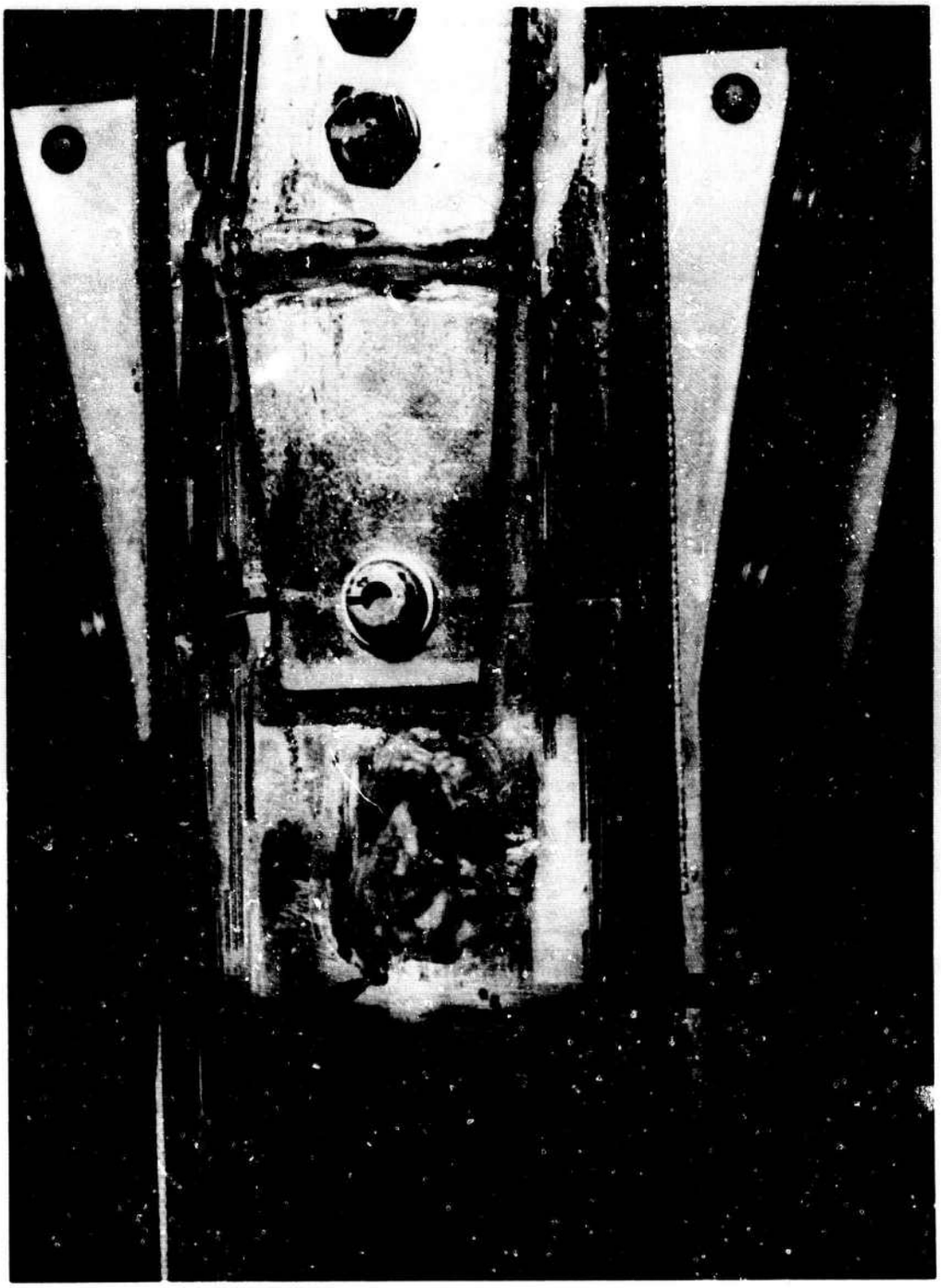

Figure 65. Blade Root-End Fatigue Test - Front Spar Fatigue Crack.

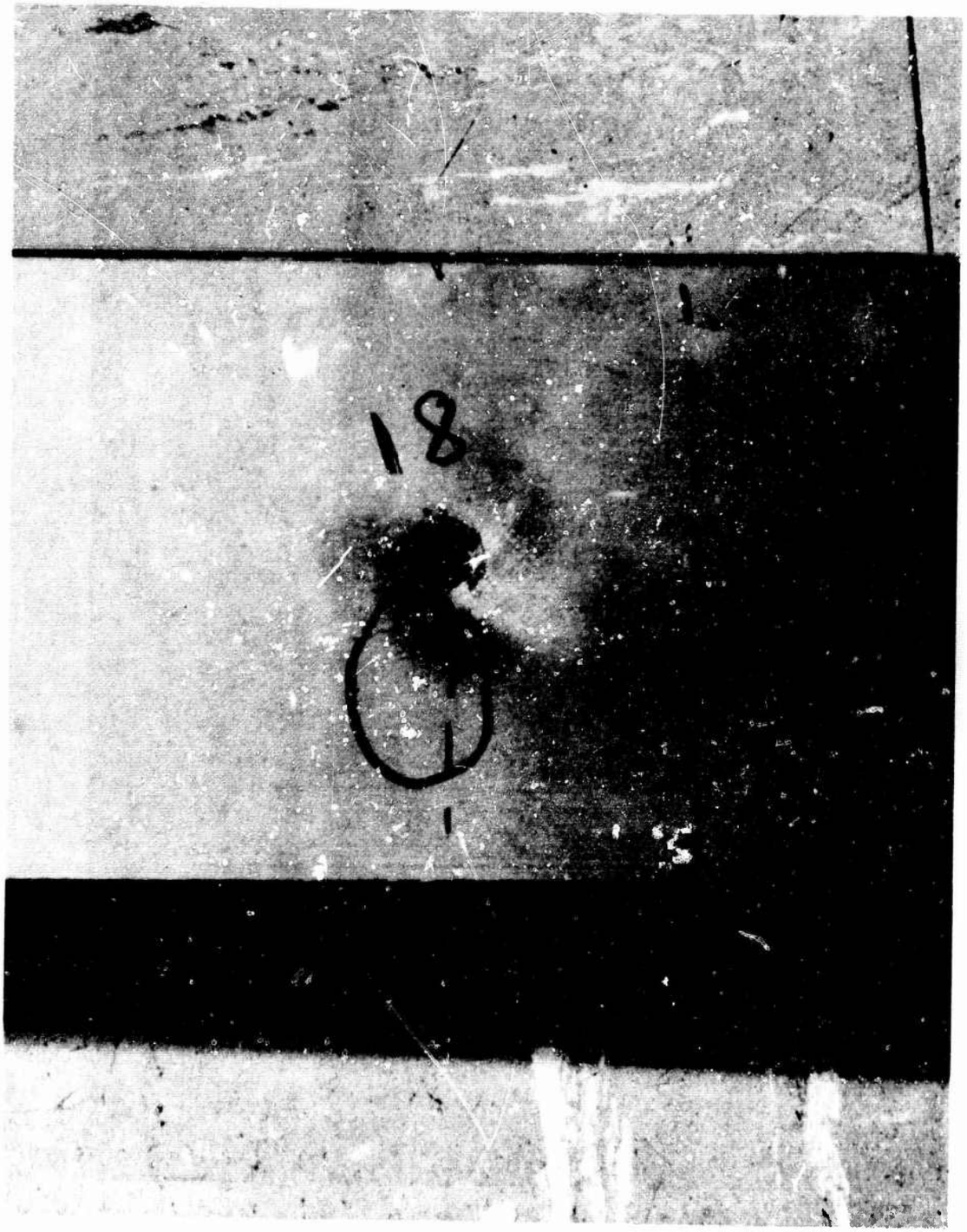

Figure 66. Blade Root-End Fatigue Test, Rear Face of Spar, Fatigue Crack.

remaining 157, 000 cycles were at Phase 2 loads previously shown under Test Procedures.

Flexure failures at 257, 000 cycles, stations 73 and 79, prompted a closer look at the flight strain data. The actual flight data revealed the flapwise and chordwise bending loads peaked in phase. However, the phasing that gives the maximum torsion loading in combination with peak chordwise moments occurs when one peak of the torsion loading coincides with the peak chordwise bending, while, due to a non-sinusoidal torsion loading, at the other end of the cycle the torsion is 90 degrees out of phase with the chordwise bending and is zero magnitude. Therefore, a reduction of the torsion to 50 percent of its former value, since the test machine applies all loads exactly in phase, was appropriate. These loads were based on a normal flight composed of takeoff, transition forward flight, turns, hovers, flares, and landings.

The chordwise bending loads were reduced from ±92, 000 inch-pounds to ±84, 300 inch-pounds based on flight test data.

The following tabulation gives the number and magnitude of the chordwise bending moment cycles to which the second specimen was inadvertently subjected when an attempt was made to adjust the spring and mass loading systems during the setup runs above the nominal ± 92, 000 inch-pounds.

Number of Cycles	Magnitude (In -Lb)
510	±125, 700
225	±115, 400
510	±107, 800

The following is a discussion of the condition of the spars after their removal subsequent to testing:

1. The most serious failure was in the first two laminations on the segment side of the front spar at station 94. 12, which failed completely across their width. They are shown in Figure 67.

2. Other minor cracks in the first lamination on the segment side of the forward spar were located through holes at stations 106. 68 and 131. 68. A typical crack is shown in Figure 68. Figure 69 shows the condition of the segment side of the forward spar and its mating area on the segments.

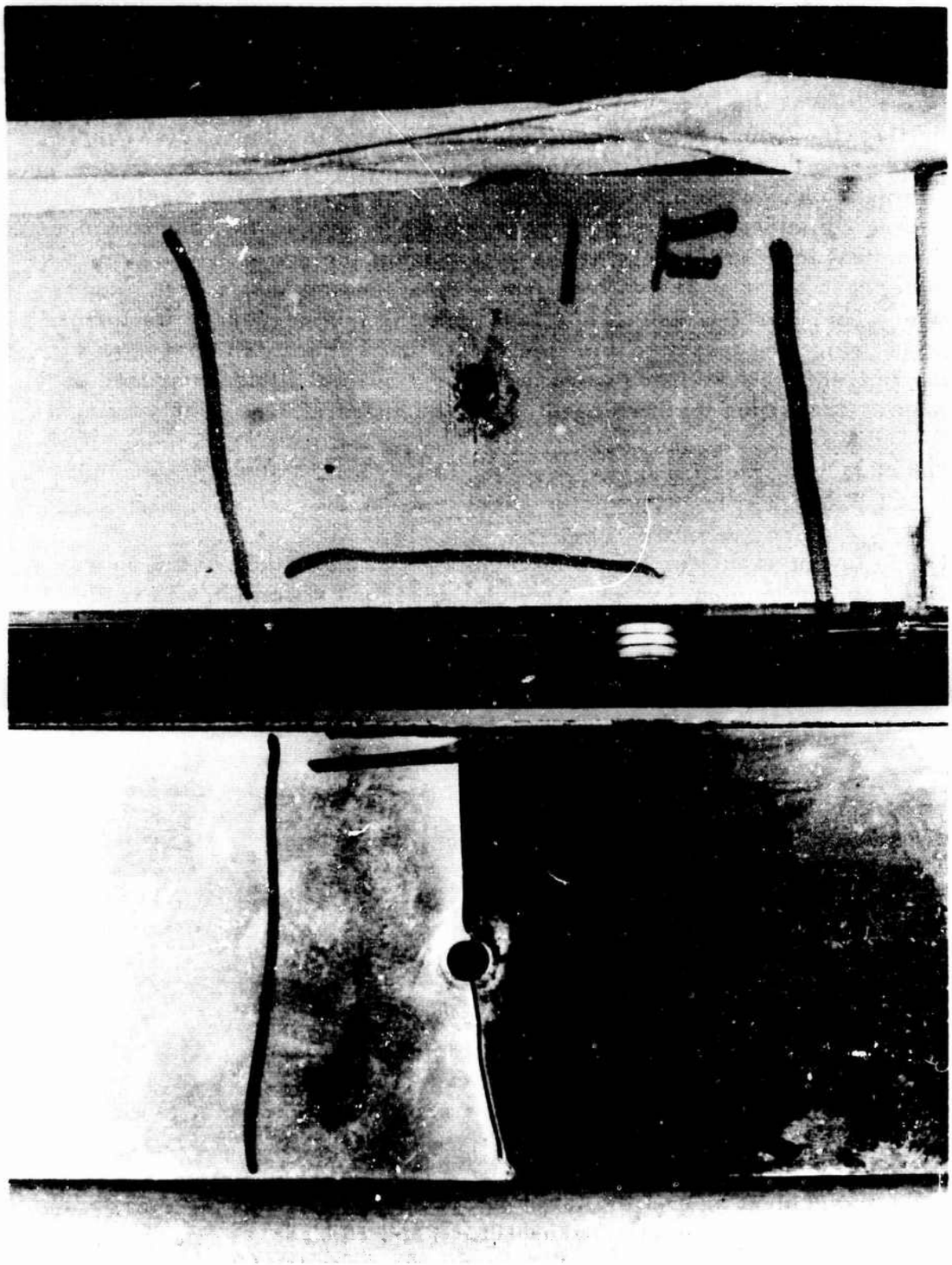

Figure 67. Cracked Laminations in Front Spar at Station 94. 12, Specimen 2.

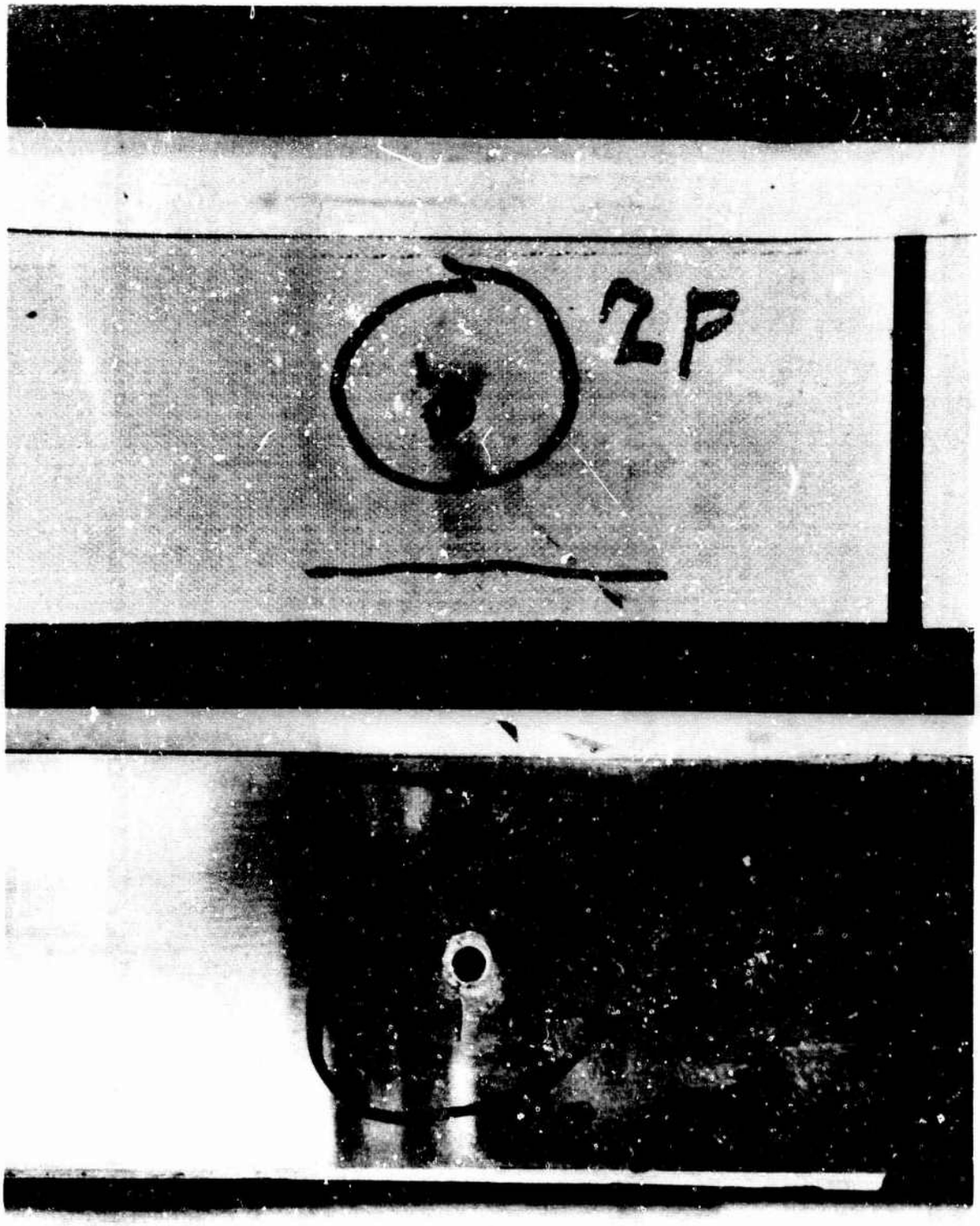

Figure 68. Typical Crack Found on the Segment Side of the Front and Rear Spars, Specimen 2.

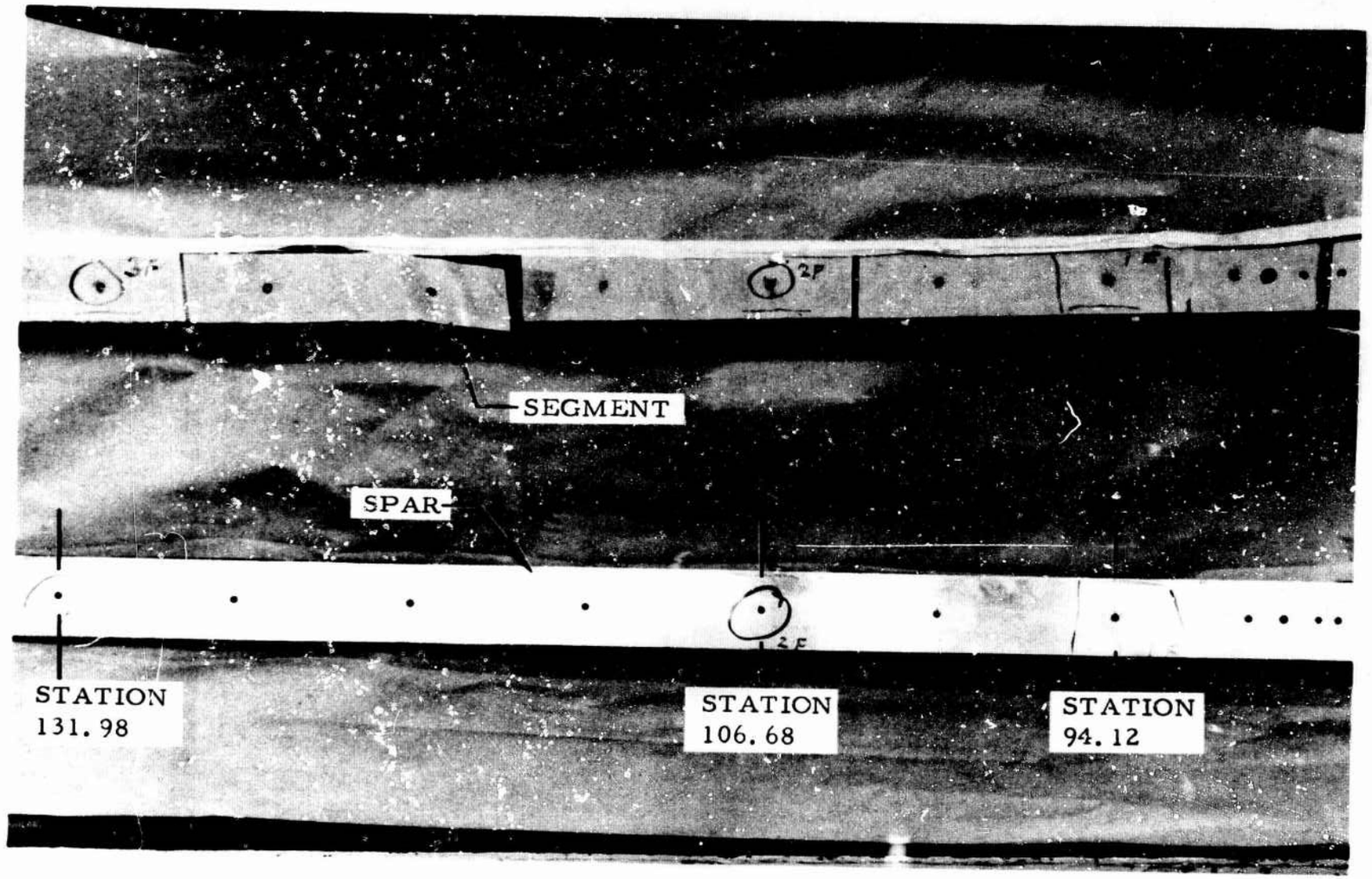

Figure 69. View of Segment Side of Front Spar Showing Location of Three Holes Where Cracks Occurred, Specimen 2.

3. Cracks in the first lamination on the segment side of the rear spar were minor, and were located at stations 74.62, 94.12, 119.12, and 144.12. They are not shown in detail, because Figure 68 is typical of their appearance.

4. Several spar-to-segment bolts (NAS 464, 1/4-inch dia) broke during the initial 250,000 cycles. They failed in different areas — one at the head, others at the root of the last imperfect thread. Conditions of typical bolts after test are shown in Figures 70 and 71.

Figure 70. Appearance of Bolt Removed From Station 94. 12, Forward Spar, Where Major Cracks Occurred, Specimen 2.

Figure 71. Appearance of Typical Bolt Removed From Segment Holes Where No Cracks Had Occurred, Specimen 2.

BLADE CONSTANT SECTION FATIGUE TESTS

SUBJECT

These tests concerned the fatigue strength of a typical XV-9A rotor blade constant section. The Phase 1 test was conducted at the whirl test site facility of HTC-AD during August 1964. The Phase 2 test was conducted at the same location during January 1965.

PURPOSE

PHASE 1 TEST

The purpose of this test was to substantiate the fatigue strength integrity of the XV-9A blade constant section for 100 flight hours, simulating conditions of loading, temperature, and pressure.

PHASE 2 TEST

The purpose of this test was to substantiate the blade section for the transient peak stresses encountered during transition and flares that were measured during flight test.

SUMMARY OF RESULTS

PHASE 1 TEST

The blade constant section specimen completed the equivalent of 100 flight hours. Inspection of the front and rear spars after the test revealed a fatigue crack propagated 0.15 inch vertically from a spar-to-segment 0.25-inch-diameter hole on the inner face 0.050-inch lamina of the rear spar at station 237.8.

PHASE 2 TEST

The specimen completed 25,000 additional cycles of load, in which the chordwise moment was increased 25 percent. The crack condition that already existed did not propagate.

TEST SPECIMENS

PHASE 1 TEST

The specimen consisted of three segments of a production blade, HTC-AD drawing 385-1100, from station 203.5 to station 241, with laminated spars extending several feet beyond the end of the specimen. The ends of the specimen were capped by bulkheads that provided a closed, pressurized, internal duct system, and also supported internal banks of electric resistance wire heaters installed in each duct. The heaters did not contact the duct walls. The test blade assembly is shown on HTC-AD drawing 385-9608.

PHASE 2 TEST

The specimen for this test was identical with that of the Phase 1 test.

TEST SETUP

The specimen was installed in a test fixture designed to apply centrifugal force and flapwise and chordwise moments. The centrifugal force was simulated by a tension load applied through flexures attached to the ends of the specimen. The specimen was feathered relative to a pinned support axis that gave the correct ratio of cyclic chordwise to flapwise bending moments.

The specimen was vibrated as a beam under axial tension loading. A spring loaded exciter, driven by a vari-drive motor connected to one of the bulkheads, induced the cyclic flapwise and chordwise bending moments.

The ducts were pressurized by air from an external source through a bulkhead connection and monitored by a pressure gage.

The heaters installed inside the ducts simulated the 1200°F gas temperature. The heated length of the test blade included the center segment and two flexure couplings. An air blower located in front of the specimen controlled the outer skin temperatures and provided cooling air over the front and rear spars. The setup details are shown in Figures 72 through 75.

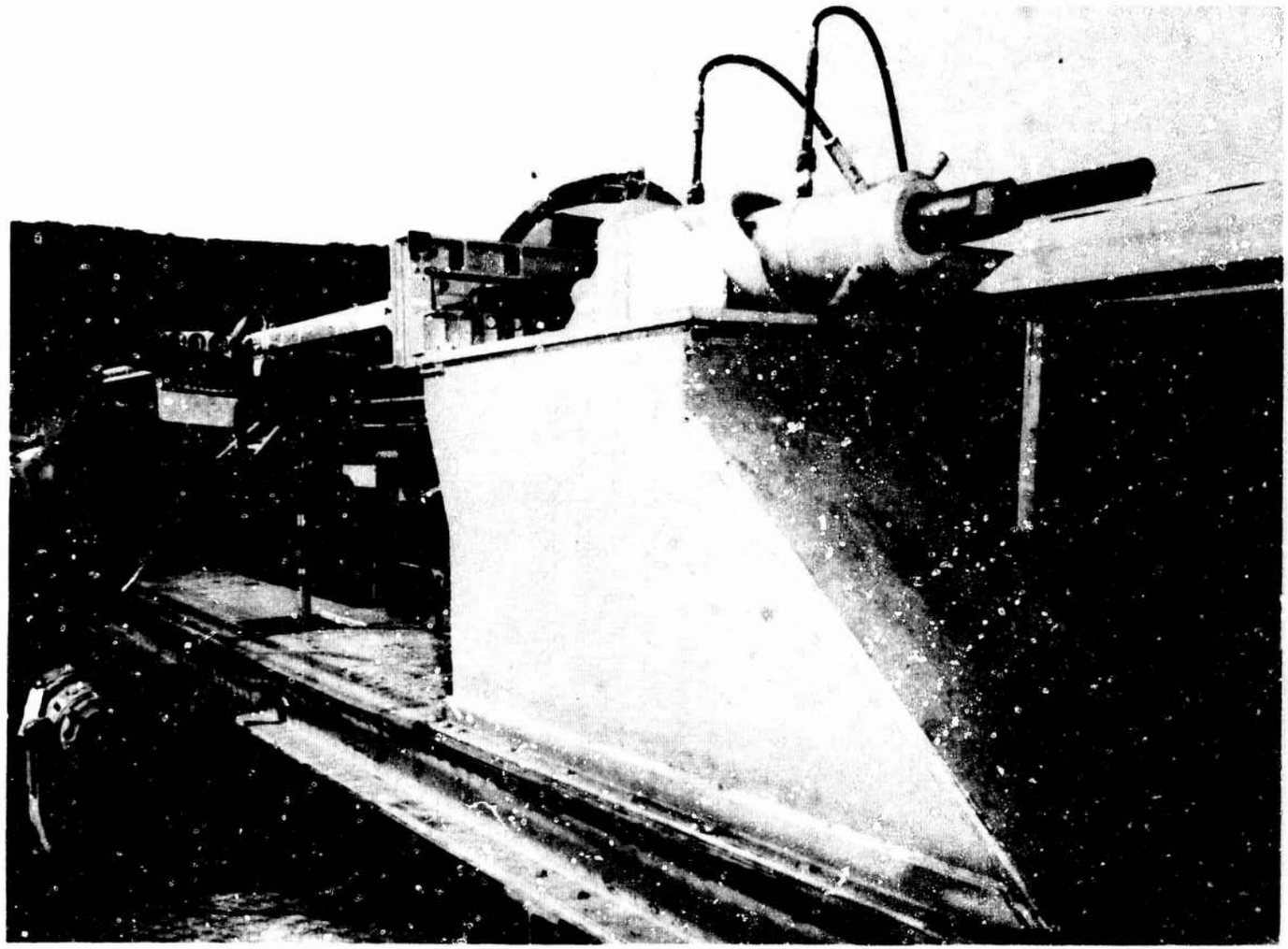

Figure 72. Blade Constant Section Fatigue Test Fixture.

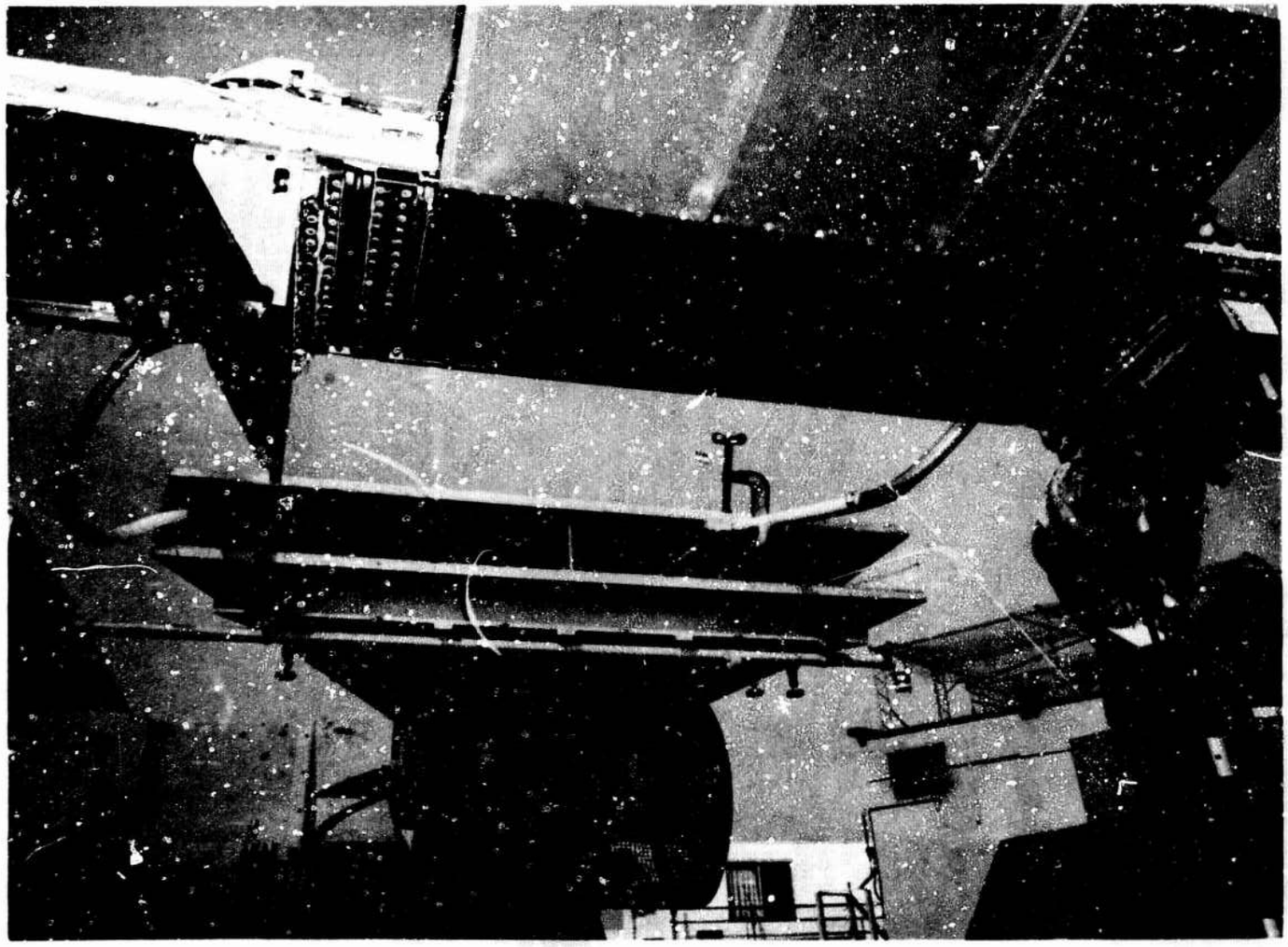

Figure 73. Blade Constant Section Fatigue Test Specimen Area and External Air Blower.

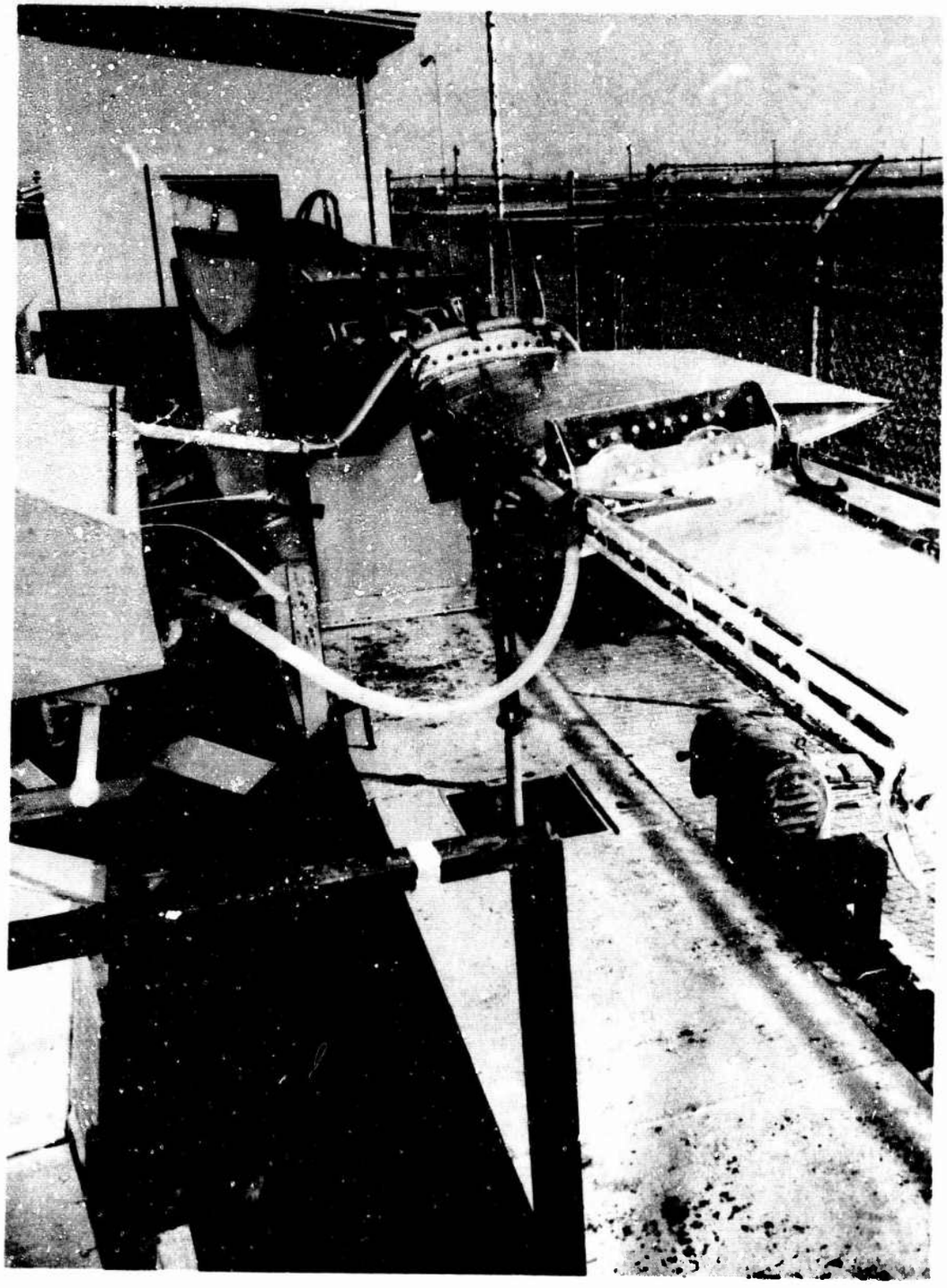

Figure 74. Blade Constant Section Fatigue Test-Specimen and Exciter Mechanism.

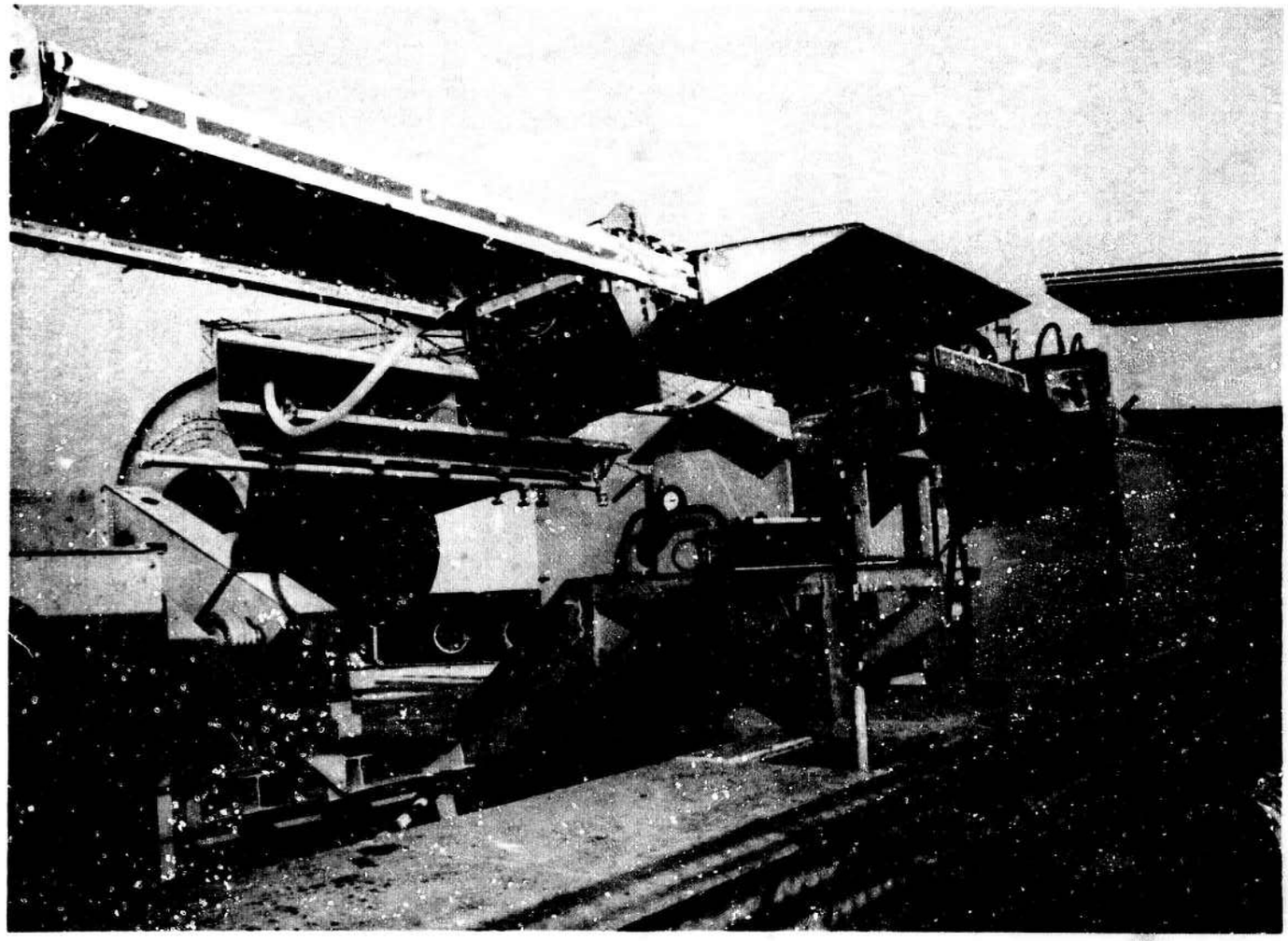

Figure 75. Blade Constant Section Fatigue Test-Specimen and Fixture.

INSTRUMENTATION

Electrical resistance strain gages were bonded to the front and rear spars. These gages were wired to sense bending or axial strains and calibrated by externally applied loads to measure axial loads and bending moments. Figure 76 shows the location of these strain-gage bridges. The output signals from these bridges were supplied to a recording oscillograph and a direct-writing oscillograph.

Chromel-alumel thermocouples were installed on the outer surfaces of the duct walls, the flexure couplings, the outer skin, and the front and rear spars. Figures 76 and 77 show the locations of thermocouples on the center segment area and spars. Additional thermocouples that were installed on the adjacent segments for control purposes are not shown in Figures 76 and 77. All thermocouples were monitored and recorded on a temperature recorder.

TEST LOADS

The specimen was tested to the following loads, based on the computed design loads reported in Reference 1 and the whirl test results reported in References 2 and 3:

	Phase 1 Test	Phase 2 Test
Centrifugal force	76,600 lb	76,600 lb
Cyclic flapwise moment	$\pm$10,000 in -lb	$\pm$10,000 in -lb
Cyclic chordwise moment	$\pm$34,000 in -lb	$\pm$42,500 in -lb
Internal duct pressure	27.5 psig	27.5 psig
Simulated gas temperature	1200°F	1200°F
Test operating frequency	10 cps	10 cps

TEST RESULTS

PHASE 1 TEST

The specimen completed the equivalent of 100 flight hours, which was based on the cyclic stress occurring at one cycle per revolution at 243 rpm for a total of 1,458,000 test cycles. The average temperatures maintained during the test on the center segment, adjacent flexure couplings, and spars are shown in Figures 76 and 77.

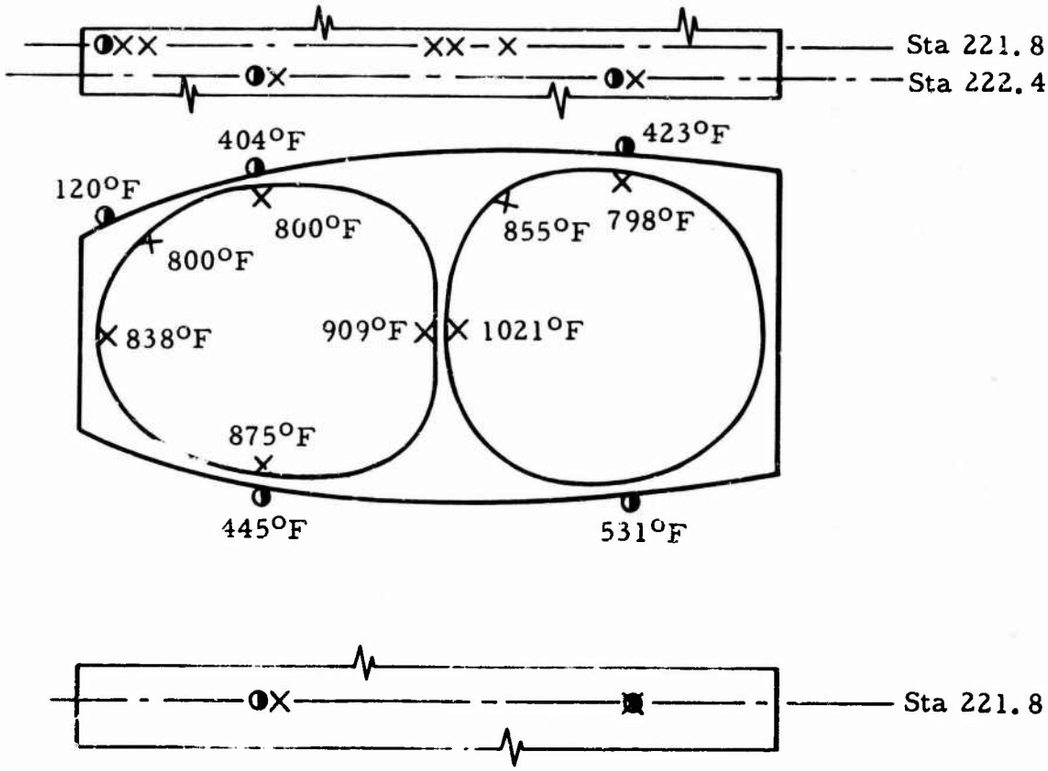

Center Segment 2

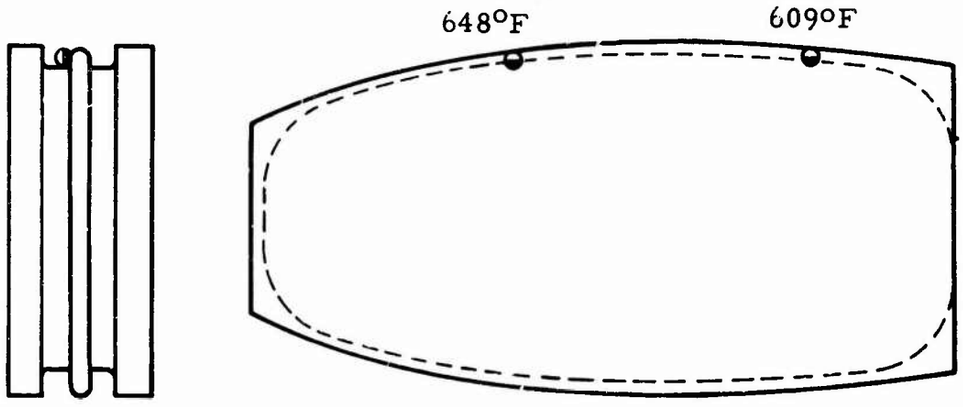

Flexure at Sta 228.5

Figure 76. Flexure and Segment Thermocouple Locations.

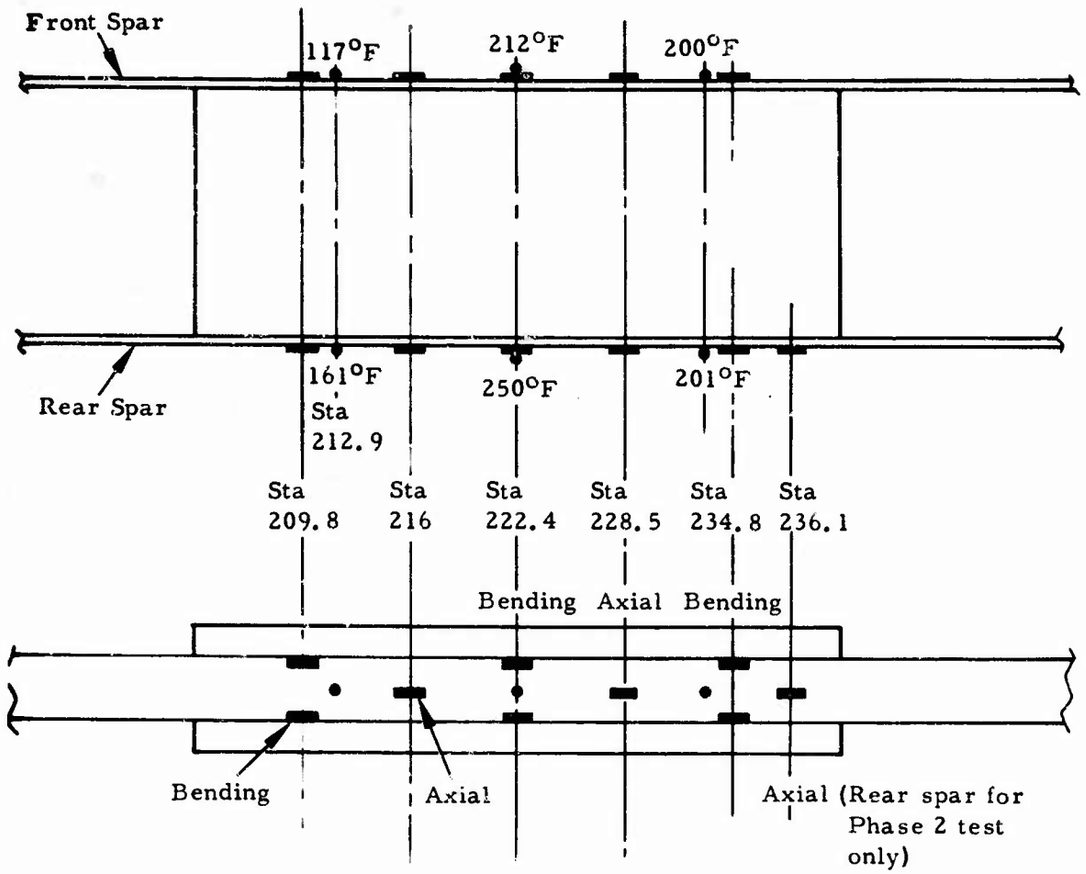

xxx°F indicates thermocouple locations and average temperatures maintained on spars during tests

Figure 77. Strain-Gage and Thermocouple Locations.

Inspection of the front and rear spars revealed a fatigue crack propagated 0. 15 inch vertically from a spar-to-segment 0. 25-inch-diameter hole on the inner face 0. 050-inch lamina of the rear spar at station 237. 8. It was noted that this station is close to the end of the test area, station 241, and may have been affected by local loading fixture constraints. Figures 78 and 79 show the fatigue crack. Fretted areas were also visible inside the bolt holes at station 225. 3, rear spar, and station 200. 5, front spar. All other holes in the spars were in satisfactory condition. No evidence of fatigue damage was found in the flexure couplings, ducts, or segment areas.

Inspection of the test segments revealed slight fretting at the outer skin and leading edge fairing faying surfaces of the center segment adjacent to the front spar.

A leakage test of the duct and flexure coupling area was conducted. This test revealed leakage of less than one cubic foot per minute.

PHASE 2 TEST

The specimen completed an additional 25, 000 cycles at chordwise bending loads equivalent to 125 percent of the chordwise moment used in the Phase 1 test. Post-test inspection, with the spars removed, indicated no change in the specimen, or in the 0. 15-inch-long crack at station 237. 8.

CONCLUSIONS

PHASE 1 TEST

The detection of a tiny crack at the bolt hole, as noted above under Test Results, page 140, resulted from a post-test examination. The crack had no detectable effect on test loads or stresses. Also, as noted, higher than intended local stresses probably occurred at this particular bolt hole, because of the immediate proximity of the loading fixture and its attending restraints. However, should a similar crack ever appear in the blade spars, it would progress slowly, as proven in reduced scale specimen tests. For example, as mentioned in the following section of this report, a crack discovered at 184, 000 cycles did not fail completely until 2, 590, 000 cycles.

PHASE 2 TEST

The specimen satisfactorily sustained the applied loads with no further indications of distress.

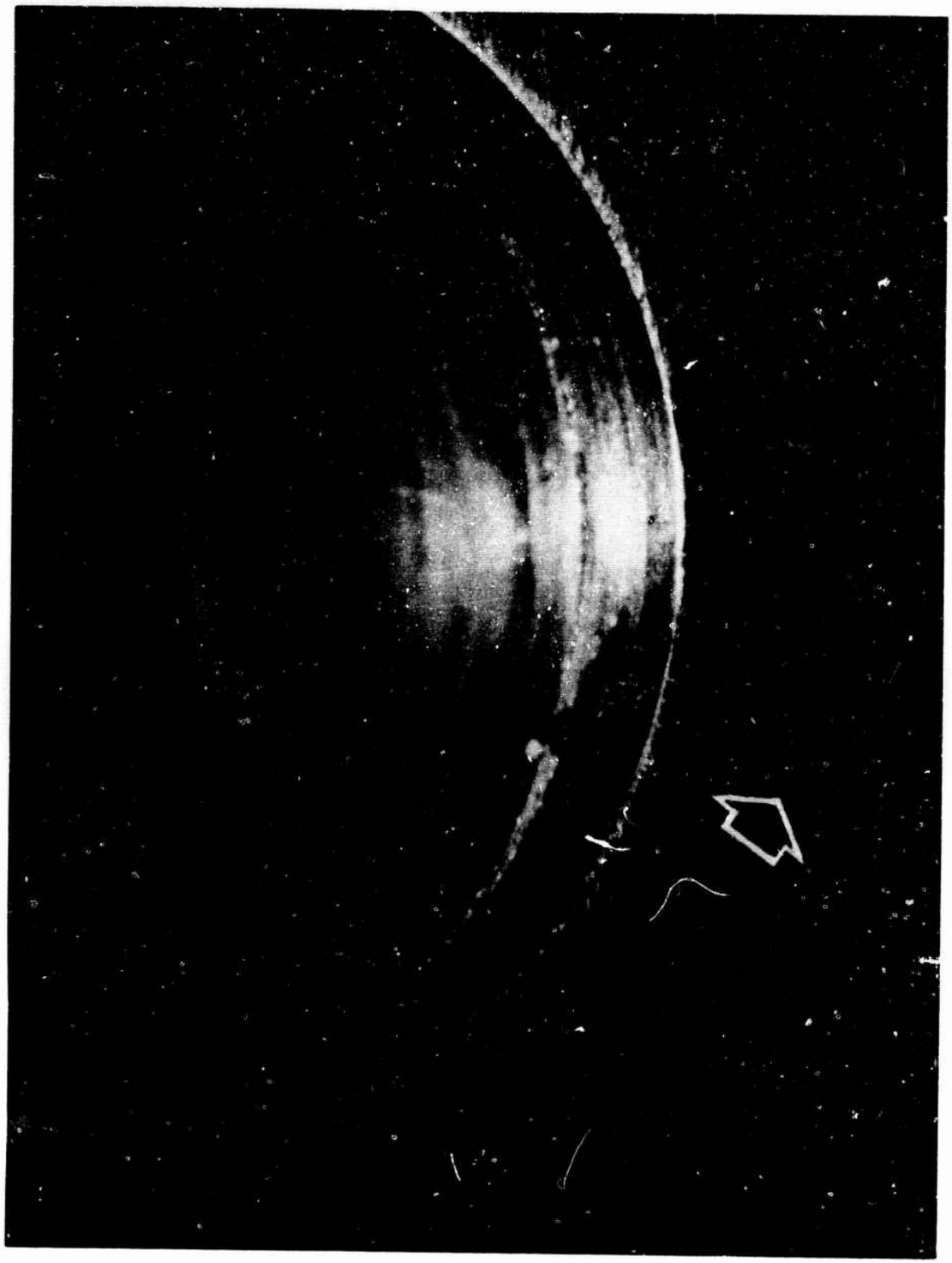

Figure 78. View of Rear Spar Fatigue Crack and Inside Bolt Hole.

Figure 79. View of Rear Spar Fatigue Crack.

REDUCED SCALE SPAR-TO-SEGMENT AND ROOT-FITTING-TO-SPAR ATTACHMENTS FATIGUE TESTS

SUBJECT

This section concerns tension-tension axial fatigue tests of reduced scale specimens of the rotor blade spars. These tests were conducted in the HTC-AD structures test laboratory from May through June 1964.

PURPOSE

The purpose of these tests was to determine the fatigue life of reduced scale specimens representing the spar-to-segment and root-fitting-to-spar attachments.

SUMMARY OF RESULTS

SEGMENT-TO-SPAR (TWO-HOLE) SPECIMENS

Tests showed that the countersunk clamp up bushing installation through a clearance hole in the spar resulted in a large improvement in fatigue life.

ROOT-FITTING-TO-SPAR (FOUR-HOLE) SPECIMENS

Tests indicated that thinning down the doubler at the first hole, loosening the fit on this bolt, and reducing bolt spacing by adding another bolt gave an approximate infinite life at 70,000 $\pm$10,000 psi fatigue strength.

TEST SPECIMENS

The test specimens were designed to simulate two areas of the blade spar: the segment-to-spar constant section area and the root-fitting-to-spar area, blade station 90. The basic configuration is shown in Figures 80 and 81. The doubler was attached to the specimen to simulate the restraint of the segment on the spar bolt holes when centrifugal force was applied. Various modifications of flanged and countersunk bushings were installed in the bolt holes for all configurations, as shown in Figures 82 and 83.

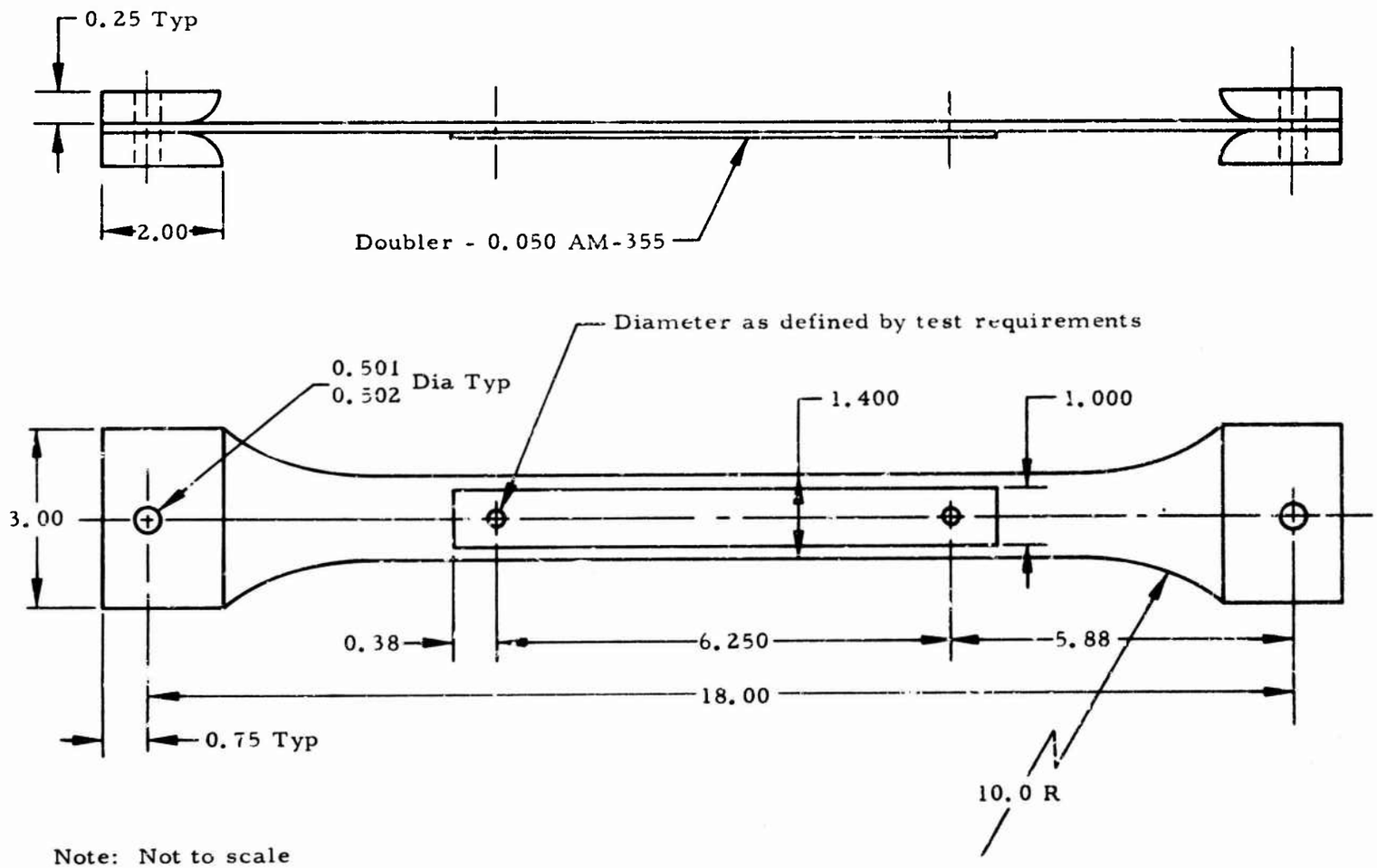

Figure 80. Segment-to-Spar (Two-Hole) Fatigue Specimen.

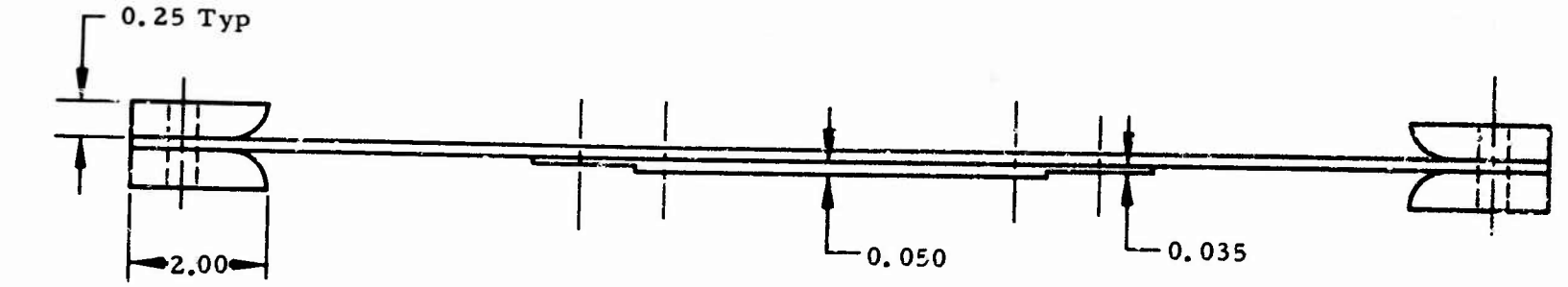

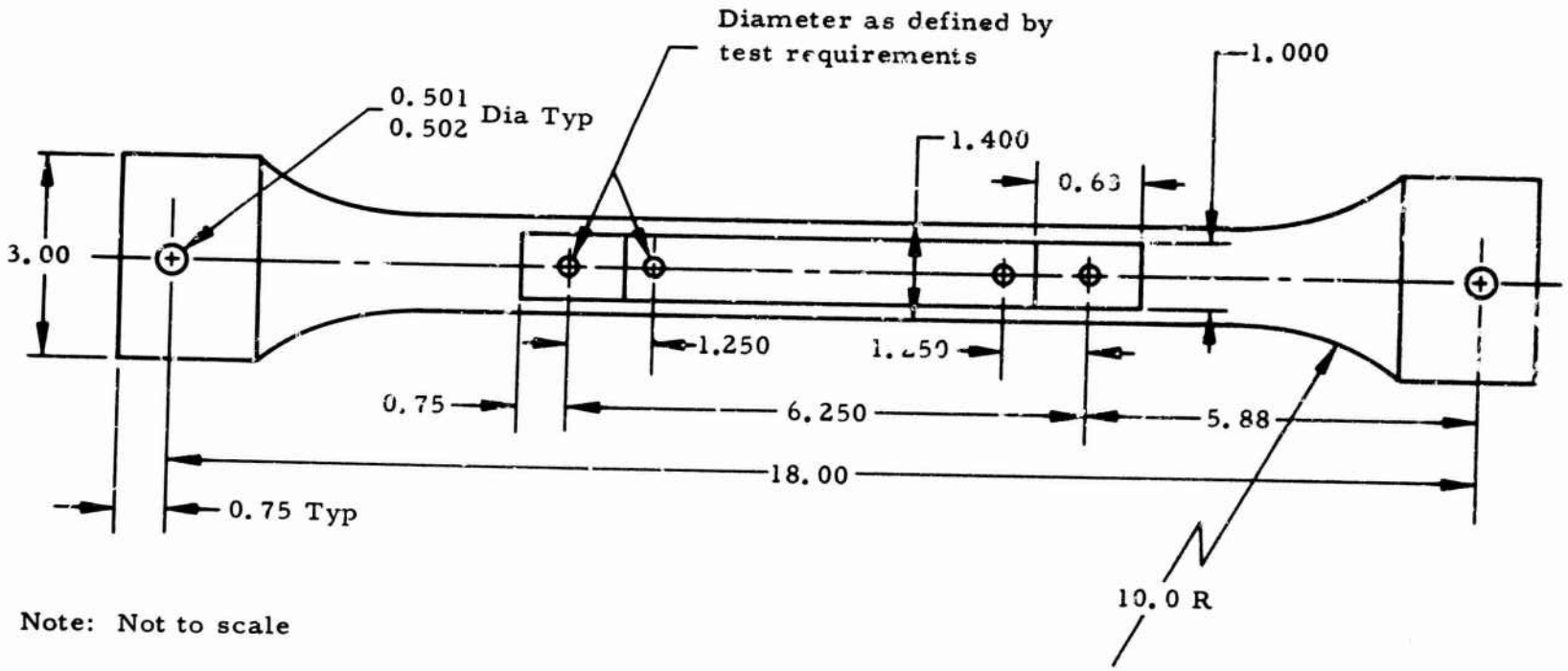

Note: Not to scale

Figure 81. Root-Fitting-to-Spar (Four-Hole) Fatigue Specimen.

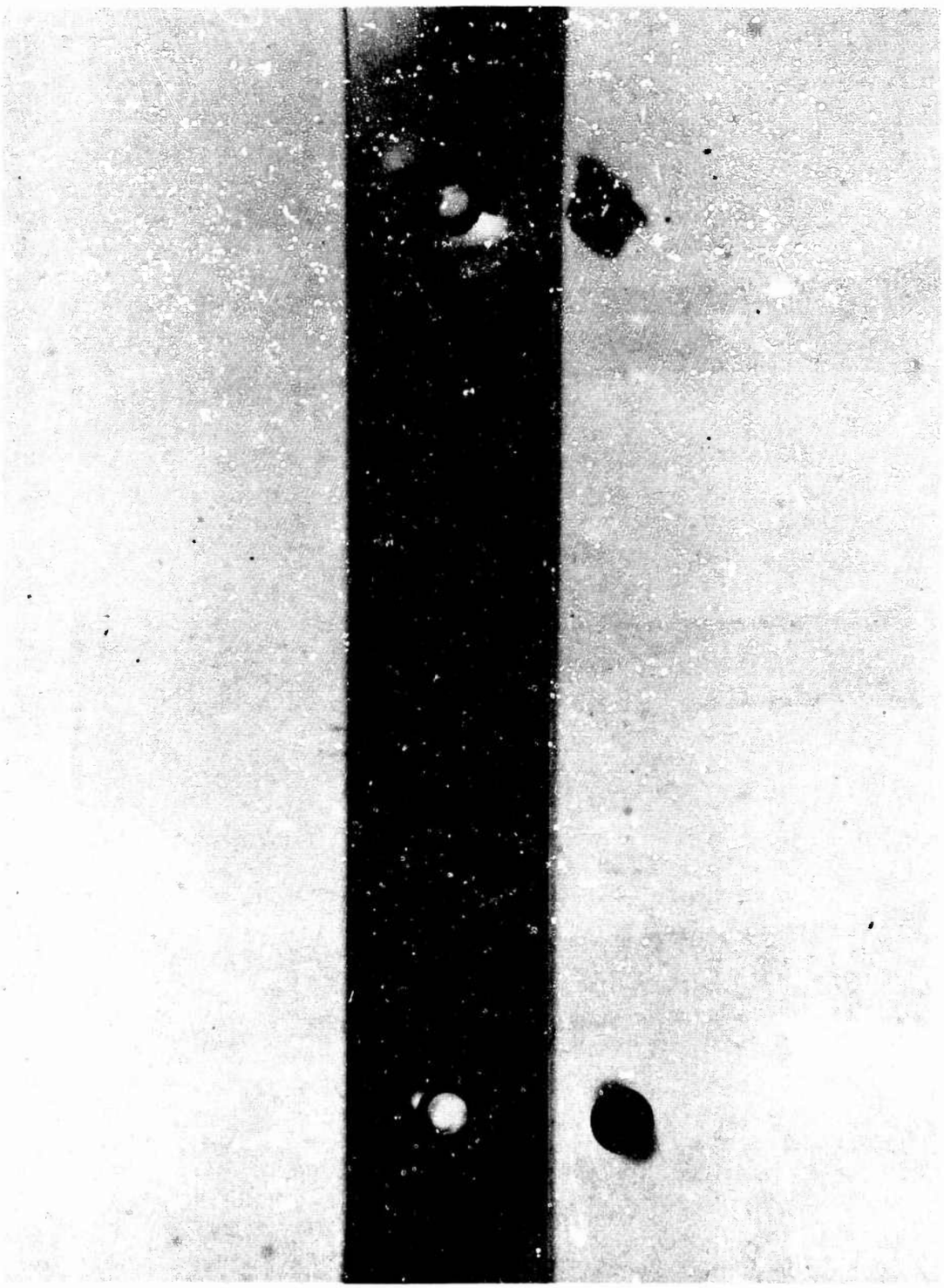

Figure 82. Typical Countersunk Threaded Bushing, Specimen 17.

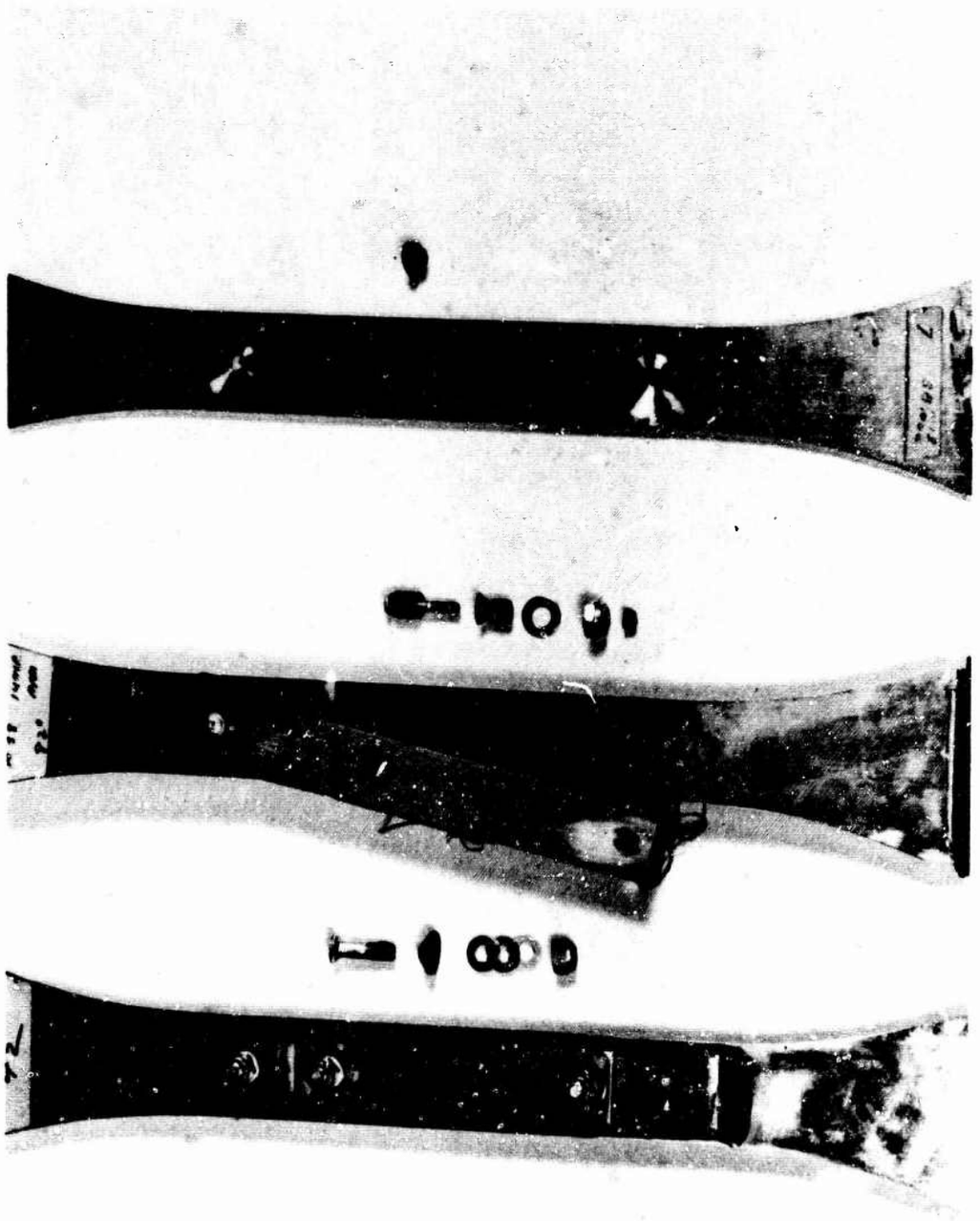

Figure 83. Various Bushing Installations.

SEGMENT-TO-SPAR (TWO-HOLE) SPECIMENS

These specimens simulated the constant section area of the spar, and were fabricated in two configurations: laminated and solid.

The laminated specimens consisted of two types: (1) eighteen laminations of 0. 007-inch-thick AM 355 steel, and (2) one 0. 025-inch, one 0. 009-inch, and thirteen 0. 007-inch-thick laminations of AM 355 steel. Both configurations were bonded together.

The type 1 specimers consisted of the following:

Configuration	Number of Specimens
Loose fit doubler, no bushing	2
Tight fit doubler, no bushing	2
Press fit bushing, 0. 25-inch diameter	4
Press fit, threaded flange clamp up bushing, 0. 25-inch diameter	4
Press fit, threaded flange clamp up bushing, 0. 313-inch diameter	3
Press fit, threaded, 100-degree countersunk clamp up bushing, 0. 25-inch diameter	2
Press fit, threaded, 100-degree countersunk clamp up bushing, 0. 313-inch diameter	6

The type 2 specimens consisted of the following:

Configuration	Number of Specimens
Undercut, threaded, 82-degree countersunk clamp up bushing, 0. 313-inch diameter	3
Undercut, threaded, 100-degree countersunk clamp up bushing, 0. 313-inch diameter	4

The solid specimens were divided into separate tests of two materials: (1) 4130 steel, ht 125, 000 psi minimum, 0. 130-inch thick; and (2) titanium, 6AL-4V, 130, 000 psi ultimate tensile strength (minimum), 0. 157-inch thick. The steel tests utilized four specimens without bushings. The titanium tests utilized two specimens without bushings and two specimens with 0. 25-inch-diameter press fit bushings.

ROOT-FITTING-TO-SPAR (FOUR-HOLE) SPECIMENS

These specimens simulated the area around blade station 90. They were fabricated in two laminated configurations: (1) eighteen laminations of 0. 007-inch-thick AM 355 steel, and (2) one 0. 025-inch, one 0. 009-inch, and thirteen 0. 007-inch-thick laminations of AM 355 steel. Both configurations were bonded together.

The type 1 tests utilized two specimens without bushings. The type 2 tests utilized five specimens with no bushings and three specimens with double countersunk holes (82-degree and 100-degree), and undercut threaded-clamp up 0. 25-inch-diameter bushings with countersunk washers.

TEST SETUP AND PROCEDURE

All specimen tests were performed on an axial tension fatigue test machine. This test machine is a below-resonance type operating at 30 cycles per second, with the cycles recorded on a mechanical counter. Steady and vibratory loads were monitored from a strain-gaged load cell set up in series with the test specimen. Figures 84 and 85 show the setup for the two configurations tested.

RESULTS

SEGMENT-TO-SPAR (TWO-HOLE) SPECIMENS

Table 12 gives the results of the test performed on the laminated specimens. Table 13 gives the results of the solid steel and titanium specimens. Graphs of cycles to failure of these specimens are shown in Figures 86 and 87. Typical failures are shown in Figures 88, 89, and 90.

ROOT-FITTING-TO-SPAR (FOUR-HOLE) SPECIMENS

The results of the laminated specimens tests are given in Table 14. A cycles-to-failure graph shows these results in Figure 91. Some typical failures of these specimens are shown in Figures 92 and 93.

CONCLUSIONS

SEGMENT-TO-SPAR (TWO-HOLE) SPECIMENS

The undercut shank, threaded, countersunk bushing installation was found to be superior in fatigue strength. This superiority was the

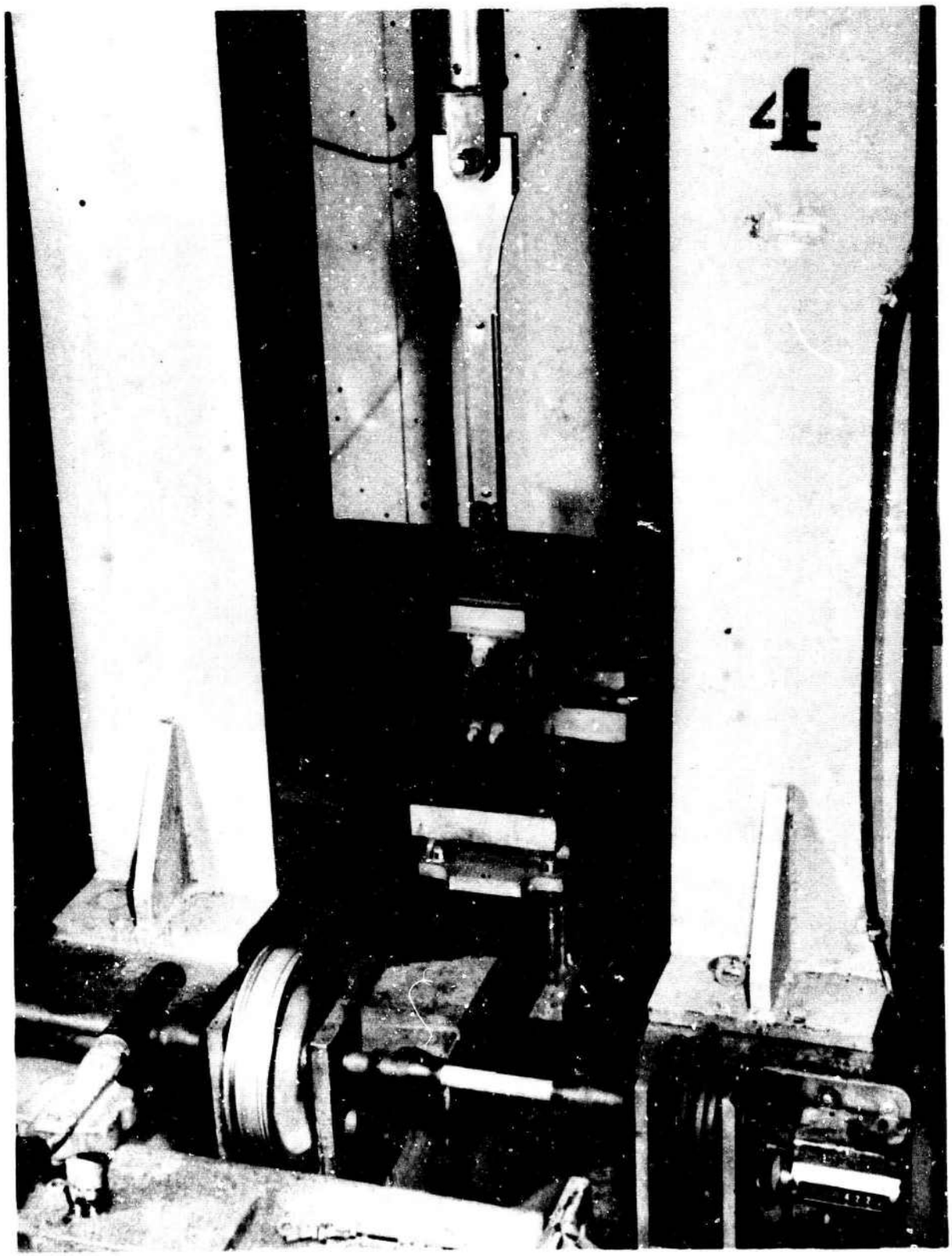

Figure 84. Two-Hole Specimen Test Setup.

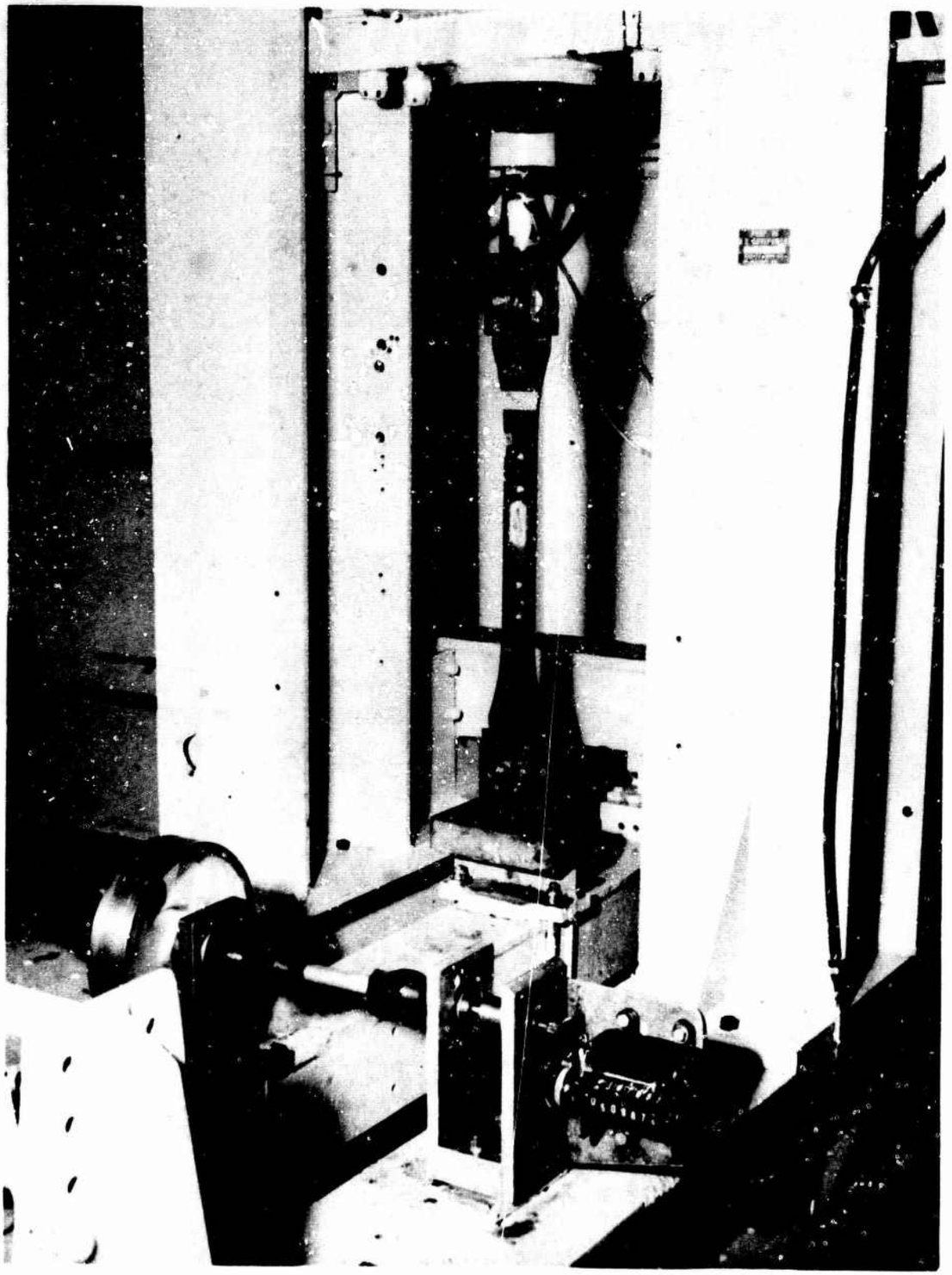

Figure 85. Four-Hole Specimen Test Setup.

TABLE 12
TWO-HOLE SPECIMENS, EIGHTEEN LAMINATIONS, 0.007-INCH AM 355 STEEL

Specimen Number	Configuration	Cycles to Failure x 10^{-6}	Load (lb)	Laminations: Distance Between Holes	Laminations: Hole Dia	Laminations: Width at Holes	Laminations: Pack t	Doubler: Distance Between Holes	Doubler: Hole Dia	Failure Location
1	Loose fit doubler	1.500	+9,600 ±1,000	6.250	0.166	1.406	0.153	6.2445	0.1655	Lower hole
		1.076	+11,000 ±1,500		0.1645	1.400			0 165	
2	Loose fit doubler	0.927	+11,000 ±1,500	6.251	0.166	1.3995	0.157	6.2465	0.165	Lower
					0.1645	1.4035	0.158		0.1645	hole
3	Tight fit doubler	0.556	+11,000 ±1,500	6.252	0.163	1.399	0.155	6.252	0.163	Lower
					0.163	1.403				hole
4	Tight fit doubler	1.868	+11,000 ±1.500	6.250	0.163	1.403	0.152	6.250	0.163	Upper
						1.399				hole
5*	Flanged 0.006-in press fit bushing, 0.25-in OD	0.206	+11,000 ±1,500	6.250	0.1635	1.400	0.144	6.250	0.165	Both
						1.404				holes
6*	Similar to specimen 5	0.190	+11,000 ±1,500	6.250	0.163	1.400	0.144	6.250	0.165	Both
						1.402				holes
7*	Similar to specimen 5	0.180	+11,000 ±1,500	6.250	0.166	1.402	0.144	6.250	0.166	Both
						1.398				holes
10	Similar to specimen 5	0.144	+11,000 ±1,500	6.250	0.163	1.410	0.153	6.250	0.165	Both
						1.4055				holes
9	Flanged threaded 0.0006-in press fit bushing, 0.25-in OD, torque = 65 in -lb	1.012	+11,000 ±1,500	6.250	0.163	1.401	0.158	6.250	0.163	Lower
						1.405				hole
8	Similar to specimen 9 except torque = 70 in -lb	5.030	+11,000 ±1,500	6.250	0.166	1.401	0.181	6.250	0.1655	Upper
						1.402	0.173		0.165	hole
12	Similar to specimen 9	3.710	+11,000 ±1,500	6.253	0.163	1.410	0.159	6.253	0.165	L er
					0.163	1.405				hole
13	Similar to specimen 9	1.397	+11,000 ±1,500	6.252	0.163	1.4095	0.161	6.251	0.166	Lower
						1.4045			0.167	hole

TABLE 12 (Continued)

Specimen Number	Configuration	Cycles to Failure x 10^{-6}	Load (lb)	Specimen: Distance Between Holes	Specimen: Hole Dia	Specimen: Width at Holes	Specimen: Spec t	Doubler: Distance Between Holes	Doubler: Hole Dia	Failure Location
20**	Flanged threaded 0.0008-in press fit bushing, 0.313-in dia, torque = 140 in -lb	0.699	+11,000 ±1,500	6.250	0.165	1.405 1.408	0.162	6.250	0.165	Lower hole
23	Similar to specimen 20, except torque = 150 in -lb	0.668	+11,000 ±1,500	6.254	0.166	1.417 1.416	0.173	6.255	0.163	Lower hole
26	Similar to specimen 23	0.993	+11,000 ±1,500	6.252	0.166	1.413 1.415	0.180	6.251	0.166	Lower hole
17	100° csk threaded 0.0006-in. press fit bushing, 0.25-in. dia, torque = 65 in -lb	0.961	+11,000 ±1,500	6.250	0.165	1.416 1.413	0.153	6.247	0.165	Upper hole
18	Similar to specimen 17	0.548	+11,000 ±1,500	6.252	0.165	1.412 1.415	0.156	6.252	0.165	Lower hole
16	100° csk threaded 0.0008-in. press fit bushing, 0.313-in. dia, torque = 140 in -lb	8.003	+11,000 ±1,500	6.250	0.165	1.414 1.411	0.158	6.249	0.165	Upper hole
19	Similar to specimen 16	10.00	+11,000 ±1,500	6.253	0.165	1.410 1.414	0.161	6.251	0.165	No failure
25	Similar to specimen 16	1.158	+11,000 ±1,500	6.254	0.164	1.417 1.414	0.160	6.253	0.163	Lower hole
27	Similar to specimen 16	0.993	+11,000 ±1,500	6.251	0.164	1.406	0.160	6.250	0.165	Upper hole

21	Similar to specimen 16, except torque = 150 in. -lb	3.633	+11,000 ±1,500	6.253	0.152	1.405	0.159	6.253	0.162	Upper hole
22	Similar to specimen 21	0.184	+11,000 ±1,500	6.250	0.165	1.405	0.156	6.251	0.166	Lower, one lamination only
32*** ****	82° csk threaded undercut bushing, 0.313-in dia, torque = 150 in -lb	15.267 0.539	+11,000 ±1,500 +11,000 ±1,875	6.254	0.164	1.411 1.413	0.170	6.255	0.163	Lower hole
35* ****	Similar to specimen 32, except torque = 140-in -lb	12.881 6.204	+11,000 ±1,500 ±1,875	6.251	0.164	1.412 1.412	0.174	6.250	0.165	Upper hole, internal
38* ****	Similar to specimen 35	23.011 →	+11,000 ±1,875	6.251	0.165	1.405 1.407	0.165	6.250	0.165	No failure
34* ****	100° csk threaded undercut bushing, 0.313-in dia, torque = 140 in -lb	12.865 7.277	+11,000 ±1,500 +11,000 ±1,875	6.250	0.164	1.412	0.164	6.250	0.165	Upper hole, internal
36* ****	Similar to specimen 34	15.121 23.242	+11,000 ±1,500 ±1,875	6.252	0.164	1.406 1.404	0.155	6.252	0.163	Lower hole, 0.025 lamination only
37* ****	Similar to specimen 34	3.566	+11,000 ±1,875	6.251	0.165	1.404	0.170	6.251	0.165	Upper hole
33****	Similar to specimen 34	1.935	+11,000 ±1,500	6.252	0.164	1.411	0.176	6.253	0.163	Adjacent to lower hole, 0.025 lamination only

*Armalon used between doubler and laminations as an antifretting material.

**Strain-gaged doubler on specimen 20 indicated +396 ±202-pound loading.

***Specimen 32 rerun and an additional 0.574 x 1[illegible] cycles accumulated before complete failure.

****These laminated specimens consisted of one 0.025-inch-thick, thirteen 0.007-inch-thick, and one 0.009-inch-thick laminations. The countersink is on the 0.025-inch-thick lamination side.

TABLE 13
TWO-HOLE SOLID SPECIMENS

Specimen Number	Configuration	Cycles to Failure x 10^{-6}	Load (lb)	Specimen				Doubler		Failure Location
				Distance Between Holes	Hole Dia	Width at Holes	Spec t	Distance Between Holes	Hole Dia	
11*	4130 steel, 125,000 psi ht tr, no bushing	13.614	+11,000 ±1,500	6.2465	0.1652	1.391 1.398	0.131	6.245	0.165	No failure
14*	Similar to specimen 11	0.902	+11,000 ±1,500	6.2475	0.166 0.164	1.3935 1.401	0.129	6.246	0.165	Lower hole
15	Similar to specimen 11	3.642	+11,000 ±1,500	6.245	0.164 0.165	1.391 1.399	0.129	6.245	0.165	Lower hole
31	Similar to specimen 11	9.863	+11,000 ±1,500	6.244	0.166	1.398 1.391	0.131	6.245	0.166	No failure
24	Titanium - 6 Al 4 V - 130,000 psi, no bushing	0.243	+11,000 ±1,500	6.250	0.165	1.408 1.406	0.157	6.245	0.165	Lower hole
28	Similar to specimen 24	0.297	+11,000 ±1,500	6.250	0.166	1.407 1.409	0.158	6.250	0.166	Upper hole
29	Titanium - 6 Al 4 V - 130,000 psi. 0.0005-in. press fit bushing, 0.25-in dia	0.070	+11,000 ±1,500	6.250	0.163	1.407 1.405	0.157	6.252	0.163	Upper hole
30* **	Similar to specimen 29	0.082	+11,000 ±1,500	6.250	0.163	1.407 1.405	0.153	6.250	0.165	Upper hole

*Armalon used between doubler and specimen as an antifretting material.
**Strain-gaged doubler on titanium specimen 30 indicated +983 ±287 pounds.

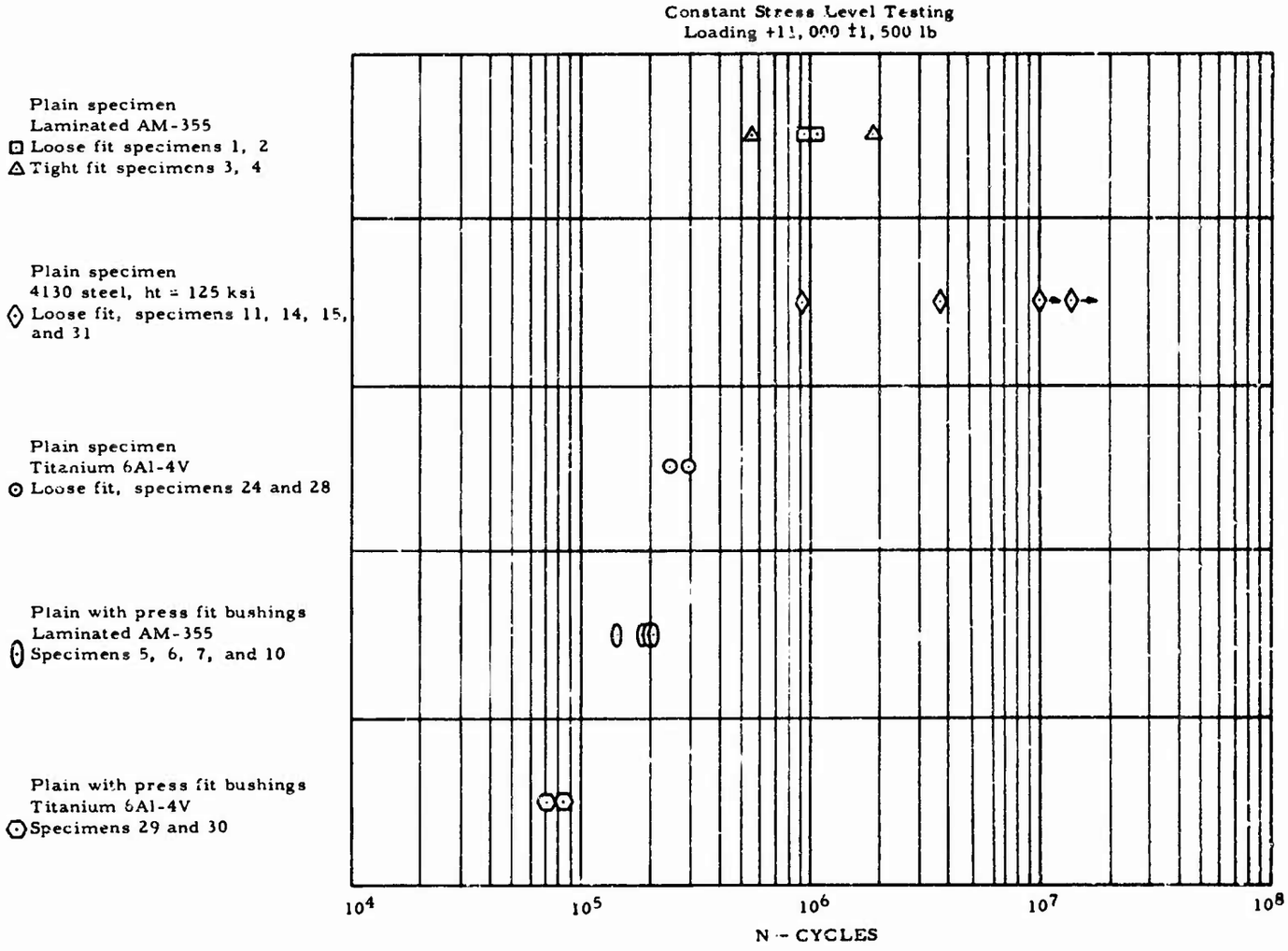

Figure 86. Two-Hole Segment Attachment-Type Specimens, Solid and Laminated.

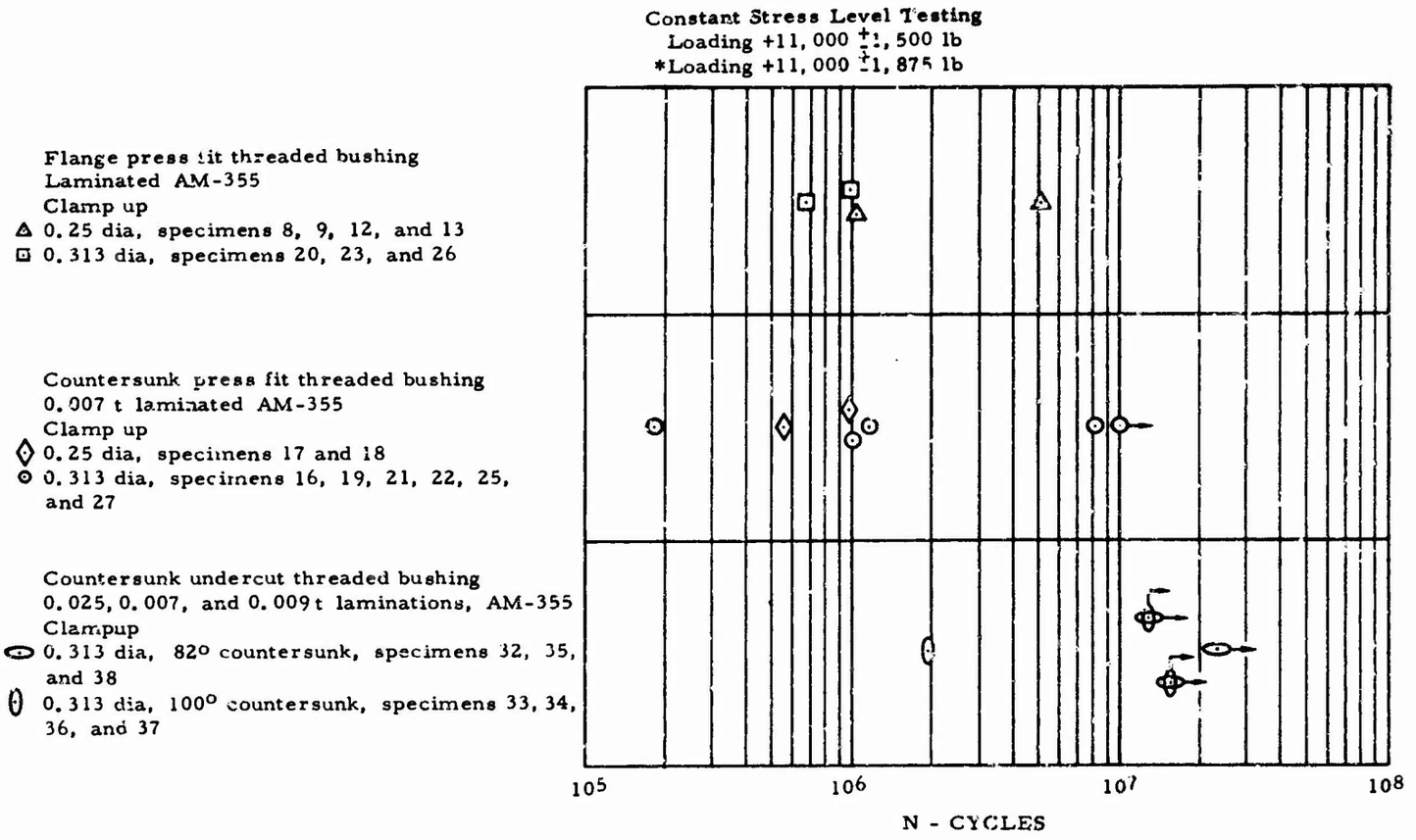

*Specimens 32, 34, 35, and 36 ran at increased loadings of +11, 000 ±1, 875 after runouts. Specimens 37 and 38 ran only at increased loading of +11, 000 ±1, 875

Figure 87. Two-Hole Segment Attachment-Type Specimens. Laminated.

Figure 88. Typical Steel Specimen Failures.

Figure 89. Typical Titanium Specimen Failures.

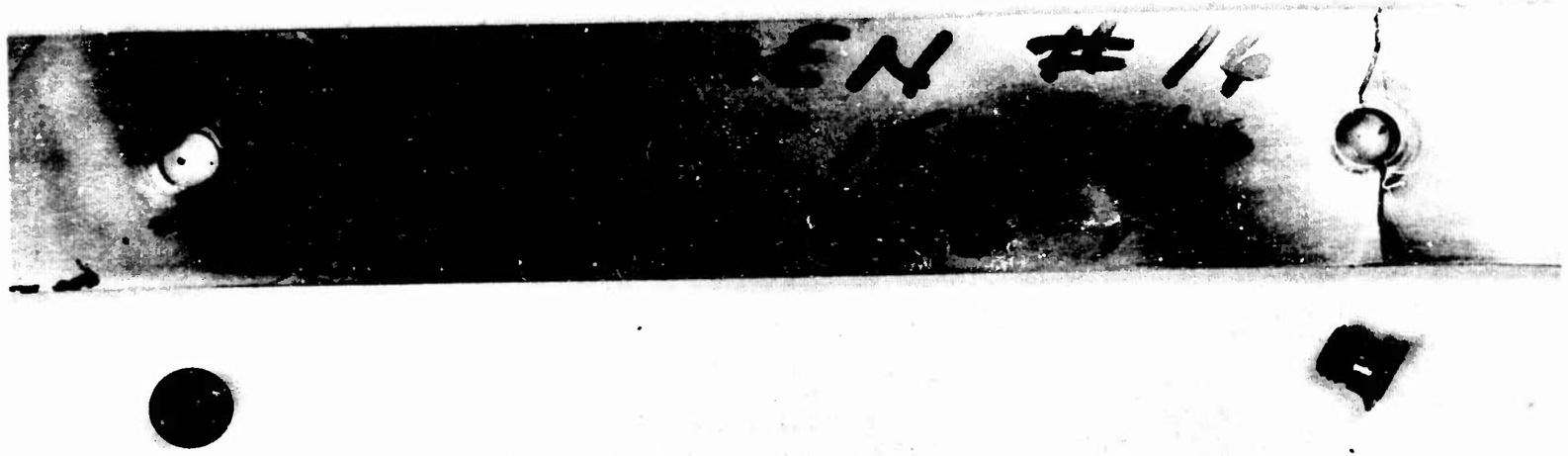

Figure 90. Typical Cracked Two-Hole Specimen.

TABLE 14
FOUR-HOLE SPECIMENS

Specimen Number	Configuration	Cycles to Failure x 10^{-6}	Load (lb)	Laminations				Doubler		Failure Location
				Distance Between Holes	Hole Dia	Width at Holes	Pack t	Distance Between Holes	Hole Dia	
39*	18 laminations, 0.007-in AM 355 steel, no bushings	0.293	+11,000 ±1,500	6.250 1.250 3.749 1.250	0.163	1.409 1.411	0.160	6.250 1.250 3.749 1.250	0.163	Lower hole
40*	Similar to specimen 39	0.317	+11,000 ±1,500	6.250 1.250 3.750 1.250	0.163	1.406	0.155	6.250 1.250 3.750 1.250	0.163	Lower hole
44*	One 0.025, thirteen 0.007, one 0.009-in laminations, AM 355 steel, no bushings, torque #8 = 7 - 9, #10 = 40 in -lb	0.468	+11,000 ±1,500	6.250 1.250 3.750 1.250	0.163 0.189 0.189 0.163	1.398	0.167	6.250 1.250 3.750 1.250	0.163 0.188 0.189 0.163	Upper hole
45*	Similar to specimen 44	10.344 16.328	+11,000 ±1,500 +11,000 ±1,875	6.249 1.251 3.749 1.249	0.166 0.189 0.189 0.166	1.398	0.158	6.250 1.251 3.750 1.249	0.167 0.189 0.189 0.167	No failure
46**	Similar to specimen 44	8.042 13.669	+11,000 ±1,500 +11,000 ±1,875	6.254 1.256 3.752 1.246	0.166 0.189 0.189 0.166	1.399 1.398	0.167	6.254 1.256 3.752 1.246	0.167 0.190 0.190 0.167	Upper hole

47** ***	Similar to specimen 44	7.516	+11,000 ±1,500	6.255 1.254	0.166 0.189	1.398	0.172	6.251 1.253	0.166 0.190	Upper hole
		2.593	+11,000 ±1,875	3.752 1.250	0.189 0.166			3.748 1.250	0.190 0.166	
48**	Similar to specimen 44	13.220	+11,000 ±1,875	6.247 1.249 3.750 1.249	0.166 0.190 0.189 0.166	1.412 1.410	0.171	6.247 1.249 3.750 1.249	0.167 0.191 0.190 0.167	No failure
41*	One 0.025, thirteen 0.007, one 0.009-in laminations, AM 355 steel, double csk specimen, threaded undercut bolt, csk washer, 0.25-in dia bolt, torque = 90 in -lb	1.405	+11,000 ±1,500	-	-	1.406 1.407	0.160	-	-	Lower hole
42*	Similar to specimen 41 except torque = 110 in -lb	20.183	+11,000 ±1,500	-	-	1.412 1.411	0.190	-	-	No failure
43*	Similar to specimen 41 except torque = 110 in -lb	0.611	+11,000 ±1,875	-	-	1.402 1.403	0.155	-	-	Upper hole

*Armalon used between doubler and laminations as an antifretting material.

**Doubler coated with 0.007 - 0.009-in thick Epon.

***Specimen 47 - two laminations (0.007 and 0.009-in) were cracked 50 percent of original width at 0.184×10^6 cycles due to fretting between doubler and laminations. An additional 2.409×10^6 cycles were accumulated before complete failure occurred.

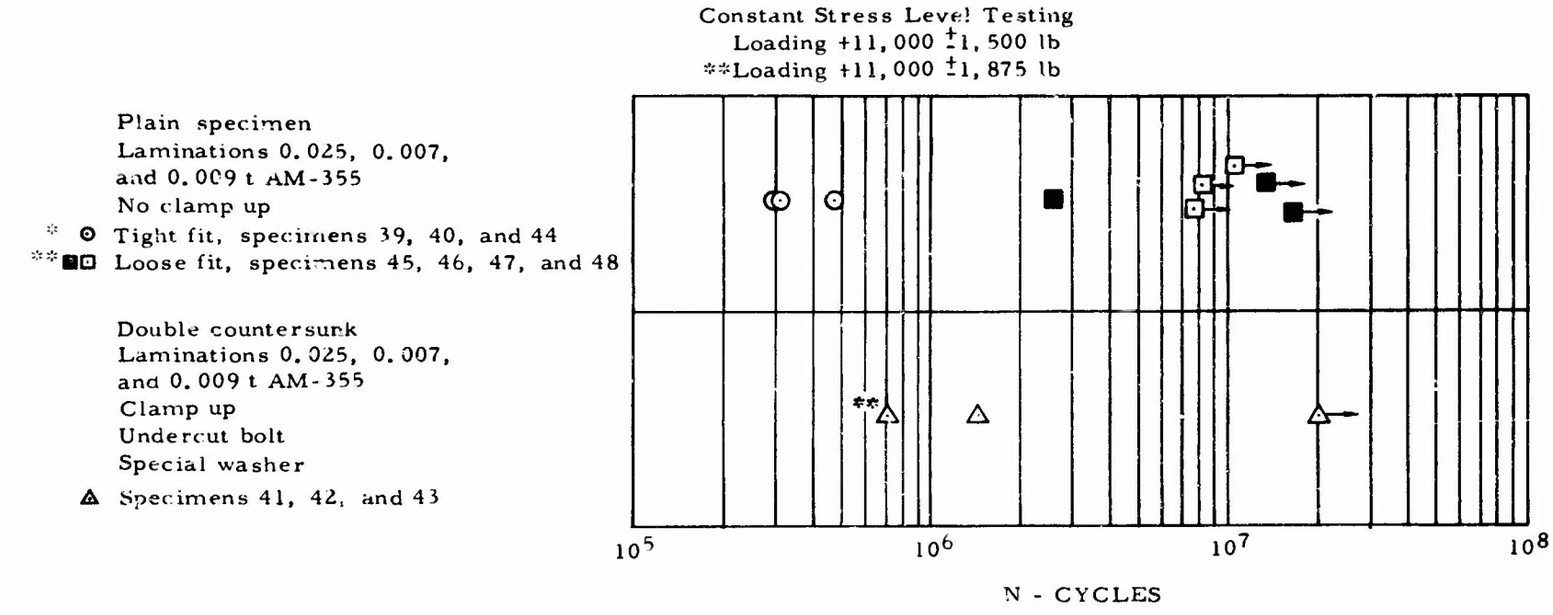

*Specimens 39 and 40 were of all the 0.007 t AM-355 laminations

**Increased loading on specimens 45, 46, 47, 48, and 43 to +11,000 ± 1,875 lb

Figure 91. Four-Hole Root-End Attachment-Type Specimen.

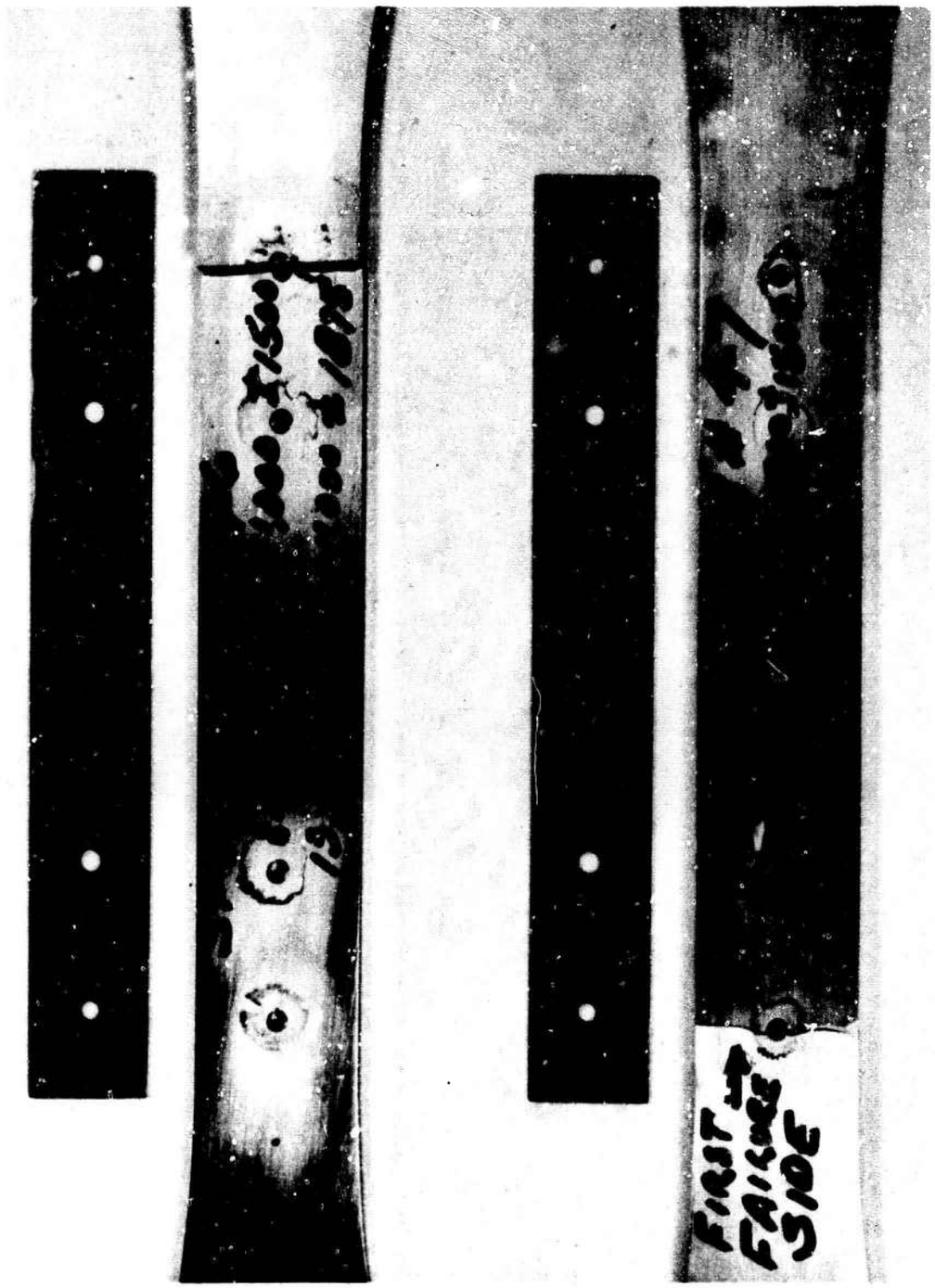

Figure 92. Typical Cracked Four-Hole Specimen.

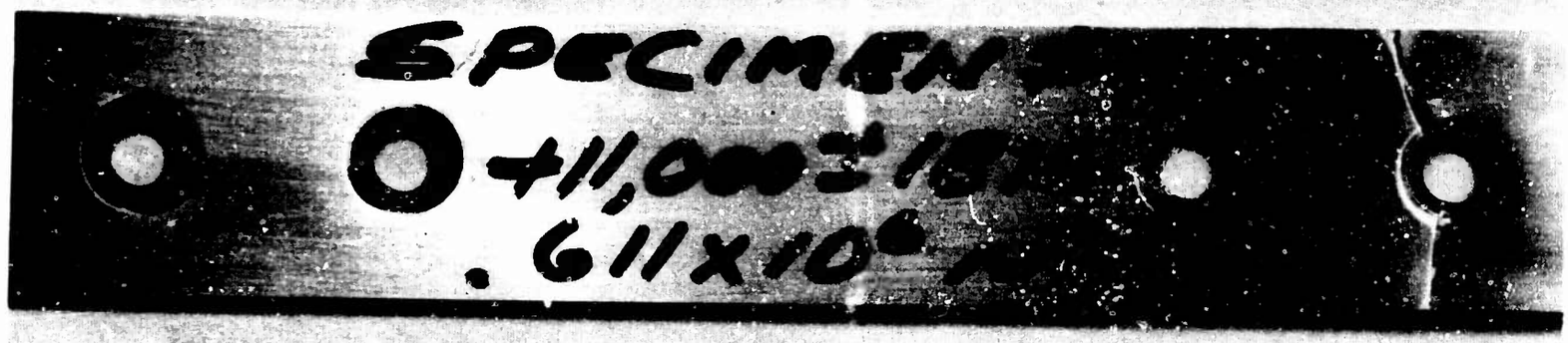

Figure 93. Typical Cracked Four-Hole Countersunk Specimen.

result of the clamping action of the bolt-bushing arrangement, which preloaded the spar bolt hole. Also, careful deburring of the bolt hole was a contributing factor in increasing the fatigue strength. In addition, fretting was practically eliminated. The spar bolt holes without bushings and the holes with press fit bushings indicated excessive fretting, and an examination of the spar holes revealed the presence of burrs on the interlaminate edges of the hole in the bond layers. This condition produced a noticeable reduction in fatigue strength when compared with the undercut clampup bushing installation.

ROOT-FITTING-TO-SPAR (FOUR-HOLE) SPECIMENS

The results of these tests indicated that thinning down the doubler at the first hole and loosening the fit at this hole gave an approximate infinite life of 70, 000 $\pm$10, 000 psi fatigue strength. The addition of another bolt to reduce the bolt spacing also contributed to the increase in fatigue strength.

FLIGHT CONTROLS HYDRAULIC SERVO ASSEMBLY ENDURANCE TESTS

SUBJECT

This section concerns the endurance testing of the hydraulic servo assembly used in the flight control system of the XV-9A. These tests were conducted during the months of September and October at the HTC-AD hydraulic laboratory.

PURPOSE

The purpose of these tests was to ensure the reliability of the hydraulic servo assembly used in the flight control system of the XV-9A helicopter.

SUMMARY OF RESULTS

The results indicate that the hydraulic servo assembly is adequate for use in the XV-9A.

TEST SPECIMEN

The specimen consisted of a hydraulic servo assembly manufactured to HTC-AD specifications.

TEST SETUP AND PROCEDURE

Servo assembly serial number 101 was mounted in a harness structure in such a manner that it could be loaded or driven with another power servo assembly. All general conditions were held throughout the entire test program as follows:

System pressure, 3200 $\pm$100 psi
Return pressure, 60 $\pm$5 psi
Oil, MIL-H-6083B
Maximum temperature, 160°F
Sine wave input, except as noted
All loads monitored by means of calibrated load cell and oscillograph

The test setup is shown in Figures 94 and 95.

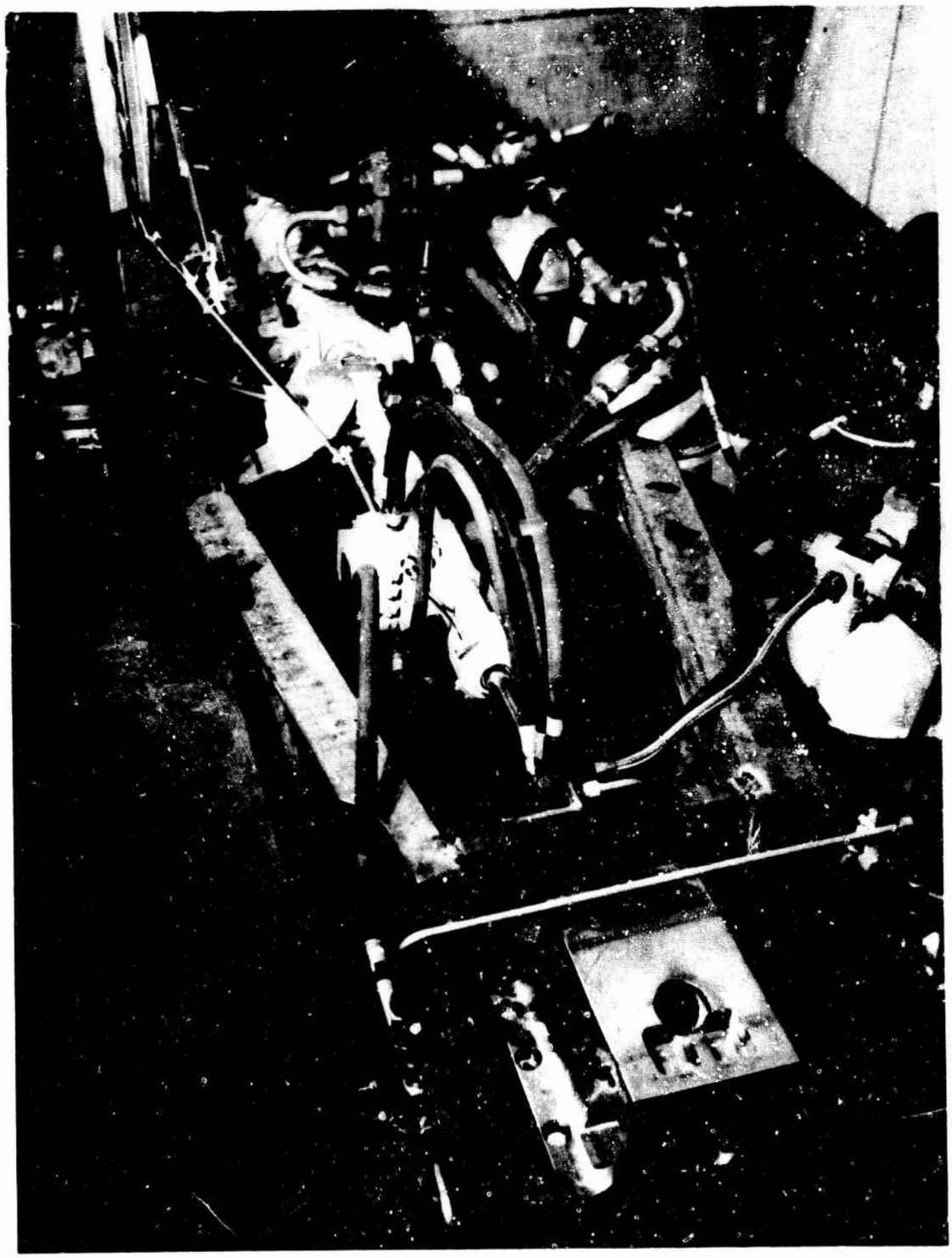

Figure 94. Hydraulic Servo Assembly Endurance Test Apparatus.

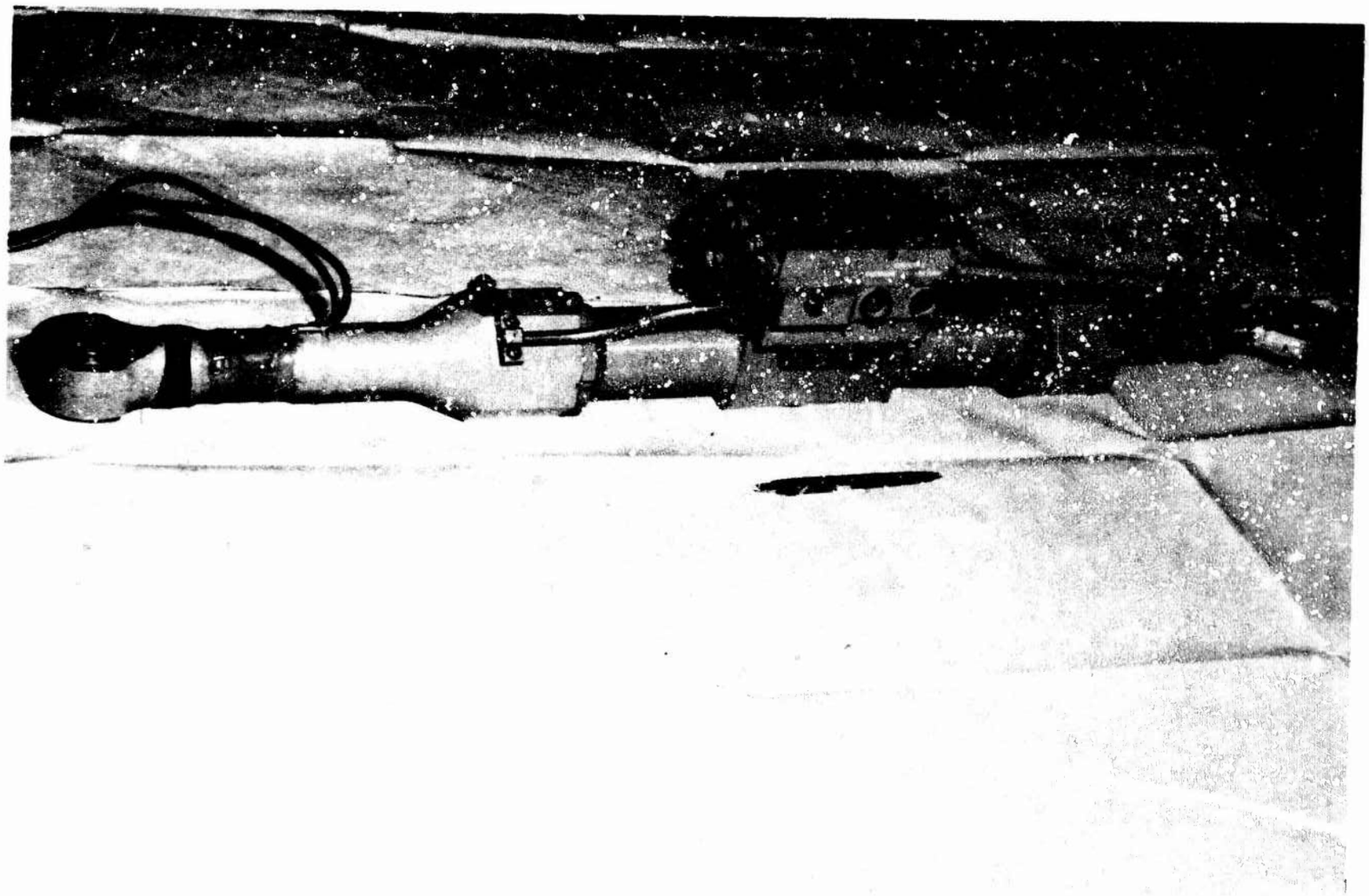

Figure 95. Hydraulic Servo Assembly.

TEST RESULTS

1. With the servo valve input stationary and the cylinder in mid position, a cyclic load of 1000 pounds (2000 pounds peak to peak) was applied at 240 cycles per minute, with the following results:

   a. With both systems operating for 850, 000 cycles

      (1) No malfunction
      (2) Force required to hold valve stationary at input shaft = 4 pounds
      (3) First leakage appeared at center vent hole at 36, 000 cycles
      (4) Measured leakage at completion of 850, 000 cycles = 3 milliliters

   b. System 1 only operating for 50, 000 cycles

      (1) No malfunction
      (2) Leakage less than 1 milliliter for the 50, 000 cycles

   c. System 2 only operating for 50, 000 cycles

      (1) No malfunction
      (2) Leakage less than 1 milliliter for this 50, 000 cycles

2. With the servo driving and load applied by the test stand cylinder acting as a pump exhausting through a relief valve, the following tests were conducted:

   a. Load, both directions, 5000 pounds; stroke 3. 4 inches; both systems operating for 15, 000 cycles. The test request called for a rate between 5. 2 and 5. 9 inches per second. However, with sine wave input, in order to even hit peaks of 5. 2 inches per second a cyclic rate of 29 cycles per minute is required. The servo would not carry the 5000-pound load at cyclic rates above 19 cycles per minute. On the recommendations of the Design Engineering Group, this phase of the test was run at 19 cycles per minute, which gives a cylinder travel peak rate of 3. 4 inches per second.

      (1) The 15, 000 cycles were completed with no malfunction
      (2) Force required to operate valve = 7 pounds
      (3) Total measurable leakage for this phase of test = 60 milliliters

b. Same as 2a, except rate asked for was 1.6 inch per second minimum with System 1 only operating. To reach peaks of 1.6 inch per second with sine wave input requires 9 cycles per minute, at which rate the servo would not carry the load. It did handle the load at 8-1/2 cycles per minute by allowing it to flatten out the peaks. (The servo valve was held wide open against its stops for 50 percent of the stroke in both directions.) The 2500 cycles were run under this condition.

(1) No malfunction
(2) Leakage 5-milliliters total for the 2500 cycles

c. Same as 2b, except with System 2 only operating. Even though the same 1.6 inch per second was called for, the highest rate at which System 2 would handle the load was 7-1/2 cycles per minute, and this by allowing the valve to be held against the stops for 50 percent of each stroke, as in 2b.

(1) No malfunction occurred during this condition
(2) Total leakage for this 2500 cycles = 5 milliliters

d. Load, both directions, 2500 pounds; both systems operating for 15,000 cycles. The test request was corrected to call for a 6.5-inch stroke rather than 6.9-inch. The test request called for 5.2-inch per second maximum, so even though both systems would carry this load at 18 cycles per minute, this phase was run at 15 cycles per minute to keep the peaks below 5.2 inches per second.

(1) Oil started dripping from the vent hole in the side of the housing at the end opposite the exposed shaft as soon as this phase of the test was started. (This probably means that the tailstock was gradually filling up during the short-stroke phases of the test.)
(2) No malfunction
(3) Total leakage for the 15,000 cycles (both vent holes and exposed shaft seal) = 240 milliliters

e. Load, 2500 pounds; full stroke; System 2 only operating. The test request called for a minimum rate of 5.0 inches per second, but the highest rate at which System 2 would handle the 2500-pound load was 6 cycles per minute, and the servo valve was bottomed 80 percent of each stroke to reach this rate.

The test was stopped after 600 cycles of this phase, and the servo assembly was removed from the test structure. The unit was taken to the manufacturer, where it was disassembled. It was found that the teflon piston-ring seals had managed to work themselves around until their slots lined up, thus providing a flow path for the fluid. This seal consists of two teflon rings in one groove with a corrugated spring under their inside diameter to exert a slight outward force. The rings are split for installation purposes, and are assembled with the cuts (or slots) 180 degrees apart.

An effort was made to use the same seals by realigning the slots so as not to have a through flow passage, but, because of wear on the outside diameter of the rings, it was impossible to get the seal to perform satisfactorily. A new seal assembly was installed.

It was also found that the teflon cap strip on the tailstock rod seal (System 1) was worn completely through. This was probably caused by a faulty installation that left a wrinkle in the thin teflon strip. This seal was also replaced.

No other seals or parts were changed. The unit was reassembled, checked out, and installed on the cycler for continuation of the life test.

The servo was remounted on the test bed and the rate was set at 16 cycles per minute (with sine wave input), and the 2500 cycles were run with no further problem except for leakage.

f. Same conditions as 2e, except System 1 only operating

(1) No malfunction
(2) Total leakage for 5000 cycles (2e and 2f) = 30 milliliters

3. The servo valve input was held stationary and force was applied by the test stand cylinder to move the tailstock end of the cylinder the required $\pm$0.200 inch (0.2 inch on both sides of neutral or the no load position — making a total travel of 0.4 inch); rate 240 cycles per minute.

a. With both systems operating (that is 3200 psi on System 1 and System 2 of the servo), the load went to more than 7500 pounds

in each direction. The stroke was cut down to ±0.062, giving a total stroke of 1/8 inch. This change produced a load of 6000 pounds in each direction at 240 cycles per minute. This condition was maintained for 40, 000 cycles.

(1) One malfunction occurred at 4000 cycles. This consisted of the failure of the brazed joint in the System 1 stainless steel transfer tube. It was removed, rebrazed, reinstalled, and gave no more trouble.

b. Same condition as 3a, except that only System 1 was operating for 5000 cycles.

(1) No malfunction, but stroke had to be increased to ±0.078, making a total stroke of 0.156, to bring the load up to 6000 pounds.

c. Same as 3b, except System 2 only operating.

(1) No malfunction
(2) Total leakage for the last 50, 000 cycles (3a, 3b, 3c) = 23 milliliters plus the amount that may be trapped in the tailstock (vent hole is on the side, so the cavity must be approximately one-half full before any leakage from the shaft seal at this end can be measured).

After completion of the endurance tests, the servo was removed from the test bed and both systems were subjected to proof pressure of 5250 psi. There was no failure and no permanent distortion.

CONCLUSIONS

Although some leakage was experienced past the piston rod seals throughout the test, this leakage never reached a value that would cause concern under normal ship operation. In most cases, the leakage appeared to decrease as the test progressed.

The assembly was removed from the test fixture (Figure 94) and partially disassembled after approximately 1, 000, 000 cycles, because of a loss in speed while operating on System 2 only. It was found that the teflon piston ring seals had worked themselves around in the groove until their slots lined up, thus providing a flow path for the fluid past the main piston. This occurrence would not be considered as a cylinder failure, because its only effect on the servo was to slow its rate when operating against a large load.

While the unit was disassembled, the seals on the System 1 piston and the piston rod were closely inspected. It was found that the teflon cap strip on the tailstock rod seal (System 1) was worn completely through. This was probably caused by a faulty installation that left a wrinkle in the thin teflon strip. This seal and the seals on the System 2 main piston were replaced. No other seals or parts were changed. The unit was reassembled, checked out, reinstalled on the cycler, and the test was continued (see Figure 96).

During the overcoming load portion of the test, a furnace-brazed connection in the tube leading from the servo valve to the outer end of the actuating cylinder (System 1) failed. Although this tube is subjected to comparatively high internal pressures during single-system operation, at the time of the rupture the pressure was probably not more than 2200 psi. However, the load being put into the test unit by the loading cylinder was greater than desired. It is believed that this high load caused an elongation between the valve body and the outboard cylinder head, thus pulling the tube from its housing.

The tube assembly was rebrazed, and the test was continued to its conclusion without further trouble.

Upon completion of the tests, the unit was partially disassembled in the following manner: The cylinder section was completely dismantled and all seals and rubbing surfaces were closely inspected. It was found that the piston ring seals on the main pistons had moved from the position they were in when the unit had been disassembled for repair. The slots were not lined up on either piston, but the fact that they had moved during the 50, 000 cycles of the overcoming load tests indicates that this seal is not the best for this application.

It was also found that the steel pin holding the piston to the piston rod on the tailstock end of the cylinder had broken during the 50, 000-cycle overcoming load test. This pin had been observed to be in satisfactory condition during the previous disassembly at the manufacturer's facility. Functionally, this pin passes through holes in the piston and piston rod, and is held in place by a lock screw, which is threaded into the piston 90 degrees from the pin and rests against a necked-down portion at the center of the pin (see Figure 97). Ordinarily, only shear loads are carried by the pin, and those loads would be at the intersection of the piston rod and the piston.

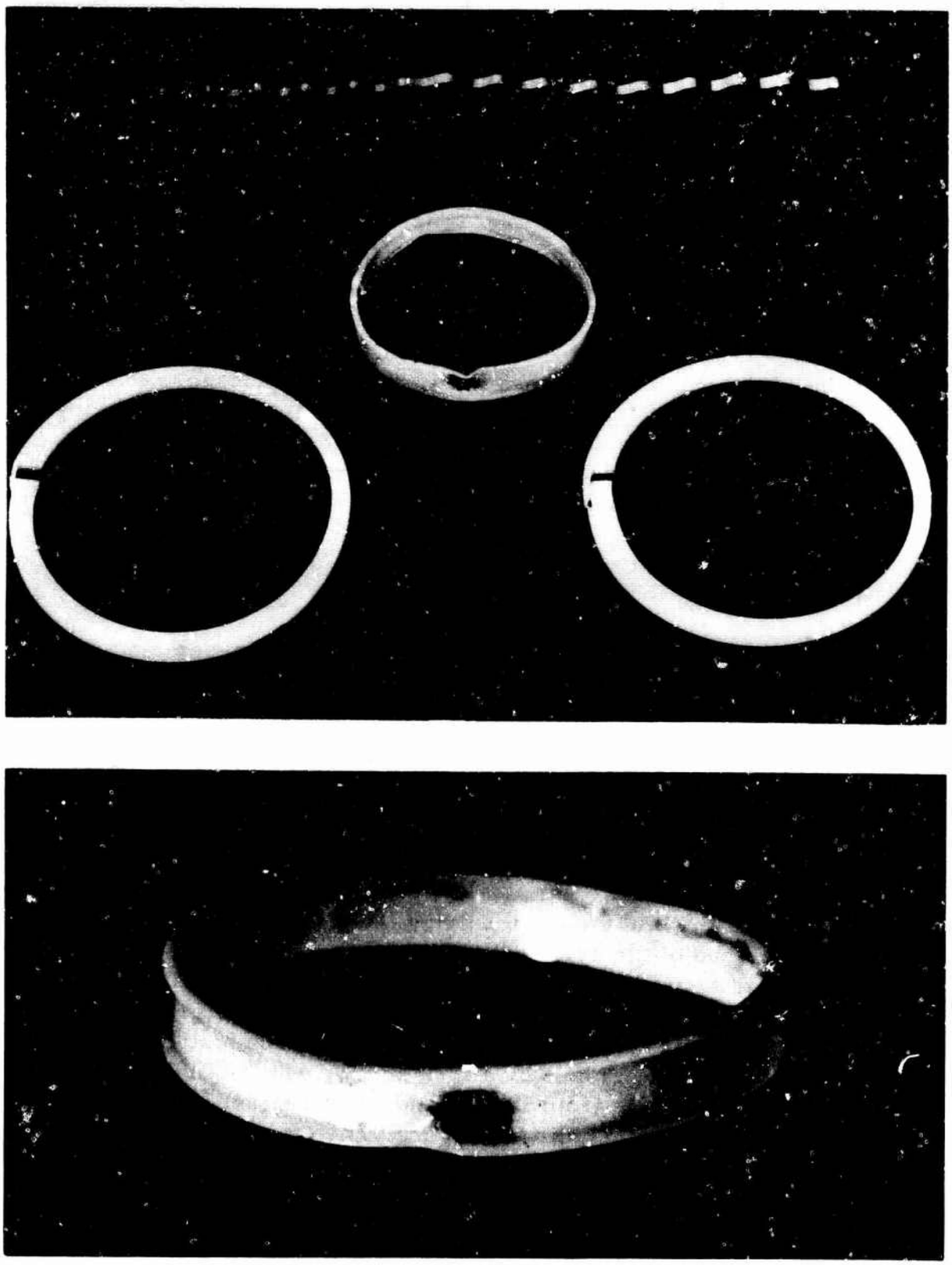

Figure 96. Damaged Seals.

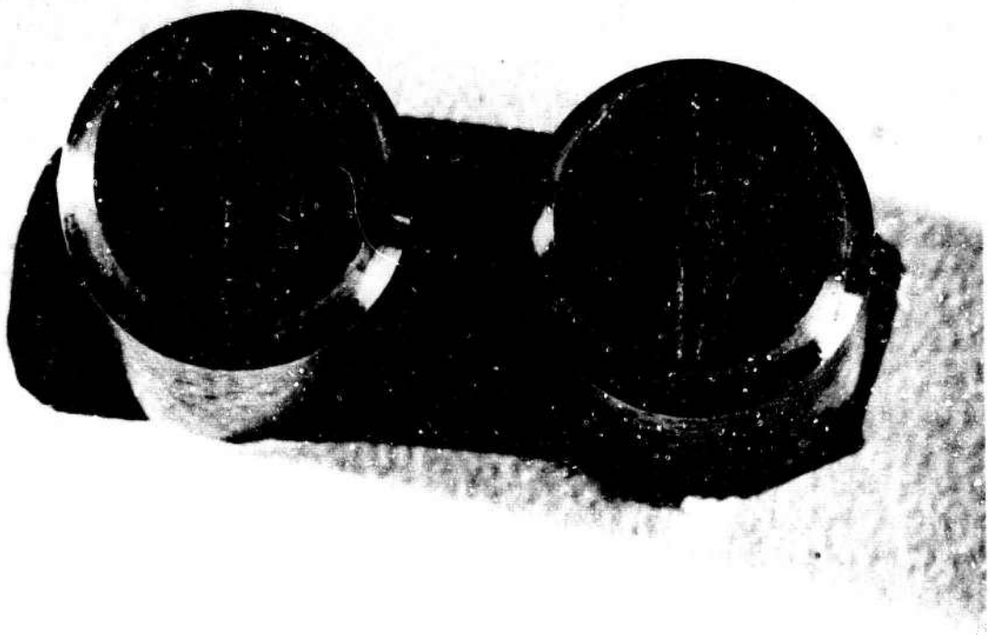

Figure 97. Broken Pin.

A visual examination of the broken pin resulted in the conclusion that the failure was caused by fatigue from a low-overstress, high-cycle reverse-bending load. A dimensional check of the pin outside diameter and the holes in the piston and the piston rod showed the maximum clearance between the pin and the rod to be 0. 004 inch. The maximum clearance between the pin and the piston was 0. 002 inch. This adds up to a clearance of 0. 006 inch between the piston and the piston rod. The detail drawings allow for pin-to-piston and pin-to-rod clearance of 0. 0007 inch maximum.

Only one end of this pin had been chamfered, and, after breaking, the unchamfered end had worked out and grooved the inside diameter of the cylinder barrel (see Figure 98).

With the above exceptions, all parts of the cylinder showed only the normal wear that would result from the more than 1, 000, 000 cycles to which the unit was subjected.

The disassembly of the valve section of the servo also showed only normal wear, with the exception of the low-pressure relief valve seats. There are four of these relief valve assemblies in the unit — two for each system. The function of these valves is to relieve the pressure from one side of the main piston to the other during dual system operation. These valves operated during the dual system overcoming load test, a total of 40, 000 cycles.

Upon examination, it was found that the valve seats had been peened in by the pounding of the valve poppets, making it impossible to remove the poppets from the cartridge. However, the poppets have adequate free movement for proper operation, and a close examination of the poppet face and the seal showed no evidence of wear that would affect their operation.

RECOMMENDATIONS

None of the aforementioned faults or failures requires an immediate change in existing hardware. However, if additional units are manufactured, the following changes are recommended:

1. Use of a different seal on the main pistons. A rubber-backed teflon slipper ring, such as used for the piston rod seal, is recommended.

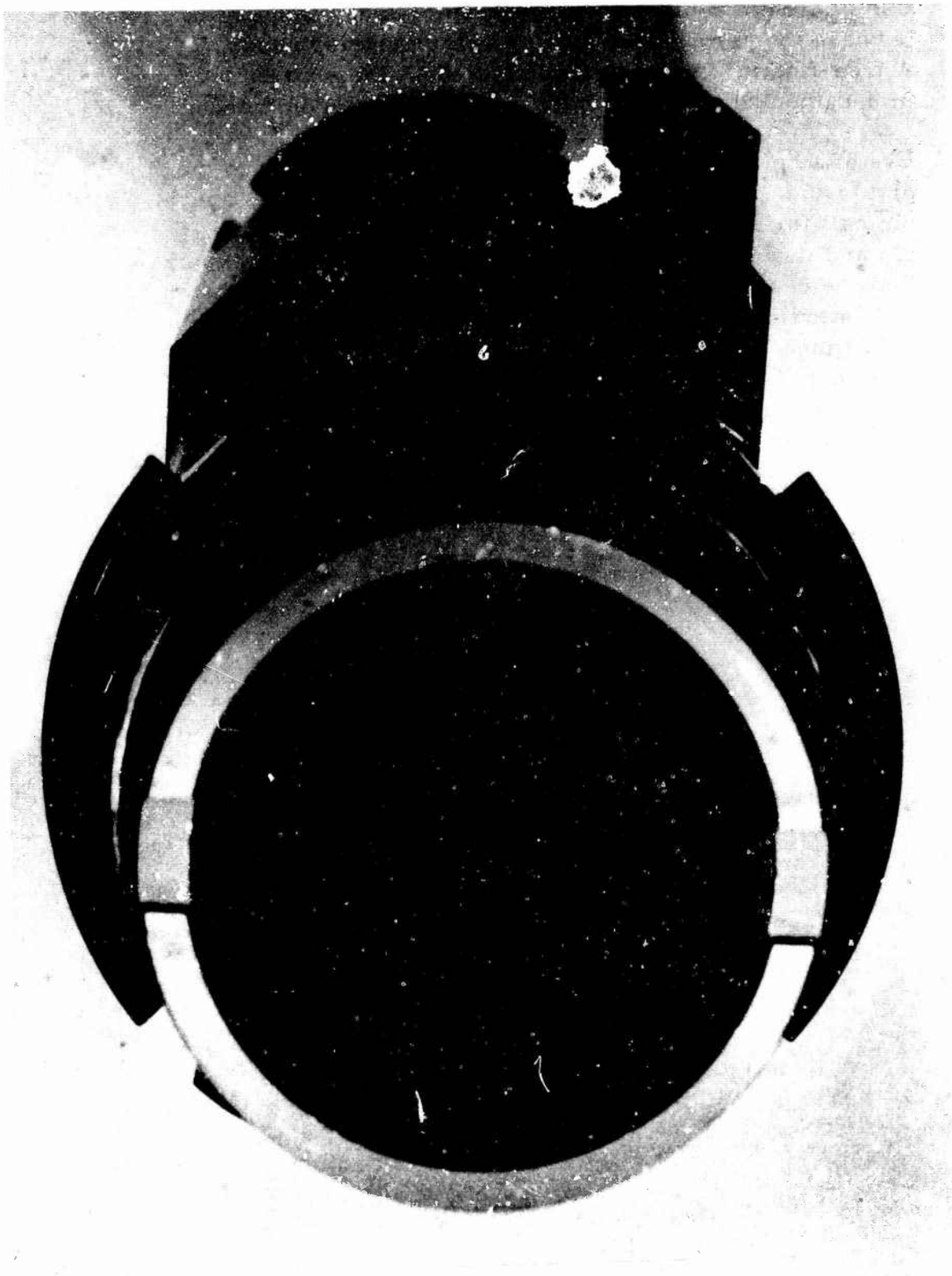

Figure 98. Cylinder Wall.

2. Use of a method other than a brazed tube as plumbing between the servo valve and the outer cylinder heads. A free-floating connection unaffected by the shortening or lengthening of the cylinder assembly is recommended.

3. Use of a better method of securing the main piston to the piston rod. The detail drawings of the piston, rod, and pin call for zero to 0.0007-inch clearance between the pin and its mating parts. The detail drawings also require that the centerline of the holes in the piston and the piston rod intersect the centerline of the respective parts within 0.001 inch. This could result in a 0.001-inch misalignment between the parts through which the pin must pass. If a maximum misalignment occurs with a zero-clearance pin, the pin must be forced into place. If this type of connection is used, it could be better to call for match drill and reaming of the piston and piston rod, so as to obtain perfect alignment.

ROTOR-SPEED FEEDBACK SYSTEM EVALUATION TESTS

SUBJECT

These tests constituted an evaluation of the rotor-speed feedback system (N_f system) designed to drive the YT-64 gas generator turbine speed governor shaft. The tests were conducted to determine signal transmission error, system natural frequency, and YT-64 governor drive torque. The tests were conducted in the HTC-AD equipment test laboratory in April 1964.

PURPOSE

The purpose of these tests was to substantiate that the rotor-speed feedback system will drive the gas generator governor at a speed proportional to the rotor speed, and will do so without speed oscillations that would cause gas-generator power oscillations.

SUMMARY OF RESULTS

The N_f system was found to have a natural frequency of approximately 15 cycles per second. Analyses conducted by HTC-AD and by the engine manufacturer indicated that the gas generator will be stable when the signal transfer system has a natural frequency above approximately 5 cycles per second. In addition, for the expected operational conditions, the N_f system is nearly critically damped. Thus, the N_f system tested is considered satisfactory from these standpoints.

When the N_f system was operated as a simple hydrostatic transmission, with no fluid extraction between pump output and motor input, the transmission error was found to be unmeasurably small over the tested range of 3270 to 4970 rpm.

The governor motor input torque was found to vary from 0.99 pound-inch at 2000 rpm to 1.72 pound-inch at 5000 rpm. This is approximately one-half the expected torque and far smaller than the capability of the smallest available piston-type hydraulic pumps and motors (15.7 pound-inch rated).

TEST SYSTEM (Figure 99)

The system tested consisted of a hydraulic pump (0.049-cubic-inch displacement) and a hydraulic motor. The high-pressure ports were

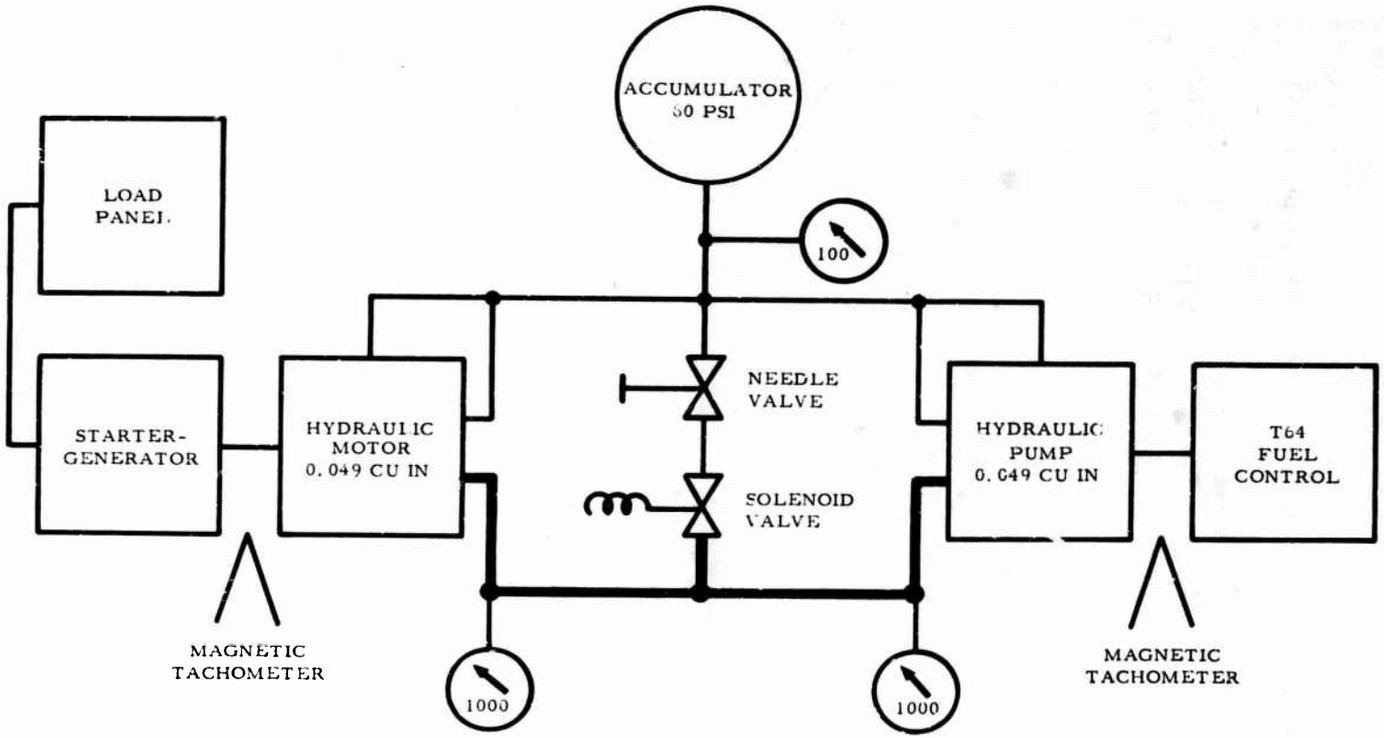

Figure 99. N_f System Schematic.

connected by a signal transfer tube, 21 feet long, of 0.250-inch diameter by 0.065-inch-wall corrosion-resistant steel tubing The low-pressure ports were both connected by 0.375-inch-diameter tube and hose to an accumulator that maintained system return pressure at 60 psi. The high-pressure signal transfer line and the return line were connected by a bypass tube. The bypass flow was controlled by a needle valve and solenoid valve in series. This system, except for the solenoid valve, effectively duplicates the systems that have been installed on the XV-9A. The solenoid valve does not change the dynamic or static characteristics of the test system, since it is installed on the low-pressure side of the bypass needle valve.

TEST APPARATUS AND INSTRUMENTATION

The test apparatus shown in Figure 100 consisted of the N_f system described above, an electric aircraft starter-generator of effectively infinite inertia, a specially prepared YT-64 fuel control, and an electric load bank to control the starter-generator speed.

The engine manufacturer prepared a YT-64 fuel control for use in these tests by locking the governor flyball servo spool to a nominal position that represents its position during normal gas generator operation. The fuel control was filled with fuel to obtain proper flyball damping and torque.

The starter-generator and fuel control were connected to the pump and motor by suitable adapter flanges and quill shafts.

The system instrumentation consists of two magnetic pickups energized by two lobes on the pump and motor quill shafts. The pickup signals were recorded by a direct-writing oscillograph. The speeds of the driving and driven members were counted by hand from the oscillograph trace. Hydraulic system return pressure was measured by a gage. Transfer line pressure was not measured during studies of dynamic characteristics, since the additional pressure system volume would compromise the test results. For test of signal accuracy, pressure gages were installed at the pump and motor high-pressure ports to determine motor torque and line losses.

PROCEDURES

DETERMINATION OF SYSTEM FREQUENCY RESPONSE

The electric starter-generator was driven by the electric load bank at a speed of approximately 3200 rpm. This speed was measured

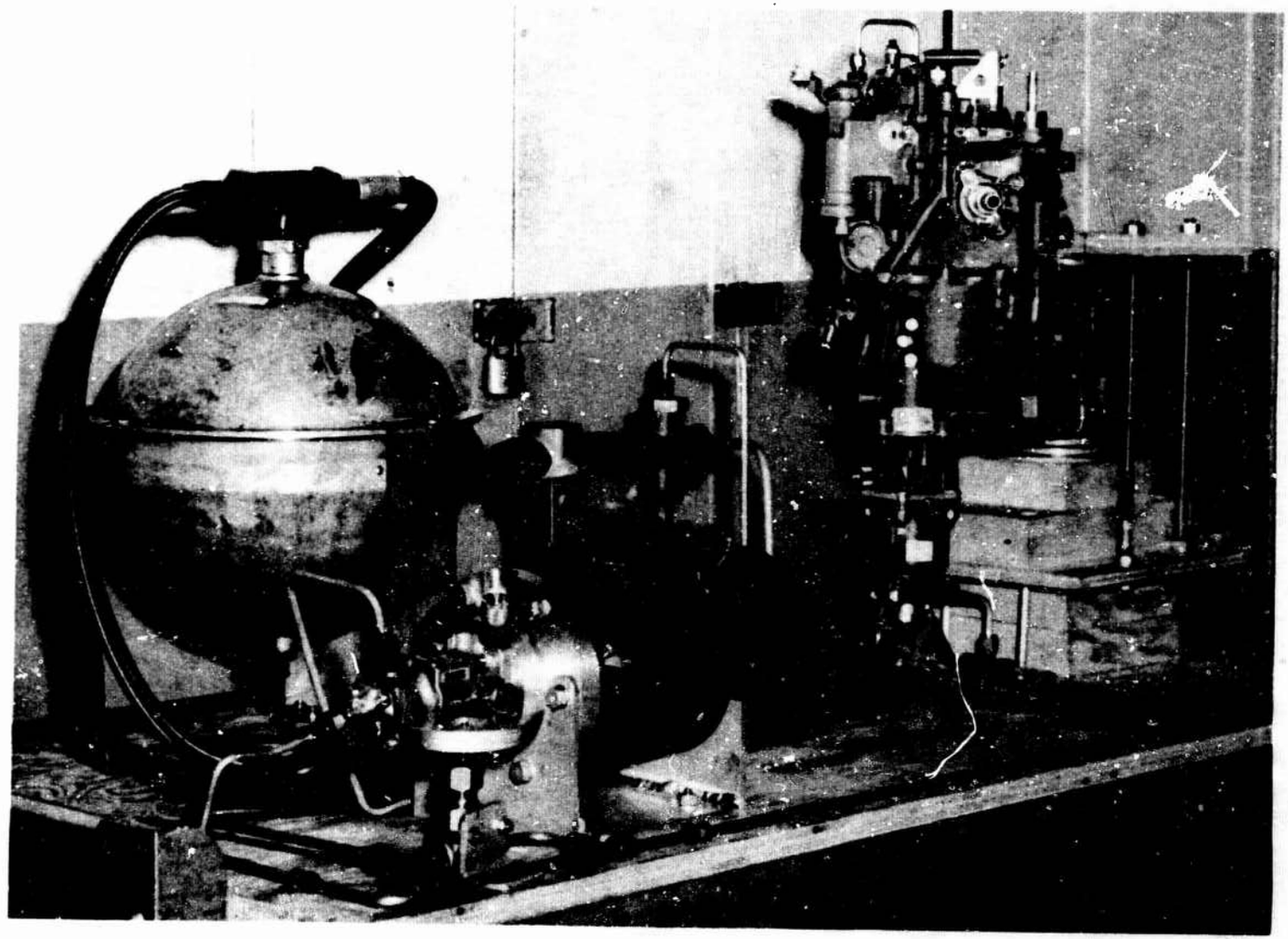

Figure 100. N_f System Test Setup.

directly by a tachometer held against the exposed starter-generator shaft. The bypass needle valve was adjusted to obtain a governor speed of approximately 2500 rpm. The bypass solenoid valve was then closed, and the system allowed to stabilize. The bypass solenoid valve was then opened for approximately 5 seconds, and then closed. During this sequence, the oscillograph was operated at high speed to record the pump and motor speed simultaneously.

The above procedure was followed for three consecutive trials; however, the last was discarded because of an instrumentation malfunction.

The pump and motor speeds were next altered to approximately 4300 and 3900 rpm, respectively, and three trials were conducted as described above.

The pump and motor speeds were determined by measuring the time interval between consecutive pips on the oscillograph trace prior to and subsequent to the time of solenoid valve actuation. The approximate instant of system excitation was obvious from examination of the plotted speed traces.

DETERMINATION OF SPEED ACCURACY

For these tests, the bypass solenoid valve was removed and pressure gages added at the pump and motor high-pressure ports.

The pump speed was adjusted to approximately 3300 rpm. The system was then allowed to stabilize with the bypass needle valve closed, and pressure data were recorded. The oscillograph was run for not less than 5 seconds to obtain motor and pump speeds.

The bypass valve was opened to obtain a motor speed of approximately 3250 rpm, and the above procedure was repeated.

The bypass valve was opened further, in arbitrary steps, to produce motor speeds as low as 2100 rpm.

The pump speed was raised to approximately 4350 rpm and the above procedure repeated. A third test was conducted at a pump speed of approximately 5000 rpm.

TEST RESULTS

FREQUENCY RESPONSE

The time-speed traces of the governor drive motor are shown in Figures 101 through 105. The pump speed was essentially constant during each trial, verifying the assumption of effectively infinite pump-starter inertia.

The speed traces of trials 1 and 2, conducted at a pump speed of 3200 rpm, definitely show the system natural frequency to be approximately 15 to 15.5 cycles per second. The damping that exists when the bypass valve is open is nearly critical. A first harmonic may be present, but data in this regard are inconclusive.

Trials 4, 5, and 6 were conducted at a pump speed of approximately 4300 rpm with the bypass valve adjusted for a motor speed of 3900 rpm. The natural frequency is seen to be 12.5 to 14.5 cycles per second.

The dashed curves indicate the possible existence of a strong first harmonic at approximately 28 cycles per second, but the instrumentation produced only two pips per revolution and has insufficient resolution to show this high frequency oscillation with any accuracy.

SPEED ACCURACY TESTS

At pump speeds ranging from 3300 to 5000 rpm, and with no bypass flow, the motor speed was the same as the pump speed with an error of less than instrumentation accuracy ($\pm$0.5 percent error).

Figure 106 presents the pump and motor power for the range of speeds tested. The difference between pump and motor power represents the transfer line pressure drop. Figure 107 presents the governor drive input torque (computed by measurement of hydraulic input and output pressure).

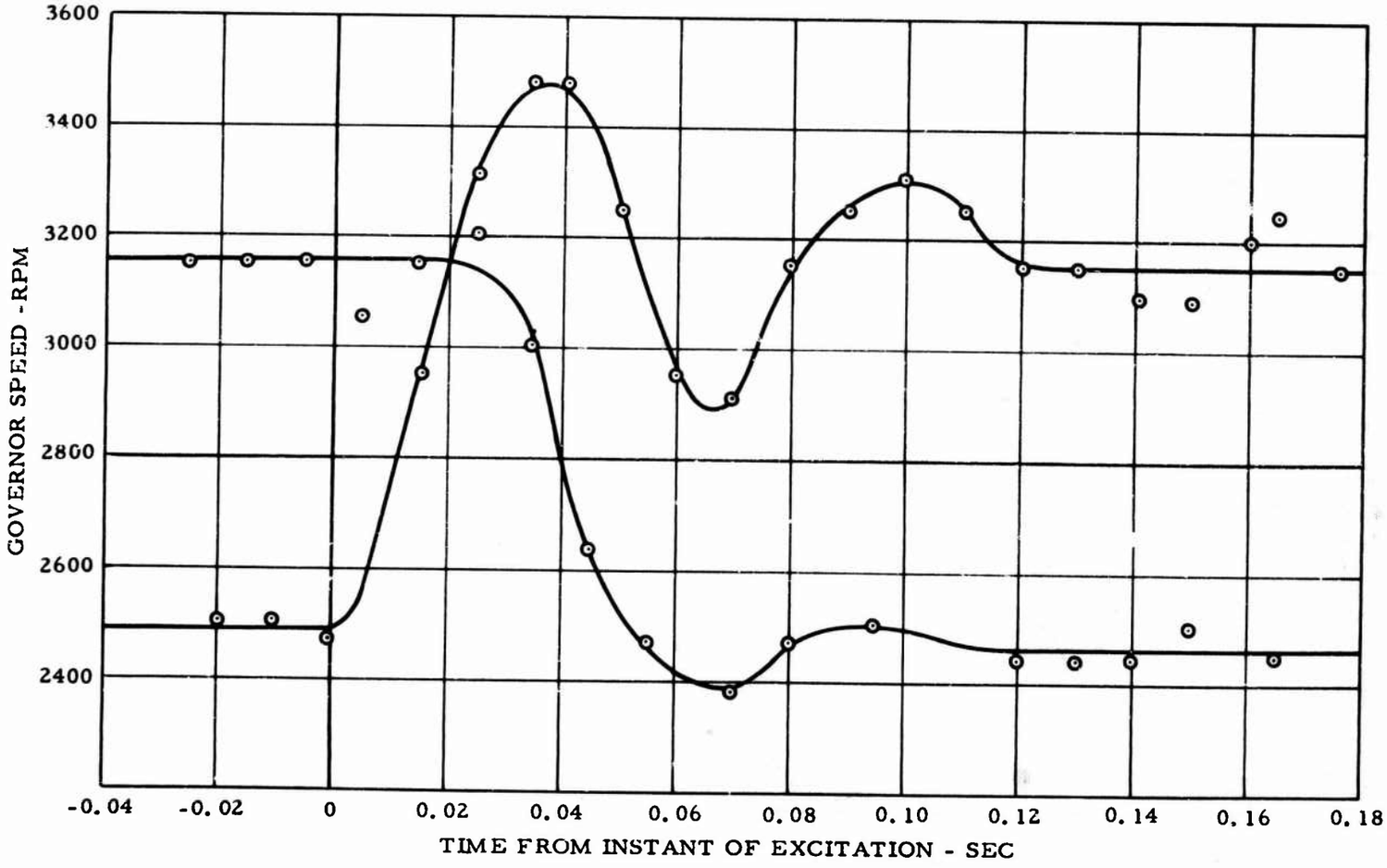

Figure 101. N_f System Frequency Response, Trial 1.

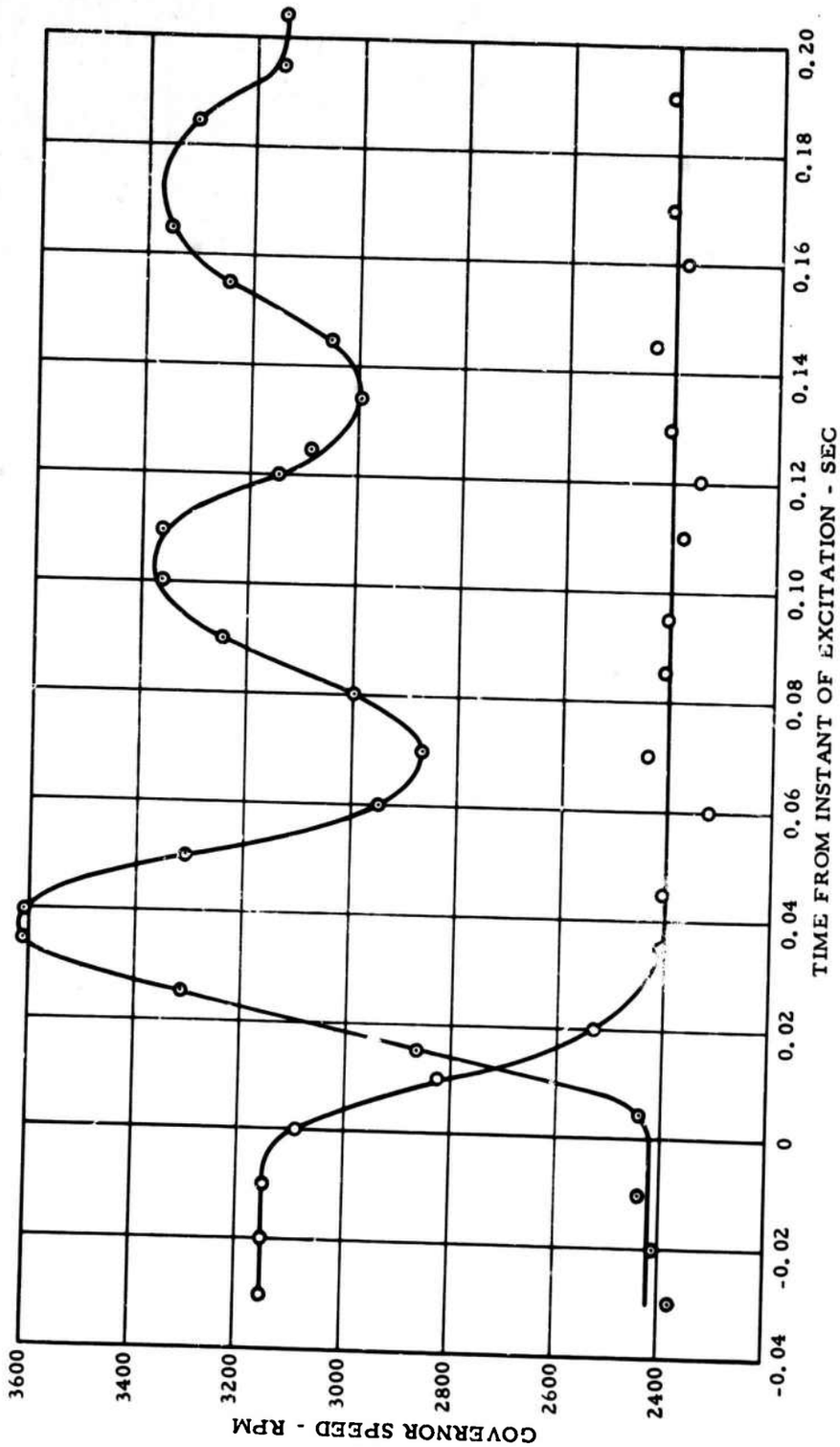

Figure 102. N_f System Frequency Response, Trial 2.

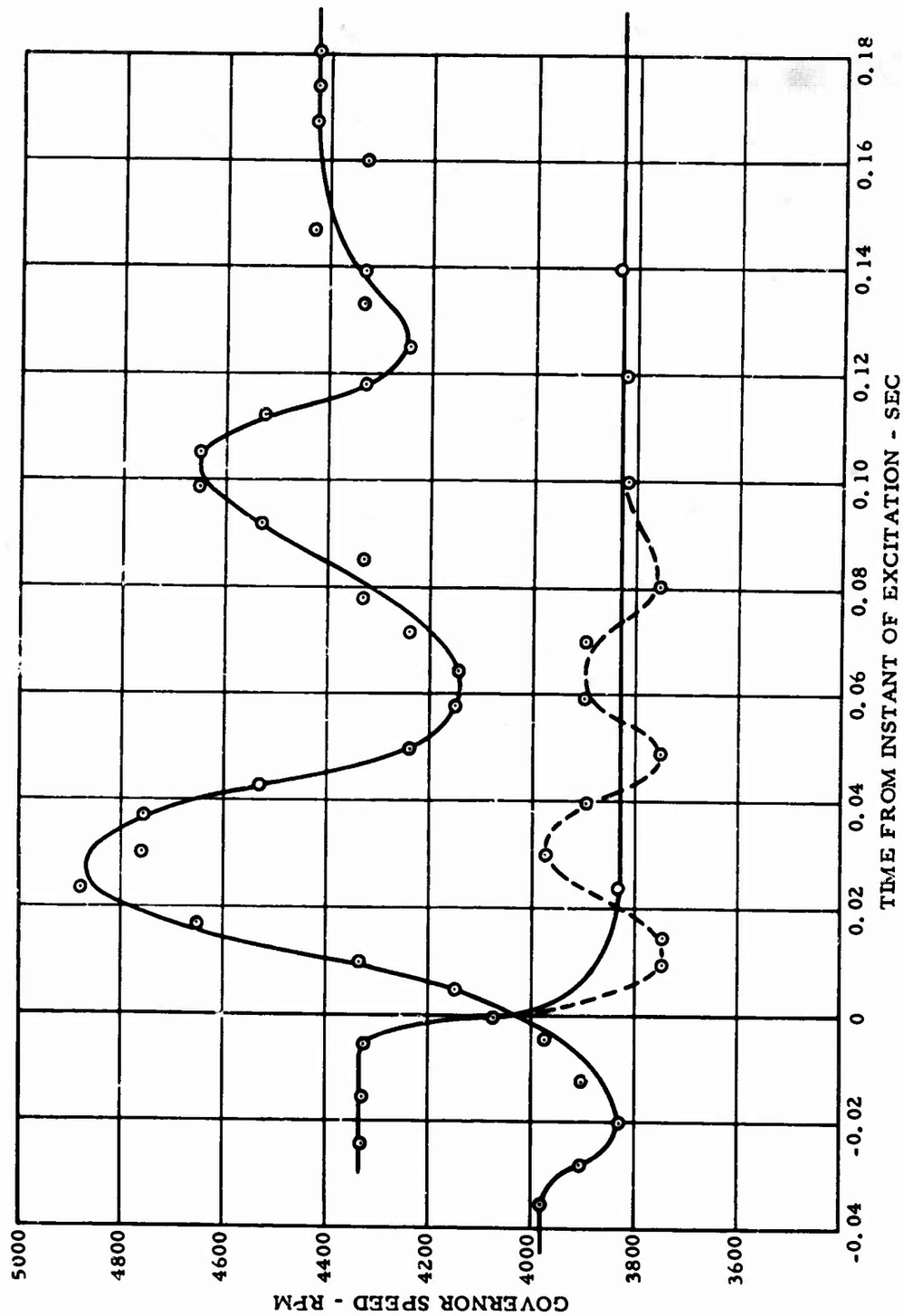

Figure 103. N_f System Frequency Response, Trial 4.

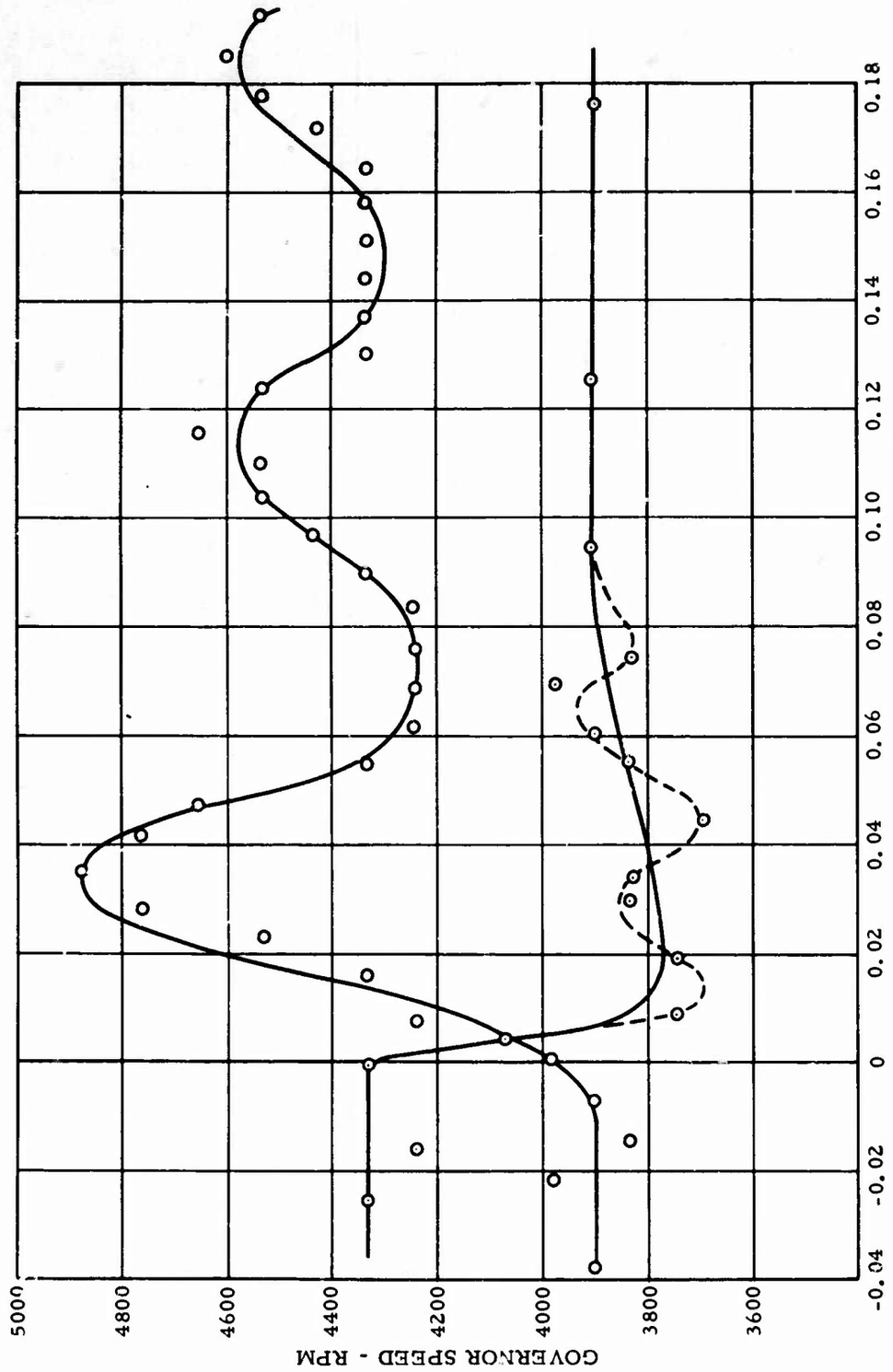

Figure 104. N_f System Frequency Response, Trial 5.

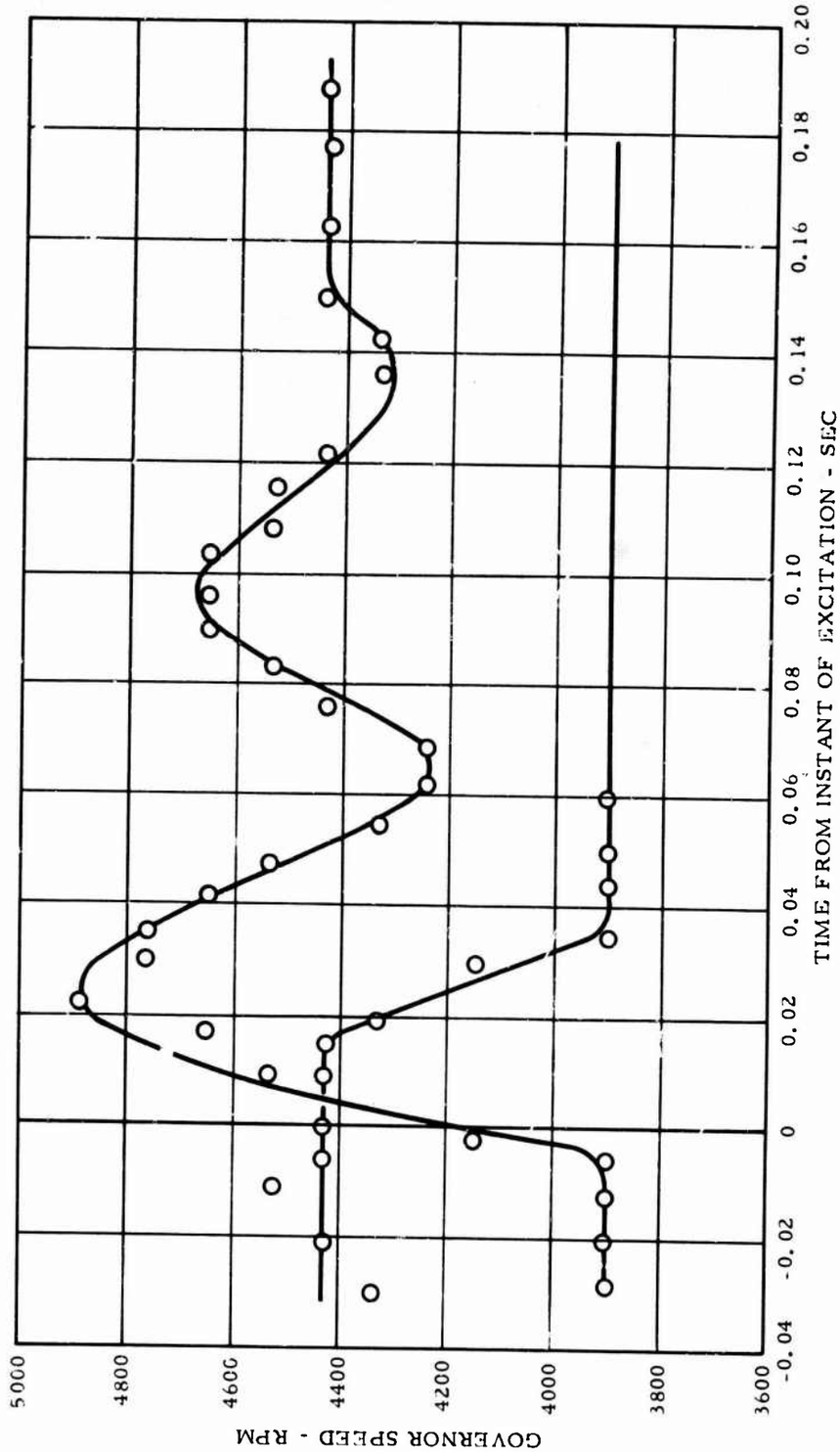

Figure 105. N_f System Frequency Response, Trial 6.

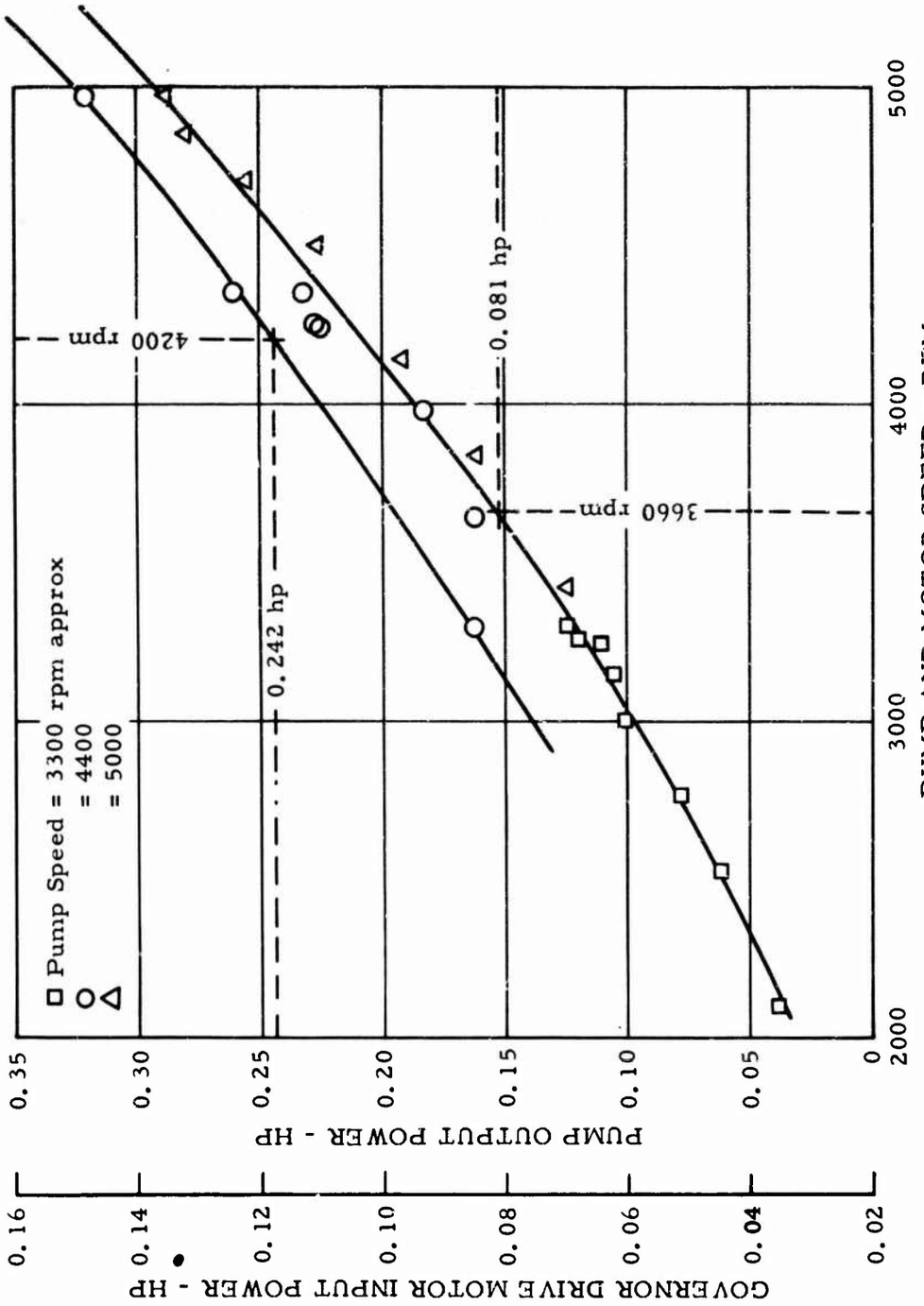

Figure 106. N_f System Power Requirements.

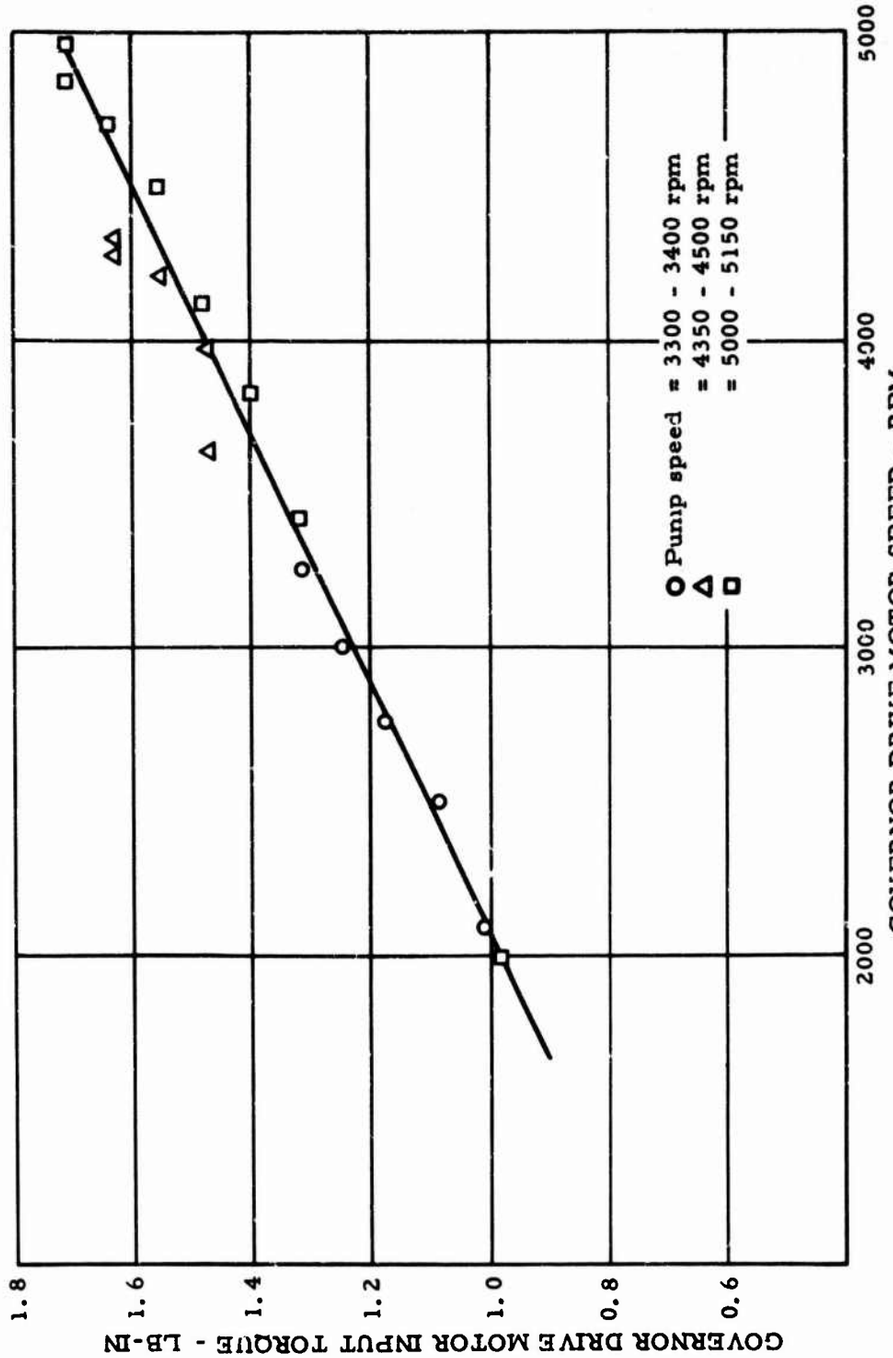

Figure 107. N_f System Governor Drive Motor Torque.

REFERENCES

1 Aircraft Design, XV-9A Hot Cycle Research Aircraft Summary Report, Hughes Tool Company - Aircraft Division Report 64-11 (385-X-05), USAAVLABS Technical Report 65-29, U. S. Army Aviation Materiel Laboratories, Fort Eustis, Virginia, August 1965.

2 Hot Cycle Rotor System Whirl Tests, Hughes Tool Company - Aircraft Division Report 62-16 (285-16), March 1962.

3 Engine and Whirl Test, XV-9A Hot Cycle Research Aircraft Summary Report, Hughes Tool Company - Aircraft Division Report 64-23, USATRECOM Technical Report 64-67, U. S. Army Transportation Research Command,* Fort Eustis, Virginia, February 1965.

*In March 1965, the name of this Command was changed to U. S. Army Aviation Materiel Laboratories.

Unclassified

Security Classification

DOCUMENT CONTROL DATA - R&D

(Security classification of title, body of abstract and indexing annotation must be entered when the overall report is classified)

1. ORIGINATING ACTIVITY *(Corporate author)* Hughes Tool Company - Aircraft Division Culver City, California	2a. REPORT SECURITY CLASSIFICATION Unclassified 2b GROUP

3. REPORT TITLE

COMPONENT TESTING, XV-9A HOT CYCLE RESEARCH AIRCRAFT

4. DESCRIPTIVE NOTES *(Type of report and inclusive dates)*

Summary Report, 29 September 1962 to 15 March 1965

5. AUTHOR(S) *(Last name, first name, initial)*

Deveaux, G. D.

6. REPORT DATE	7a. TOTAL NO. OF PAGES	7b. NO. OF REFS
November 1965	197	3

8a. CONTRACT OR GRANT NO. DA 44-177-AMC-877(T) b. PROJECT NO. Task IM121401D14403 c. d.	9a. ORIGINATOR'S REPORT NUMBER(S) USAAVLABS Technical Report 65-38 9b. OTHER REPORT NO(S) *(Any other numbers that may be assigned this report)* HTC-AD 64-26 (385-T-16)

10. AVAILABILITY/LIMITATION NOTICES

Qualified requesters may obtain copies of this report from DDC.
This report has been furnished to the Department of Commerce for sale to the public.

11. SUPPLEMENTARY NOTES	12. SPONSORING MILITARY ACTIVITY
	U.S. Army Aviation Materiel Laboratories Fort Eustis, Virginia

13. ABSTRACT

This report presents the tests conducted on various structural components of the XV-9A Hot Cycle Research Aircraft. These component tests provided information necessary for design development of the aircraft and supplied data necessary for rotor system fatigue-life calculations.

DD FORM 1 JAN 64 1473

Unclassified

Security Classification

Security Classification

14. KEY WORDS	LINK A		LINK B		LINK C	
	ROLE	WT	ROLE	WT	ROLE	WT

INSTRUCTIONS

1. ORIGINATING ACTIVITY: Enter the name and addresa of the contractor, subcontractor, grantee Department of Defense activity or other orgunization *(corporate author)* issuing the report.

2a. REPORT SECURITY CLASSIFICATION: Enter the overall security classification of the report. Indicate whether "Restricted Data" ia included. Marking is to be in accordance with appropriate security regulations.

2b. GROUP: Automatic downgrading is specified in DoD Directive 5200.10 and Armed Forces Industrial Manual. Enter the group number. Also, when applicable, show that optional markings have been used for Group 3 and Group 4 as authorized.

3. REPORT TITLE: Enter the complete report title in all capital letters. Titles in all cases should be unclassified. If a meaningful title cannot be aelected without classification, show title classification in all capitals in parenthesis immediately following the title.

4. DESCRIPTIVE NOTES: If appropriate, enter the type of report, e.g., interim, progress, summary, annual, or final. Give the incluaive dates when a specific reporting period is covered.

5. AUTHOR(S): Enter the name(s) of author(a) as shown on or in the report. Enter last name, first name, middle initial. If military, show rank and branch of aervice. The name of the principal author ia an absolute minimum requirement.

6. REPORT DATE: Enter the date of the report as day, month, year, or month, year. If more than one date appears on the report, use date of publication.

7a. TOTAL NUMBER OF PAGES: The total page count should follow normal paginatlon procedures, i.e., enter the number of pagea containing information.

7b. NUMBER OF REFERENCES: Enter the total number of references cited in the report.

8a. CONTRACT OR GRANT NUMBER: If appropriate, enter the applicable number of the contract or grant under which the report was written.

8b, 8c, & 8d. PROJECT NUMBER: Enter the appropriate military department identification, auch as project number, subproject number, syatem numbers, taak number, etc.

9a. ORIGINATOR'S REPORT NUMBER(S): Enter the official report number by which the document will be Identified and controlled by the originating activity. This number must be unique to this report.

9b. OTHER REPORT NUMBER(S): If the report has been asaigned any other report numbers *(either by the originator or by the sponsor)*, also enter this number(s).

10. AVAILABILITY/LIMITATION NOTICES: Enter any limitations on further dissemination of the report, other than those imposed bv security classification, using standard statements such as:

(1) "Qualified requesters may obtain copies of thia report from DDC."

(2) "Foreign announcement and dissemination of this report by DDC is not authorized."

(3) "U. S. Government agencies may obtain copies of this report directly from DDC. Other qualified DDC users ahall request through _____."

(4) "U. S. military agencies may obtain copies of this report directly from DDC. Other qualified users shall request through _____."

(5) "All distribution of this report is controlled. Qualified DDC users shall request through _____."

If the report has been furnished to the Office of Technical Services, Department of Commerce, for sale to the public, indicate this fact and enter the price, if known.

11. SUPPLEMENTARY NOTES: Use for additional explanatory notes.

12. SPONSORING MILITARY ACTIVITY: Enter the name of the departmental project office or laboratory sponsoring *(paying for)* the research and development. Include address.

13. ABSTRACT: Enter an abstract giving a brief and factual summary of the document indicative of the report, even though it may also appear elsewhere in the body of the technical report. If additional space is required, a continuation sheet shall be attached.

It is highly desirable that the abstract of classified reports be unclassified. Each paragraph of the abstract shall end with an indication of the military security classification of the information in the paragraph, represented as *(TS)*, *(S)*, *(C)*, or *(U)*.

There is no limitation on the length of the abstract. However, the suggested length is from 150 to 225 words.

14. KEY WORDS: Key words are technically meaningful terms or short phrases that characterize a report and may be used as index entries for cataloging the report. Key words must be selected so that no security classification is required. Identifiers, such as equipment model designation, trade name, military project code name, geographic location, may be used as key words but will be followed by an indication of technical context. The assignment of links, rules, and weights is optional.

Security Classification

6864-65